Extracellular Matrix Remodeling and the Inflammatory Response during Skeletal Muscle Regeneration in Sarcopenic Obese Mice

Lemuel Arthur Brown
University of Arkansas, Fayetteville

Extracellular Matrix Remodeling and the Inflammatory Response during
Skeletal Muscle Regeneration in Sarcopenic Obese Mice

A dissertation submitted in partial fulfillment
of the requirements for the degree of
Doctor of Philosophy in Kinesiology

by

Lemuel Brown
University of Connecticut
Bachelor of Science in Exercise Science, 2010
Eastern Washington University
Master of Science in Exercise Science, 2012

December 2016
University of Arkansas

This dissertation is approved for recommendation to the Graduate Council

_____
Dr. Tyrone Washington
Thesis Director

_____   _____
Dr. Nicholas Greene   Dr. Jeffrey Wolchok
Committee Member   Committee Member

_____   _____
Dr. Cynthia Sides   Dr. Walter Bottje
Committee Member   Committee Member

Abstract

AIM: Sarocpenic obesity is a national concern within the United States because this metabolic syndrome is tied with reduced mobility and quality of life. Both obesity and aging are associated with insulin-resistance, chronic low-grade inflammation and muscle weakness. Skeletal muscle regeneration is a process that involves the coordinated effort of myogenic regulatory factors (MRFs), inflammatory signaling, and extracellular matrix (ECM) remodeling for optimal regeneration. It has been demonstrated that obesity and aging have a reduction in muscle regeneration. It has not been examined if sarcopenic obesity will further reduce muscle mass and the regenerative process. The purpose of this study was to determine how sarcopenic obesity alters inflammatory signaling and extracellular remodeling in mouse skeletal muscle. **METHODS:** One hundred two male C57BL6/J mice (4 weeks old) were randomly assigned to either a high fat diet (HFD, 60% fat) or normal chow. Both young (3 months old) and aged mice (22-24 months old) were injected with either PBS or bupivacaine. Muscles were excised 3 or 21 days after injection. **RESULTS:** Mean cross-sectional area was reduced by 26% in aged HFD mice. The aged lean mice had 9% greater mean cross-sectional area 21 days following muscle damage but no changes were observed in aged HFD. Aged mice had nearly 2-fold collagen III content than young mice. P-STAT3/STAT3 was reduced by 82% in the aged HFD mice in the TA. NF-κB was 3-5 fold greater in the aged HFD mice compared to the aged lean mice in the gastrocnemius and the TA. There was a main effect of injury to reduce collagen I and III content in aged injured, and a main effect of diet with a decrease of collagen I, collagen III, and MMP-9 gene expression in aged HFD mice 3 days following muscle damage. **CONCLUSION:** Sarcopenic obese mice have reduced cross-sectional area than aged mice along with increase collagen III content and basal

alterations in MyoD, ECM proteins, and inflammation gene expression. During skeletal muscle regeneration sarocopenic obese mice had dysregulated inflammatory signaling and reduced ECM gene expression. These data suggest further impairment in the regenerative process in sarcopenic obese mice.

Acknowledgements

I would first like to thank my doctoral advisor Dr. Tyrone Washington for his mentorship over the past four years. Your guidance has helped me grow as a proficient scientist in exercise science. To my advisory and dissertation committees, your input has tremendously improved this project and I thank you for the time you've spent working alongside me during my years as a doctoral student. To my friends and graduate students within the Human Performance Laboratory, I thank you for your constant support during my progression to complete my doctoral degree. Your countless assistance in meetings, journal clubs, seminars, courses, conferences and laboratory procedures has helped me immensely. Funding for this dissertation was primarily provided by the Arkansas Biosciences Institute. Animals were provided by Rigel Pharmaceuticals.

Table of Contents

CHAPTER 1

REVIEW OF LITERATURE

Sarcopenic obesity is a metabolic syndrome that is rising in the United States and around the globe due to the increased rate of obese adults (Villareal, Apovian, Kushner, & Klein, 2005). This is alarming to several health organizations because roughly a third of older adults are obese yet little is known about symptoms and health risks involved in this population (Batsis et al., 2013; Flegal, Carroll, Kit, & Ogden, 2012). Moreover, there are several devastating symptoms that are linked with sarcopenia alone that may lead to poor quality of life, increased healthcare cost, and increase mortality rate. Functional independence is necessary for older adults to complete daily life tasks without assisted living. If older adults do not need to rely on aides and medications related to physical movement there would be a substantial reduction in disability associated healthcare cost (Bowne, Russell, Morgan, Optenberg, & Clarke, 1984).

Skeletal muscle regeneration is a process that occurs following damage after physical activity or exercise and has been investigated with sarcopenia and obese populations because it is necessary for skeletal muscle repair and growth. Skeletal muscle regeneration relies on a coordinated effort from inflammation, myoblast proliferation and differentiation (myogenesis), and ECM remodeling. It has been heavily supported in the literature that exercise can be beneficial in functional movement, reduction in body weight, and muscle growth (Kraemer et al., 1999; Rubenstein et al., 2000; Shumway-Cook, Gruber, Baldwin, & Liao, 1997). Certainly, the overall objective for sarcopenic obese individuals is to increase lean mass and reduce fat free mass because both sarcopenia and obesity are associated with reduced regenerative capacity in skeletal muscle, insulin resistance, systemic low-grade

inflammation, and altered ECM remodeling (Barrett-Connor, 1990; Gregor & Hotamisligil, 2011; Hotamisligil et al., 1996). Nevertheless, both sarcopenia and obesity contribute to reduced mobility which may prevent sarcopenic obese individuals in participating in resistance training and aerobic activity. The literature review for this topic will focus on sarcopenic obesity and skeletal muscle regeneration. The major areas of focus in muscle regeneration for this dissertation are 1) myogenesis 2) the inflammatory response and 3) the extracellular matrix.

Sarcopenic obesity

To better understand sarcopenic obesity both obesity and sarcopenia have to be clearly defined. Obesity is a metabolic disease involving excess adipose tissue that increases health risk. It is most commonly measured by body mass index (BMI). Individuals with a BMI within 25-30 kg/m^2 are considered overweight whereas individuals that have a BMI $\geq$ 30 kg/m^2 are classified as obese. Measuring body fat percentage and Hip-Girth ratio are alternative methods to examine obesity. Classifying obesity is important because there are several health risk associated with the metabolic disease such as high blood pressure, systemic low-grade inflammation, and insulin resistance (Barrett-Connor, 1990; Gregor & Hotamisligil, 2011; Hotamisligil et al., 1996). Over time obesity can lead to pathological disease. Hence, obese individuals are more at risk for cardiovascular disease, diabetes, and stroke (Barrett-Connor, 1990; Steppan et al., 2001; Van Gaal, Mertens, & De Block, 2006). Within skeletal muscle specifically obese individuals exhibit delayed muscle regeneration, muscle fibrosis, increased advanced glycation of end products that is related to muscle stiffness that can negatively impact mobility (Akhmedov & Berdeaux, 2013; L. A. Brown et al., 2015; Gaens, Stehouwer, & Schalkwijk, 2013).

Sarcopenia was first defined by Rosenberg in 1989 as an age-related decline in muscle mass (Rosenberg, 1989). In the past few decades it has been redefined as progressive age-related loss of muscle mass and associated muscle weakness (Lynch, 2011). There are many documented symptoms that are related to the loss of skeletal muscle mass including increase risk of falls, muscle frailty, decrease mobility, and reduced strength (Rubenstein et al., 2000; Shumway-Cook et al., 1997). In clinical research however the definition of sarcopenia is broader in scope. Individuals that suffer from certain disease and illnesses that have similar symptoms may be classified as sarcopenic. For the objective of this dissertation, Rosenberg's definition will be used to examine sarcopenic obesity.

The occurrence of sarcopenia in older adults is usually initiated in the fifth decade (Janssen, Heymsfield, & Ross, 2002). It is around this time that it is assumed that majority of the population will suffer from this disease. In a clinical setting sarcopenia is measured by the reduction in muscle mass, muscle strength, and/or physical performance (Stenholm et al., 2008). The most common clinical equipment and testing for sarcopenia are DXA, handgrip strength, and usual gait speed (Stenholm et al., 2008). While there are several types of measurements to classify sarcopenia by decline in muscle mass, it is well accepted that a loss in muscle grip strength of 40% would be sarcopenia (Choong & Mak, 1991; Stenholm et al., 2008). Although other studies have diagnosed sarcopenia by 2 standard deviations below or lower quintiles of muscle mass compared to young adults (Stenholm et al., 2008). In the literature a 30-50% loss of muscle mass is most common in older adults 50-80 year old (Lynch, 2011). Older adults who suffer from sarcopenia are also more susceptible to a reduction of size in type II muscle fibers than type I fibers (Muscaritoli et al., 2010). Thus, there is drastic decline in strength physical performance. Older adults with sacropenia will

3

also have a reduction in protein turnover, which may partially be involved with the reduction in muscle quality (Proctor, Balagopal, & Nair, 1998). It has been examined in older adults that there is roughly a 50% reduction in muscle stem cells or satellite cells that are needed in the muscle regeneration process. Although, satellite cells are important for muscle fiber repair and growth there are many factors involved that may impact the regenerative capacity (Conboy et al., 2005). Whether these symptoms or underlying mechanisms are involved in sarcopenic obesity is not very well known.

Sarcopenic obesity can be defined as the age-related decline in mass while excessive adipose tissue is preserved or gained (Santilli, Bernetti, Mangone, & Paoloni, 2014). It has been reported that sarcopenic obesity is more closely associated with metabolic syndrome than either disease alone (Lim et al., 2010). This is due to the evidence discovered in numerous studies linking both sarcopenia and obesity to increase mortality and metabolic diseases (J. C. Brown, Harhay, & Harhay, 2014; Fried et al., 2001; Stenholm et al., 2008). This is troubling to sarcopenic obese individuals because the combination of the two co-morbidities could be more damaging to skeletal muscle integrity, repair, and function, but it's classification as a metabolic syndrome is milder because it is less understood. It has been suggested that both sarcopenia and obesity may work synergistically to negatively impact mobility, mortality, and metabolism (Fried et al., 2001; Proctor et al., 1998; Rejeski, Marsh, Chmelo, & Rejeski, 2010). Recent investigations examining sarcopenic obesity have reported reductions of muscle loss that is not based solely muscle mass decline (Santilli et al., 2014). It has also been reported that sarcopenic obese individuals have altered muscle composition due to fat infiltration in the muscle (Santilli et al., 2014). Excessive fat infiltration in skeletal muscle has been linked to a decline in muscle quality and physical performance (Santilli et al.,

4

2014). Systemic low grade inflammation is also exhibited in sarcopenic individuals and may be of more concern then sarcopenic or obese individuals. Chronic signaling of inflammatory cytokines has been reported to promote muscle wasting and apoptosis. The pro-inflammatory cytokine serum IL-6 is associated with excess adipose tissue while TNF-α is inversely related with total muscle mass (Cesari et al., 2005; Schaap, Pluijm, Deeg, & Visser, 2006).

Sarcopenic obesity Animal model

There are very few published studies investigating sarcopenic obese mice and therefore the animal model is relatively new. From a clinical standpoint obese mice that exhibit muscle wasting by disease or genetic modification have been examined (Nilsson et al., 2013). The common model used are middle aged mice and rats that have a deletion of the leptin gene. As a result these mice will gain excessive body fat due to higher rates of food consumption. A more physiological model to examine sarcopenic obesity is diet-induced obesity in old mice. In this model the C57BL/6 strain is given a western or high-fat diet to mimic the excessive calories consumed in western countries. These mice will be kept on this diet until tissue extraction for biochemical analysis. Tissue extraction in these mice will take place at 18-24 months of age which would be the human equivalent of 56-69 years old. The current studies in the literature using this model are predominately focused on heart and liver tissues. There have been a few investigations in sarcopenic obese muscle, but the majority of these studies are in human models where cellular mechanisms are overlooked.

Myogenesis

Once muscle damage occurs from physical activity or exercise, the muscle will have to repair and remodel. This process is known as skeletal muscle regeneration. One aspect of muscle regeneration is the formation of muscle tissue through stem cells, which is termed

myogenesis. There are several phases that are involved with myogenesis including satellite cell (SC) activation, myoblast proliferation, myoblast differentiation, and fusion to the myofiber. SC cells are muscle progenitor cells that have the capability to proliferate and differentiate into myoblasts. Moreover, SC activity is tightly regulated by transcription factors or myogenic regulatory factors (MRF) that will bind to the E-Box region of the DNA sequence (Satoh, Araki, & Satou, 1996). At rest almost all SC cells are localized under the basement membrane beneath the basal lamina and nearly all SC cells will express the transcription factor paired box homeotic gene 7 (Pax7).

Upon skeletal muscle damage, quiescent satellite cells will become activated and the majority of the population will express Pax7 and myogenic differentiation (MyoD). MyoD is a basic helix-loop-helix transcription factor that is expressed during myoblast proliferation and differentiation and is important for myogenic commitment. Upon, SC activation nearly all cells will express MyoD within 24 hours (Zammit et al., 2002). Once MyoD expression is upregulated, SC cells will begin to co-express the MRF myogenic factor 5 (Myf5), which is necessary for proliferation of myoblast (Grefte, 2011). In fact, MyoD is tightly regulated by Myf5 as well as Pax3 and Six homeoproteins (Relaix et al., 2013).

It has been demonstrated that growth factors and cytokines may also be involved with the regulation of MyoD (Engert, Berglund, & Rosenthal, 1996; Serrano, Baeza-Raja, Perdiguero, Jardi, & Munoz-Canoves, 2008). There are also several negative regulators of MyoD including myostatin and TGF-β signaling that are necessary too for myogenesis so that myoblasts can enter the later stages to ultimately lead to myofiber repair and growth (Langley et al., 2002). Chronic activation of these signals, however, can be very detrimental to the regenerative process (Burks & Cohn, 2011). Myoblast proliferation will reach its peak about

2-3 days after injury and will transition into myoblast differentiation to form myotubes. At this point Pax7 will be downregulated and the myoblast will express MyoD, myogenic factor 4 (myogenin), and in some cases Myf5. The expression of both MyoD and myogenin has been reported as early as 12 hours, although the peak of myogenin is around 3 days (Rantanen, Hurme, Lukka, Heino, & Kalimo, 1995).

Myogenin is a MRF that is essential for the initiation of terminal differentiation and fusion (Yin, Price, & Rudnicki, 2013). Myogenin is also involved with the regulation of the contractile proteins myosin and actin to restore muscle function (Benchaouir et al., 2007). Moreover, myogenin can repress Pax7 expression to promote its major functions (Olguin, Yang, Tapscott, & Olwin, 2007). It has recently been discovered that myogenin expression can be regulated by MyoD (Gillespie et al., 2009). Because binding is essential for MRFs to promote their function, they can be negatively regulated by proteins that do not allow them to bind to the E-box region. Ids are a group of proteins that will take the place of MRFs and heterodimerize with E proteins at the E-box (Yin et al., 2013). This will allow the cessation of myogenesis following muscle damage. Thus, MRFs are essential in muscle repair and recovery from muscle damage and are tightly regulated by numerous proteins that are localized in the muscle tissue.

Inflammatory response and Skeletal muscle

The inflammatory response is regarded as the first responders during skeletal muscle regeneration. As such, non-resident phagocytes and other inflammatory proteins will migrate to the site of injury. Moreover, these inflammatory proteins will be involved in the early stages of repair including clearance of necrotic tissue, myoblast proliferation, and differentiation. As muscle regeneration continues there is a shift in function to focus on migration, fusion, and remodeling of the musculature. Anti-inflammatory proteins will regulate these processes and macrophages will secrete these proteins to facilitate these changes. Hence, inflammation has a regulatory role all throughout muscle regeneration.

It has been reported in numerous metabolic and pathological diseases that expression and concentration of these inflammatory proteins and signals are altered that will negatively impact the regenerative capacity of skeletal muscle tissue. More specifically, sarcopenic obesity has been classified as metabolic syndrome that reduces regenerative capacity and leads to skeletal muscle loss. Therefore, it is imperative to identify the changes in the inflammatory response so that future interventions and therapeutics can be utilized to optimize skeletal muscle regeneration in sarcopenic obese individuals.

Phagocytes & Cytokines

Upon skeletal muscle damage there have been several cytokines observed in the skeletal muscle that are upregulated. Interleukin-6 (IL-6) and tumor necrosis factor alpha (TNF-α) have been examined extensively in regards to muscle regeneration because they are necessary for optimal regeneration and have many regulatory functions (S. E. Chen et al., 2005; T. A. Washington et al., 2011; Zhang et al., 2013). IL-6 is a pleiotropic interleukin protein that is a part of the IL-6 family. During infection or injury IL-6 is upregulated to

8

promote an immune response that will protect against pathogens and cellular damage. Upon skeletal muscle regeneration specifically, IL-6 will be secreted by resident and infiltrating macrophages which will promote a pro-inflammatory response. It has been well documented that IL-6 can function as anti-inflammatory myokine when secreted by muscle cells (Petersen & Pedersen, 2005). In addition, IL-6 is secreted by over 20 other cell types and common mesenchymal cells to perform diverse functions (Croker et al., 2003; Kamimura, Ishihara, & Hirano, 2003). At the onset skeletal muscle damage, IL-6 will bind to its signaling receptor glycoprotein 130 (gp130), which will activate a signaling cascade that ultimately results in cell growth, proliferation, and differentiation. Once gp130 is activated, Janus kinase (JAK) will bind to membrane proximal region of the receptor and gp130 will be phosphorylated (Croker et al., 2003; Heinrich et al., 2003). Phosphorylation of gp130 allows signal transducers and activators of transcription (STAT) to dock on Src Homology 2 (SH2) of the tyrosine kinase JAK1. Once phosphorylated, STATs will form dimers and translocate to the nucleus where the will function as transcription factors along with other proteins to regulate cell function. IL-6 signaling leads to dimerization of predominately STAT3 (Tyr705) along with STAT1.

IL-6 signaling will increase exponentially upon infection and/or trauma thus there are multiple inhibitors and phosphatases responsible for the deactivation and degradation of IL-6. Specifically, examining myotoxin induced muscle damage IL-6 has been observed on average to increase 10–fold 48 hours following damage (Hirata et al., 2003). It has been established that both PIAS and SOCS can suppress IL-6 activity to control its function (Croker et al., 2003; Heinrich et al., 2003). It has also been reported that the upregulation of IL-6 at the onset of regeneration increases myoblast proliferation and differentiation and is necessary for the

regenerative process (Kamimura et al., 2003; Toth et al., 2011; Zhang et al., 2013). However, it appears that the overexpression of basal IL-6 in skeletal muscle has been implicated in muscle pathological disease states such as DMD, cachexia, and myopathies (Iwase, Murakami, Saito, & Nakagawa, 2004; Lundberg, Brengman, & Engel, 1995). IL-6 is one of a few cytokines that are observed in nearly all obese individuals that will exhibit low-chronic grade inflammation. However, these individuals may have a reduction in muscle IL-6 at rest and a blunted response of IL-6 expression in muscle a few days following muscle damage (J. C. Brown et al., 2014).

In aging individuals it appears that basal levels of IL-6 in skeletal muscle are similar to younger adults while levels of skeletal muscle IL-6 expression may be different following exercise (Hamada, Vannier, Sacheck, Witsell, & Roubenoff, 2005; Pedersen et al., 2004; Przybyla et al., 2006). A few studies reported a significant upregulation of skeletal muscle IL-6 following muscle damage (Pedersen et al., 2004; Przybyla et al., 2006). In contrast, Hamada and colleagues observed a significant increase of skeletal muscle IL-6 mRNA expression in younger adults, but did not find any differences in IL-6 mRNA expression following exercise in older adults (Hamada et al., 2005). Whether IL-6 expression is blunted in older adults remains unclear. Moreover, the fate of IL-6 is uncertain in older adults. It is not known if IL-6 signaling is leading towards an anti-inflammatory response by STAT3 activation or a pro-inflammatory immune response. When IL-6 is membrane bound to the IL-6 receptor (IL-6R), it will activate STAT3 and have anti-inflammatory effects. This is referred as classical IL-6 signaling. IL-6 trans signaling occurs in chronic inflammatory disease states and leads to activation of the immune system (Kishimoto, 2006). Thus, IL-6 signaling needs to be further explored in aging and sarcopenic obese adults.

TNF-α is a pro-inflammatory cytokine that is a member of the TNF family and is known for its role as a pro-apoptotic gene. In classical signaling, the TNF-α ligand will bind to either TNFR1 or TNFR2 transmembrane receptor. A major target of TNF-α, Nuclear Factor-κB (NF-κB), is involved with promoting apoptosis in various cells including muscle cells. NF-κB has multiple isoforms, which are involved with different outcomes of the cell. Typically in skeletal muscle the p50/p65 heterodimer will be activated and will lead to cellular apoptosis. Because TNF-α is a pro-apoptotic cytokine and is necessary for skeletal muscle regeneration it has been examined for its involvement of damaged tissue (S. J. Chen et al., 1999). Pathological and metabolic diseases have demonstrated that increased levels of chronic systemic TNF-α expression are involved with muscle wasting (Argiles, Busquets, Toledo, & Lopez-Soriano, 2009; Cai et al., 2004; Tisdale, 1997). Chronic systemic inflammation is also found in aging and obese populations as well (Chmelar, Chung, & Chavakis, 2013; Gregor & Hotamisligil, 2011). Far less is known about TNF- α signaling at basal levels and during acute regeneration in skeletal muscle. In human studies with various exercise interventions both TNF-α has been reported as either no change or upregulated in elderly skeletal muscle compared to younger adults (Peake, Della Gatta, & Cameron-Smith, 2010). Thus, IL-6 and TNF signaling are crucial components in the skeletal muscle regeneration process with distinct roles. Furthermore, alterations in these cytokines can have a negative impact on regenerative capacity and should be further examined in sarcopenic obese populations.

Recruitment and infiltration of phagocytes

One process involved with the initial inflammatory response during skeletal muscle regeneration is infiltration of phagocytes (Kharraz, Guerra, Mann, Serrano, & Munoz-Canoves, 2013; Kragstrup, Kjaer, & Mackey, 2011; Serrano et al., 2008; Thornell, 2011;

11

Yang et al., 2012). Non-resident phagocytes play a predominant role in phagocyte recruitment and plasma proteins to remove damaged tissue and repair skeletal muscle (Zhang et al., 2013). Resident macrophages perform these functions as well, but to a lesser extent. At the onset of muscle damage, resident macrophages located at the epimysium and perimysium connective tissue will secrete muscle cytokines that will serve as a chemoattractant to phagocytes and plasma proteins to the site of damage (De Bleecker & Engel, 1994). These recruited phagocytes will remove necrotic tissue and aid in the repair and remodeling of the skeletal muscle tissue. Neutrophils are the first phagocytes to infiltrate the endothelium to the site of injury. Their role in regeneration is not completely understood in skeletal muscle but they may take partial responsibility in removing damaged tissue and facilitating myoblast proliferation (Cassatella, 1999). After 48 hours neutrophils are downregulated whereas macrophage infiltration is increased. Macrophages are activated monocytes that phagocytose microbes and damage tissues and are necessary in the muscle regeneration response (Kharraz et al., 2013). The recruitment of neutrophils and monocytes (non-activated macrophages) is a coordinated response between several specific ligands and receptors.

Recruitment of phagocytes and inflammatory cells is a multi-step process that has been studied extensively in the immune response. Furthermore, phagocyte recruitment in regards to muscle damage is an emerging field in the muscle regeneration process. Cytokines, chemokines, integrins, and adhesion molecules are important proteins in the recruitment process. Adhesion molecules are a group of proteins that are involved with recruiting circulating phagocytes for infiltration into the skeletal muscle tissue. Naïve neutrophils and monocytes have receptors that correspond with selectins and integrins that will bind with specific ligands on the endothelium. The sheer force of blood will cause the phagocytes to roll

on the endothelium wall until the muscle cytokine, which serves as a chemoattractant, recognizes a chemokine receptor on the immune cell. Afterwards, a conformational change will take place on an integrin, which is a cell surface protein that is involved with cell-cell adhesion. The β2 integrin will change from a low to high confirmation and *tether* the phagocyte near the site of damage. The tethering of the phagocyte will lead towards infiltration into the extracellular matrix, then towards damaged skeletal muscle tissue. Each phagocyte has a specialized β2 heterodimeric integrin that is involved with migration and may explain for the difference in regulation. The integrin located on neutrophils is called lymphocyte function-associated antigen 1 (LFA-1) whereas macrophages integrins are called macrophage-1 antigen (Mac-1 or $\alpha_M\beta_2$). Intercellular adhesion molecule 1 (ICAM-1) is an adhesion molecule and a member of the immunoglobulin family that binds with LFA-1 and Mac-1 (Dearth et al., 2013). ICAM-1 consist of five extracellular domains, a transmembrane, and cytoplasmic tail (Gahmberg, Tolvanen, & Kotovuori, 1997). The extracellular immunoglobulin domain, CD11b, has been implicated as an essential domain for binding to β2 integrins (Gahmberg et al., 1997).

The induction of adhesion molecules have been investigated in skeletal muscle growth, regeneration, and disease. Dearth and colleagues investigated ICAM-1 in a muscle overload animal model, because ICAM-1 interacts with β2-integrins that is needed for macrophage infiltration during muscle damage. The authors suggested that the overexpression of the ligand ICAM-1 may be beneficial during muscle regeneration to improve the migration of immune cells (Dearth et al., 2013). Sonnet examined whether ICAM-1 is expressed upon muscle regeneration and its functional role in skeletal muscle (Sonnet et al., 2006). The researchers discovered that not only was ICAM-1 expressed in muscle upon regeneration, but

that it is involved in the survival of macrophages (Sonnet et al., 2006). De Bleecker and Engel examined ICAM-1 and its expression in myopathies associated with chronic inflammation (De Bleecker & Engel, 1994). They reported an upregulation of ICAM-1, which was associated with an increase of cytokines in the muscle. Thus, ICAM-1 may have supported the chronic influx of macrophages to the site of muscle damage that could alter inflammation signaling.

Whether or not these alterations occur in aging or obese population have yet to be explored. Previously mentioned older adults and obese individuals exhibit chronic systemic low grade inflammation, but there inflammatory profile may be reduced in skeletal muscle. It has been observed in skeletal muscle of obese mice that macrophage count is reduced a few days following injury (Nguyen, Cheng, & Koh, 2011). Moreover, it appears that inflammatory cytokines are reduced in skeletal muscle of obese mice and that cytokine secretion is blunted at the onset of muscle damage (L. A. Brown et al., 2015). Yet, it has not been investigated if adhesion molecules may be responsible for the reduction of inflammatory signaling in obese or aging skeletal muscle. This process warrants further investigation in obese, aging, and sarcopenic obese individuals.

Macrophage Polarization

Macrophages serve many functions to assist in the regenerative process of skeletal muscle. The two primary functions are, a) removing damaged or necrotic tissue, and b) repairing and remodeling. The function that a macrophage will perform is dependent on the phenotype and the changing of the functional state is referred as macrophage polarization. M1 macrophages are known as classically activated macrophages that will remove damaged/necrotic tissue. In contrast, M2 macrophages (alternatively activated macrophages)

14

are partially responsible for the repair process (Zhang et al., 2013) (Figure1-1). M2 macrophage subsets include M2a, M2b, and M2c which are mediated by cytokines, hormones, and signals and are based on the state of the cell (Martinez & Gordon, 2014). M2a macrophages are mediated by IL-4 and IL-13 and primarily function to kill parasites and protect against allergic reactions (Martinez & Gordon, 2014). M2b macrophages are mediated by toll-like receptor ligands and immune complexes and serve as immunoregulatory macrophages (Martinez & Gordon, 2014). Finally, M2c macrophages are mediated by IL-10 and TGF-β and are involved in matrix deposition and tissue remodeling (i.e. muscle damage from injury) (Martinez & Gordon, 2014). No matter the phenotype, macrophages will secrete cytokines that promote their function. The homeostatic balance between the two phenotypes is key for optimal skeletal muscle regeneration (Rigamonti & Zordan, 2014). In a normal response to muscle damage after an exercise bout, initially M1 macrophages will be expressed during regeneration followed by a phenotypic switch towards M2 macrophage expression. If the balance between the phenotypes are modified, it may result in less optimal muscle regeneration (Villalta, Nguyen, Deng, Gotoh, & Tidball, 2009).
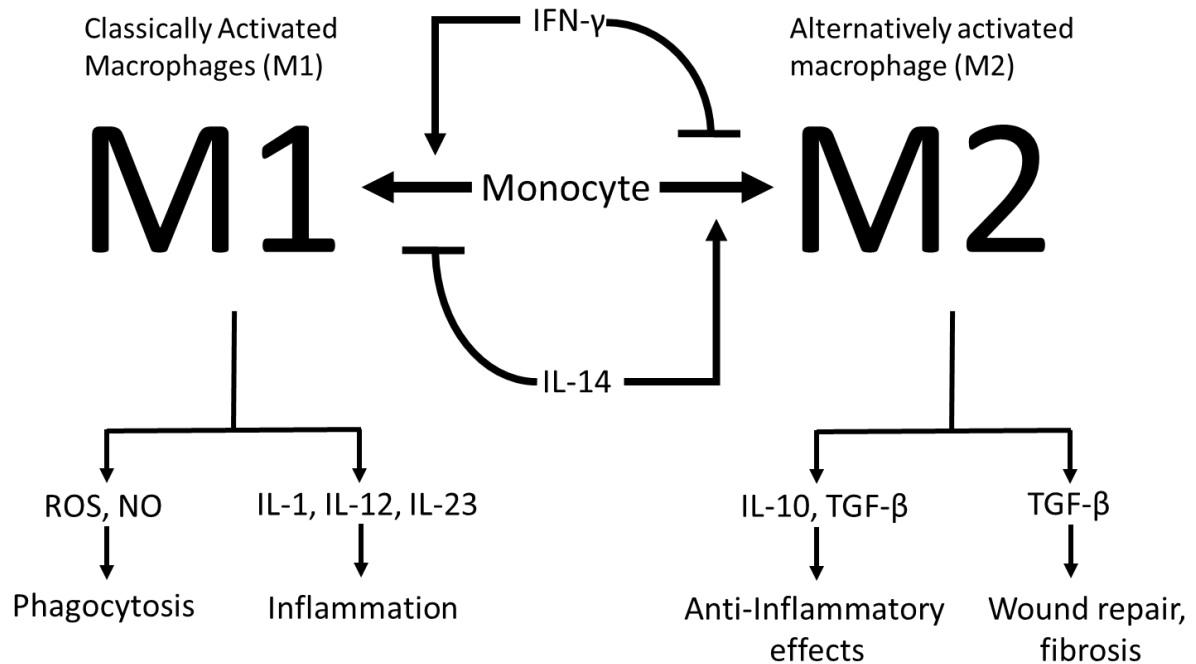
Figure 1-1. Macrophage Polarization. Adapted from Cellular and molecular biology by A. K. Abbas, A. H. H. Lichtman, S. Pillai, 2011, . Philadelphia, PA: Elsevier Saunders. Copyright 2011.

The adaptive immune system is primarily responsible for regulating macrophage phenotype. After damage occurs to the skeletal muscle tissue, dendritic cells will present the damaged peptides to T lymphocytes. The T lymphocytes will recognize the damaged tissue with the T cell receptor and will begin the differentiation to either a T_H1 or T_H2 cells. T_H1 cells will secrete IFN-γ, which dictates a pro-inflammatory response by M1 macrophages. M1 macrophages will secrete pro-inflammatory cytokines such as IL-6, IL-1β, and TNF-α. IL-6 will signal through the JAK2/STAT3 pathway leading to cell survival of monocytes, T-lymphocytes, and B-lymphocytes. TNF-α and IL-1β will signal through the NF-κB pathway. This response is necessary in the inflammatory response because it promotes acute inflammation and stimulates the adaptive immunity. M1 macrophages appear to be upregulated during myoblast proliferation and may aide in myoblast proliferation (Toth et al.,

2011). Toth and colleagues wanted to determine whether or not IL-6 played a role in muscle regeneration because skeletal muscle cells secrete IL-6 after damage around the same time point myoblast begin proliferation (Hiscock, Chan, Bisucci, Darby, & Febbraio, 2004; Toth et al., 2011). STAT3 is a downstream target of IL-6 known to increase expression *c-Myc* (Kiuchi et al., 1999). Increased *c-Myc* expression induces proliferation in myoblast cells (Z. Li et al., 2012). Toth found that induction of STAT3 by IL-6 occurred in the nuclei of human satellite cells following eccentric contraction (Toth et al., 2011). Overall, classical activation of M1 macrophages are required for the earlier response in regeneration.

Conversely, T_H2 will mediate anti-inflammatory cytokines such as IL-13 and IL-14 that will facilitate a change from M1 to M2 expression. M2 macrophages will promote wound repair and ECM remodeling. To date, IL-10 and TGF-β are the most understood anti-inflammatory cytokines secreted by M2 macrophages. TGF-β has many functions in skeletal muscle regeneration, the most important being skeletal muscle repair. TGF-β commonly signals through Smad proteins and promotes growth of collagen, fibroblast, and increases in matrix proteins. In addition, TGF-β will reduce the activation of neutrophils and macrophages. IL-10 is a negative feedback regulator of M1 macrophages that signals through JAK1 and TYR2/STAT3 signaling. It can also be signaled by regulatory T cells that are involved with suppressing the immune response. Nevertheless, IL-10 is partially involved in bringing expression of inflammation back to baseline levels. Regulation of the switching between the two phenotypes is still not well understood and requires further investigation. M2 macrophages may also promote myoblast differentiation (Sakaguchi et al., 2014). One study focused on the function of M2 macrophages 3-5 days post muscle damage *in vitro* and *in vivo*. The study observed that *in vitro,* differentiating myoblast in M2 macrophage media

upregulated differentiation markers, myogenin and MyHC (Sakaguchi et al., 2014). They concluded that M2 macrophages may need to be further explored in terms of differentiation but may be necessary for the differentiating phase of muscle regeneration (Sakaguchi et al., 2014).

The balance between M1 and M2 macrophages is very delicate in the regeneration process. Prolonged expression in either macrophage phenotype can lead to a suboptimal repair in skeletal muscle fibers (Villalta et al., 2009; Yang et al., 2012). Yang and colleagues reported distinct differences between lean and obese mice in the ratio between M1/M2 macrophage expressions (Yang et al., 2012). They included SIRT1 knockout (MSKO) mice in their experiment because it is a master regulator of metabolism and inflammation (X. Li, 2013; Yang et al., 2012). They found that deletion of SIRT1 switched M2 alternative macrophages activation to M1 classical activation. They also found increases in total M1 macrophages expressed in adipose tissue in MSKO mice (Yang et al., 2012). An imbalance of M2/M1 is also not favorable in certain tissues. Prolonged expression of M2 occurs in muscular dystrophies (Yang et al., 2012). Villalta noticed that during muscle regeneration that there was a severe reduction in M1 expression in mdx mice (Villalta et al., 2009). After further investigation, it appeared that M2 macrophages inhibit the expression of M1 macrophages. Thus, individuals that suffer from muscular dystrophies may benefit from therapies that improve M1 macrophages early in the regeneration process (Villalta et al., 2009).

In conclusion, the balance between M1 and M2 macrophages is essential in regenerating skeletal muscle fibers. M1 macrophages will be upregulated first to promote the removal of damage necrotic muscle tissue. Afterwards, anti-inflammatory M2 macrophages

will assist in the repair and remodeling of muscle tissue. Prolonged responses in both M1 and M2 macrophages have been shown to negatively impact repair of skeletal muscle tissue. Thus, it is essential to determine if there are changes in macrophage phenotypes in regards to muscle regeneration.

Extracellular matrix of skeletal muscle

The extracellular matrix (ECM) provides structural support to skeletal muscle and is comprised of several proteins that serve a variety of functions in skeletal muscle such as repair, growth, remodeling, and stability. The earliest experiments described the ECM as only a structural protein to support functional movement and resist tension from stress. Yet, in the past few decades this notion has been disproven through deeper investigation. Studies examining localization of dormant SC cells, growth factors, myokines, and resident macrophages that are involved in the regenerative process have discovered that these proteins all reside in the basement membrane of the ECM. Hence, following studies have uncovered physical interactions with ECM proteins and proteins involved with skeletal muscle regeneration. Furthermore, upon mechanical stress ECM proteins will initiate the regenerative process and the inflammatory proteins that reside in the ECM will assist in the regulation of ECM remodeling for optimal regeneration. Thus, the extracellular matrix is more than just a structural protein for muscle, it is essential in muscle repair and is involved with other processes that are necessary for muscle function.

The extracellular matrix requires tight regulation because it is comprised of several proteins that all perform diverse functions in numerous processes. It has been demonstrated in metabolic and pathological diseases that the ECM will be dysregulated and reduce the regenerative capacity of skeletal muscle. The major consequence in altered ECM is skeletal muscle fibrosis, which can be defined as improper healing of connective tissue leading to scar tissue formation. As a result of fibrosis there is a reduction of force transmission (muscle weakness) and stability of the muscle (excessive muscle stiffness) as well as sub-optimal muscle regeneration upon damage. Thus, it is essential to know about the components that

comprise the ECM and understand the remodeling process upon muscle damage to identify potential problems in regenerating muscle of sarcopenic obese individuals.

ECM structure and function

The ECM is localized in several areas of skeletal muscle with a varied distribution of extracellular proteins to best suit its function (Light & Champion, 1984). The most outer layer of the ECM is referred as the epimysium, which is the sheath that covers the entire belly of the muscle and extends to the tendon. Collagen accounts for nearly a quarter of the connective tissue in the epimysium that is predominately collagen I and has minor amounts of collagen III (Light & Champion, 1984). The ECM that covers the surrounding muscle bundles along with the blood vessels and nerves is the perimysium. Collagen comprises nearly all of the connective tissue content in the perimysium and is predominately Collagen I with a minor amount of Collagen III and trace amounts of Collagen V (Light & Champion, 1984). Lastly, there is the endomysium that covers each individual muscle fiber and is in direct contact of the basement membrane where quiescent SC cells reside. The blood vessels and nerves will actually extend into the endomysium. The endomysium is comprised predominately of collagen I and collagen III fibrils and accounts for half of the connective tissue content (Light & Champion, 1984). Macrophages, adipocytes, and fibroblast cells are all localized in the endomysium and are involved in the skeletal muscle regeneration process. Overall, skeletal muscle ECM makes up about 5% of the skeletal muscle dry weight and is comprised of collagens, glycoproteins, glycoaminoglycans, and proteoglycans (Light & Champion, 1984; Schiaffino & Partridge, 2008).

Collagens are the most abundant proteins in the human body that are highly diverse in

composition (Myllyharju & Kivirikko, 2004). The collagen family is composed of 3 polypeptide α chains that are coiled into a triple helix configuration that allow them to be structural proteins by nature (Schiaffino & Partridge, 2008). Collagens are rich in glycine, proline, and hydroxyproline. The proline in collagen is responsible for maintaining the formation of helical orientation of each alpha chain. Glycine is essential in the structure of collagen because of its size. Glycine is the only amino acid that can fit in the interior of the helical collagen structure. All collagens have at least one rod-like collagen domain and one noncollagenous domain. Collagen structures have tensile strength and elastic properties that allow functional movement in mammals whereas noncollagneous proteins in the ECM provide compressive strength. Collagen fibrils are synthesized by fibroblasts and are usually made up of 2 or more collagen isoforms. To date there are over 45 genes that code for 28 isoforms of collagen (collagen type based on domain structure homology) that have been discovered in human tissue and organs (Mecham, 2011) (Table 1-1). Collagen types I-III, V, and XI are fibril forming collagens that are 285 kDa and provide tensile strength to the skeletal muscle (Table 1-1). Collagen I and III are the most abundant fibrillar collagens in skeletal muscle (Purslow & Duance, 1990). The composition of the basement membrane however has a high abundance of collagen IV, a network type collagen.

Type	Class	Distribution
I	Fibrillar	dermin, bone, tendon, ligament
II	Fibrillar	cartilage, vitreous
III	Fibrillar	skin, blood vessels, intestine
IV	Network	basement membranes
V	Fibrillar	bone, dermis, cornea, placenta
VI	Network	bone, dermis, cornea, cartilage
VII	Anchoring fibrils	dermis, bladder
VIII	Network	dermis, brain, heart, kidney
IX	FACIT	cartilage, cornea, vitreous
X	Network	cartilage
XI	Fibrillar	cartilage, invertebral disc
XII	FACIT	dermis, tendon
XIII	MACIT	endothelial cells, dermis, eye, heart
XIV	FACIT	bone, dermis cartilage
XV	MULTIPLEXIN	capillaries, testis, kidney, heart
XVI	FACIT	dermis, kidney
XVII	MACIT	hemidesmosomes in epithelia
XVIII	MULTIPLEXIN	basement membrane, liver
XIX	FACIT	basement membrane
XX	FACIT	cornea
XXI	FACIT	stomach, kidney
XXII	FACIT	tissue junctions
XXIII	MACIT	heart, retina
XXIV	Fibrillar	bone, cornea
XXV	MACIT	brain, heart, testis
XXVI	FACIT	testis, ovary
XXVII	Fibrillar	cartilage
XXVIII	-	dermis, sciatic nerve

Table 1-1. Types, class, and composition of collagen. Adapted from Collagen: basis of life from S. Jain, H. Kaur, G. Pandav, A. Dewan, and D. Saxena, 2014, *Universal Research Journal of Dentistry*, *4*, p.1. Copyright 2014 by Wolters Kluwer Medknow Publications.

Collagen I is the most abundant form of fibrillar collagen in the human body that has been extensively researched in skeletal muscle biology. Collagen I is made up of nearly 1,000 amino acids and is composed of two α1(I) chains and one α2(I) chain. Collagen I is known as

the thickest collagen fibrils (~ 400 kDa) in mammals. Upon, injury the COL1A1 gene is upregulated to increase collagen turnover at the site of injury.

Collagen III has been examined less extensively as collagen I within skeletal muscle. One of the earliest findings of collagen III in skeletal muscle was documented in 1977 by Bailey's meat science laboratory (Duance, Restall, Beard, Bourne, & Bailey, 1977). Collagen III is composed of three α1(III) chains. Similar to COL1A1, the COL3A1 gene is upregulated after muscle damage and is regulated by similar growth factors and myokines, but differences in upregulation may occur in traumatic injury and disease. Processing of collagen I and III are very similar, but several differences do exist in the post-translational steps during procollagen formation inside the fibroblast (Fleischmajer, MacDonald, Perlish, Burgeson, & Fisher, 1990). During post-translational modifications, Collagen III will lose a carboxy propeptide and then amino peptide, which is reversed in collagen I processing (Fessler, Timpl, & Fessler, 1981). Collagen III and I will actually share similar cleavage sites during post-translational modifications but use different proteinase specific enzymes (Morikawa, Tuderman, & Prockop, 1980). Collagen III is considered an incomplete processed collagen because the enzymes involved in processing leave a C-telopeptide and partially processed N-propeptide (Mecham, 2011). Thus, collagen III is a thinner collagen fibril that can withstand more deformation compared to collagen I. Flesichmajer and colleagues observed that collagen I with increasing diameter lack amino propeptides, whereas collagen III fibrils, which do not grow keep the amino propeptide on the surface (Fleischmajer et al., 1990). The amino propeptide specifically prevents the formation of thick collagen III fibrils.

It has been suggested that collagen III is essential for fibrillogenesis, processing of collagen I and determination collagen I diameter (Liu, Wu, Byrne, Krane, & Jaenisch, 1997).

24

It is well known that collagen fibrils are made up of at least two collagen fibrils and that collagen III is co-localized in all collagen I tissues in humans (Liu et al., 1997; Mecham, 2011). Liu et al., discovered that COL3A1 knockout mice had a reduction of collagen fibrils and disorganized fibrils (Liu et al., 1997).

The synthesis of collagen is an important aspect of collagen turnover that takes place in many cell types including fibroblasts, myofibroblast, osteoblasts, fibroadipocytes, adipocytes, macrophages, mast cells, plasma cells, and leukocytes. These cells will reside on collagen fibers and will regulate collagen remodeling and turnover via cell-cell interactions (Kjaer, 2004; Schiaffino & Partridge, 2008). Alterations in these cell populations can interfere with collagen structure and direct cell-cell interactions. For example, in hypertrophic obesity preexisting adipocytes will expand. The expansion of these cells will forcibly push collagen fibrils to the side.

Fibril forming collagen synthesis involves many steps usually starting with mechanical stress. Upon mechanical load the ECM will serve as scaffold for the adhesion of cells that are mediated by glycoproteins, proteoglycans (PG), and integrins (Brakebusch, Bouvard, Stanchi, Sakai, & Fassler, 2002; Ingber et al., 1994; Kjaer, 2004). The interaction between the ECM and particular adhesion molecules will activate cellular signaling pathways (MAPK, PKC, NF-κB) and rearrangement of the cytoskeleton (Burridge & Chrzanowska-Wodnicka, 1996; Chiquet, Matthisson, Koch, Tannheimer, & Chiquet-Ehrismann, 1996; Reynolds et al., 2000). Concurrently, the glycosaminoglycan (GAG) side chains on PGs will be able to bind specific growth factors and present these factors to their respected receptor (i.e. TGF-β, IGF-1, FGF, VEGF) (Kjaer, 2004). The ECM can also release growth factors that is dependent on the level of mechanical stimulation (Kjaer, 2004). These growth factors will serve as transcription

25

factors and are responsible for the upregulation of collagen genes. Afterwards, translation of

procollagen will take place in the endoplasmic reticulum of the fibroblast. Then the alpha

chains are folded and procollagen will go through a series of posttranslational modifications

before it is stable. The assembling of procollagen, conversion to collagen, and cross-linking of

collagen fibrils are all major steps that finalize collagen processing. Collagen degradation

involves specializes proteases known as matrix metalloproteinases (MMP) and will be

discussed later in this section.

Glycoproteins are another population of proteins in the ECM that are made up of an

oligosaccharide chain and polypeptide side-chains. Fibronectin is one of the most researched

glycoproteins in the ECM that is abundant in skeletal muscle. Fibronectin is a large (440

kDa), fibril, adhesive glycoprotein that has a soluble, insoluble, and cell surface form.

Fibronectin is responsible for binding to collagen as well as other important ECM proteins to

assist in cell adhesion and migration (Kjaer, 2004; Mecham, 2011). More specifically,

fibronectin will bind with collagen type I and III between residue 775 and 776 (Kleinman,

Martin, & Fishman, 1979). This is important in regards to activated satellite cells that will

need to migrate and interact with other cell types. Fibronectin will bind to integrins located on

ECM proteins to activate several signaling pathways. It is evident that fibronectin is involved

with the regenerative process because of its high affinity for denatured collagens (Jilek &

Hörmann, 1978). Fibronectin is also classified as a fibrillogenesis organizer which is

important process in ECM remodeling. Assembly of collagen fibrils with fibronectin require

interactions with integrins and other collagen fibrils (Kadler, Hill, & Canty-Laird, 2008; Mao

& Schwarzbauer, 2005). It has been demonstrated that the blocking of integrins on fibronectin

will inhibit collagen fibril assembly.

The ECM in skeletal muscle is also comprised with several proteoglycans (PG) that have many distinct functions. PGs can be described as a specialized class of glycoproteins that are heavily glycosylated. All PGs are carbohydrate-rich soluble polyanions that are attached to a protein and glycosaminoglycan (GAG) chain (Scott, 1990). Glycoaminoglycans (GAGs) are long branched heteropolisacchrides that have repeating dissachaarides units with one or both sugars containing a sulfate group. The rigidity in GAGs structure assist in structural integrity of the ECM while allowing cell migration to take place. GAGs are highly negative molecules that bind and organize water molecules while repelling other negative molecules. This property of GAG allows lubricating fluid in joints. The most noted PGs that have been discovered in muscle are decorin, biglycan, and versican. One of the major roles of PGs in the ECM is to link collagen fibrils (Scott, 1990).

Decorin is a small leucine rich proteoglycan (SLRP) named after its ability to decorate the collagen fibers (Mecham, 2011). Its major functions involve the assembly of collagen fibrils and the protection of the collagen from collagenases. Specifically, decorin works as a steric barrier that will prevent collagenase from accessing their cleavage site in most scenarios (Mecham, 2011). A reduction of decorin in tendons leads to larger diameter collagen fibrils and structurally abnormal fibrils (Ameye et al., 2002; Danielson et al., 1997). Decorin will bind and interact with fibril collagens and inhibit cell growth. The deletion of decorin slows bone growth and possibly skeletal muscle growth (Xu et al., 1998). Decorin can also bind with growth factors that regulate ECM proteins through binding with cell surface receptors. In addition, decorin signaling will lead to intracellular signaling (Mecham, 2011). Decorin has been classified as an antifibrotic reagent because it will bind and inactivate TGF-β (Kjaer, 2004). MMPs will cleave decorin when bound to TGF-β to activate TGF-β activity. Decorin

27

works synergistically with TGF-β to inhibit myoblast differentiation and modulate myoblast proliferation (Mecham, 2011). Decorin can also interact with IGF-1 and myostatin (Miura et al., 2006).

ECM Regulation

As mentioned earlier, the extracellular matrix is very complex because it is composed of several different proteins that are involved with several processes that assist in wound healing and repair. As such, the ECM is tightly regulated by several factors including mechanical stress, inflammatory proteins, growth factors, and specialized proteases. The following cytokines are secreted by fibroblasts and other cells to regulate collagen turnover: IL-1α,β, IL-6, and TNF-α. IL-1 is pro-inflammatory cytokine that has been implicated as an activator of MMPs to degrade collagen synthesis (Unemori et al., 1994). IL-1β is secreted by fibroblast upon mechanical loading to the tissue (Shimizu et al., 1994). IL-1β can also stimulate other signals involved with collagen turnover including MMP-1, MMP-3, IL-6, and COX-2 (Tsuzaki et al., 2003). It has been suggested that inflammatory cytokines may also regulate ECM proteins through tissue inhibitors of matrix metalloproteinases (TIMPs) (Y. Y. Li, McTiernan, & Feldman, 1999). Li and colleagues have found that stimulation of IL-1β will increase TIMP-1 and suppress TIMP-3 mRNA expression and proteins in cardiac myocytes (Y. Y. Li et al., 1999).

IL-6 is a pleiotropic cytokine that also promotes collagen degradation. Fibroblast cells will secrete IL-6 during tension to muscle and tendons (Kjaer, 2004). It has been suggested that pro-inflammatory cytokines also regulate MMP activity. In osteoblasts stimulated with either IL-1 or IL-6 induced MMP-2, MMP-3, and MMP-13 (Kusano et al., 1998). Interestingly, the

experiments performed by Kusano et al. reported that the increase in MMP mRNA was markedly enhanced by IL-1 but only moderately by IL-6 (Kusano et al., 1998). These results may suggest that regulation of MMPs is cytokine specific. Similar to IL-1 and IL-6, TNF-α is a pro-inflammatory cytokine secreted by macrophages and fibroblast cells that will also promote collagen degradation. It has been reported in cardiac fibroblast that the stimulation of TNF-α will induce MMP-3 activity (Siwik, Chang, & Colucci, 2000). This is supported by Li and colleagues that found TNF-α stimulation will downregulated TIMP-3 activity, an inhibitor of MMPs (Y. Y. Li et al., 1999).

Perhaps more understood than inflammatory regulation of ECM proteins, growth factors are major regulators of ECM turnover and remodeling. TGF-β has been regarded as a master regulator and transcription factor of collagen I and III. TGF-β is secreted by macrophages and platelets that will assist in the regulation of ECM proteins and fibroblast activity. *In vitro* studies have demonstrated fold increases of collagen I and III in response to cardiac fibroblast in media supplemented with TGF-β (Butt & Bishop, 1997; Siwik et al., 2000). TGF-β will upregulate collagen genes transcription via Smad proteins (S. J. Chen et al., 1999; Ge et al., 2012) and can also be upregulated independent of Smad signaling (Hocevar, Brown, & Howe, 1999). TGF-β will also upregulate several other matrix proteins including aggrecan and biglycan (Kjaer, 2004). TGF-β can also stimulate TIMPs that will reduce collagen degradation by inhibiting MMPs. The combination of TGF-β with mechanical loading has been shown to activate other growth factors such as connective growth factor (CTGF). CTGF's role is prominent in wound healing specifically scar formation but is not very well understood skeletal muscle (Leask, Holmes, & Abraham, 2002).

Fibroblast growth factor (FGF) is another essential stimulator of fibroblast activity that are

involved in collagen synthesis and perform other functions vital to ECM remodeling (i.e. fibroblast proliferation) (Harwood, Grant, & Jackson, 1976). Similar to TGF-β, FGF can also be activated by mechanical load and injury (Clarke & Feeback, 1996). It has been theorized that FGF may also play a role in intracellular communication from the conversion of mechanotransduction to biochemical signaling (Kjaer, 2004). Finally, Insulin-like Growth Factor (IGF-1) has been shown to increase collagen synthesis by stimulating fibroblast activity *in vitro* and *in vivo* (Butt & Bishop, 1997; Wilson, Rattray, Thomas, Moreland, & Schulster, 1995). However, IGF-1 itself can become inactivated through MMPs or pro-inflammatory cytokines. Pro-inflammatory cytokines will also increase IGF-BP1 that will bind to IGF-1 and inactivate this growth factor (Samstein et al., 1996).

Another essential regulator of collagen turnover are highly specialized proteases that are referred to as matrix metalloproteinases (MMPs). MMPs were first discovered in tadpoles in 1962 and identified as zinc-dependent endopeptidases that operate as zymogens (inactive enzyme precursor) (Gross & Lapiere, 1962). MMPs are unique proteases that are members of the metzincin group, because they have a Met residue and zinc ion at the active site (Bode, Gomis-Ruth, & Stockler, 1993; Page-McCaw, Ewald, & Werb, 2007; Stocker et al., 1995). The latent form of MMPs will have a peptide (also known as pro-domain) that blocks the active or catalytic site of the protein (Libby & Lee, 2000; Page-McCaw et al., 2007). The pro-domain will need to be cleaved, which can occur autocatalytically or heterocatalytically through the use of other active MMPs (Libby & Lee, 2000). Thus, the latent and active form of MMPs vary in size. There are over 20 known MMPs that degrade collagen and other ECM proteins (Table 1-2) (Page-McCaw et al., 2007). MMPs also participate in a variety of functions that promotes skeletal muscle regeneration including myoblast proliferation,

differentiation, and migration (Carmeli, Moas, Reznick, & Coleman, 2004; Lei, Leong, Smith, & Barton, 2013; Page-McCaw et al., 2007; Schiaffino & Partridge, 2008; Urso, Wang, Zambraski, & Liang, 2012).

MMP Member	Common name/Synonym	Cellular Localization
MMP1	Collagenase-1/ Interstitial collagenase	
MMP8	Collagenase-2/ Neutrophil collagenase	
MMP13	Collagenase-3	
MMP2	Gelatinase A/ 72kDa gelatinase	Secreted
MMP9	Gelatinase B/ 92kDa gelatinase	
MMP12	Macrophage metalloelastase	
MMP7	Matrilysin/ Uterine	
MMP26	Matrilysin-2/ Endometase	
MMP14	MT1-MMP	
MMP15	MT2-MMP	
MMP16	MT3-MMP	TM type I
MMP24	MT5-MMP	
MMP17	MT4-MMP	
MMP25	MT6-MMP/ Leukolysin	
MMP3	Stromelysin-1/ progelatinase	
MMP10	Stromelysin-2	
MMP11	Stromelysin-3	
MMP28	Epilysin	
MMP18	Collagenase 4	Secreted
MMP19	RASI-1	
MMP20	Enamelysin	
MMP27	-	
MMP21	MMP23A	
MMP22	MMP23B	TM type II

Table 1-2. MMPs function, localization and domain structure Adapted from Matrix metalloproteinases (MMPs) and tissue inhibitors of metalloproteinases (TIMPs): Positive and negative regulators in tumor cell adhesion by D. Bourboulia, and W. G. Stetler-Stevenson, 2010, *Seminars in cancer biology, 20,* pp. 161-168. Copyright 2010 by Academic Press.

There have only been a few MMPs identified in skeletal muscle that serve a role in muscle repair and remodeling. Most notably, MMP-2 and MMP-9 have been implicated as essential proteases in the regenerative process, because they are highly expressed upon muscle damage and serve specific functions to promote repair and remodeling (Lei et al., 2013; Schiaffino & Partridge, 2008). Furthermore, they are unique in that they contain fibronectin type 2 repeats in their structure that allow collagen binding which allow these MMPs to release TGF-β from ECM proteins (Page-McCaw et al., 2007; Yu & Stamenkovic, 2000). MMP-2, MMP-7, MMP-9 are also involved with infiltration of inflammatory cells by the cleavage of ligands that are chemoattractants of macrophages and neutrophils (McQuibban et al., 2000; Overall, McQuibban, & Clark-Lewis, 2002). MMP-2 is transiently increased during injury, and is secreted by myoblasts amongst other cell types present in skeletal muscle (Kherif et al., 1999; Schiaffino & Partridge, 2008). Moreover, MMP-2 (Gelatinase-A) is responsible for the degradation of collagen I-V and can also degrade fibronectin, and other ECM proteins (Kherif et al., 1999; Page-McCaw et al., 2007). MMP-2 is constitutively active and its expression will peak at 7 days after muscle injury and will slowly decrease for weeks (Kherif et al., 1999; Lei et al., 2013). It has been reported that MMP-9 will also degrade collagen fibrils, but its regulation and activity suggest a different role than MMP-2. MMP-9 (Gelatinase-B) MMP-9 is secreted and regulated predominately by inflammatory cells and expressed at very low levels until damage occurs in skeletal muscle (Kherif et al., 1999). MMP-9 is highly elevated 24 hours following muscle damage and will return to basal levels around 2 weeks (Kherif et al., 1999). More recently, MMP-13 (Collagenase-3) has been demonstrated to assist in myoblast migration (Lei et al., 2013). MMP-13 is an interstitial collagenase that cleaves collagen I-IV and other ECM proteins (Freije et al., 1994; Leeman, Curran, & Murray, 2002).

MMP-13 can be activated by MMP-2, MMP-3, and MMP-14 (MT1-MMP) and can activate MMP-2 and MMP-9 (Lei et al., 2013). MMP-13 expression is induced 7 days following muscle injury and appears to peak at around 11 days (Lei et al., 2013). MMP-7 is also involved in skeletal muscle regeneration and skeletal muscle hypertrophy. MMP-7 is highly expressed by myoblasts and promotes migration of myoblasts (Caron, Asselin, Morel, & Tremblay, 1999). Other notable MMPs such as MT1-MMP, MMP-3, MMP-24, and MMP-25 have been examined in skeletal muscle due to their regulation of ECM remodeling, but their specific role in the regenerative process has yet to be elucidated (Bernal, Hartung, & Kieseier, 2005).

Specific proteins named for their inhibition of MMPs, Tissue inhibitors of matrix metalloproteinases (TIMPs), have been identified as glycoproteins that have a high affinity for the active region of MMPs. The N-terminal regions of TIMPs bind with the catalytic domain of MMPs to inhibit their activity (Bourboulia & Stetler-Stevenson, 2010). Also, the C-terminal region of TIMPs can interact with MMP-2 and MMP-9's hemopexin domains to stabilize the inhibitor complex (Bourboulia & Stetler-Stevenson, 2010). Four TIMPs have been identified in mammals that can bind with all MMPs, but will have a higher affinity for certain MMPs (Bourboulia & Stetler-Stevenson, 2010; Mecham, 2011; Page-McCaw et al., 2007; Schiaffino & Partridge, 2008). TIMP-1 has been identified to inhibit predominately MMP-1 MMP-3, MMP-7, and MMP-9 (Bourboulia & Stetler-Stevenson, 2010). TIMP-2 has been reported as an inhibitor of MT1-MMP and MMP-2 and is the only current TIMP known to also function as an activator of MMPs (i.e. MMP-2) (Bourboulia & Stetler-Stevenson, 2010; Z. Wang, Juttermann, & Soloway, 2000). It has been reported that TIMP-1 and TIMP-2 activity will increase following muscle damage (Hirata et al., 2003; Koskinen et al., 2001).

Hence, they will be involved in reducing MMP activity at certain time points of muscle regeneration. TIMP-3 and TIMP-4 activity, expression, and function have not been thoroughly examined in skeletal muscle, but their roles in MMP are being examined. Basal gene expression data has reported that TIMP-3 is highly expressed prenatally and will inhibit MMP-2 and MMP-9 (Bourboulia & Stetler-Stevenson, 2010). Whereas TIMP-4 is highly expressed in the brain, heart, and adipocytes and will inhibit MT1-MMP and MMP-2 (Bourboulia & Stetler-Stevenson, 2010). Altogether, the regulation of collagen and other ECM proteins is sophisticated in nature and requires further examination to fully understand aging and pathophysiological disease.

Overview ECM remodeling during muscle damage

After exercise or administration of a myotoxin a cascade of signals will lead to optimal ECM repair and remodeling to best suit mammalian skeletal muscle function. Proteins and cells involved with ECM repair will be activated as early as a few minutes upon myotrauma. In exercise if mechanical load is sufficient, integrins will be activated and work as mechanosensors that will facilitate activation of cellular signaling pathways causing mecanotransduction (Ingber et al., 1994). Mechanical stress imposed on the cells will need to be converted to biochemical signals and it is theorized that FGF is involved with this process (Bishop, Butt, Dawes, & Laurent, 1998). At this point the MMP activation cascade will be induced first by self-activating MT1-MMP (Bonfil & Cher, 2011). The activation of MT1-MMP will assist in the activating the rest of the proMMPs to active MMPs to start degrading collagen and ECM proteins and allowing the migration of mesenchymal cells. Concurrently, Resident inflammatory cells in skeletal muscle along with systemic inflammatory cells that have been successfully recruited and infiltrate the musculature will be activated (see events of

inflammation in skeletal muscle). Certain muscle cells and M1 macrophages will secrete the

pro-inflammatory cytokines IL-6, IL-1, and TNF-α. In respect to ECM turnover, these

cytokines will bind to their receptor and activate intracellular signaling pathway that will

result in collagen degradation through MMP activation and downregulation of TIMPs. How

these pro-inflammatory cytokines specifically activate latent MMPs is still unclear. MMP-2

and MMP-9 will allow the release of growth factors that are bound on ECM proteins that are

involved with myoblast proliferation and collagen synthesis. At the onset of muscle damage,

fibronectin will be upregulated because it is has a high-affinity for denatured collagen and is

involved in early steps of fibrillogenesis and proliferation of cells. MMP-1 will

simultaneously be activated and will play a role in myoblast differentiation, migration, and

collagen degradation (W. Wang, Pan, Murray, Jefferson, & Li, 2009). Furthermore, decorin

will be upregulated to inhibit the myoblast proliferation. The MMPs involved with

differentiation are also directly involved with myoblast migration or indirectly involved by

activating MMPs involved in migration (MMP-9 and MMP-13) (Lo, Dalkara, & Moskowitz,

2003). At about 14 days after muscle damage the remodeling of collagen fibrils will begin

(Sato et al., 2003). Once new collagen is synthesized, Collagen V and XI known as nucleators

will nucleate collagen fibrils for self-assembly (Blaschke, Eikenberry, Hulmes, Galla, &

Bruckner, 2000; Wenstrup et al., 2004). Afterwards, ECM proteins involved with regulating

fibril organization will regulate collagen fibrils. The organization of collagen fibrils including

the interactions and packing of collagens are made possible by fibril-associated collagens with

interrupted triple helix (FACIT) collagens (i.e. Collagen IX, XII, XIV, and XX) (Mecham,

2011). Sevilla and colleagues has implicated that fibronectin is involved with fibril

organization when observing Fibronectin-null mice with altered fibril formation (Sevilla,

Dalecki, & Hocking, 2010). The last documented step of fibrillogenesis is linear and lateral growth that is dictated by ECM regulators. SLRPs and FACITs are predominately responsible for fibril growth (Danielson et al., 1997). Studies involving SLRP deficient and FACIT absent mice have demonstrated that fibril growth is blunted (Ameye et al., 2002; Hemmavanh, Koch, Birk, & Espana, 2013). Thus, the ECM repair and remodeling process is intricate involving several process including inflammatory recruitment, infiltration, collagen biosynthesis, and fibrillogenesis. All of these processes are tightly regulated by growth factors and ECM proteins. Any alterations in expression of these ECM proteins and/or inflammatory cytokines may be detrimental to ECM remodeling.

ECM during aging and obesity

Aging and obesity are two populations with unique metabolic states and are associated with insulin resistance and chronic low grade inflammation. Although roughly a third of the world is currently overweight or obese, and a third of the global population is expected to be 65 or older by 2040, little is known about ECM composition and remodeling in these groups (**CDC**). Moreover, virtually no research study has examined ECM composition and remodeling in the sarcopenic obese sub-population. As mentioned previously, aging is associated with many negative symptoms that cause a deficit in skeletal muscle mass. In regards to the ECM, collagen content appears to much higher than young adults. Brooks and colleagues found a 2-fold increase in hydroxyproline in old mice which is an indicator of collagen content (Wood et al., 2014). Another outcome of aging is a reduction collagen turnover that alters the ECM (Bailey, 2001; Goldspink, Fernandes, Williams, & Wells, 1994). It has been reported in older adults that there is a reduction of collagen turnover and increased fibrosis that may suggest an imbalance in collage turnover. (Avery & Bailey, 2005; Kragstrup

36

et al., 2011). It has also been observed that fibril diameter decreases in older adults

(Nakagawa, Majima, & Nagashima, 1994). This may be due to an upregulation of decorin

which a major regulator of fibril diameter size. It is also known that collagen III is a small

diameter fibril compared to collagen I that has more elastic properties. It may be possible that

older adults will shift from collagen I to III expression. Tissue stiffness has also been

identified in aging individuals (DeGroot et al., 2001). In younger adults that participate in

chronic strength and power training muscle stiffness is a positive outcome from training.

However, in older adults muscle stiffness is also observed. The muscle stiffness observed in

younger adults is beneficial to sport and exercise performance and thus the mechanisms

involved may differ than older adults. Muscle stiffness in older adults occurs from higher

glycation of collagen fibrils (DeGroot et al., 2001). Glycation crosslinks are non-enzymic and

occur when glucose reacts with collagen side-chains that form advanced glycation end

products (AGE). This process will only occur in a low collagen turnover environment and will

cause stiffness that is not functional for movement (Avery & Bailey, 2005, 2006). Other ECM

proteins that play major roles in ECM remodeling such as fibronectin and decorin have not

been thoroughly examined and require more attention. It is also important to mention that

sarcopenia leads to muscle frailty and increased susceptibility to injury. Because ECM is

involved with passive tension and force transmission, it is likely that alterations in the ECM is

at least partially responsible for these conditions in older adults.

There have been a couple reports that have discovered changes an ECM composition

and remodeling in obese individuals as well. Hwang et al. examined an increase ECM gene

expression in human skeletal muscle when increasing plasma lipids through infusion.

Specifically, they found an increase in collagen I-VI, CTGF, fibronectin-1, MMP-2, MMP-11,

MMP-28, and TIMP-1 compared to leaner individuals (Hwang et al., 2010). In confirmation, Berria and colleagues reported an increase in hydroxyproline as well as collagen I and III in human skeletal muscle (Berria et al., 2006). More recently, it has been reported that fibrillogenesis and adipogenesis originate from common mesenchymal progenitors in skeletal muscle (Joe et al., 2010; Uezumi et al., 2011). Both PGFRα and fibroadipogenic cells have the ability to promote fibrosis and increase adipocytes in muscle tissue and have an increase concentration in obese individuals. Thus aging and obese have unique consequences that alter ECM composition and remodeling which may reduce the regenerative capacity and integrity of skeletal muscle tissue. Sarcopenic obesity must be examined to understand how the combination of these metabolic states may influence ECM.

CHAPTER 2

Doctoral dissertation proposal:

EXTRACELLULAR MATRIX REMODELING AND THE
INFLAMMATORY RESPONSE DURING SKELETAL MUSCLE
REGENERATION IN SARCOPENIC OBESE MICE

by

Lemuel Brown

October 19, 2016

SPECIFIC AIMS AND HYPOTHESES

Specific Aim #1. To examine basal markers of regenerative capacity in skeletal muscle in C57BL/6 sarcopenic obese mice.

Experiment #1. Experiment 1 tested the hypothesis that skeletal muscle mass and cross-sectional area is reduced in sarcopenic obese mice. Muscle weight to tibia length and cross-sectional area was measured to examine skeletal muscle mass in the gastrocnemius, tibialis anterior, and soleus.

Experiment #2. Experiment 2 tested the hypothesis that myogenic transcription factors are depressed in sarcopenic obese mice at basal levels. RNA expression of MRFs were measured to examine composition in the gastrocnemius, tibialis anterior, and soleus.

Experiment #3. Experiment 3 tested the hypothesis that inflammatory signaling is reduced in sarcopenic obese mice. Protein and RNA expression of muscle cytokines were measured to examine composition in the gastrocnemius, tibialis anterior, and soleus.

Experiment #4. Experiment 4 tested the hypothesis that ECM promotes are upregulated in sarcopenic obese mice at basal levels. This was completed through examination of RNA expression of collagen I, collagen III, and proteins involved with collagen turnover in the gastrocnemius, tibialis anterior, and soleus.

Specific aim #2. To examine monocytes/neutrophils activity in the muscle in sarcopenic obese mice during muscle regeneration.

Experiment #1 Experiment #1 tested the hypothesis that there is a reduction of adhesion molecules in the tibialis anterior muscle. We induced muscle damage with through a myotoxin injection, bupivacaine. RNA expression of ICAM-1 etc. was examined as an indirect measure of activity.

Experiment #2. Experiment 2 tested the hypothesis that there is a reduction of muscle

cytokines at the onset of muscle regeneration. RNA expression and protein levels of IL-6, TNF-α, STAT3, etc. will be examined as an indirect measure of activity.

Specific aim #3. To examine how sarcopenic obesity alters ECM remodeling during skeletal muscle regeneration.

Experiment #1. Experiment 1 tested the hypothesis that collagen content is greater in sacropenic obese mice. This will be accomplished by examining stains of collagen I and collagen III.

Experiment #2. Experiment 2 tested the hypothesis that ECM proteins and promoters of collagen are blunted in sarcopenic obese mice at the onset of muscle regeneration. The expression of RNA of collagen I, collagen III, fibronectin 1, and TGF-β were examined.

Experiment #3. Experiment 3 tested the hypothesis that MMPs are exacerbated in sarcopenic obese mice at the onset of muscle regeneration as a result of reduced TIMP-1 mRNA abundance. The expression of RNA of MMP-2, MMP-9, TIMP-1 were examined.

WORKING MODEL

The skeletal muscle regeneration process involves the coordination of the inflammatory response, activation of MRFs, and ECM remodeling. Several of these factors will be involved with regulating other aspects within muscle regeneration thus the
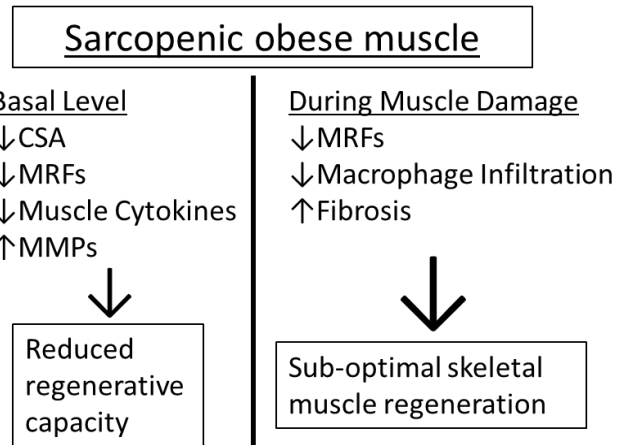
Figure 2-1. Potential alterations in sarcopenic

repair process is tightly regulated. Because skeletal muscle is a coordinated response, changes in signaling in any of these factors may negatively influence the regenerative capacity of skeletal muscle tissue and result in sub-optimal muscle regeneration. For example, the absence of IL-6 will have impaired ECM remodeling and a decrease in myoblast proliferation and differentiation resulting in sub-optimal regeneration.

It has been demonstrated that changes in muscle morphology and metabolic state can alter cellular signaling pathways involved with muscle regeneration. A previous study from our laboratory demonstrated changes in mice on a high-fat diet i.e. reduction of MRFs and cytokines at basal levels. These changes could influence regenerative capacity potential and favor muscle mass loss. Sarcopenia which is the loss of muscle mass due to aging, has a reduced regenerative capacity. The mechanisms involved with sarcopenia are not completely understood, but inflammation, MRF inactivity, and protein turnover has been implicated. As a result fibrosis and sub-optimal muscle regeneration are outcomes following muscle injury in older adults. These two co-morbidities both have sub-optimal regeneration and may work synergistically to negatively impact the regenerative process.

PRELIMINARY STUDIES

The specific aims that were created for this dissertation stem from preliminary data from our lab. In our initial assessment of diet-induced obese mice, there was an increase in muscle weight and tibialis anterior weight relative to tibia length (Figure 2-2) (L. A. Brown et al., 2015). This was not observed in the diet-induced obese mice (Figure 2-2) (L. A. Brown et al., 2015). This data suggested that muscle regeneration was impaired or possibly delayed in obese mice.
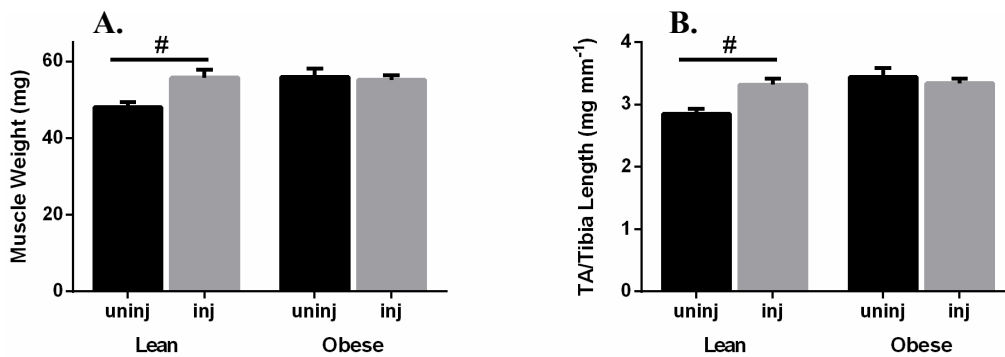
Figure 2-2. Skeletal muscle in 4 month old lean and obese mice 28 days following myotoxin-induced muscle damage. (A) tibialis anterior muscle weight, (B) tibialis anterior muscle weight to tibia length

Following this study, old obese mice were obtained and muscle weights and tibia length were taken from both old 21 days following muscle damage. There was no difference between the injured and uninjured old obese mice (Figure 2-3) (L. A. Brown et al., 2015). Similar to the obese mice, muscle regeneration appeared to be impaired in the old obese mice.
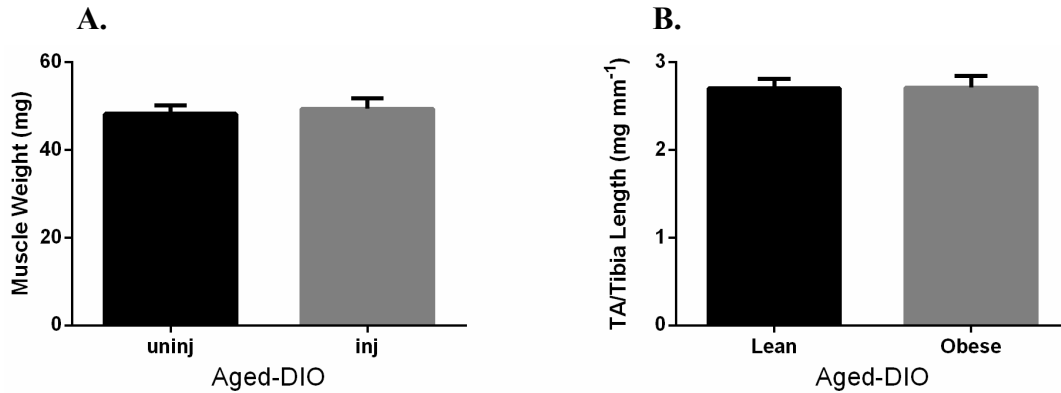
Figure 2-3. Skeletal muscle in 22-24 month old obese mice 21 days following myotoxin-induced muscle damage. (A) tibialis anterior muscle weight, (B) tibialis anterior muscle weight to tibia length. *Abbreviation* DIO = Diet-induced obesity

Inflammation, MRFs, and the ECM were examined to further investigate whether skeletal muscle regeneration was impaired in these populations. The young obese mice had an 80% reduction of IL-6 expression in the TA compared to the young lean mice (Figure 2-4) (Brown et al., 2015).
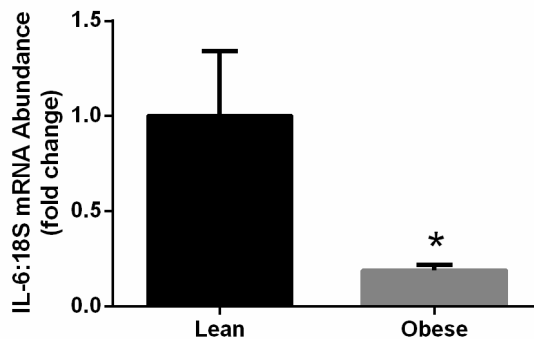
Figure 2-4. IL-6 mRNA abundance in 4 month old lean and obese uninjured mice.

A few days following muscle damage the young obese and lean mice had a similar response for upregulating IL-6 (data not shown). However, western blot analysis showed a blunted response of STAT3 in obese mice (Figure 2-5) (L. A. Brown et al., 2015).
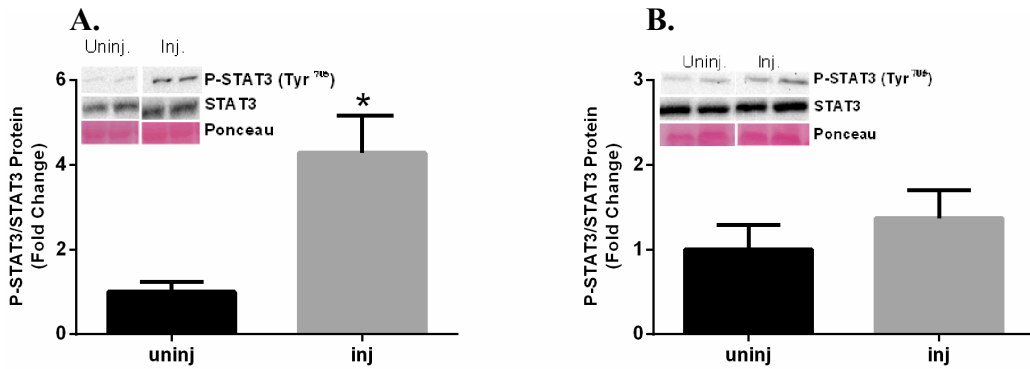
Figure 2-5. P-STAT3/STAT3 protein in 4 month old lean and obese mice 3 days following myotoxin-induced muscle damage. (A) lean, (B) obese.

TNF-α expression was altered in obese mice as well. Upon skeletal muscle damage, TNF-α expression is upregulated because it is needed for skeletal muscle regeneration. Upregulation of TNF-α was blunted in obese mice 3 days following myotoxin-induced muscle damage (Figure 2-6) (L. A. Brown et al., 2015).
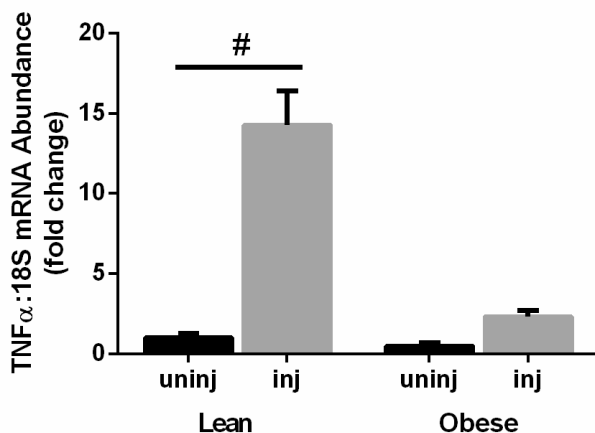
Figure 2-6. TNF-α mRNA abundance in 4 month old lean and obese mice 3 days following myotoxin-induced muscle damage.

Our lab also observed changes with basal MRF expression in young obese mice. Obese mice had more than a 20% reduction of MyoD expression compared to the lean control (Figure 2-7) (L. A. Brown et al., 2015). However, there were no differences found in the obese group three days following injury (data not shown).

45
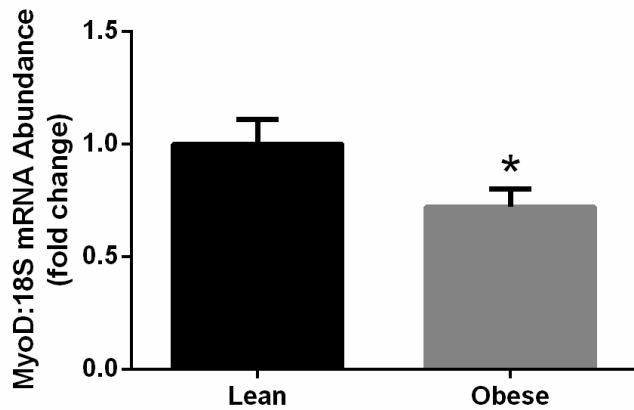
Figure 2-7. MyoD mRNA abundance in 4 month old lean and obese uninjured mice.

MyoD expression was also examined in the aged lean and obese mice three days following

muscle damage. There was a trend for a reduction of MyoD expression in the obese group

(Figure 2-8). It is important to note that the sample size was not sufficient in this experiment

(n = 3).
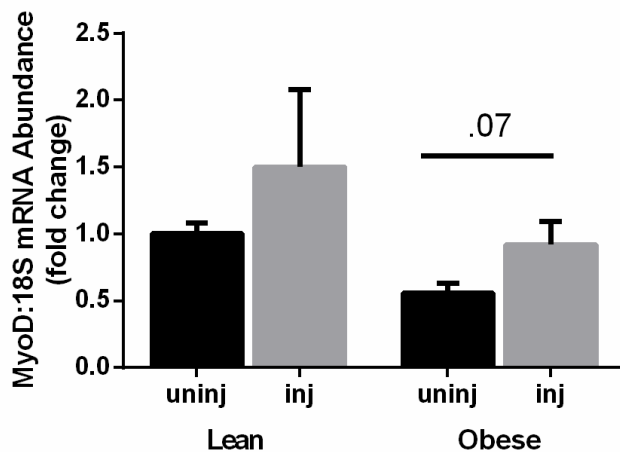
Figure 2-8. MyoD mRNA abundance in 22-24 month old lean and obese mice 3 days
following myotoxin-induced muscle damage.

To further investigate if muscle regeneration was altered in young obese mice, ECM

composition was examined. Three days following muscle damage, fibronectin is upregulated

2-5 fold greater compared to the control mice. Also, the obese mice had a significantly higher

expression of fibronectin compared to the lean mice (Figure 2-9).
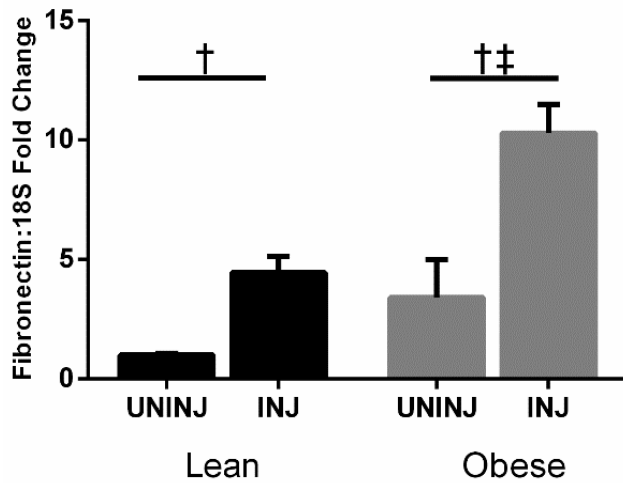
Figure 2-9. Fibronectin mRNA abundance in 3 month old lean and obese mice 3 days following myotoxin-induced muscle damage.

We then examined the collagen ratio, which has been used as a measure of fibrosis. Collagen III/I was much lower in the young obese mice compared to the young lean mice (Figure 2-9). Three days following injury the collagen III/I was reduced in lean mice, but not in obese mice (Figure 2-10).
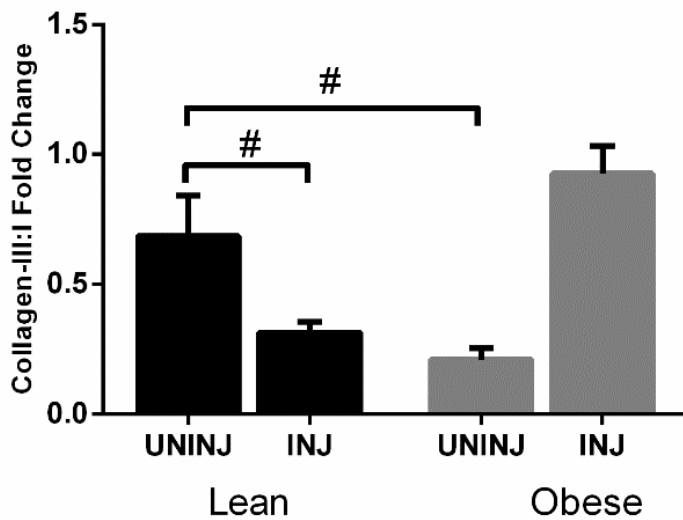
Figure 2-10. Collagen III/I mRNA abundance in 3 month old lean and obese mice 3 days following myotoxin-induced muscle damage.

RESEARCH DESIGN AND METHODS

Specific Aim #1. To examine basal markers of regenerative capacity in skeletal muscle in C57BL/6 sarcopenic obese mice.

Rationale. Sarcopenic obesity is a metabolic syndrome in older adults that have a BMI ≥ 30 and leads to many diseases. Roughly one third of older adults are classified as obese and this population is growing. The major symptoms involved with sarcopenic obese individuals are a loss of skeletal muscle due to aging and systemic chronic low-grade inflammation. The mechanisms that are involved with a loss of skeletal muscle has been examined in aging studies, but has not been explored in sarcopenic obesity. Some of the mechanisms involved with the loss of skeletal muscle mass are related to the regenerative capacity of skeletal muscle. The inflammatory response, MRFs, and ECM composition are involved with muscle regeneration and the reduction and/or chronic expression at basal levels and can negatively impact muscle metabolism and repair. Previous work in our lab has demonstrated that expression of inflammatory cytokines are reduced in obese individuals. This will contribute to altered signaling in skeletal muscle. The expression of these regulators involved with regenerative capacity of skeletal muscle are poorly understood in sarcopenic obese skeletal muscle and needs to be explored. **The overall objective of these experiments is to characterize sarcopenic obese skeletal muscle.**

Experimental design for specific aim #1. This aim will examine muscle morphology, inflammation, MRF's, and ECM in 4 uninjured animal groups 1) young lean, 2) young obese, 3) aged lean, 4) aged obese. Experiment #1 will examine TA weight relative to tibia length and bodyweight in 3-4 mo-old and 22-24 mo-old male mice. In addition, CSA will be measured an all animal groups. If feasible, CSA fiber size distribution and other histological

markers will be measured in all animal groups. Experiment #2 will examine the MRFs MyoD and myogenin in TA, gastrocnemius, plantaris, and soleus of all animal groups. Experiment #3 will examine cytokines IL-6, TNF-α, STAT3, NF-κB in TA, gastrocnemius, plantaris, and soleus of all animal groups. Experiment #4 will examine ECM targets collagen I, collagen III, TGF-β, and fibronectin in TA, gastrocnemius, plantaris, and soleus of all animal groups. If feasible decorin and other ECM proteins will be measured.

Animal treatment groups related to specific aim #1.

Experiment #1-4.

These experiments examined basal markers of regenerative capacity in sarcopenic obese skeletal muscle in C57BL/6 mice.

Animals. C57BL/6 male mice (Jackson Laboratories) were housed in the University of Arkansas' animal facility. The room was maintained on a 12:12 light:dark cycle with the light period starting at 0700. Mice were randomly assigned to either standard rodent chow or high fat diet (HFD, 60% kcals fat, Research Diets, New Brunswick, New Jersey). Mice had ad libitum access to both food and water. All mice were sacrificed at 3-4 mo-old or 22-24 mo-old (Table 2-1). All animal experimentation was approved by the University of Arkansas' Institutional Animal Care and Use Committee.

Table 2-1. Animal treatment groups for specific aim #1

Diet	Age	n
Lean	3-4 mo-old	8-12
HFD	3-4 mo-old	8-12
Lean	22-24 mo-old	8-12
HFD	22-24 mo-old	8-12

Methodology related to specific aim #1.

PBS Injection. At twelve wks of age, phosphate buffered solution (PBS) injections were performed as previously described (Tyrone A Washington et al., 2013). Mice were anesthetized with a subcutaneous injection of a cocktail containing ketamine hydrochloride (45 mg/kg body weight), xylazine (3 mg/kg body weight), and acepromazine (1 mg/kg body weight). Roughly 0.03 ml of PBS were injected in the left and right tibialis anterior muscles (TA). A 25-gauge, 5/8 (0.5 x 16 mm) needle was inserted along the longitudinal axis of the muscle, and the PBS was injected slowly as the needle was withdrawn.

Muscle and Tibia Extraction. Muscle and tibia extractions was performed as previously described (Tyrone A Washington et al., 2013; T. A. Washington et al., 2011). Three and 21 days post-injection, the TA and tibias was extracted from each mouse. Mice were anesthetized with a subcutaneous injection of a cocktail containing ketamine hydrochloride (90 mg/kg body weight), xylazine (3 mg/kg body weight), and acepromazine (1 mg/kg body weight). The left TA was frozen in liquid nitrogen and stored at -80°C for protein and gene expression analysis, the right TA was cut at the midbelly, mounted in optimum cutting temperature compound (OCT), and dropped in liquid nitrogen cooled isopentane. Once frozen, samples were be stored at -80°C for morphological analysis. The tibias were removed and measured with a plastic caliper (VWR, Radnor, PA, USA). Tibia measurements were utilized to normalize muscle weights to an estimate of total body size.

Tibialis Anterior Morphology. Cross-sectional area (CSA) was performed as previously described (T. A. Washington et al., 2011). Each TA muscle section (n = 8-12) was stained with hematoxylin and eosin, imaged with a Nikon camera (Sight DS-Vi1) mounted on an Olympus CKX41 inverted microscope at 20X magnification (Olympus), and analyzed with

Nikon NIS Elements BR software package (Nikon). Each fiber was traced and the number of

pixels traced will be calibrated to obtain CSA of the muscle. All fibers in the cross section

images were quantified unless the sarcolemma was not intact. Approximately 100 fibers were

traced per sample.

Western blotting. Muscle tissues were homogenized as previously described (N. P. Greene et

al., 2015; Perry Jr et al., 2016). Briefly, tissue were homogenized with glass homogenizers in

0.2 mL of complete protein loading buffer containing 5- mM Trsi-HCL, pH 6.8, 1% sodium

dodecyl sulfate (SDS), 10% glycerol, 20 mM dithiothreitol, 127 mM 2-mercaptoethanol, and

0.01% bromophenol blue, supplemented with protease inhibitors (Roche, Nutley, NJ) and

phosphatase inhibitors (Sigma-Aldrich, St. Louis, MO). The muscle homogenates (10-30 μg)

were transferred to microfuge tubes, heated for 5 min at 95°C, and centrifuges in a microfuge

for 5 min at 13,000 RPM at room temperature. Protein concentrations of each sample were

determined using the RC/DC assay (Bio-Rad, Hercules, CA), and 40 μg of protein were

resolved on an 8-15% SDS-polyacrylamide gel (SDS-PAGE). The gel was transferred to a to

polyvinylidene difluoride (PVDF) membrane. Membranes were stained with Ponceau S before

blotting to verify equal loading of the gels. Membranes were incubated in a 5% nonfat dried

milk dissolved with Tris-buffered saline with tween (TBS-T). Primary antibodies for NF-κB,

P-Stat3 (Tyr705), and Stat3 (Cell Signaling Technologies, Danvers, MA) were diluted 1:1,000

to 1:5,000 in 5% milk, in TBST, and incubated at 4°C overnight. Anti-rabbit monoclonal

secondary antibodies (Cell Signaling Technologies, Danvers, MA) were diluted 1:2,000 to

1:5,000 in 5% milk, in TBST, and then incubated at room temperature for one hour. Enhanced

Chemiluminescence (ECL) were performed using Fluorochem M imager (Protein Simple,

Santa Clara, California) to visualize antibody-antigen interaction. Blotting images were

quantified by densitometry using AlphaView software (Protein Simple). The Ponceau-stained

membranes were digitally scanned, and the 45-kDa actin bands will be quantified by densitometry and used as a protein loading correction factor for each lane.

RNA Isolation, cDNA Synthesis, quantitative RT-PCR. The following procedures were completed as previously described (N. P. Greene et al., 2015; Tyrone A Washington et al., 2013). RNA was extracted with Trizol reagent (Life Technologies, Grand Island, NY, USA). TA muscles were homogenized in Trizol. Total RNA was isolated, DNase treated and concentration and purity was determined by fluorometry using the Qubit 2.0 (Life Technologies). cDNA was reverse transcribed from 1 μg of total RNA using the Superscript Vilo cDNA synthesis kit (Life Technologies, Carlsbad, CA, USA). Real-time PCR was performed, and results were analyzed by using the StepOne Real-Time PCR system (Life Technologies, Applied Biosystems, Grand Island, NY). cDNA was amplified in a 25 μL reaction containing appropriate primer pairs and TaqMan Universal Mastermix (Applied Biosystems). Samples were be incubated at 95°C for 4 min, followed by 40 cycles of denaturation, annealing and extension at 95°C, 55°C and 72°C respectively. TaqMan fluorescence was measured at the end of the extension step each cycle. Fluorescence labeled probes for MyoD (FAM dye), myogenin (FAM dye), TNFα (FAM dye), IL-6 (FAM dye), ICAM-1 (FAM dye), TGF-β (FAM dye), collagen I (FAM dye), collagen III (FAM dye), fibronectin (FAM dye), MMP-2 (FAM dye), MMP-9 (FAM dye), TIMP-1 (FAM dye), and 18S (VIC dye) were purchased from Applied Biosystems and quantified with TaqMan Universal mastermix. Cycle threshold (Ct) was determined, and the ΔCt value was calculated as the difference between the Ct value and the 18s Ct value. Final quantification of gene expression was calculated using the ΔΔCT method Ct = [ΔCt(calibrator) − ΔCt(sample)]. Relative quantification was calculated as 20-ΔΔCt. Melt curve analysis was performed at the end of the PCR run to verify no primer dimers were formed.

Statistical analysis. All data was analyzed using Statistical Package for the Social Sciences

(SPSS version 22.0, Armonk, NY). Results were reported as mean ± SEM. A two-way ANOVA

was performed to analyze main effects of treatment and diet and if there were any interactions

between the dependent variables. When a significant interaction was detected, differences among

individual means were assessed with Fisher's LSD post-hoc analysis. Statistical significance was

set at $P \leq 0.05$. The $\chi2$ analysis was used to detect differences in the proportion of small fibers ($<$

$400\,\mu m^2$) and large fibers ($> 900\,\mu m^2$) between treatment groups.

Anticipated results.

Hypothesis #1. Skeletal muscle mass and cross-sectional area will be reduced in sarcopenic obese mice as measured by relative weight data and CSA size.

Hypothesis #2. Myogenic regulatory factors will be reduced in sarcopenic obese mice, as measured by mRNA abundance.

Hypothesis #3. Inflammatory cytokines will be reduced in sarcopenic obese mice, as measured by mRNA abundance and protein.

Hypothesis #4. ECM proteins will be reduced in sarcopenic obese mice, as measured by mRNA abundance.

Alternative hypotheses.

It is possible that there will be no changes in mRNA abundance and protein of sarcopenic obese mice compared to the lean and young control mice. Although it has been observed that aging and obesity alter inflammation, MRFs, and ECM; the two co-morbidities may counteract each other.

Study Limitations.

The study uses C57BL/6 mice that are 22-24 month old mice, which would be equivalent to 63-69 years old in humans. Moreover, to induce obesity mice are given a diet that consists of 60% fat to mimic obese humans. Although these methods are used to create a sarcopenic obese model in mice these results cannot be directly applied to humans because of the slight differences in muscle morphology, gene expression, and protein levels.

Specific aim #2. To examine monocytes/neutrophils activity in the muscle in sarcopenic obese mice during muscle regeneration.

Rationale. Aging, obesity, and muscle pathologies are associated with systemic low-grade inflammation. It has been reported that some muscle pathologies also exhibit chronic inflammation in skeletal muscle. It was under the assumption in the literature that aging and obesity would exhibit chronic inflammation in skeletal muscle as well. Our lab has recently demonstrated that inflammatory cytokines are blunted in obese mice at the onset of muscle regeneration. In support of our findings, a study examining obese mice found a reduction of macrophages in obese mice following skeletal muscle injury. Thus, the reduction of macrophages and secreted cytokines may be due to reduced monocyte recruitment and infiltration to the muscle. Adhesion molecules are essential to macrophage infiltration from the blood into the skeletal muscle following muscle injury. It is possible that the reduced expression of adhesion molecules may result in less infiltration of macrophages and result in reduced cytokine expression. Moreover, it has not yet been examined if sarcopenic obese skeletal muscle has a reduction of cytokines and macrophage infiltration following muscle damage. **The overall purpose of this aim is to determine whether cytokines in skeletal muscle is altered in sarcopenic obese mice at the onset of skeletal muscle regeneration and if these changes are associated with phagocyte infiltration**

Experimental design for Specific Aim #2.

This aim examined macrophage activity as defined by macrophage recruitment and secretion of cytokines. Macrophage activity will be examined in 8 animal groups (Table 2-2, Table 2-3). Experiment #1 examined the adhesion molecule ICAM-1 in TA of all animal groups. Experiment #3 examined ECM targets inflammatory cytokines IL-6 and TNF-α and intracellular signaling of IL-6 and TNF-α.

Animal treatment groups related to specific aim #2.

Experiment #1-3.

These experiments examined macrophage activity in the TA of sarcopenic obese mice during muscle regeneration.

Animals. The same mice mentioned in specific aim #1 were randomly assigned in 8 groups (Table 2-2, Table 2-3). During the myotoxin-induced muscle damage protocol, each mouse was administered bupivacaine (experimental) or PBS (control) in the TA. TA extraction will take place at either 3 or 21 days following injection. All animal experimentation were approved by the University of Arkansas' Institutional Animal Care and Use Committee.

Table 2-2. Young animal treatment groups for specific aim #2-3

Timepoint	Diet	Treatment	n
3 Day	Lean	Uninjured	5-6
3 Day	Lean	Injured	5-6
3 Day	HFD	Uninjured	5-8
3 Day	HFD	Injured	5-8
21 Day	Lean	Uninjured	5-6
21 Day	Lean	Injured	5-6
21 Day	HFD	Uninjured	5-8
21 Day	HFD	Injured	5-8

Table 2-3. Old animal treatment groups for specific aim #2-3

Timepoint	Diet	Treatment	n
3 Day	Lean	Uninjured	7-8
3 Day	Lean	Injured	7-8
3 Day	HFD	Uninjured	5-6
3 Day	HFD	Injured	5-6
21 Day	Lean	Uninjured	7-8
21 Day	Lean	Injured	7-8
21 Day	HFD	Uninjured	5-6
21 Day	HFD	Injured	5-6

Methodology related to specific aim #2.

Bupivaine Injection. At twelve wks of age, bupivacaine (Hospira, Lake Forest, IL) injections were performed as previously described (L. A. Brown et al., 2015; T. A. Washington et al., 2011). Mice were anesthetized with a subcutaneous injection of a cocktail containing ketamine hydrochloride (45 mg/kg body weight), xylazine (3 mg/kg body weight), and acepromazine (1 mg/kg body weight). Muscle damage were induced by injecting 0.03ml of 0.75% bupivacaine (Marcaine) in the left and right tibialis anterior muscles (TA). A 25-gauge, 5/8 (0.5 x 16 mm) needle was inserted along the longitudinal axis of the muscle, and the bupivacaine was injected slowly as the needle was withdrawn. The control group was injected with 0.03 ml of PBS.

Muscle and Tibia Extraction. Muscle and tibia extractions was performed as previously described (Tyrone A Washington et al., 2013; T. A. Washington et al., 2011). Three and 21 days post-injection, the TA and tibias was extracted from each mouse. Mice were anesthetized with a subcutaneous injection of a cocktail containing ketamine hydrochloride (90 mg/kg body weight), xylazine (3 mg/kg body weight), and acepromazine (1 mg/kg body weight). The left TA was frozen in liquid nitrogen and stored at -80°C for protein and gene expression analysis, the right TA was cut at the midbelly, mounted in optimum cutting temperature compound (OCT), and dropped in liquid nitrogen cooled isopentane. Once frozen, samples were be stored at -80°C for morphological analysis. The tibias were removed and measured with a plastic caliper (VWR, Radnor, PA, USA). Tibia measurements were utilized to normalize muscle weights to an estimate of total body size.

Tibialis Anterior Morphology. Cross-sectional area (CSA) was performed as previously described (Washington et al., 2011). Each TA muscle section (n = 8-12) was stained with hematoxylin and eosin, imaged with a Nikon camera (Sight DS-Vi1) mounted on an Olympus CKX41 inverted microscope at 20X magnification (Olympus), and analyzed with Nikon NIS

Elements BR software package (Nikon). Each fiber was traced and the number of pixels traced will be calibrated to obtain CSA of the muscle. All fibers in the cross section images were quantified unless the sarcolemma was not intact. Approximately 100 fibers were traced per sample.

Western Blotting. Muscle tissues were homogenized as previously described (N. P. Greene et al., 2015; Perry Jr et al., 2016).Briefly, tissue were homogenized with glass homogenizers in 0.2 mL of complete protein loading buffer containing 5- mM Trsi-HCL, pH 6.8, 1% sodium dodecyl sulfate (SDS), 10% glycerol, 20 mM dithiothreitol, 127 mM 2-mercaptoethanol, and 0.01% bromophenol blue, supplemented with protease inhibitors (Roche, Nutley, NJ) and phosphatase inhibitors (Sigma-Aldrich, St. Louis, MO). The muscle homogenates (10-30 µg) were transferred to microfuge tubes, heated for 5 min at 95°C, and centrifuges in a microfuge for 5 min at 13,000 RPM at room temperature. Protein concentrations of each sample were determined using the RC/DC assay (Bio-Rad, Hercules, CA), and 40 µg of protein were resolved on an 8-15% SDS-polyacrylamide gel (SDS-PAGE). The gel was transferred to a to polyvinylidene difluoride (PVDF) membrane. Membranes were stained with Ponceau S before blotting to verify equal loading of the gels. Membranes were incubated in a 5% nonfat dried milk dissolved with Tris-buffered saline with tween (TBS-T). Primary antibodies for NF-κB, P-Stat3 (Tyr705), and Stat3 (Cell Signaling Technologies, Danvers, MA) were diluted 1:1,000 to 1:5,000 in 5% milk, in TBST, and incubated at 4°C overnight. Anti-rabbit monoclonal secondary antibodies (Cell Signaling Technologies, Danvers, MA) were diluted 1:2,000 to 1:5,000 in 5% milk, in TBST, and then incubated at room temperature for one hour. Enhanced Chemiluminescence (ECL) were performed using Fluorochem M imager (Protein Simple, Santa Clara, California) to visualize antibody-antigen interaction. Blotting images were quantified by densitometry using AlphaView software (Protein Simple). The Ponceau-stained

membranes were digitally scanned, and the 45-kDa actin bands will be quantified by densitometry and used as a protein loading correction factor for each lane.

RNA Isolation, cDNA synthesis, and quantitative RT-PCR. The following procedures were completed as previously described (N. P. Greene et al., 2015; Nicholas P Greene et al., 2014; Tyrone A Washington et al., 2013). RNA was extracted with Trizol reagent (Life Technologies, Grand Island, NY, USA). TA muscles were homogenized in Trizol. Total RNA was isolated, DNase treated and concentration and purity was determined by fluorometry using the Qubit 2.0 (Life Technologies). cDNA was reverse transcribed from 1 µg of total RNA using the Superscript Vilo cDNA synthesis kit (Life Technologies, Carlsbad, CA, USA). Real-time PCR was performed, and results were analyzed by using the StepOne Real-Time PCR system (Life Technologies, Applied Biosystems, Grand Island, NY). cDNA was amplified in a 25 µL reaction containing appropriate primer pairs and TaqMan Universal Mastermix (Applied Biosystems). Samples were be incubated at 95°C for 4 min, followed by 40 cycles of denaturation, annealing and extension at 95°C, 55°C and 72°C respectively. TaqMan fluorescence was measured at the end of the extension step each cycle. Fluorescence labeled probes for TNF-α (FAM dye), IL-6 (FAM dye), ICAM-1 (FAM dye), and 18S (VIC dye) were purchased from Applied Biosystems and quantified with TaqMan Universal mastermix. Cycle threshold (Ct) was determined, and the ΔCt value was calculated as the difference between the Ct value and the 18s Ct value. Final quantification of gene expression will be calculated using the ΔΔCT method Ct = [ΔCt(calibrator) – ΔCt(sample)]. Relative quantification will be calculated as 20-ΔΔCt. Melt curve analysis was performed at the end of the PCR run to verify no primer dimers were formed.

Statistical analysis. All data was analyzed using Statistical Package for the Social Sciences (SPSS version 22.0, Armonk, NY). Results was reported as mean ± SEM. A two-way ANOVA was performed to analyze main effects of treatment and diet and if there were any interactions between the dependent variables for 3 and 21 days post-bupivacaine injection. When a significant interaction is detected, differences among individual means was assessed with Fisher's LSD post-hoc analysis. The $\chi 2$ analysis was used to detect differences in the proportion of small fibers ($< 400\,\mu m2$) and large fibers ($> 900\,\mu m2$) between treatment groups. Statistical significance will be set at $P \leq 0.05$.

Anticipated results.

Hypothesis #1. There will be a reduction in macrophage infiltration in sarcopenic obese muscle at the onset of skeletal muscle regeneration, as measured by ICAM-1 mRNA abundance.

Hypothesis #2. There will be a reduction in cytokines in sarcopenic obese skeletal muscle at the onset of muscle regeneration, as measured by IL-6, TNF-α mRNA abundance and STAT3, NF-κB protein.

Alternative hypotheses.

It is possible that there will be no changes in mRNA abundance and protein of sarcopenic obese mice compared to the lean and young control mice. Although it has been observed that aging and obesity are associated with systemic low-grade inflammation these changes to inflammatory signaling may not exist within skeletal muscle during regeneration.

Study limitations.

This study uses myotoxin-induced muscle damage that mimics traumatic eccentric damage

observed in exercise. Because these methods are used to isolate the regenerative process in mice these results cannot be directly compared to studies involving exercise models because of the lack of mechanical movement and involvement of whole-body metabolism. Moreover, the experimental design in this study does not distinguish between resident and non-resident macrophages, thus the origin of macrophages discovered in the TA cannot be definitely stated.

Specific aim #3. To examine how sarcopenic obesity alters ECM remodeling during skeletal muscle regeneration

Rationale. An important step involved with skeletal muscle regeneration is ECM remodeling. The ECM will interact with muscle cells and release growth factors necessary to promote regeneration. Moreover, resident macrophages are localized within the ECM. Alterations in ECM and its regulation have been reported in disease and traumatic (type II) injury during muscle damage. As a result optimal muscle regeneration was not achieved in these individuals. Previously, our lab demonstrated that skeletal muscle in obese mice regenerates sub-optimally. In support, preliminary data examining obese mice 3 days following muscle damage had an increase in collagen III/I, which is an indicator of fibrosis. It is known in the literature that fibrosis is one of the negative outcomes of regenerating muscle fibers in aging mice. The ECM remodeling process in sarcopenic obese mice is not known and needs to be further explored. **The purpose of this aim was to examine how sarcopenic obesity alters ECM remodeling during skeletal muscle regeneration.**

Experimental design for specific aim #3.

This aim examined components of the ECM and its regulation both to understand how sarcopenic obesity may alter ECM remodeling. Experiment #1 visually examined ECM morphology by collagen I and collagen III staining in the TA cross-section. Experiment #2 examined ECM proteins collagen I, collagen III, and fibronectin in the TA of all animal groups. Experiment #3 examined the regulation of ECM as measured by TGF-β, MMP-2, MMP-9 and TIMP-1.

Methodology related to specific aim #3.

Experiment #1-3.

These experiments examined collagen and its regulation in sarcopenic obese mice during muscle regeneration.

Animals. Tissues were used from the animal experiments described in specific aim #2 (See Table 2-2, Table 2-3).

Immunofluorescence. Immunostaining for collagen I and III were performed as previously described (Kim, Kasukonis, Brown, Washington, & Wolchok, 2016). Each TA muscle cross-section was cut at 10 μm (n = 4-7) using the cryostat and placed on a slide. First, slides were permeabilized in 0.1% 10X Triton then rinsed in PBS. Then slides were blocked in PBS with 4% goat serum and 0.05% sodium azide for 30 minutes at room temperature. Afterwards, slides were incubated on primary antibodies for 3 hours at room temperature; rabbit-polyclonal anti-collagen I IgG (1:500, Sigma Aldrich, St. Louis, MO), rabbit-polyclonal anti-collagen III (1:500, Sigma Aldrich, St. Louis, MO). Slides were then washed with PBS and incubated in Alexa Fluor 488 (1:500, Life Technologies Carlsbad, CA). Images of the slide were acquired with a Nikon camera (Sight DS-Vi1) mounted on an Olympus CKX41 inverted microscope at 20X magnification (Olympus), and analyzed with MATLAB. Total ECM area was determined by dividing the number of green pixels by the total number of pixels in the image.

RNA Isolation, cDNA synthesis, and quantitative RT-PCR. The following procedures were completed as previously described (Nicholas P Greene et al., 2014; Tyrone A Washington et al., 2013). RNA was extracted with Trizol reagent (Life Technologies, Grand Island, NY, USA). TA muscles were homogenized in Trizol. Total RNA was isolated, DNase treated and concentration and purity was determined by fluorometry using the Qubit 2.0 (Life Technologies). cDNA was reverse transcribed from 1 μg of total RNA using the Superscript Vilo cDNA synthesis kit (Life Technologies, Carlsbad, CA, USA). Real-time PCR was performed, and results were analyzed by using the StepOne Real-Time PCR system (Life Technologies, Applied Biosystems, Grand Island, NY). cDNA was amplified in a 25 μL reaction containing appropriate primer pairs and TaqMan Universal Mastermix (Applied Biosystems). Samples were be incubated at 95°C for 4 min, followed by 40 cycles of

denaturation, annealing and extension at 95°C, 55°C and 72°C respectively. TaqMan

fluorescence was measured at the end of the extension step each cycle. Fluorescence labeled

probes for collagen I (FAM dye), collagen III (FAM dye), fibronectin (FAM dye), TGF-β

(FAM dye), MMP-2 (FAM dye), MMP-9 (FAM dye), TIMP-1 (FAM dye), and 18S (VIC

dye) were purchased from Applied Biosystems and quantified with TaqMan Universal

mastermix. Cycle threshold (Ct) were determined, and the ΔCt value was calculated as the

difference between the Ct value and the 18s Ct value. Final quantification of gene expression

was calculated using the ΔΔCT method Ct = [ΔCt(calibrator) – ΔCt(sample)]. Relative

quantification was calculated as 20-ΔΔCt. Melt curve analysis was performed at the end of

the PCR run to verify no primer dimers were formed

Statistical analysis. All data was analyzed using Statistical Package for the Social Sciences

(SPSS version 22.0, Armonk, NY). Results were reported as mean ± SEM. A two-way ANOVA

was performed to analyze main effects of treatment and diet and if there were any interactions

between the dependent variables for 3 and 21 days post-bupivacaine injection. When a

significant interaction is detected, differences among individual means were assessed with

Fisher's LSD post-hoc analysis. Statistical significance was set at $P \leq 0.05$.

Anticipated results.

Hypothesis #1. Collagen fibrils content will not change in sarcopenic obese mice at the onset of skeletal muscle regeneration as visually inspected by collagen staining.

Hypothesis #2. ECM promoters are blunted in sarcopenic obese mice at the onset of skeletal muscle regeneration, as measured by collagen I, collagen III, TGF-β, and fibronectin mRNA abundance.

Hypothesis #3. MMP mRNA abundance is greater in sarcopenic obese mice at the onset of skeletal muscle regeneration, as measured by MMP-2, MMP-9 and a result of blunted TIMP-1 mRNA abundance.

Alternative hypotheses.

It is possible that there will be no changes in mRNA abundance and protein of sarcopenic obese mice compared to the lean and young control mice. Although it has been observed that aging and obesity are associated with ECM protein and ECM regulation, these changes to the ECM may not exist within the combination of the two co-morbidities during skeletal muscle regeneration.

Study limitations.

This study uses myotoxin-induced muscle damage that mimics traumatic eccentric damage observed in exercise. Because these methods are used to isolate the regenerative process in mice these results cannot be directly compared to studies involving exercise models because of the lack of mechanical movement and involvement of whole-body metabolism.

Chapter 3

Basal level markers of skeletal muscle regenerative capacity are altered in sarcopenic obese mice skeletal muscle

[1,2]Lemuel A. Brown, [1,2]Richard A. Perry, [1,2]Wesley S. Haynie, [2]David E. Lee, [2]Megan E. Rosa, [2]Jacob L. Brown, [2]Nicholas P. Greene, and [1,2]Tyrone A. Washington

[1]Exercise Muscle Biology Laboratory, [2]Human Performance Laboratory, Department of Health, Human Performance and Recreation, University of Arkansas, Fayetteville AR 72701

Running Title: Aged Diet-induced obesity and muscle regeneration

Corresponding author:
Tyrone A. Washington, Ph.D.
University of Arkansas
Department of Health, Human Performance, and Recreation
155 Stadium Dr. HPER 308H
Fayetteville AR 72701

Office Phone: 479-575-6693
Fax: 479-575-5778
tawashin@uark.edu

Abstract

AIM: Currently, in the United States sarcopenic obesity is growing at an alarming rate. This is a major concern because sarcopenic obese individuals are associated with insulin-resistance, chronic low-grade inflammation, and reduced muscle quality and integrity. Previous studies examining either aging or obesity have reported a reduction in cross-sectional area in both groups and have implicated alterations in ECM and inflammatory signaling as a major culprit. It has not been examined if the combination of these two-comorbidities will further reduce muscle mass and regenerative potential. The purpose of this study was to determine how Sarcopenic obesity alters inflammatory signaling and extracellular remodeling in mouse skeletal muscle. **METHODS:** Twenty-four male C57BL6/J mice (4 weeks old) were randomly assigned to either a high fat diet (HFD, 60% fat) or normal chow for either 8 weeks or 21-23 months. At 3-4 months or 22-24 months the TA, soleus, and gastrocnemius were excised. **RESULTS:** Mean cross-sectional area was reduced by 26% in aged HFD mice compared to the aged lean mice. Aged mice had nearly 2-fold collagen III content than young mice. P-STAT3/STAT3 was reduced by 82% in the aged HFD mice compared to the aged lean mice in the TA. NF-κB was 5-fold greater in the aged HFD mice compared to the aged lean mice in the TA. MMP-2 was reduced by more than 40% in the aged HFD mice compared to the aged lean mice in all muscles. **CONCLUSION:** Sarcopenic obese mice have reduced cross-sectional area than aged lean mice which may be linked to markers of muscle fibrosis and basal alterations an inflammatory signaling.

Keywords: high fat, aging, inflammation, myogenic regulatory factors, extracellular matrix

Introduction

Sarcopenic obesity is a growing concern to several health organizations due to the increase in health risk and healthcare cost. The age-related progressive decline in muscle mass and excessive adipose tissue are associated with numerous health risks that can ultimately lead to increase mortality (Lynch, 2011; Stenholm et al., 2008). Obese and sarcopenic individuals are subjected to a reduction of quality in vital organs and tissues including skeletal muscle which is needed for mobility, energy metabolism, and acts as a reservoir for essential growth factors and amino acids needed for survival (Biolo, Fleming, Maggi, & Wolfe, 1995; Stump, Henriksen, Wei, & Sowers, 2006). Specifically, older adults that suffer from sarcopenia will lose 30-50% muscle mass along with reductions that contribute to muscle frailty (Cesari et al., 2005; Fried et al., 2001). Obesity has also recently been implicated in reductions in muscle mass and muscle fibrosis which may negatively impact muscle function (Drake, Alway, Hollander, & Williamson, 2010; Hu et al., 2010; Uezumi et al., 2011). The combination of these two co-morbidities could potentially accelerate the decay of muscle tissue.

Skeletal muscle tissue integrity can be compromised when signaling pathways and regulators of myogenesis are irreversibly impaired. Several myopathies, metabolic disease and severe injury have implicated repression or chronic elevation of myogenic regulatory factors (MRFs) that are involved in myoblast proliferation and differentiation (Kim et al., 2016; Luz, Marques, & Santo Neto, 2002; Megeney, Kablar, Garrett, Anderson, & Rudnicki, 1996). A reduction of MRFs have been reported in myopathies and aging at basal levels which may implicate reduced regenerative potential of the muscle fibers (Thornell, 2011; Verdijk et al., 2007). Our laboratory has recently demonstrated reductions of MyoD mRNA abundance in

young HFD mice skeletal muscle (L. A. Brown et al., 2015).

Skeletal muscle function is also essential in muscle quality and is compromised in aging and obese individuals. The extracellular matrix (ECM) is one component surrounding the muscle fiber and fiber bundles that are involved in passive tension and force transmission (Gillies & Lieber, 2011; Kjaer, 2004). In skeletal muscle the fibril collagens I and III are predominant and are more resilient to stress than other ECM proteins. Muscle fibrosis has been documented in aging as well as muscle stiffness (DeGroot et al., 2001). Insulin resistant populations such as diabetics and elder populations are more susceptible to muscle stiffness and thus obese individuals may have alterations in ECM content (Song & Schmidt, 2012). The ECM also serves as reservoir for inflammatory proteins that regulate muscle mass and are involved in muscle function.

There are several key inflammatory proteins such as phagocytes that are involved with the regulation of muscle mass. Monocytes in the blood stream will be recruited by secreted ICAM-1 adhesion molecules to facilitate phagocyte infiltration into the muscle ECM. (Abbas, Lichtman, & Pillai, 2011; Dearth et al., 2013; Schiaffino & Partridge, 2008). This process will allow these non-resident macrophages to secrete cytokines involved in muscle repair (Abbas et al., 2011; Schiaffino & Partridge, 2008). It has been observed that populations that are associated with insulin resistance such as obesity and aging will also exhibit chronic elevation of pro-inflammatory cytokines at basal levels that can eventually lead to muscle atrophy over time (Petersen & Pedersen, 2005). In aging individuals the chronic expression of the inflammatory TNF-α will activate NF-κB that once activated may lead to apoptosis. On the contrary there have been findings in reduced macrophages and inflammatory cytokines in resting conditions in obese skeletal muscle (L. A. Brown et al., 2015; Nguyen et al., 2011).

73

Whether the differences in inflammatory proteins and signaling will positively or negatively impact sarcopenic individuals has yet to be determined.

Both sarcopenia and obesity have been investigated in skeletal muscle research extensively, yet these two co-morbidities have not been thoroughly examined together in how key proteins involved with repair may influence muscle quality and integrity. Thus, the purpose of this study is to examine how sarcopenic obesity alters basal levels of inflammation and ECM proteins in mice. We hypothesized that the combination of aging and obesity will further impair inflammatory signaling and ECM remodeling at rest.

Methods

Animals and Housing

Twelve young adult C57BL/6 male mice (n=12) and twelve aged C57BL/6 male mice (n=12) were purchased from Jackson Laboratories. Animals were housed in the University of Arkansas Central Laboratory Animal Facility. Young and aged mice were randomly fed a normal chow (lean; 17% kcals fat Research Diets, New Brunswick, New Jersey) or a high fat diet (HFD; 60% kcals fat, Research Diets, New Brunswick, New Jersey). The following four groups were formed: 1) young lean (n = 6); 2) young obese (n = 6); 3) aged lean (n = 6); 4) aged obese (n = 6). All procedures were approved by the University of Arkansas Institutional Animal Care and Use Committee (IACUC).

Muscle and Tibia Extraction

At either 3-4 mo or 22-24 mo of age, muscle and tibia extractions were performed as previously described (Tyrone A Washington et al., 2013; T. A. Washington et al., 2011). The gastrocnemius, soleus, TA, and tibias were extracted while the mice were anesthetized with a subcutaneous injection of a cocktail containing ketamine hydrochloride (90 mg/kg body weight), xylazine (3 mg/kg body weight), and acepromazine (1 mg/kg body weight). The left TA was snap frozen in liquid nitrogen and stored at -80°C for protein and gene expression analysis, the right TA was cut at the midbelly, mounted in optimum cutting temperature compound (OCT), and then dropped in liquid nitrogen cooled isopentane. Once frozen, samples were stored at -80°C for morphological analysis. After the muscles was dissected out, the tibia was removed and measured with a plastic caliper (VWR, Radnor, PA, USA). Tibia measurements were utilized to normalize muscle weights to an estimate of total body size.

Morphological Analysis

Fiber distribution and cross-sectional area (CSA) were performed as previously described (L. A. Brown et al., 2015; T. A. Washington et al., 2011). Each gastrocnemius muscle section (n = 6) was stained with hematoxylin and eosin, imaged with a Nikon camera (Sight DS-Vi1) mounted on an Olympus CKX41 inverted microscope at 20X magnification (Olympus), and analyzed with Nikon NIS Elements BR software package (Nikon). Each fiber was traced with a mouse and the number of pixels traced was calibrated to obtain CSA of the muscle. All fibers in the cross section images were quantified unless the sarcolemma was not intact. Approximately 100 fibers were traced per sample. Immunostaining for collagen I and III were performed as previously described (Kim et al., 2016). Each TA muscle cross-section was cut at 10 µm (n = 4-7) using the cryostat and placed on a slide. First, slides were permeabilized in 0.1% 10X Triton then rinsed in PBS. Then slides were blocked in PBS with 4% goat serum and 0.05% sodium azide for 30 minutes at room temperature. Afterwards, slides were incubated on primary antibodies for 3 hours at room temperature; rabbit-polyclonal anti-collagen I IgG (1:500, Sigma Aldrich, St. Louis, MO), rabbit-polyclonal anti-collagen III (1:500, Sigma Aldrich, St. Louis, MO). Slides were then washed with PBS and incubated in Alexa Fluor 488 (1:500, Life Technologies Carlsbad, CA). Images of the slide were acquired with a Nikon camera (Sight DS-Vi1) mounted on an Olympus CKX41 inverted microscope at 20X magnification (Olympus, Tokyo, Japan), and analyzed with MATLAB. Total ECM area was determined by dividing the number of green pixels by the total number of pixels in the image.

Western blotting

Muscle tissues were homogenized as previously described (Lee et al., 2016). Approximately 10-40 mg of gastrocnemius, soleus, and TA was homogenized in glass dounce type homogenizers in 0.30 ml of complete protein loading buffer (50 mM Tris·HCl, pH 6.8, 1% sodium dodecyl sulfate (SDS), 10% glycerol, 20 mM dithiothreitol, 127 mM 2-mercaptoethanol, and 0.01% bromophenol blue supplemented with protease inhibitors (Roche) and phosphatase inhibitors (Sigma-Aldrich, St. Louis, MO). After homogenization, samples were transferred to sterile 1.5mL microcentrifuge tubes, heated for 5 minutes at 95°C to denature protein and then centrifuged for 5 minutes at 13,000 rpm. Protein concentrations were determined using a commercially available RC/DC assay kit. Muscle homogenate (40 μg) was fractionated in 10% SDS-polyacrylamide gels. Gels were transferred to polyvinylidene difluoride (PVDF) membranes. Membranes were stained with *Ponceau S* before blotting to verify equal loading of the gels. Membranes were blocked in 5% milk, in Tris-buffered saline with 0.1% Tween-20 (TBST), for 2 hours. Primary antibodies for P-Stat3 (Tyr[705]), Stat3 (Cell Signaling Technologies, Danvers, MA), and NF-κB p65 (Santa Cruz, Dallas, TX) were diluted 1:1000 to 1:2000 in 5% milk, in TBST, and incubated at 4°C overnight. Anti-rabbit and Anti-mouse monoclonal secondary antibodies (Cell Signaling Technologies, Danvers, MA) were diluted 1:2,000 in 5% milk, in TBST, and then incubated at room temperature for one hour. Enhanced Chemiluminescence (ECL) was performed using Fluorochem M imager (Protein Simple, Santa Clara, California) to visualize antibody-antigen interaction. Blotting images were quantified by densitometry using AlphaView software (Protein Simple). The Ponceau-stained membranes were digitally scanned, and the 45-kDa

actin bands were quantified by densitometry and used as a protein loading correction factor for each lane.

RNA Isolation, cDNA synthesis, and quantitative RT-PCR

The following procedures were completed as previously described (L. A. Brown et al., 2015; Nicholas P Greene et al., 2014; Tyrone A Washington et al., 2013). RNA was extracted with Trizol reagent (Life Technologies, Grand Island, NY, USA). TA muscles were homogenized in Trizol. Total RNA was isolated, DNase treated and purity and concentrations were determined using 260/280nm ratios read on a BioTek Take3 microvolume microplate with a BioTek PowerWave XC microplate reader (BioTek Instruments Inc., Winooski, VT). cDNA was reverse transcribed from 1 µg of total RNA using the Superscript Vilo cDNA synthesis kit (Life Technologies, Carlsbad, CA, USA). Real-time PCR was performed, and results were analyzed by using the StepOne Real-Time PCR system (Life Technologies, Applied Biosystems, Grand Island, NY). cDNA was amplified in a 25 µL reaction containing appropriate primer pairs and TaqMan Universal Mastermix (Applied Biosystems). Samples were incubated at 95°C for 4 min, followed by 40 cycles of denaturation, annealing and extension at 95°C, 55°C and 72°C respectively. TaqMan fluorescence was measured at the end of the extension step each cycle. Fluorescence labeled probes for MyoD (FAM dye), myogenin (FAM dye), TNFα (FAM dye), IL-6 (FAM dye), Collagen I (FAM dye), Collagen III (FAM dye), Fibronectin (FAM dye), MMP-2 (FAM dye), MMP-9 (FAM dye), TGF-β (FAM dye), TIMP-1 (FAM dye), and 18S (FAM dye) were purchased from Applied Biosystems and quantified with TaqMan Universal mastermix. Cycle threshold (Ct) was determined, and the ΔCt value was calculated as the difference between the Ct value and the 18S Ct value. Final quantification of gene expression was calculated using the ΔΔCT method

Ct = [ΔCt(calibrator) − ΔCt(sample)]. Relative quantification was then calculated as $20^{-\Delta\Delta Ct}$.

Melt curve analysis was performed at the end of the PCR run to verify no primer dimers were formed.

Statistical Analysis

All data was analyzed using Statistical Package for the Social Sciences (SPSS version 22.0, Armonk, NY). Results are reported as mean ± SEM. A two-way ANOVA was performed to analyze main effects of treatment and diet and if there were any interactions between the dependent variables for 3 and 21 days post-bupivacaine injection. When a significant interaction was detected, differences among individual means were assessed with Fisher's LSD post-hoc analysis. The χ^2 analysis was used to detect differences in the proportion of small fibers ($< 400\ \mu m^2$) and large fibers ($> 900\ \mu m^2$) between treatment groups. Statistical significance was set at $P \le 0.05$.

Results

Animal weight characteristics and muscle morphology

Body weight in the young HFD mice was 24% greater than young lean mice (Table 1). Body weight in the aged HFD mice was 35% greater than aged lean mice (Table 1). TA muscle weight relative to tibia length in the in the young HFD mice was 4% greater compared to the lean mice. TA muscle weight was reduced by 8% in the aged HFD mice compared to the aged lean mice. Soleus muscle weight relative to tibia length in the in the young HFD mice was 16% greater in compared to the lean mice. In the aged mice there was no difference in soleus muscle weight relative to tibia length in the HFD mice compared to the lean mice. Gastrocnemius muscle weight relative to tibia length in the in the young HFD mice was 9% greater in compared to the lean mice. Gastrocnemius muscle weight was reduced by 6% in the aged HFD mice compared to the aged lean mice.

In the young mice, gastrocnemius mean cross-sectional area was 17% smaller in the HFD mice compared to the lean mice (Fig. 1B). In the aged mice, gastrocnemius mean cross-sectional area was 26% smaller in the HFD mice compared to the lean mice (Fig. 1B). In the young mice there were 21% (Fig. 1C) more small ($< 400\ \mu m^2$) fibers in the HFD group compared to the lean group in the gastrocnemius. Also, in the young mice there were 75% (Fig. 1C) less large fibers ($> 900\ \mu m^2$) in the HFD group compared to the lean group. In the aged mice there were 3-fold (Fig. 1D) more small ($< 400\ \mu m^2$) fibers in the HFD group compared to the lean group in the gastrocnemius. Also, in the aged mice there were 74% (Fig. 1D) less large fibers ($> 900\ \mu m^2$) in the HFD group compared to the lean group in the gastrocnemius. There was no difference in collagen I content in in the gastrocnemius in all groups (Fig. 2B). There was a main effect of with an increase of collagen III in the aged

80

groups compared to the young groups in the gastrocnemius (Fig. 2D).

MRF gene expression

There was no difference of MyoD mRNA abundance in the TA in all groups (Fig. 3A). There was a main effect of diet with a decrease of MyoD mRNA abundance in the HFD groups compared to the lean groups in the soleus (Fig. 3B). There was a main effect of diet with an increase of MyoD mRNA abundance in the HFD groups compared to the lean groups in the gastrocnemius (Fig. 3C). There was a main effect of age with an increase of MyoD mRNA abundance in the aged groups compared to the young groups in the gastrocnemius (Fig. 3C). There was a main effect of diet with a decrease of myogenin mRNA abundance in the HFD groups compared to the lean groups in the TA (Fig. 3D). There was no difference of myogenin mRNA abundance in the soleus in all groups (Fig. 3E). In the young mice, myogenin mRNA abundance was not different in the HFD group compared to the lean group in the gastrocnemius (Fig. 3F). In the aged mice, myogenin mRNA abundance was not different in the HFD group compared to the lean group in the gastrocnemius (Fig. 3F).

Inflammation gene expression

There was no difference of IL-6 mRNA abundance in the TA in all groups ($P = 0.05$, Fig. 4A). There was a main effect of age with an increase of IL-6 mRNA abundance in the aged groups compared to the young groups in the soleus (Fig. 4B). There was no difference of IL-6 mRNA abundance in the gastrocnemius in all groups (Fig. 4C). There was no difference of TNF-α mRNA abundance in the TA in all groups (Fig. 4D). There was a main effect of diet with a decrease of TNF-α mRNA abundance in the HFD groups compared to the lean groups in the soleus (Fig. 4E). There was a main effect of age with an increase of TNF-α mRNA abundance in the aged groups compared to the young groups in the soleus (Fig. 4E). There

81

was a significant interaction of TNF-α mRNA abundance in the gastrocnemius (Fig. 4F). However, in the young mice, TNF-α mRNA abundance was not different in the HFD group compared to the lean group in the gastrocnemius (Fig. 4F). Also, in the aged mice, TNF-α mRNA abundance was not different in the HFD group compared to the lean group in the gastrocnemius (Fig. 4F). There was a main effect of age with a decrease of ICAM-1 mRNA abundance in the aged groups compared to the young groups in the TA (Fig. 4G). There was a main effect of age with an increase of ICAM-1 mRNA abundance in the aged groups compared to the young groups in the soleus (Fig. 4H). There was no difference of ICAM-1 mRNA abundance in the gastrocnemius in all groups (Fig. 4I).

Inflammation protein expression

In the young mice, phosphorylated STAT3 relative to STAT3 was not different in the HFD group compared to the lean group in the TA (Fig. 5A). In the aged mice, phosphorylated STAT3 relative to STAT3 was reduced by 82% in the HFD group compared to the lean group in the TA (Fig. 5A). In the young mice, NF-κB was not different in the HFD group compared to the lean group in the TA (Fig. 5B). In the aged mice, NF-κB was 5-fold greater in the HFD group compared to the lean group in the TA (Fig. 5B). There was a main effect of diet with a decrease of phosphorylated STAT3 relative to STAT3 in the aged groups compared to the young groups in the TA (Fig. 5C). There was a main effect of diet with an increase of NF-κB in the HFD groups compared to the lean groups in the soleus (Fig. 5D). There was a main effect of age with an increase of NF-κB in the aged groups compared to the young groups in the soleus (Fig. 5D). There was no difference of phosphorylated STAT3 relative to STAT3 in the gastrocnemius in all groups (Fig. 5E). In the young mice, NF-κB was not different in the HFD group compared to the lean group in the gastrocnemius (Fig. 5F). In the aged mice, NF-

82

κB was 3-fold greater in the HFD group compared to the lean group in the gastrocnemius (Fig. 5F).

Collagen & TGFβ gene expression

There was a main effect of diet with a decrease of TGF-β mRNA abundance in the HFD groups compared to the lean groups in the TA (Fig. 6A). There was a main effect of age with a decrease of TGF-β mRNA abundance in the aged groups compared to the young groups in the TA (Fig. 6A). There was a significant interaction of TGF-β mRNA abundance in the soleus (Fig. 6B). However, in the young mice, TGF-β mRNA abundance was not different in the HFD group compared to the lean group in the soleus (Fig. 6B). Also, in the aged mice, TGF-β mRNA abundance was not different in the HFD group compared to the lean group in the soleus (Fig. 6B). There was no difference of TGF-β mRNA abundance in the gastrocnemius in all groups (Fig. 6C). There was a main effect of age with a decrease of collagen I mRNA abundance in the aged groups compared to the young groups in the TA (Fig. 6D). In the young mice, collagen I mRNA abundance was 2-fold greater in the HFD group compared to the lean group in the soleus (Fig. 6E). In the aged mice, collagen I mRNA abundance was not different in the HFD group compared to the lean group in the soleus (Fig. 6E). In the young mice, collagen I mRNA abundance was 5-fold greater in the HFD group compared to the lean group in the gastrocnemius (Fig. 6F). In the aged mice, collagen I mRNA abundance was not different in the HFD group compared to the lean group in the gastrocnemius (Fig. 6F). In the young mice, collagen III mRNA abundance was 2-fold greater in the HFD group compared to the lean group in the TA (Fig. 6G). In the aged mice, collagen III mRNA abundance was not different in the HFD group compared to the lean group in the TA (Fig. 6G). In the young mice, collagen III mRNA abundance was 2-fold greater in the

83

HFD group compared to the lean group in the soleus (Fig. 6H). In the aged mice, collagen III mRNA abundance was not different in the HFD group compared to the lean group in the soleus (Fig. 6H). In the young mice, collagen III mRNA abundance was 6-fold greater in the HFD group compared to the lean group in the gastrocnemius (Fig. 6I). In the aged mice, collagen III mRNA abundance was reduced by 73% in the HFD group compared to the lean group in the gastrocnemius (Fig. 6I). There was a significant interaction of fibronectin 1 mRNA abundance in the TA (Fig. 6J). However, in the young mice, fibronectin 1 mRNA abundance was not different in the HFD group compared to the lean group in the TA (Fig. 6J). Also, in the aged mice, fibronectin 1 mRNA abundance was not different in the HFD group compared to the lean group in the TA (Fig. 6J). In the young mice, fibronectin 1 mRNA abundance was not different in the HFD group compared to the lean group in the soleus (Fig. 6K). In the aged mice, fibronectin 1 mRNA abundance was reduced by 56% in the HFD group compared to the lean group in the soleus (Fig. 6K). In the young mice, fibronectin 1 mRNA abundance was 2-fold greater in the HFD group compared to the lean group in the gastrocnemius (Fig. 6L). In the aged mice, fibronectin 1 mRNA abundance was not different in the HFD group compared to the lean group in the gastrocnemius (Fig. 6L).

MMP and TIMP gene expression

In the young mice, MMP-2 mRNA abundance was not different in the HFD group compared to the lean group in the TA (Fig. 7A). In the aged mice, MMP-2 mRNA abundance was decreased by 42% in the HFD group compared to the lean group in the TA (Fig. 7A). In the young mice, MMP-2 mRNA abundance was 2-fold greater in the HFD group compared to the lean group in the soleus (Fig. 7B). In the aged mice, MMP-2 mRNA abundance was decreased by 43% in the HFD group compared to the lean group in the soleus (Fig. 7B). In the

84

young mice, MMP-2 mRNA abundance was 2-fold greater in the HFD group compared to the lean group in the gastrocnemius (Fig. 7C). In the aged mice, MMP-2 mRNA abundance was decreased by 45% in the HFD group compared to the lean group in the gastrocnemius (Fig. 7C). There was a main effect of diet with a decrease of MMP-9 mRNA abundance in the HFD groups compared to the lean groups in the TA (Fig. 7D). There was a main effect of age with a decrease of MMP-9 mRNA abundance in the aged groups compared to the young groups in the TA (Fig. 7D). There was a main effect of diet with a decrease of MMP-9 mRNA abundance in the HFD groups compared to the lean groups in the soleus (Fig. 7E). There was a main effect of diet with a decrease of MMP-9 mRNA abundance in the HFD groups compared to the lean groups in the gastrocnemius (Fig. 7F). There was a significant interaction of TIMP-1 mRNA abundance in the TA (Fig. 7G). However, in the young mice, TIMP-1 mRNA abundance was not different in the HFD group compared to the lean group in the TA (Fig. 7G). Also, in the aged mice, TIMP-1 mRNA abundance was not different in the HFD group compared to the lean group in the TA (Fig. 7G). There was no difference in TIMP-1 mRNA abundance in in the soleus in all groups (Fig. 7H). There was no difference in TIMP-1 mRNA abundance in the gastrocnemius in all groups (Fig. 7I).

Discussion

The primary goal of this study was to examine how sarcopenic obesity alters basal levels of inflammation and ECM proteins in mice. We hypothesized that the combination of aging and obesity would further impair myogenesis, inflammatory signaling and ECM remodeling at rest. To our knowledge we are the first to demonstrate a reduction in mean CSA, greater frequency of smaller fibers, reduced P-STAT/STAT3, increase collagen III content, and chronically activated NF-κB expression in sarcopenic obese mice. All of these changes observed in sarcopenic obese indicate reduced regenerative capacity and also suggest further progressive decline exacerbated by the comorbidity of sarcopenic obesity.

To determine whether sarcopenic obese mice were subjected to further exacerbated declines in muscle mass loss, we first examined muscle weights relative to tibia length and mean CSA in all animal groups. Aged HFD mice had an 8% and 6% reduction in TA and gastrocnemius muscle weight relative to tibia length but no change in the soleus. It has been reported that aging muscle is more susceptible to muscle mass losses in type II fibers than type I fibers which we observed in the mean-cross sectional area of aging HFD mice (Muscaritoli et al., 2010). Then we examined mean CSA and observed a 17% and 26% reduction in the young HFD and aged HFD compared to their lean counterparts, respectively. Next, we examined fiber distribution in both young and aged mice. The HFD mice in both young and aged mice had a higher frequency for smaller fibers and lower frequency of larger fibers suggesting that there is reduction of CSA in young HFD and aged HFD mice. Taken together it appears that muscle mass is much greater in sarcopenic obese mice.

In this study we noticed that changes in MRFs were influenced by aging. In the soleus and gastrocnemius muscle there was a main effect of age to increase MyoD expression. Marsh

86

and colleagues had similar findings reporting higher elevated MyoD in old rats compared to young rats (Marsh, Criswell, Carson, & Booth, 1997). It is possible that MyoD may be chronically expressed to try and repair the muscle because in aging muscle there is a loss of motor neurons that will result in denervated muscle fibers (Hashizume, Kanda, & Burke, 1988; Marsh et al., 1997). There were no changes reported with myogenin expression in skeletal muscle which is consistent with Schefer that reported no changes in myogenic differentiation in aging skeletal muscle *in vitro* (Shefer, Van de Mark, Richardson, & Yablonka-Reuveni, 2006).

Next we examined inflammatory cytokines and adhesion molecules in skeletal muscle. There were no differences in IL-6 expression except for an increase of IL-6 in the soleus of aged mice. There was also an increase of ICAM-1 in the soleus of aged mice. ICAM-1 is an adhesion that recruits naïve macrophages from circulation to the site of injury (Abbas et al., 2011). It is possible that slow twitch muscle fibers might be more susceptible to macrophage infiltration to facilitate muscle repair an aging muscle. It is important to note that the soleus was the only hindlimb muscle fiber that did not result in a decrease muscle weight relative to tibia length and therefore the IL-6 could be playing a preservative role in aging type I muscle fibers. This would be supported by aging literature that has demonstrated more pronounced reductions in type II fibers (Muscaritoli et al., 2010). On the contrary, the downstream target of IL-6, STAT3, was downregulated in aging mice. It has been confirmed that IL-6 can be alternatively activated by other intracellular proteins resulting apoptosis signaling observed an inflammatory diseases (Kishimoto, 2006). Thus more investigation is required to determine if IL-6 is playing a beneficial or negative role in slow twitch muscle fibers. Interestingly, there was a decrease of ICAM-1 expression in the highly glycolytic TA muscle which could

indicate less macrophage infiltration and thus less removal of damaged muscle fibers. Hence, there may be a differential response of IL-6 signaling in different muscle fiber types.

It has been a major assumption that pro-inflammatory cytokines are chronically activated in populations that are associated with systemic low grade inflammation. This study found no differences in TNF-α expression in either the TA or gastrocnemius. However, in the soleus there was a decrease of TNF-α expression in the HFD mice and an increase in TNF-α expression in the aged mice. The increase in TNF-α corroborates with the findings of increased IL-6 and ICAM-1 expression in the soleus and advocates a greater population of macrophages in aging soleus muscle. Because there was an increase of TNF-α expression in aged soleus muscle we investigated the downstream target NF-κB. We reported a main effect of HFD and aging to increase NF-κB expression in the soleus and 3-5 fold changes in aged HFD TA and gastrocnemius muscle. Moreover, there were no changes of TNF-α expression in the TA and gastrocnemius aging muscle. It has been demonstrated that NF-κB can be chronically activated independent of TNF-α and will cause atrophy in cancer cachexia (He et al., 2013). These findings may provide an explanation of the further decline in sarcopenic obese muscle mass and should be further investigated.

Muscle fibrosis has also been observed in both aging and obese populations and can negatively impact regenerative capacity. In the gastrocnemius we observed no changes of collagen I content, but almost 2-fold greater collagen III in aged mice. It appears that excess collagen exhibited in aging gastrocnemius is predominately collagen III (Wood et al., 2014). Collagen III is different in structure in collagen I that it is more elastic and may suggest a higher susceptibility to injury in older adults. Gene expression was also investigated and there was a differential response in hindlimb muscles. The major finding within aging HFD

mice was reduced collagen III gene expression in the gastrocnemius and fibronectin 1 in soleus at basal levels. These findings did not match the excessive collagen III content witnessed in aging muscle and require more attention. It is possible that MMPs are still being activated in aging mice even though aging reduces favors low collagen turnover. Because MMP activity was not directly measured, further investigation is required.

Altogether, aging HFD mice have reduced regenerative capacity and further progressive muscle mass loss at rest. This was evident in the aging and aging HFD muscle because there were reductions in muscle mass, CSA, impaired inflammatory signaling and altered ECM remodeling. Interestingly, it does appear that type II muscle are more negatively impacted and should be targeted for future therapeutic strategies to preserve muscle in sarcopenic obese populations.

Table 1

Tibia anterior weight, soleus weight, gastrocnemius weight, bodyweight, tibia anterior relative to tibia

length, soleus relative to tibia length, gastrocnemius relative to tibia length, in male C57BL/6 mice.

Treatment	TA (mg)	Soleus (mg)	Gastrocnemius (mg)	Bodyweight (g)	TA/TL (mg mm^{-1})	Soleus/TL (mg mm^{-1})	Gastrocnemius/TL (mg mm^{-1})
Young							
Lean	55.07 ± 1.41	9.67 ± 0.22	149.33 ± 3.32	28.91 ± 0.45	3.18 ± 0.09	0.56 ± 0.01	8.61 ± 0.23
HFD	56.90 ± 0.86	$11.58 \pm 0.18^{\#}$	$162.38 \pm 2.49^{\#}$	$38.14 \pm 0.64^{\#}$	$3.31 \pm 0.05^{\#}$	$0.67 \pm 0.01^{\#}$	$9.44 \pm 0.14^{\#}$
Aged							
Lean	52.03 ± 8.34	10.29 ± 0.47	152.44 ± 4.99	35.14 ± 2.09	2.83 ± 0.11	0.56 ± 0.02	8.29 ± 0.28
HFD	$46.78 \pm 1.16^{\$}$	9.83 ± 0.51	$140.51 \pm 3.82^{\$}$	$53.70 \pm 2.48^{\$}$	$2.59 \pm 0.07^{\$}$	0.54 ± 0.03	$7.76 \pm 0.17^{\$}$

Values are means $\pm$ SEM. *Note.* BW = bodyweight, TL = tibia length. Significant difference from the young lean distinguished by [#]. Significant difference from the old lean distinguished by [$], $P \leq 0.05$.

Figure Legends

Figure 1. Tibialis anterior mean cross sectional area and fiber distribution (A) Representative H&E staining of muscle cross section of young lean (a), young HFD (b), aged lean (c), and aged HFD (d); (B) Mean cross-sectional area of the tibialis anterior in young lean and HFD mice. (C) Myofiber distribution in young lean and young HFD mice (D) Myofiber distribution in young lean and young HFD mice. Frequency histograms and the frequency of fibers $< 400 \, \mu m^2$ and $> 900 \, \mu m^2$ were compared by a χ^2 analysis as previously described (Washington et al., 2011). Values are reported in the frequency percentage of a given fiber size (μm^2). Differences between two groups distinguished by *, $P \leq 0.05$.

Figure 2. Immunofluorescent staining of collagen on the tibialis anterior muscle. (A) Representative collagen I staining of muscle cross section of young lean (a), young HFD (b), aged lean (c), and aged HFD (d); (B) Collagen I content percentage in young and aged mice. (C) Representative collagen III staining of muscle cross section of young lean (a), young HFD (b), aged lean (c), and aged HFD (d); (D) Collagen III content percentage in young and aged mice. Main effects of age distinguished by ‡.

Figure 3. Myogenic regulatory factors in young and aged mice in the TA, soleus, and gastrocnemius. (A-C) MyoD mRNA abundance. (D-F) Myogenin mRNA abundance. All data was normalized to the young lean. Main effects of diet distinguished by † and age by ‡. Significant differences between young lean and young HFD and aged lean and aged HFD distinguished by [#]. $P \leq 0.05$.

Figure 4. Inflammatory cytokines and ICAM-1 mRNA Abundance in young and aged mice in the TA, soleus and gastrocnemius. (A-C) IL-6 mRNA abundance. (D-F) TNF-α mRNA abundance. (G-I) ICAM-1 mRNA abundance All data was normalized to the young

lean. Main effects of diet distinguished by † and age by ‡. Significant differences between young lean and young HFD and aged lean and aged HFD distinguished by #. P ≤ 0.05.

Figure 5. P-STAT3/STAT3 and NF-κB65 protein in young and aged mice in the TA, soleus, and gastrocnemius. (A) P-STAT3/STAT3 in the TA; (B) NF-κB65 in the TA. (C) P-STAT3/STAT3 in the soleus; (D) NF-κB65 in the soleus. (E) P-STAT3/STAT3 in the gastrocnemius; (F) NF-κB65 in the gastrocnemius. Main effects of diet distinguished by † and age by ‡. Significant differences between young lean and young HFD and aged lean and aged HFD distinguished by #. P ≤ 0.05. Abbreviations: YL, young lean; YH, young high fat diet; AL, aged lean; AH, aged high fat diet.

Figure 6. Collagen and promoters of collagen in young and aged mice in the TA, soleus and gastrocnemius. (A-C) TGF-β mRNA abundance. (D-F) Collagen I mRNA abundance. (G-I) Collagen III mRNA abundance (J-L) Fibronectin 1 mRNA abundance All data was normalized to the young lean. Main effects of diet distinguished by † and age by ‡. Significant differences between young lean and young HFD and aged lean and aged HFD distinguished by #. P ≤ 0.05.

Figure 7. MMPs and TIMP-1 mRNA Abundance in young and aged mice in the TA, soleus and gastrocnemius. (A-C) MMP-2 mRNA abundance. (D-F) MMP-9 mRNA abundance. (G-I) TIMP-1 mRNA abundance All data was normalized to the young lean. Main effects of diet distinguished by † and age by ‡. Significant differences between young lean and young HFD and aged lean and aged HFD distinguished by #. P ≤ 0.05.
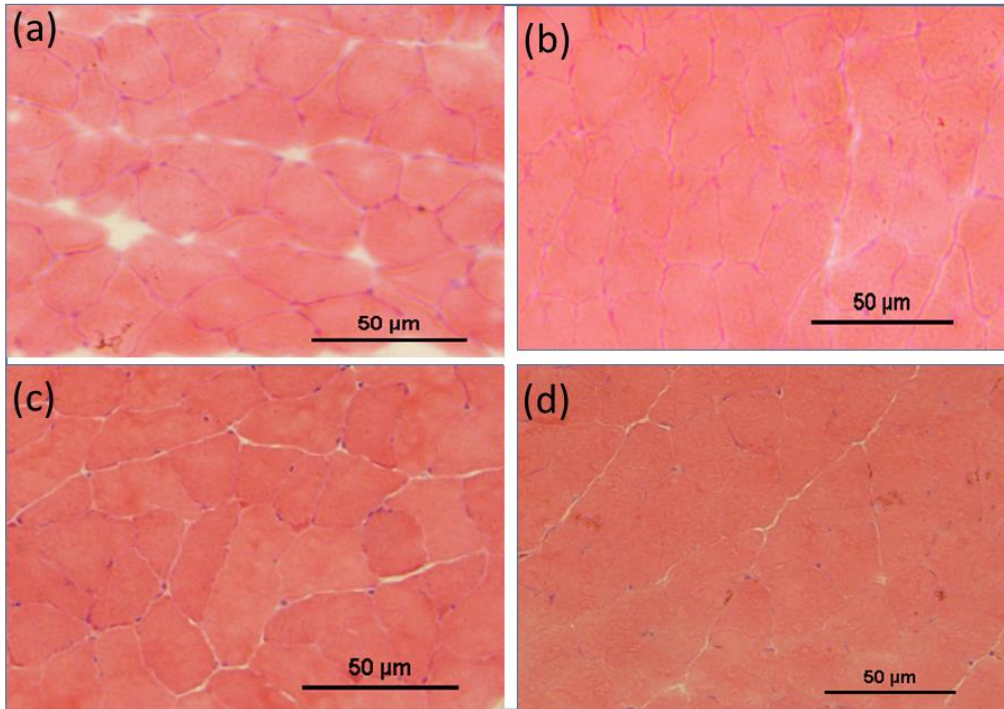
Figures

Figure 1
A.

B.
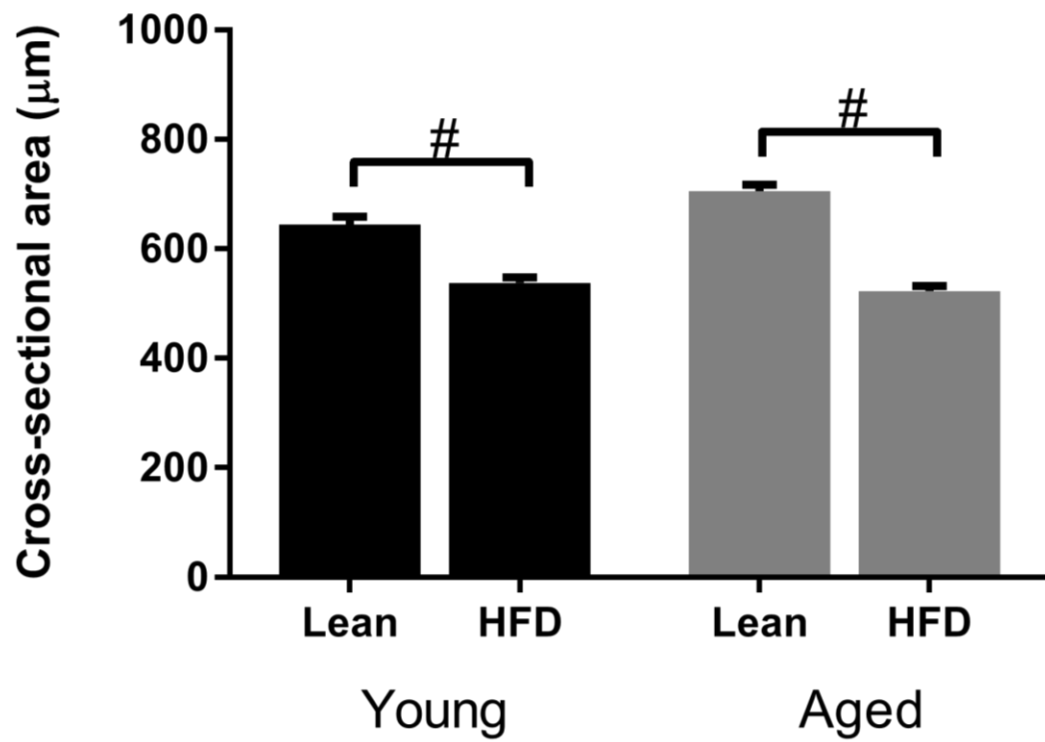
C.
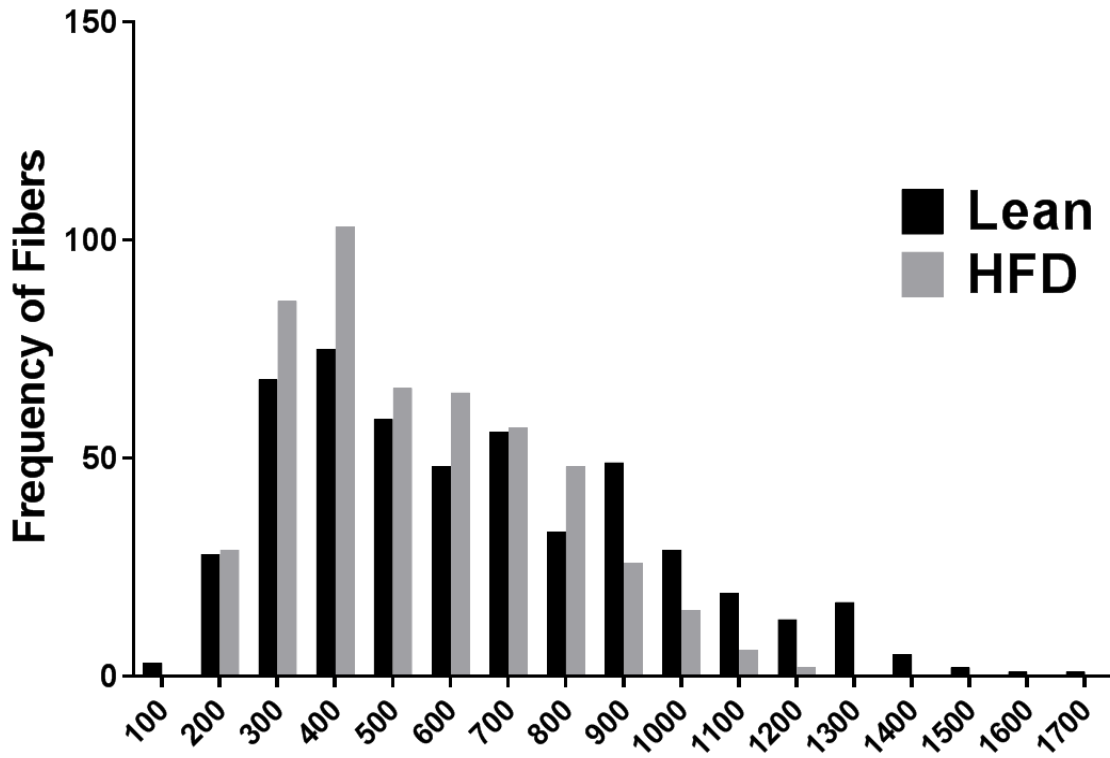
D.
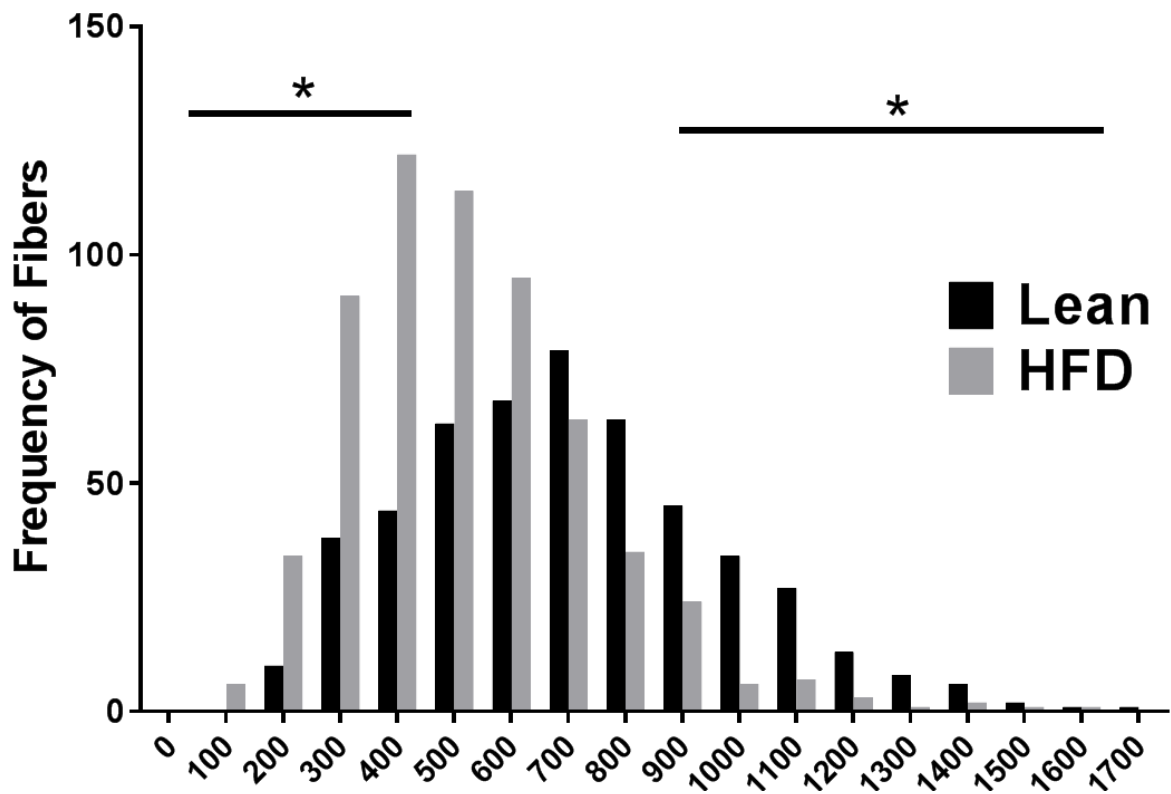
Figure 2

A.
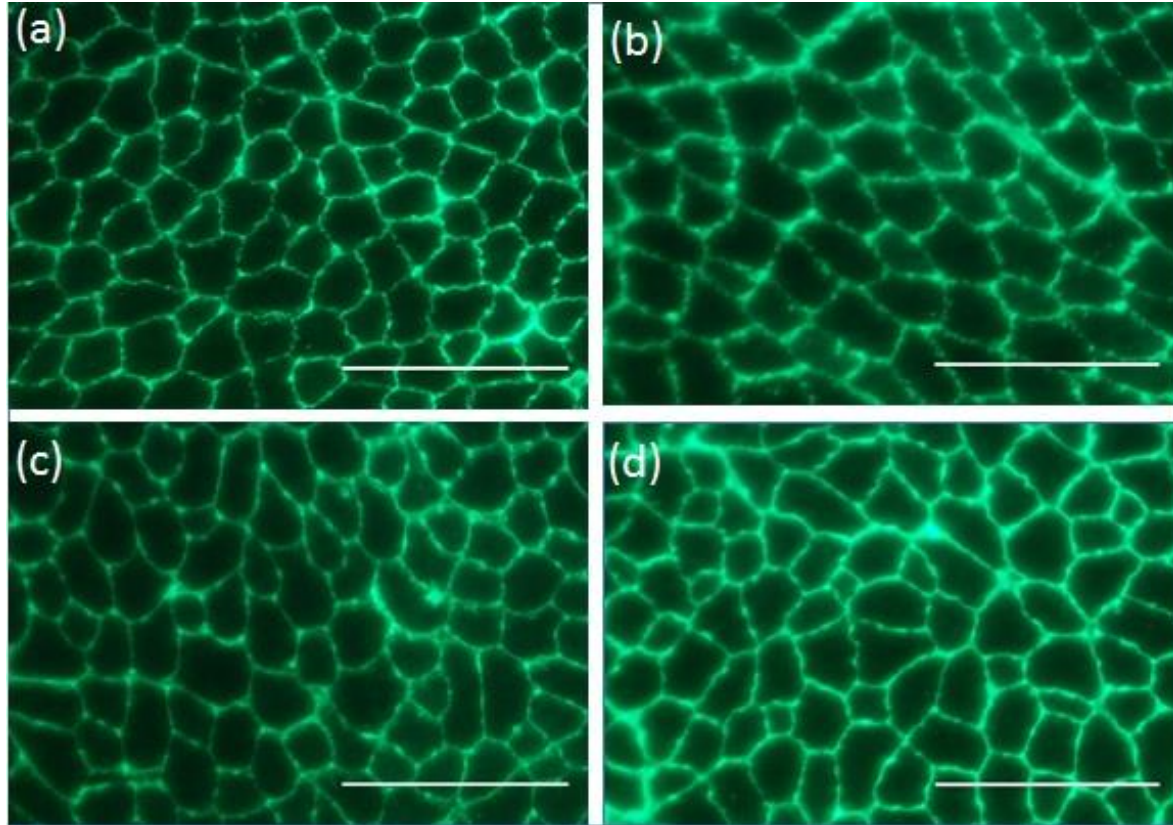
B.
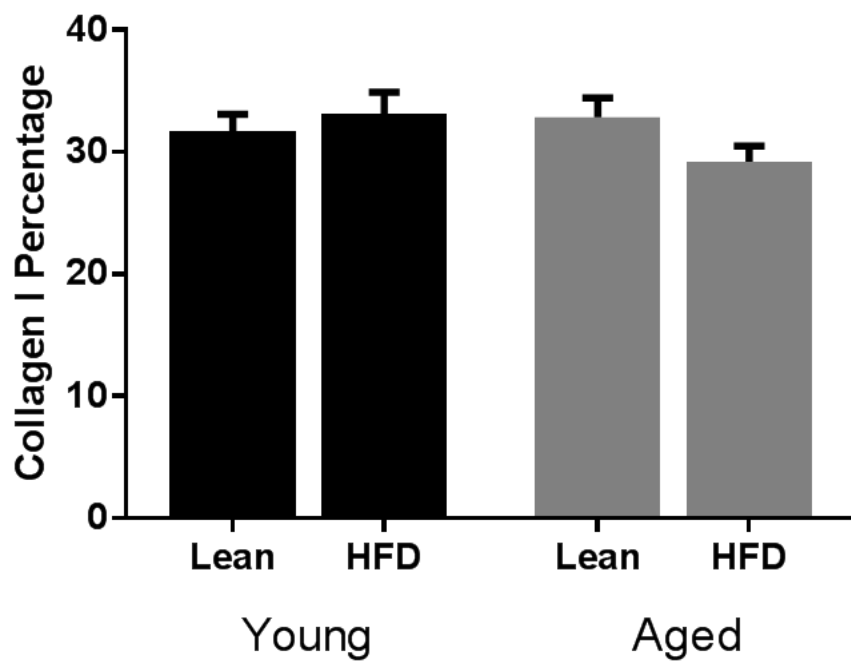
C.
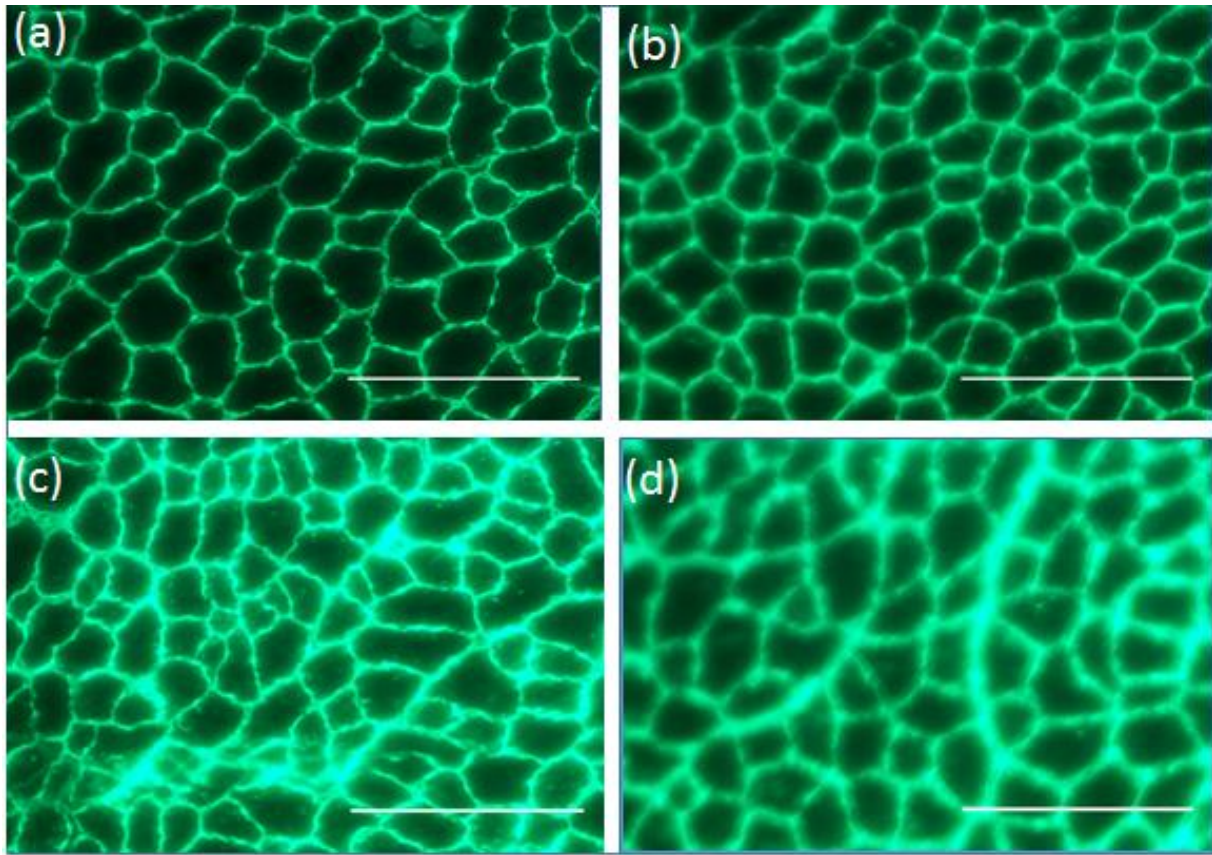
D.
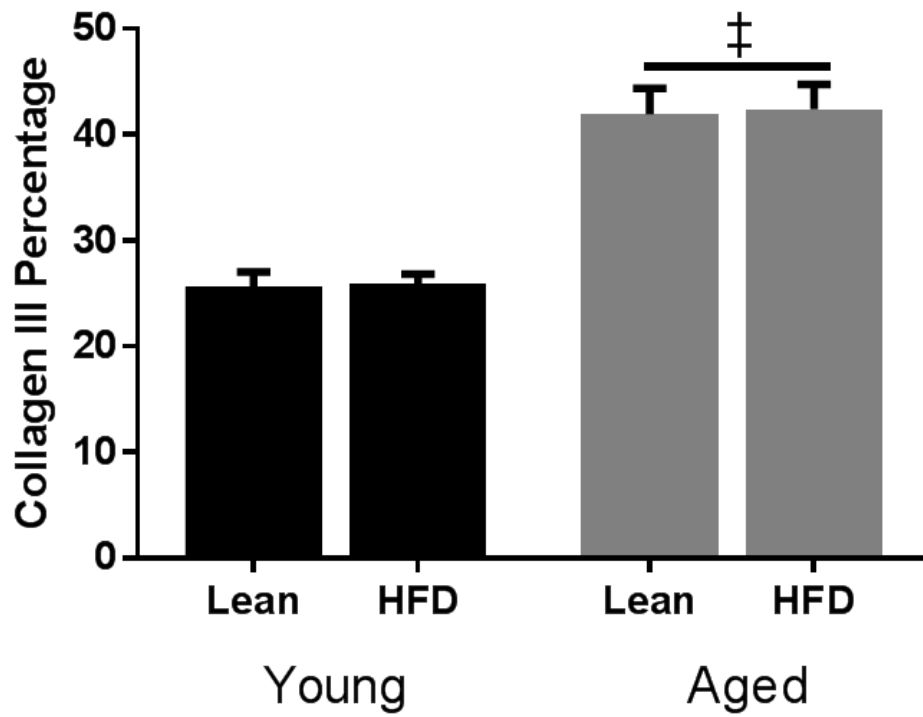
Figure 3

A.
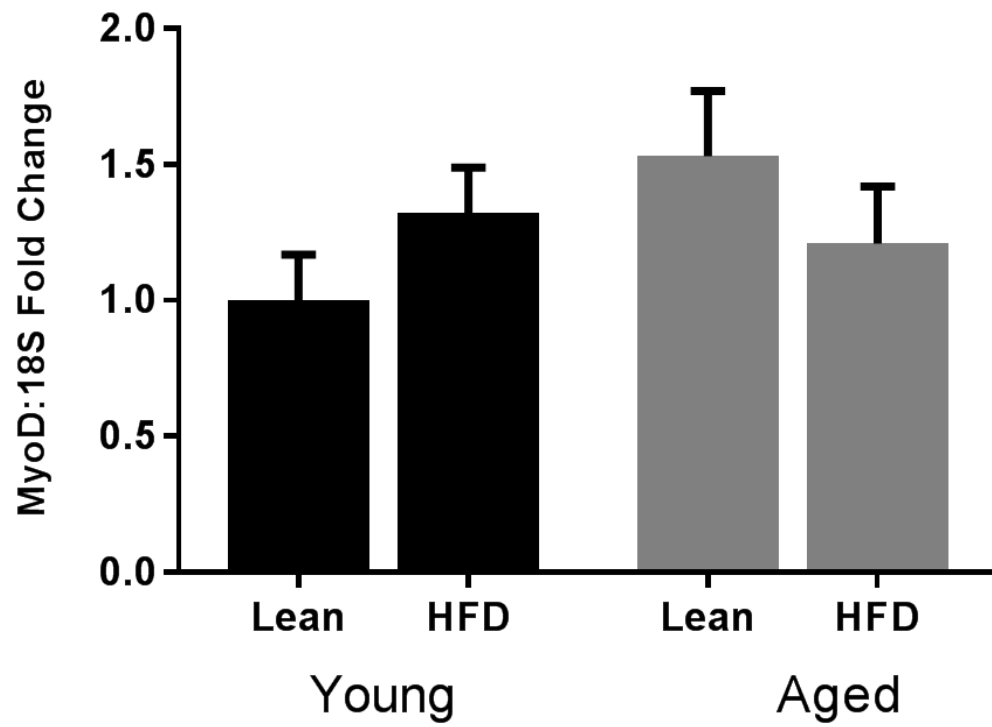
B.
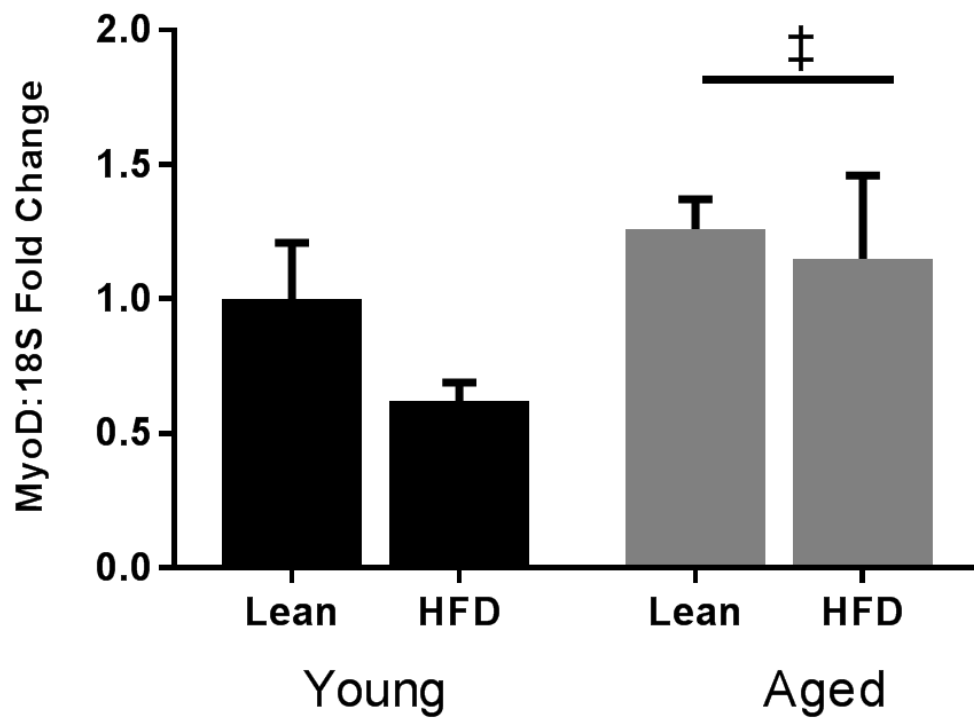
C.
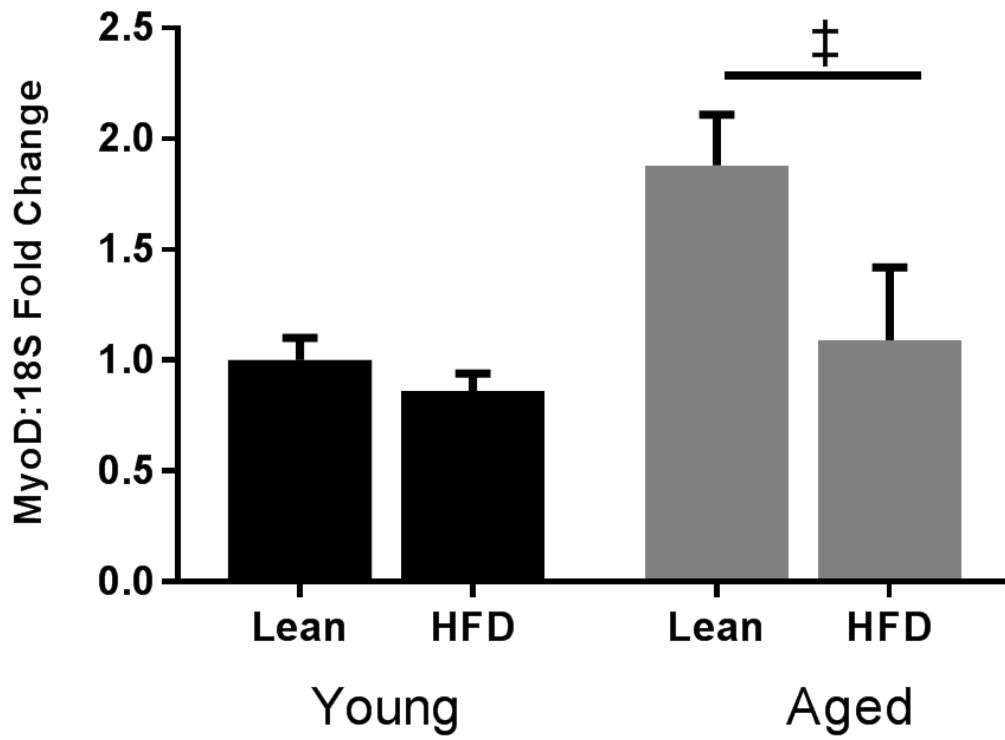
D.
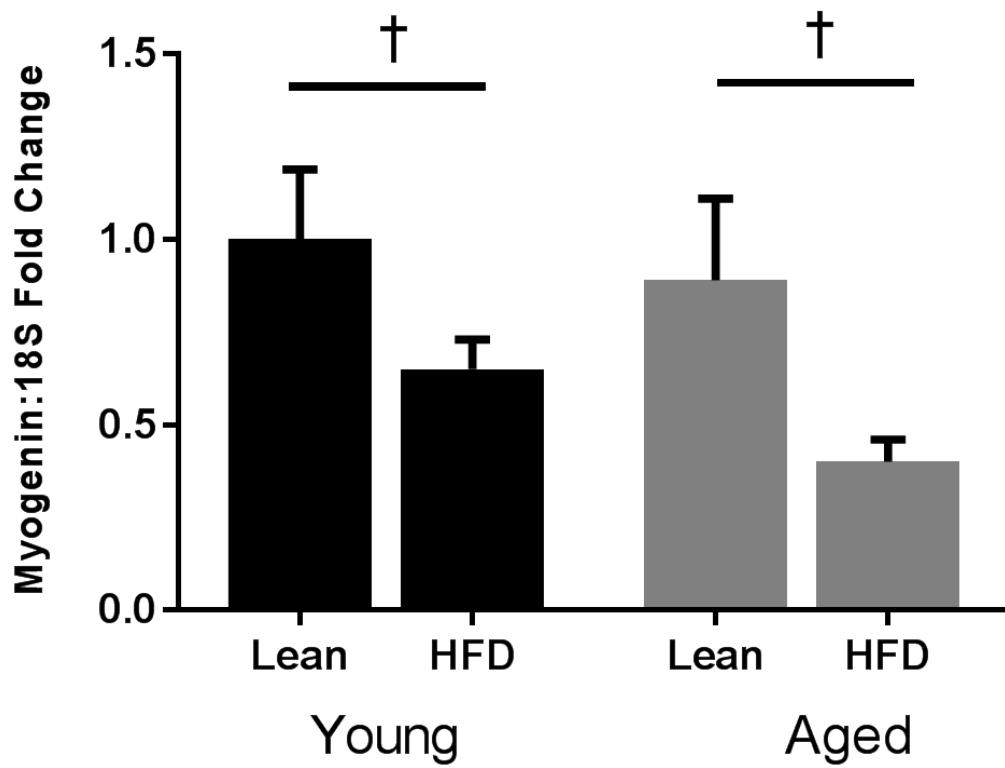
E.
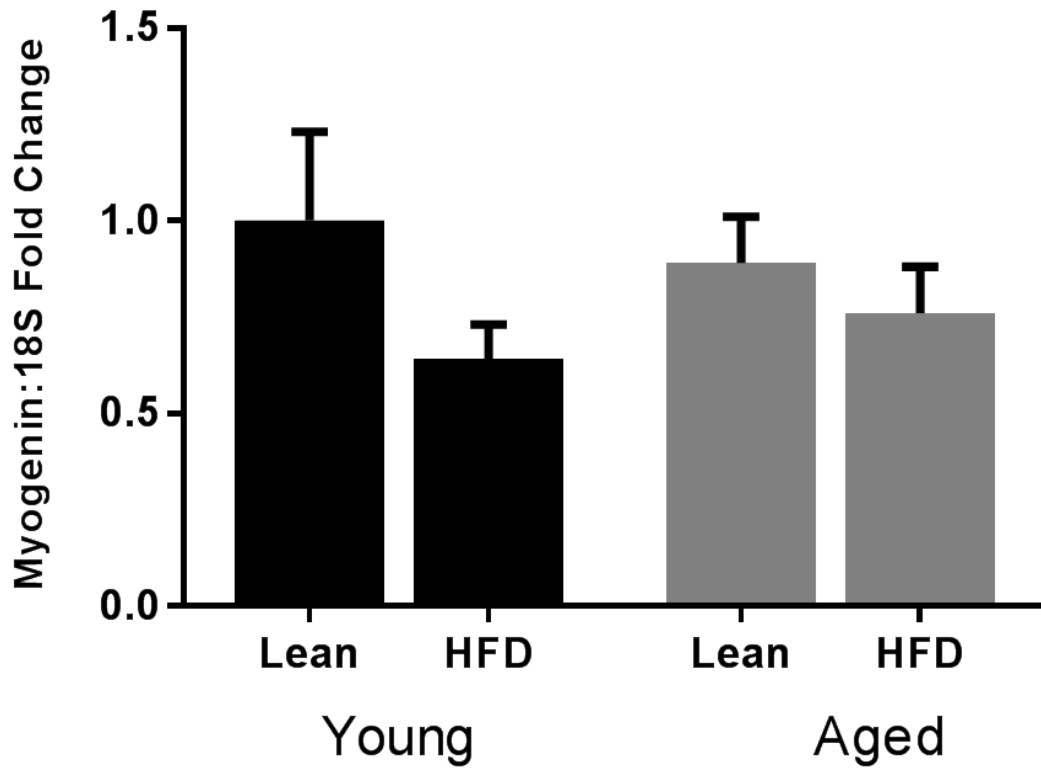
F.
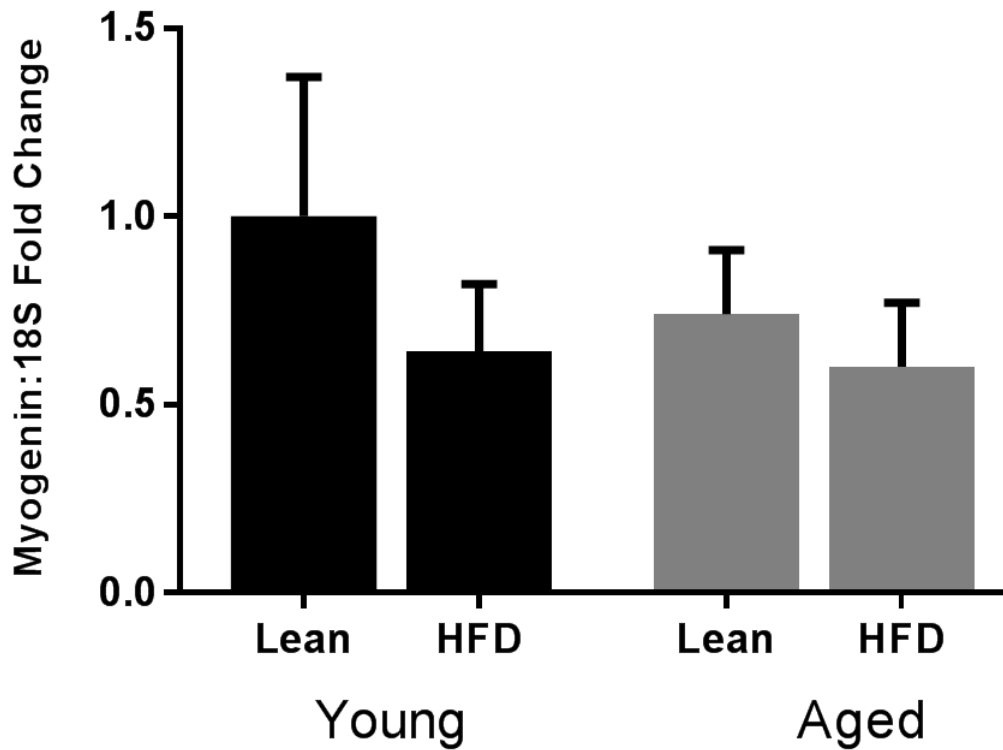
Figure 4
A.
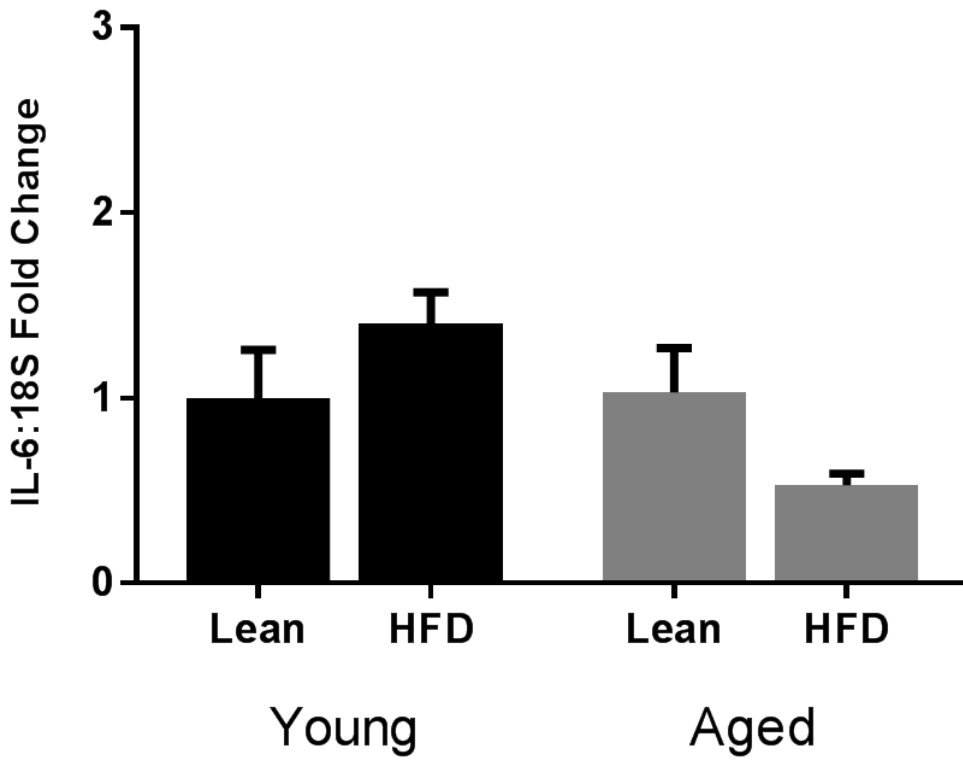
B.
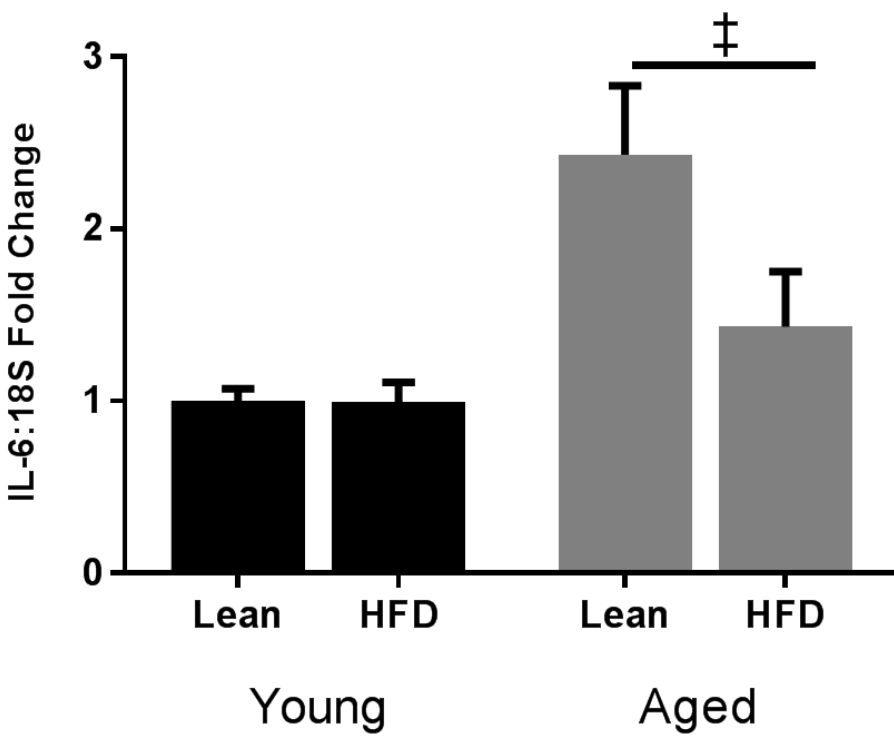
C.
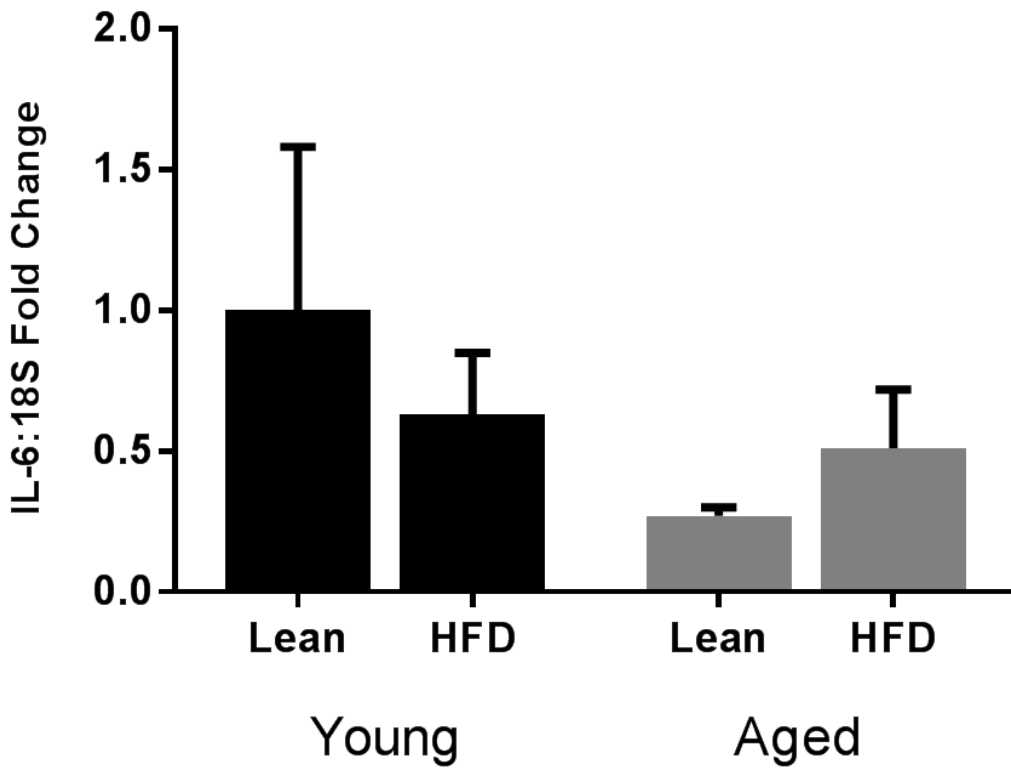
D.
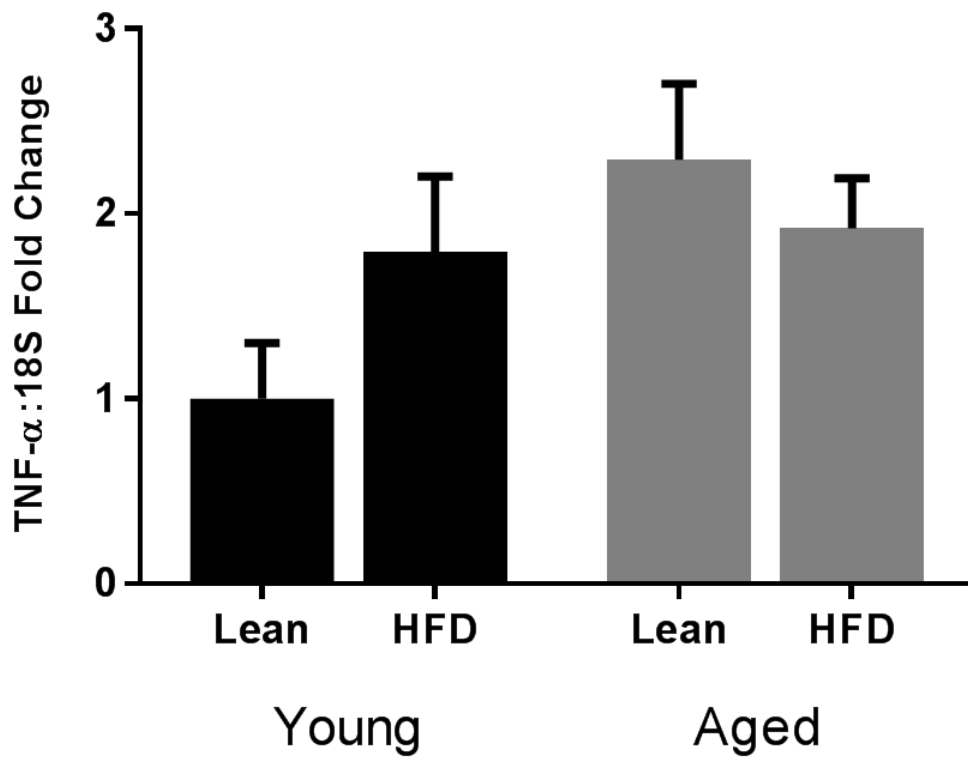
E.
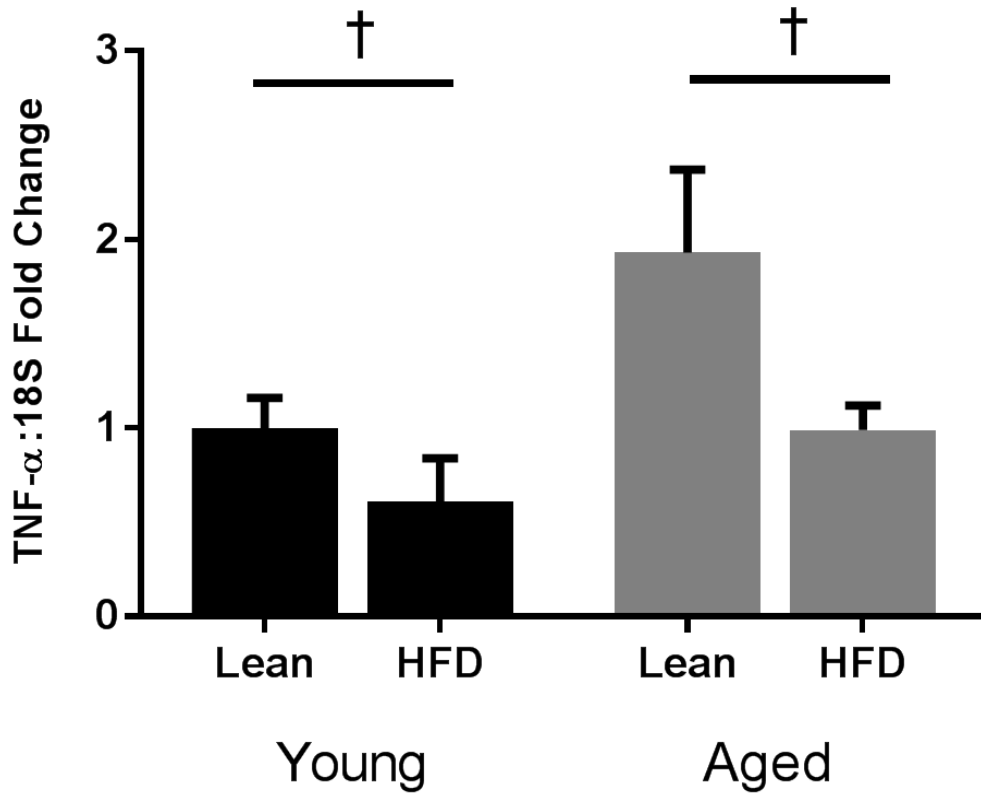
F.
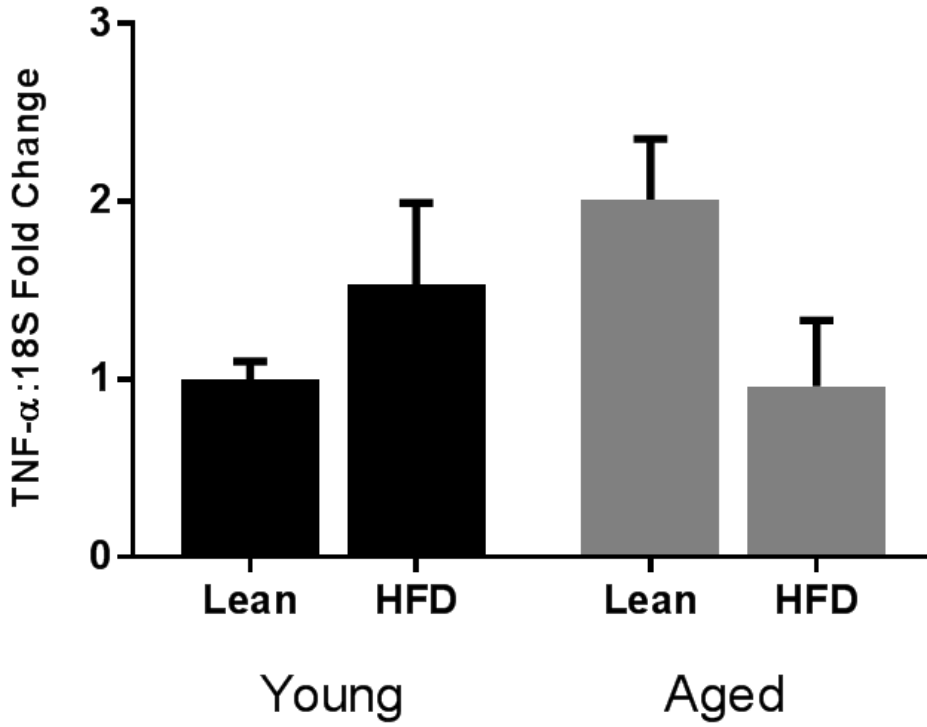
G.
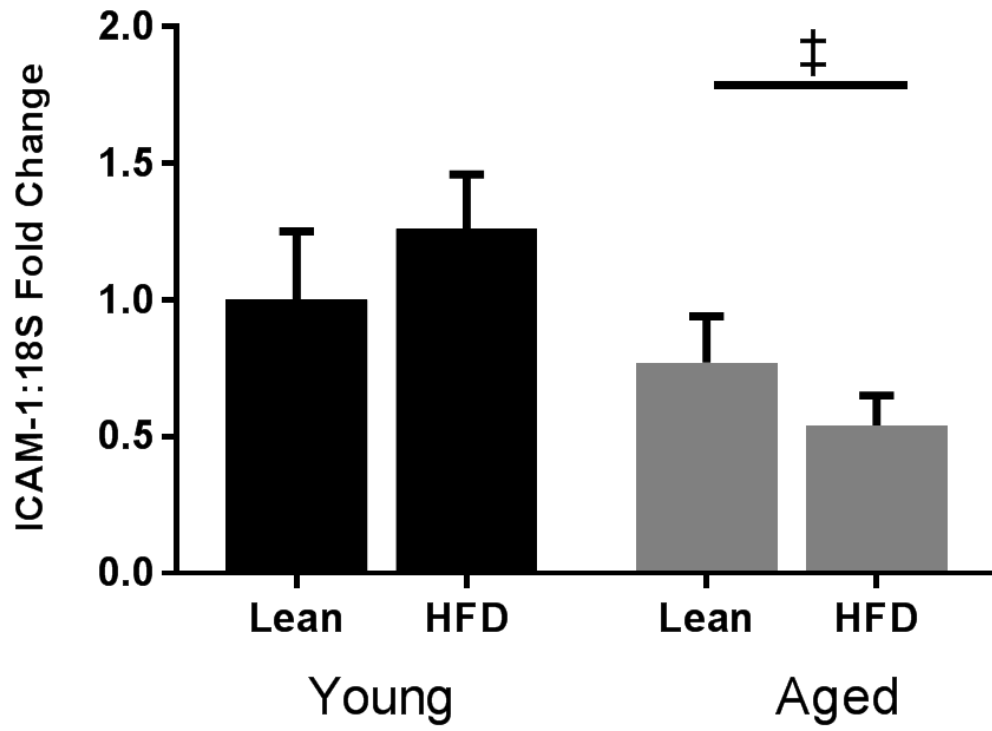
H.
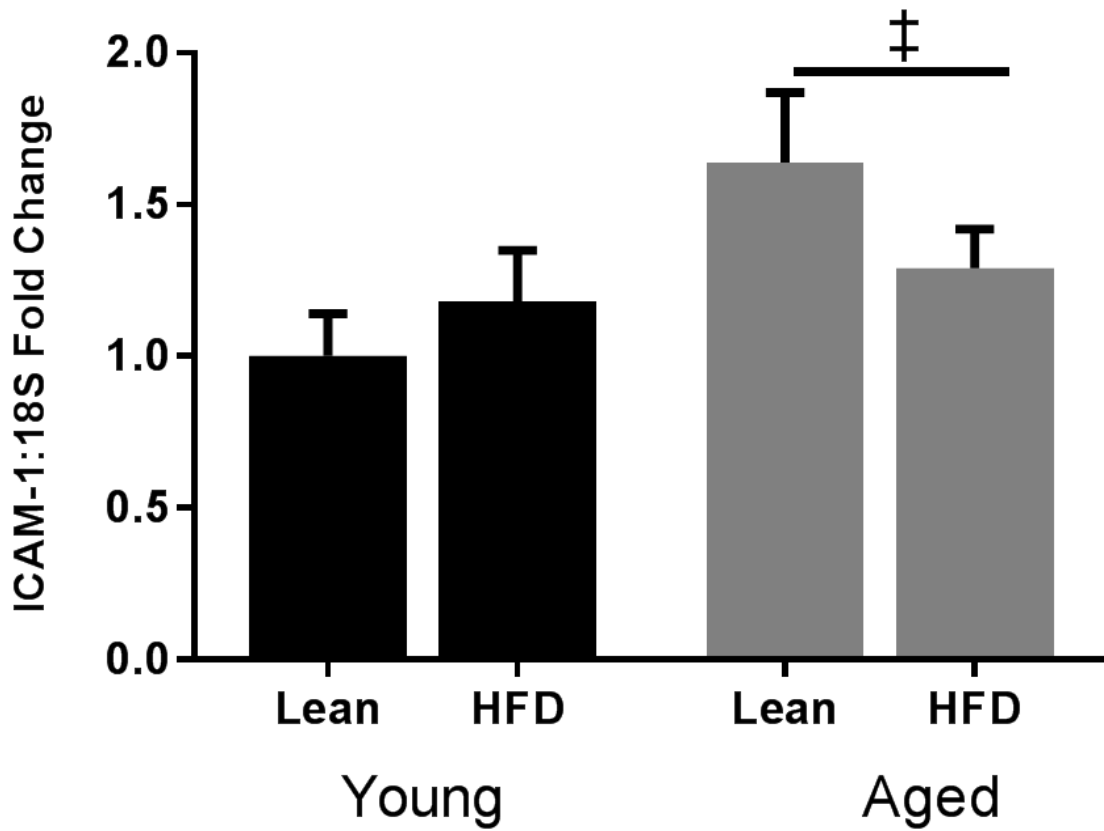
I.
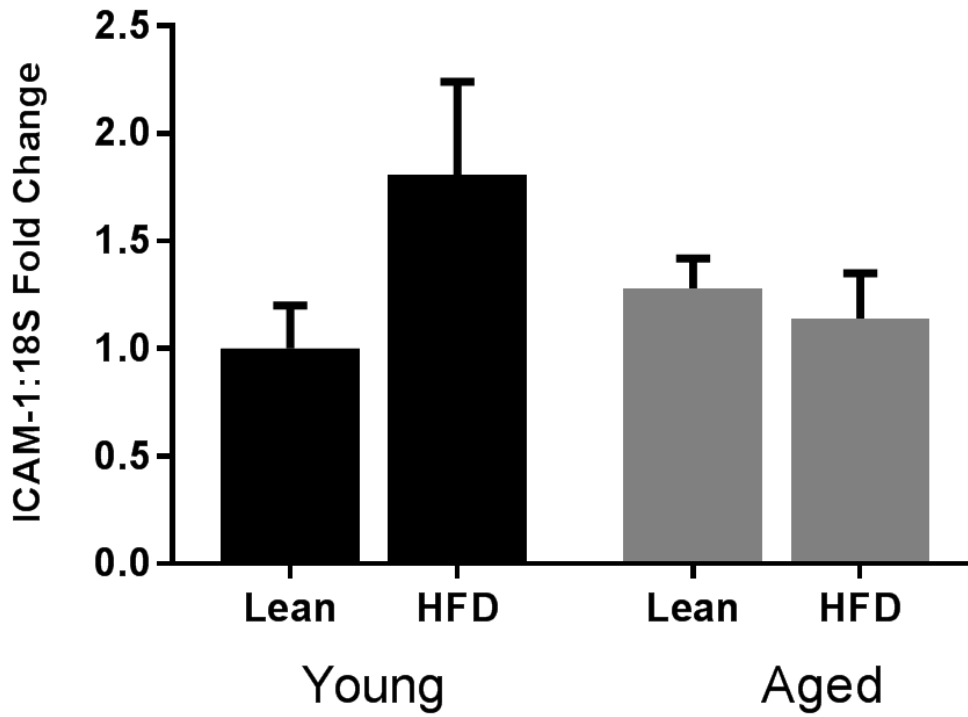
Figure 5
A.
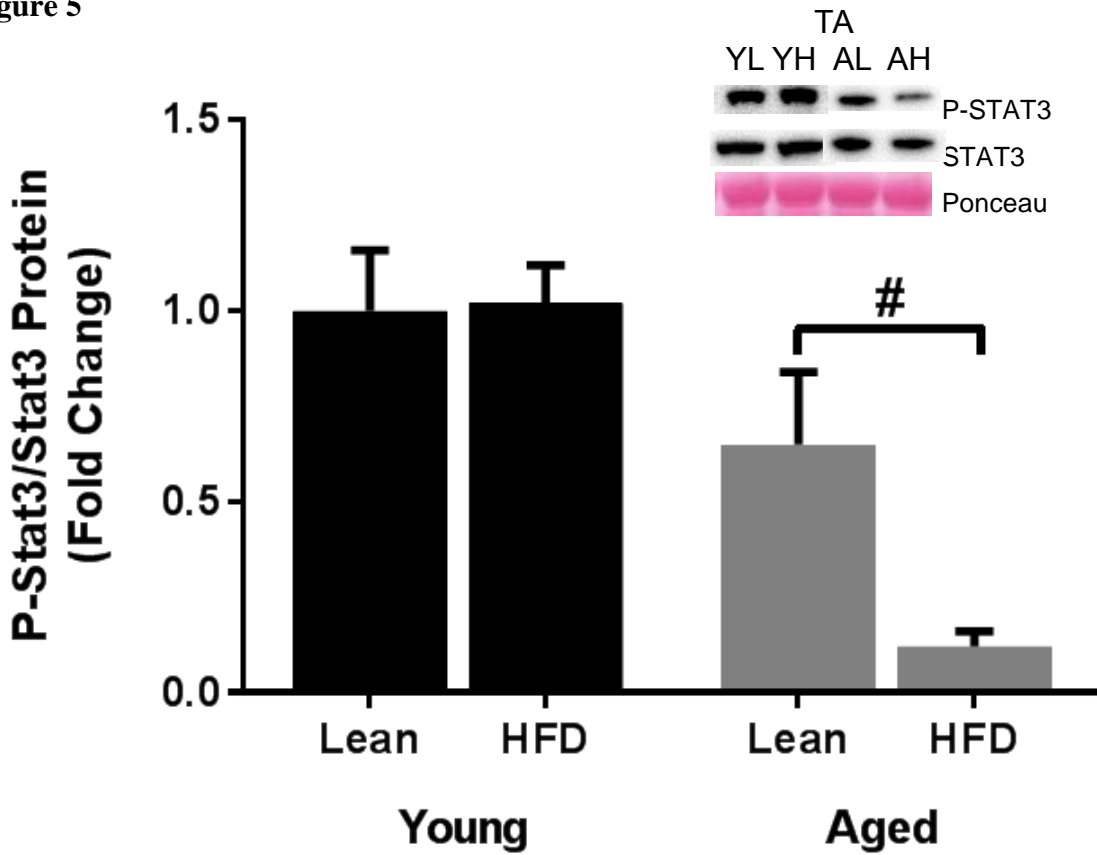
B.
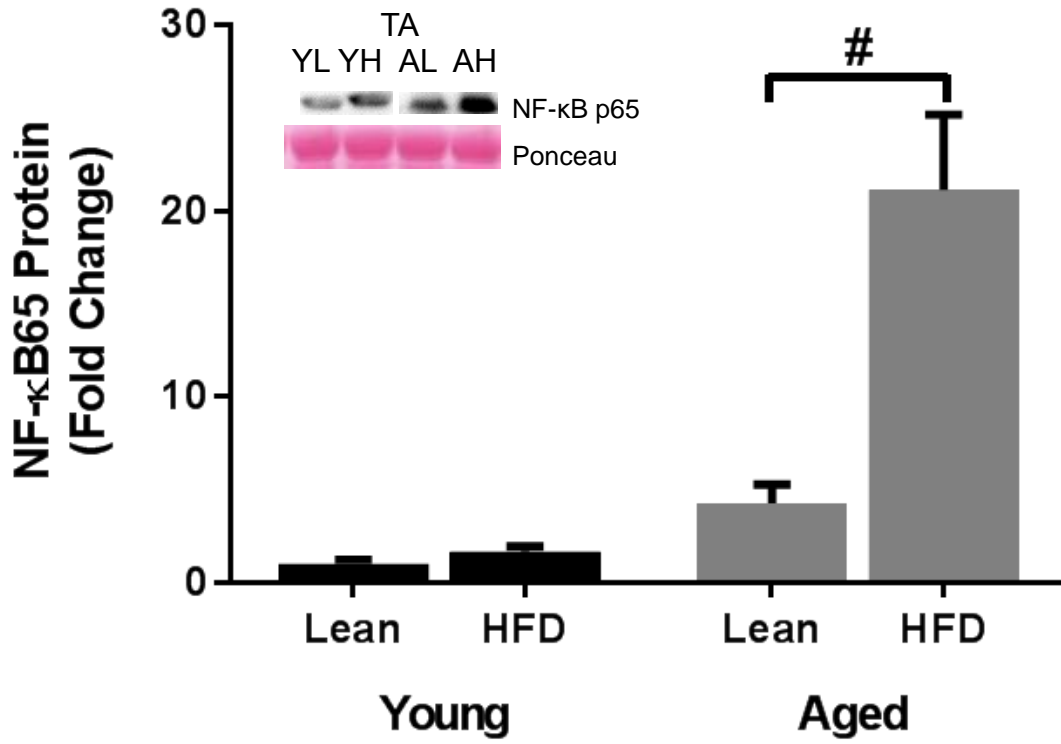
C.
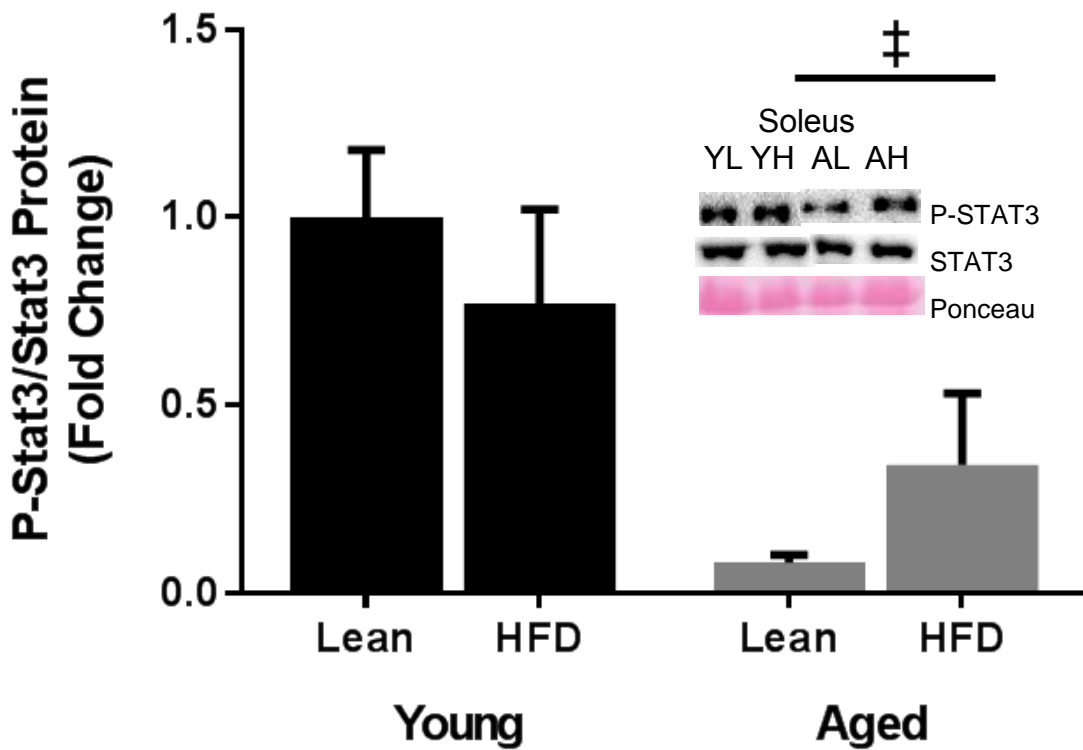
D.
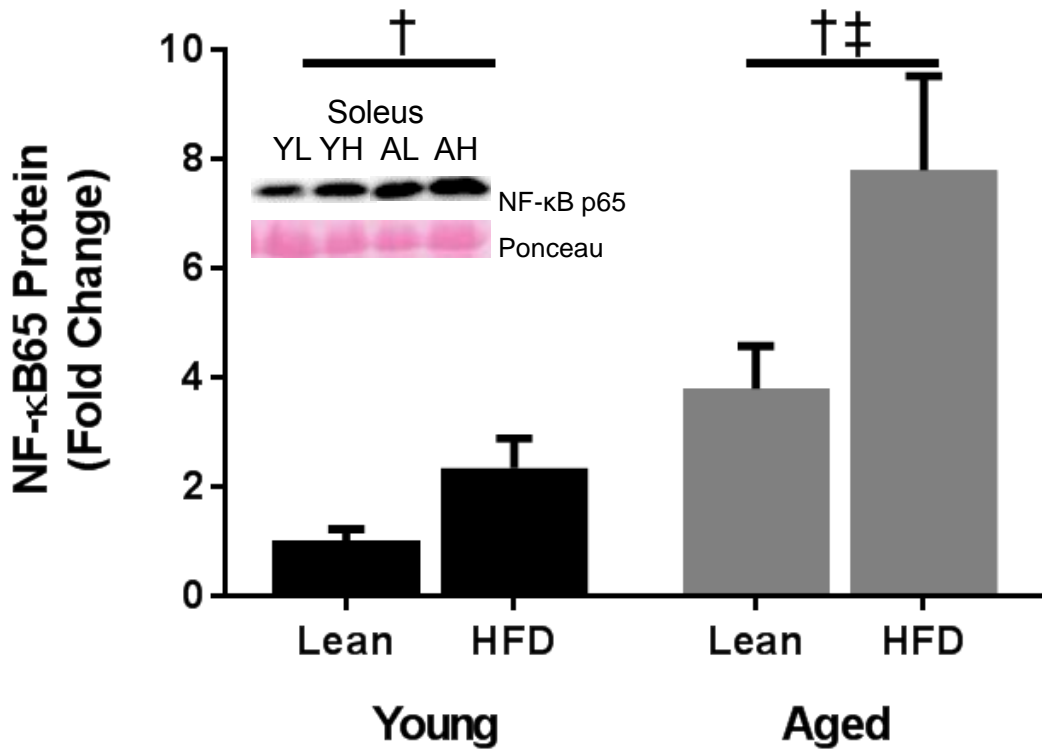
E.
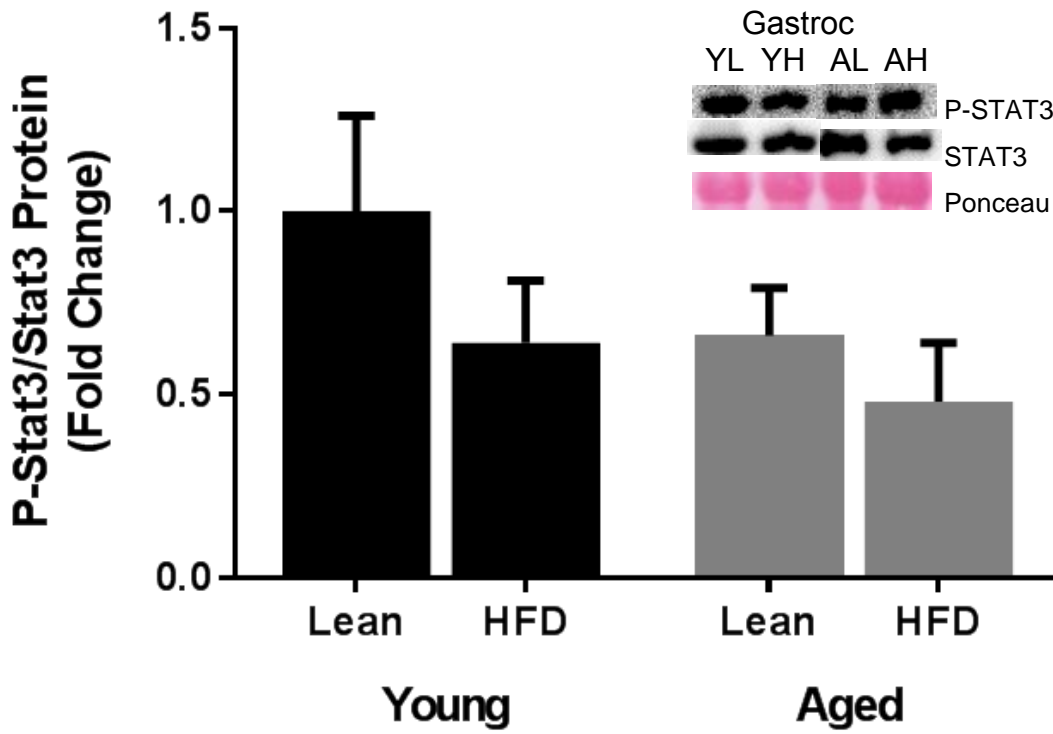
F.
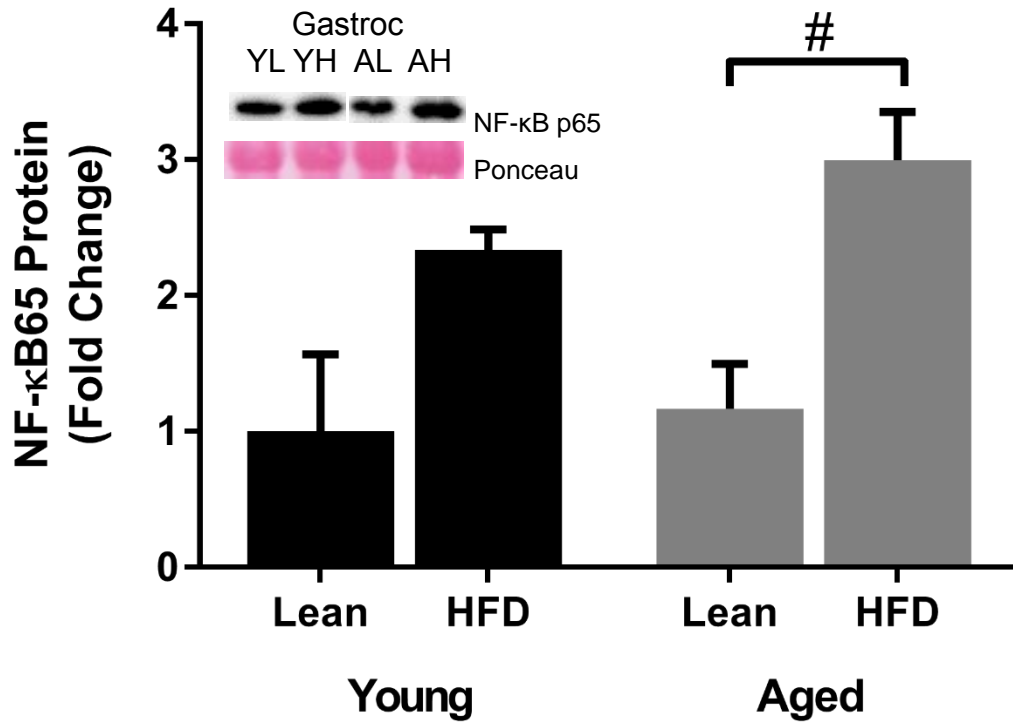
Figure 6

A.
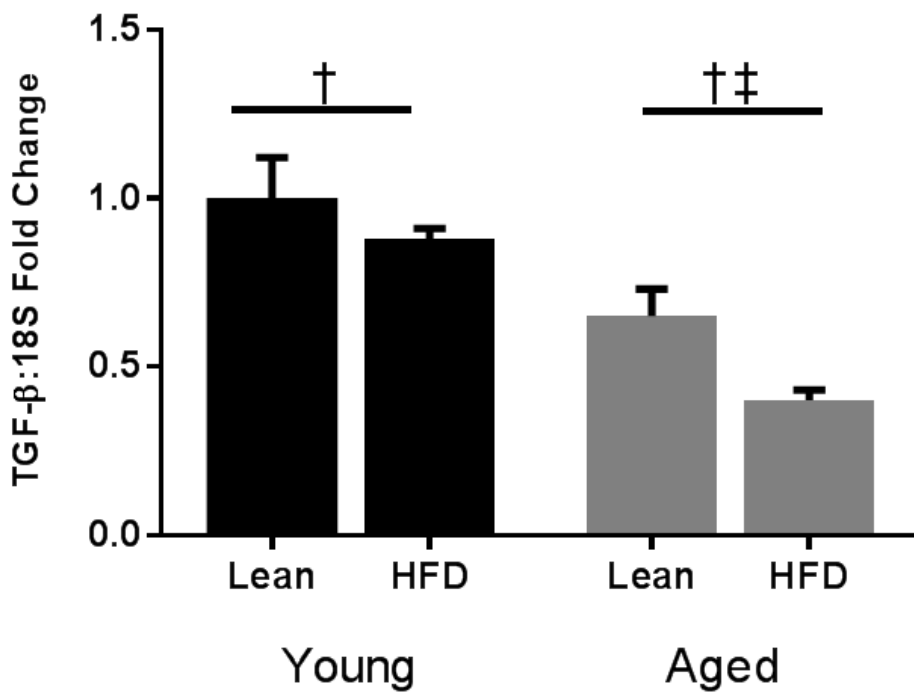
B.
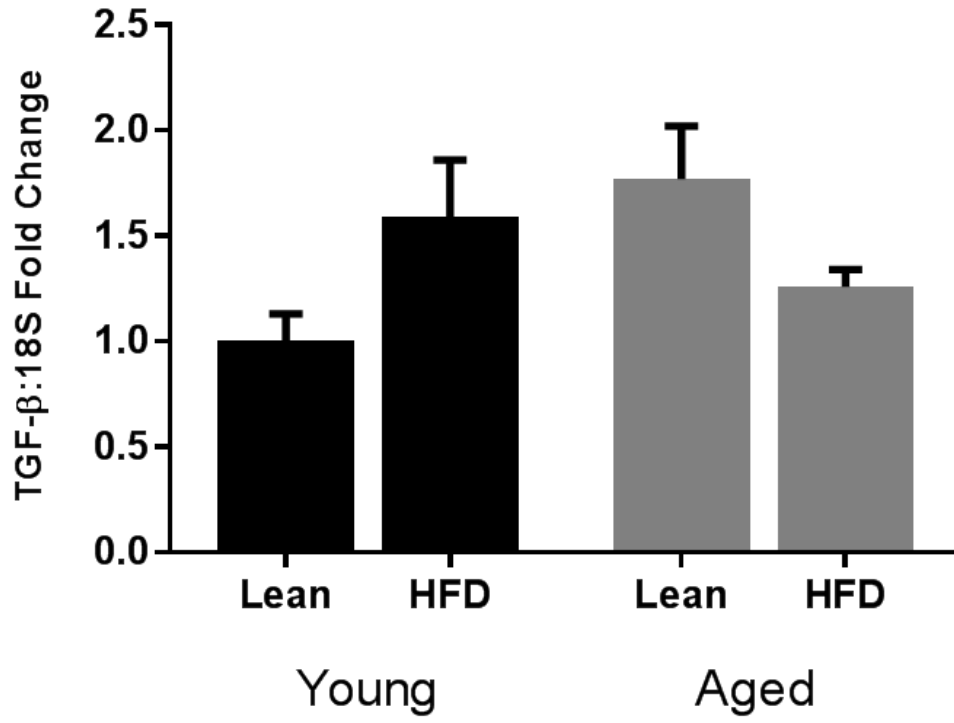
C.
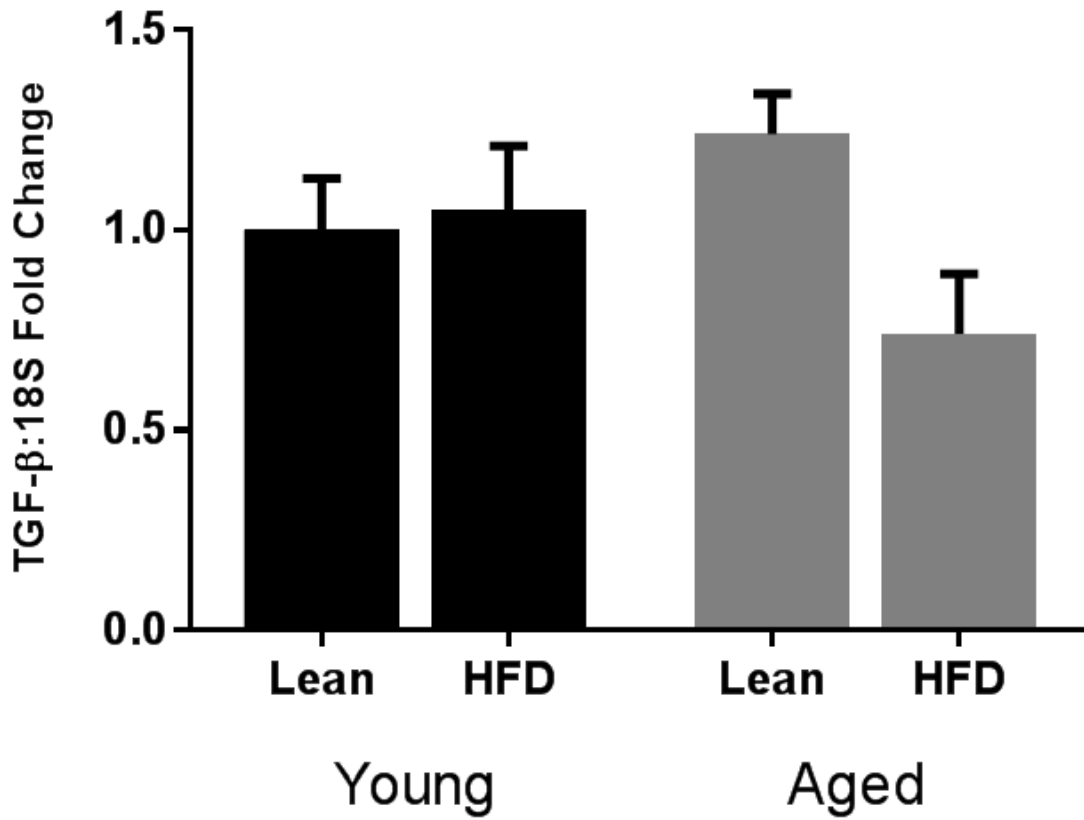
D.
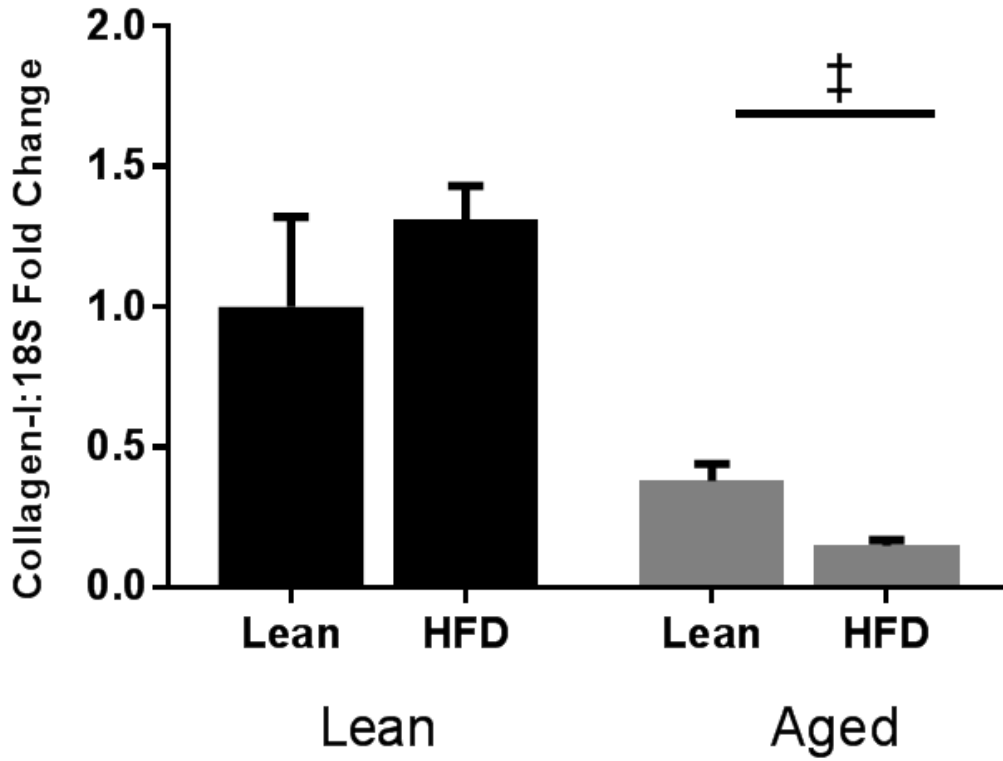
E.
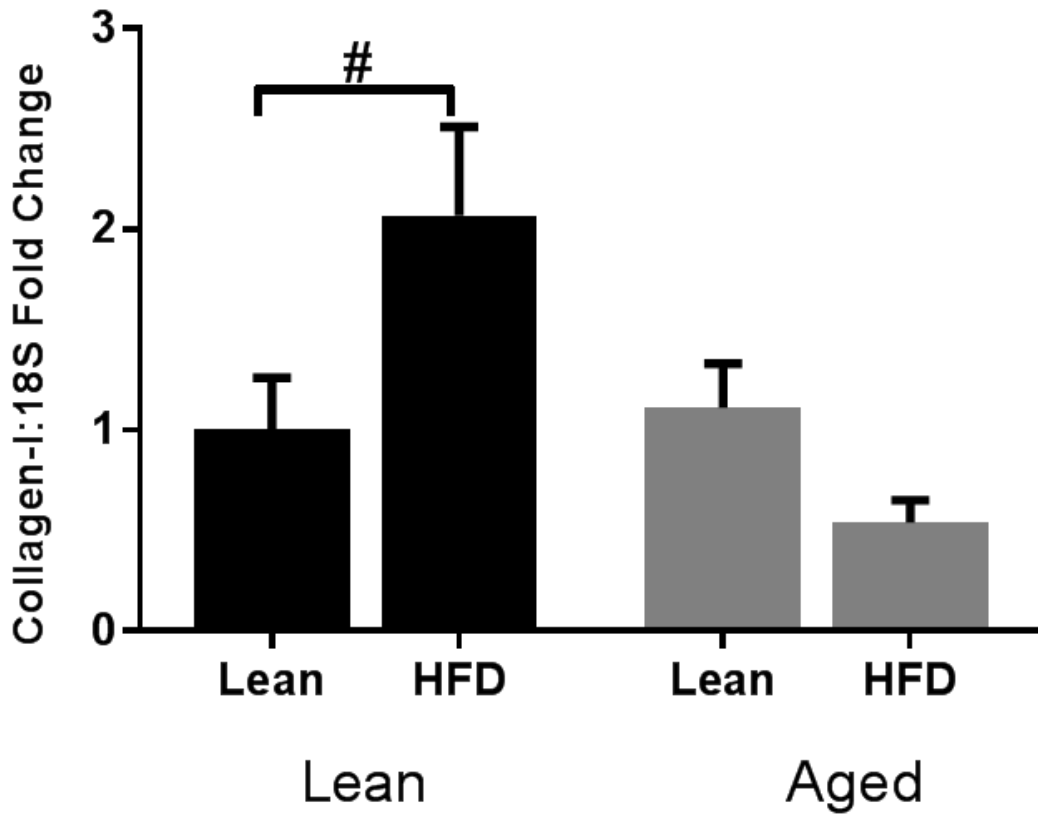
F.
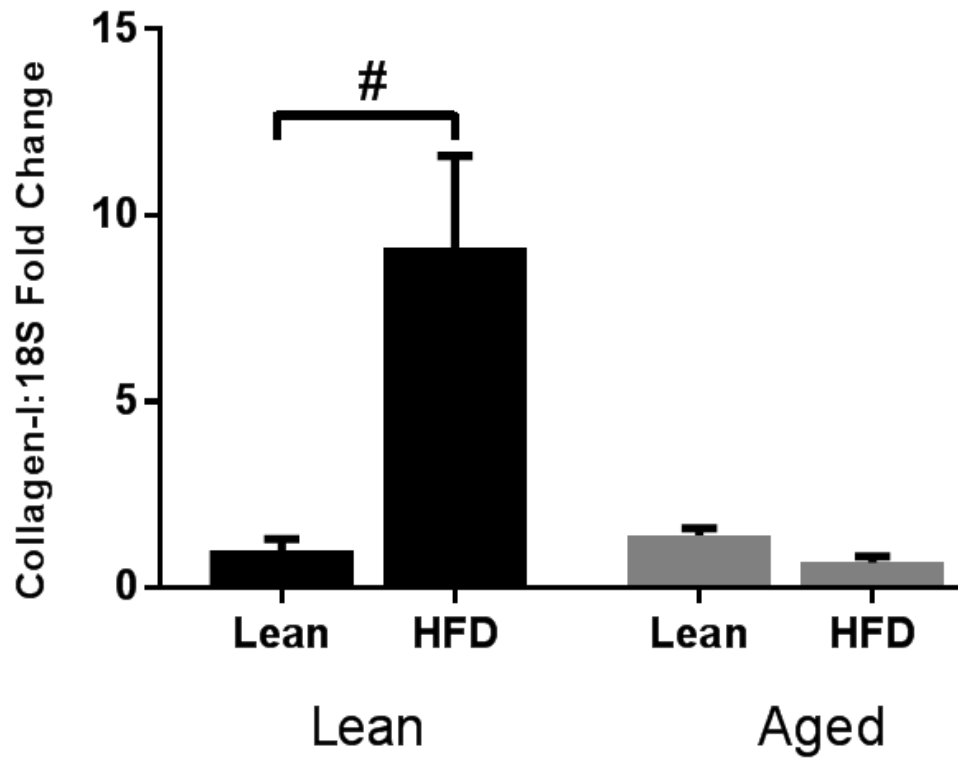
G.
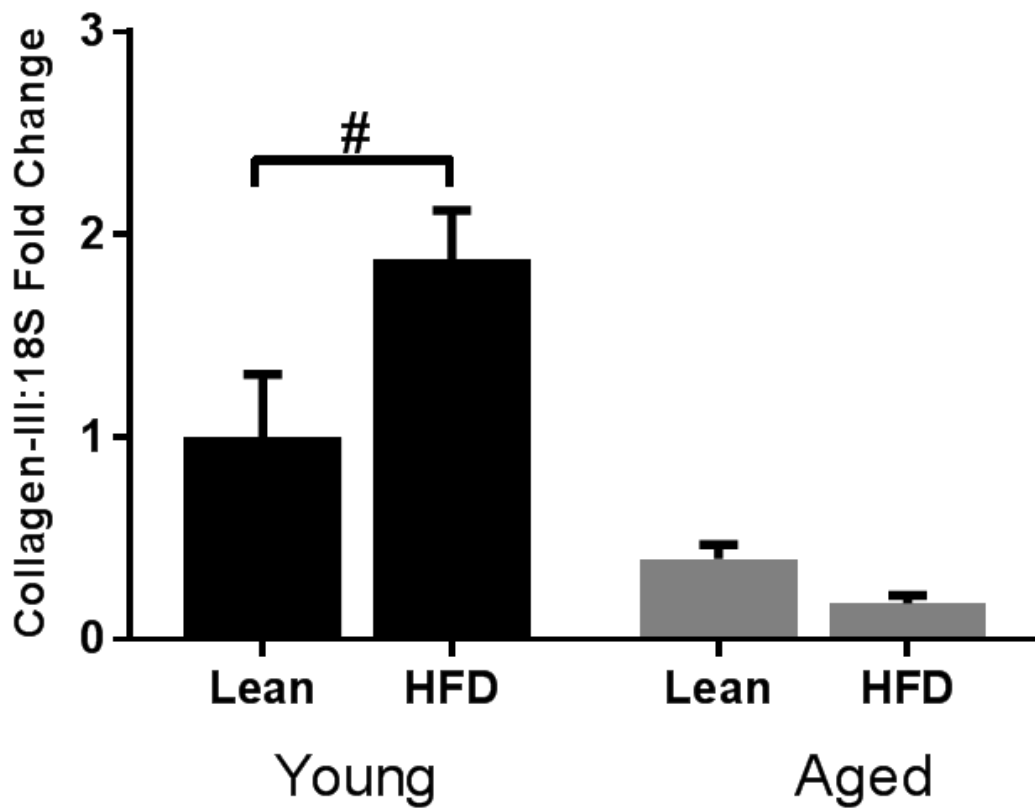
H.
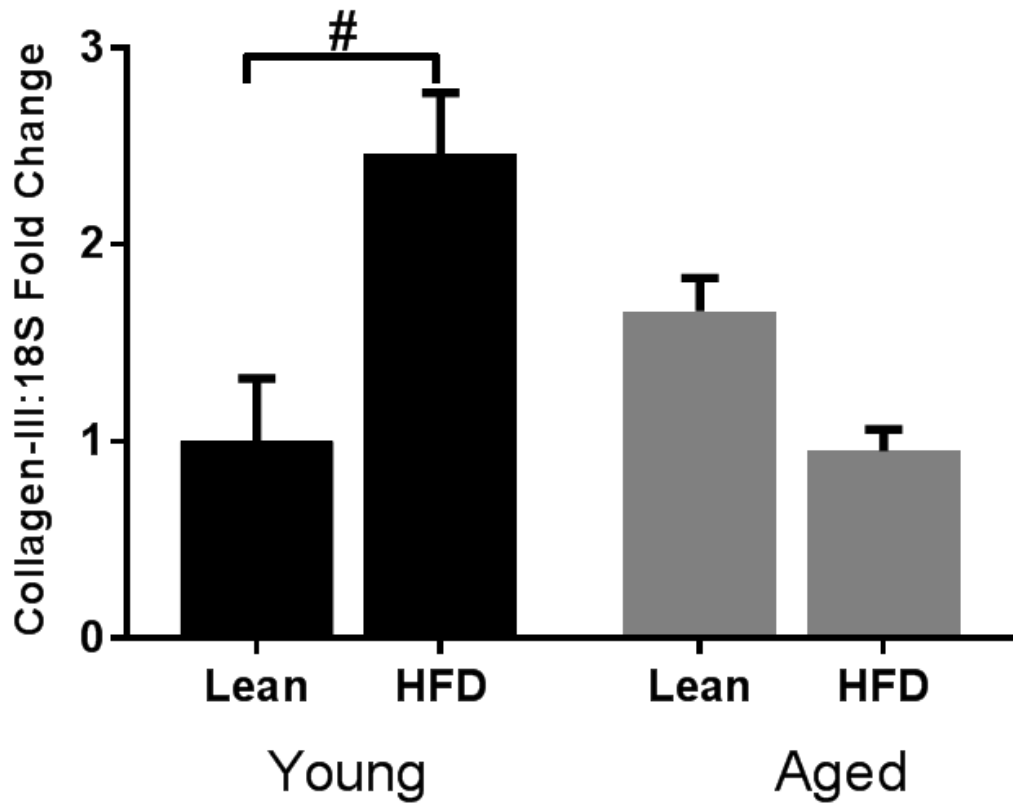
I.
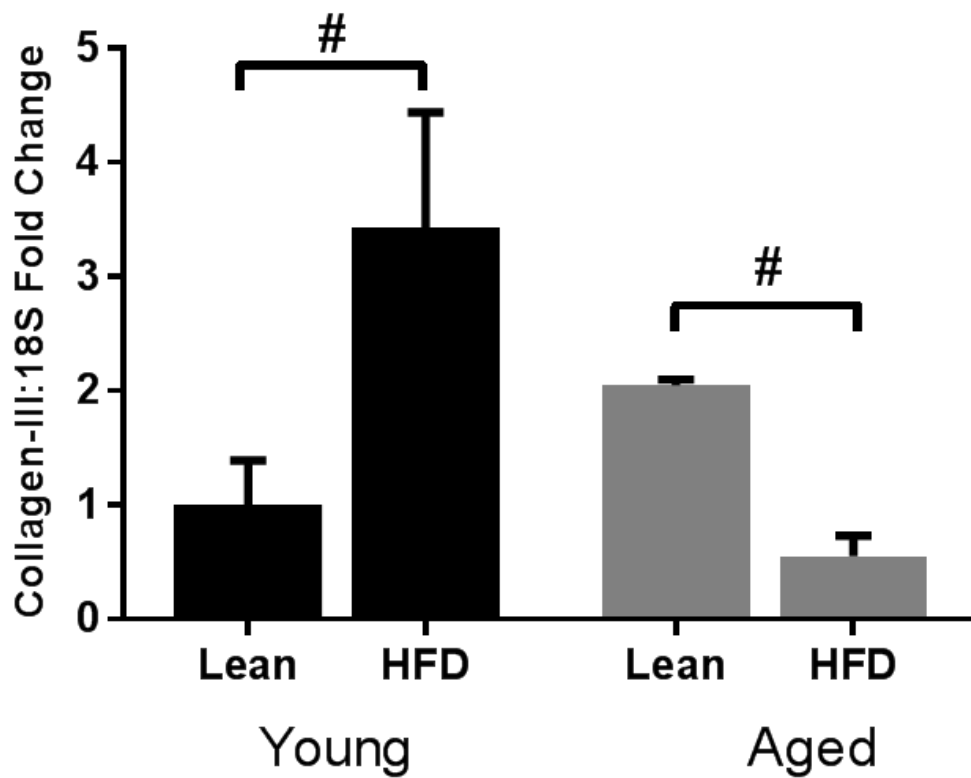
J.
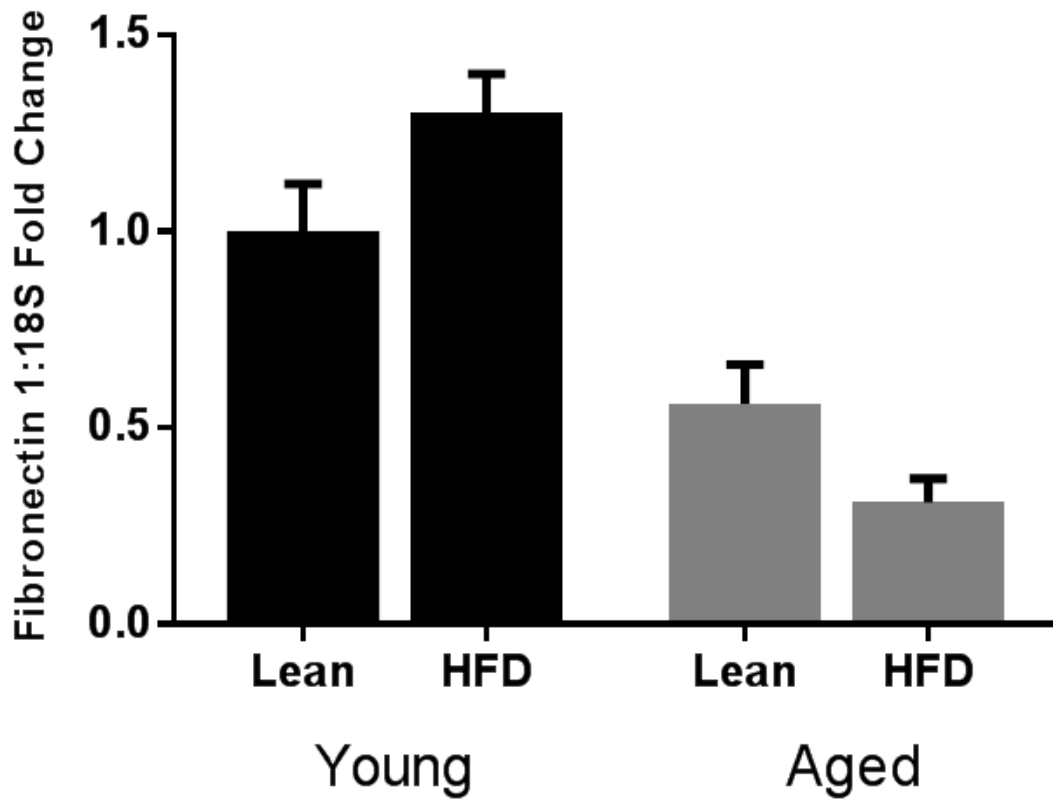
K.
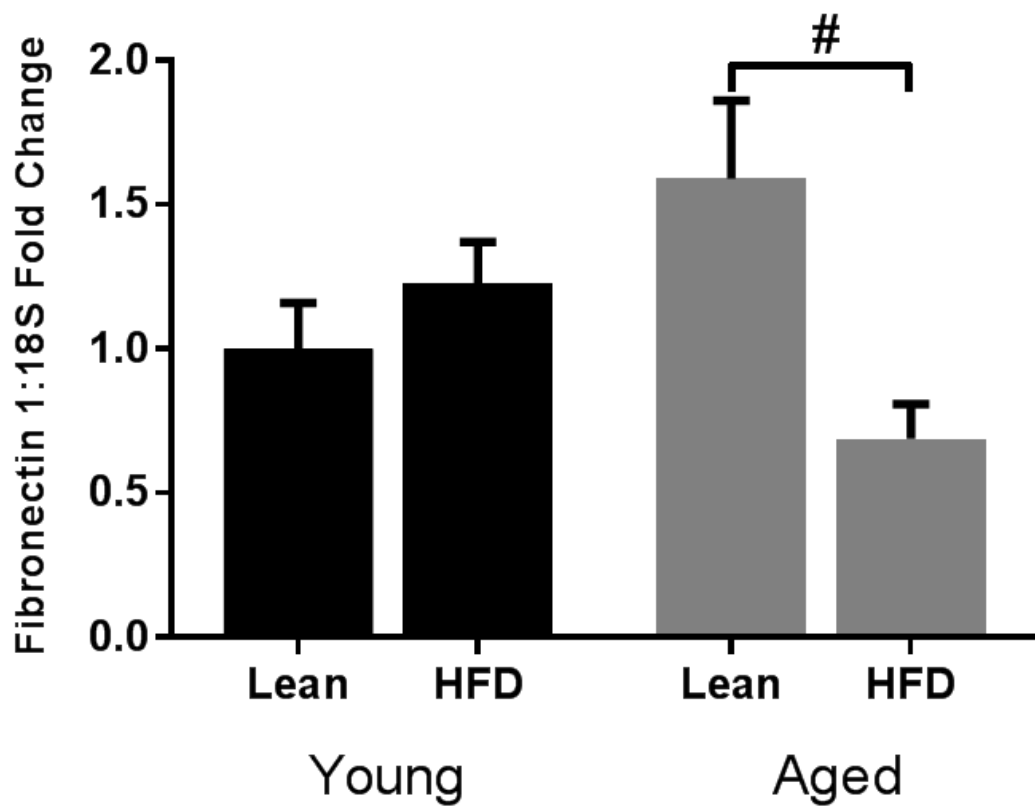
L.
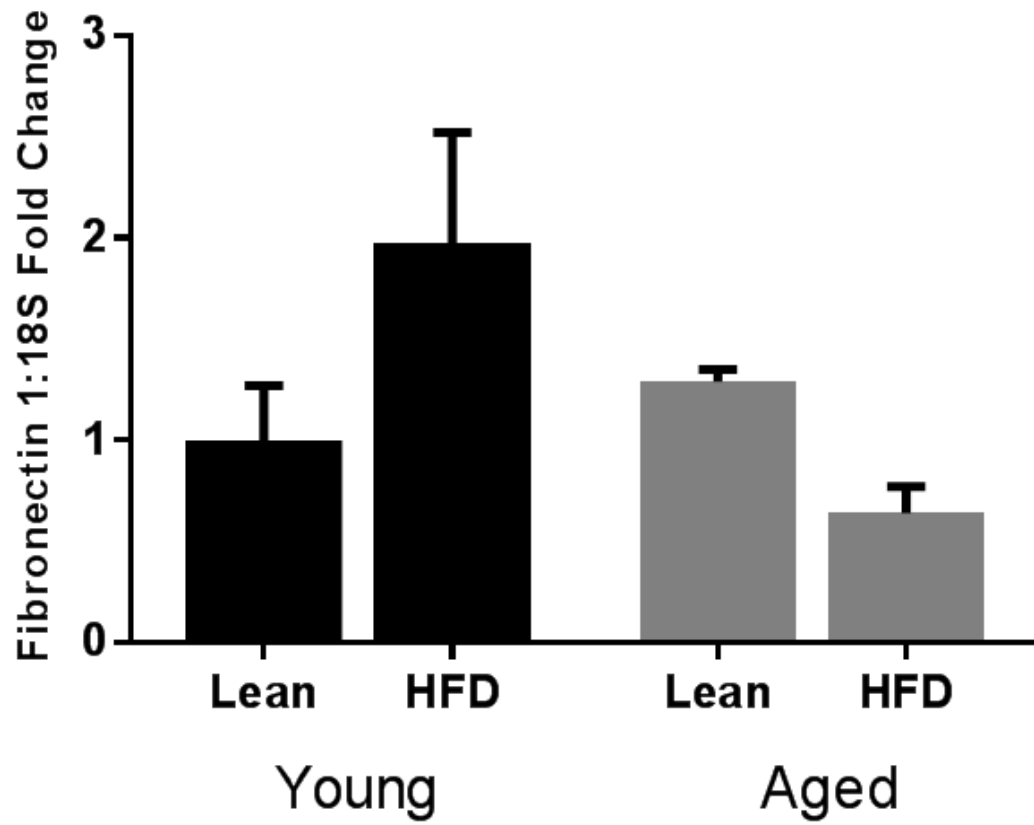
Figure 7
A.
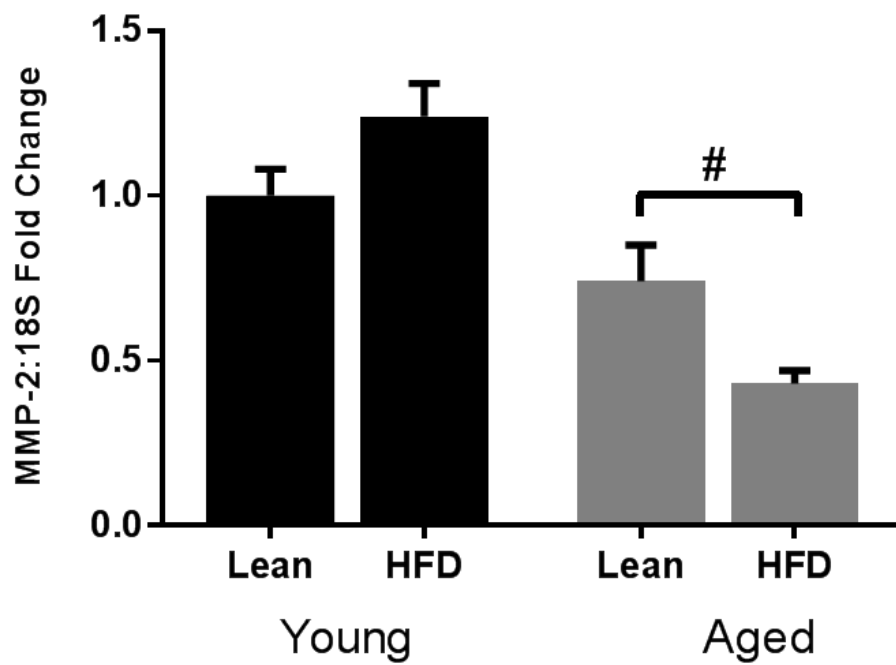
B.
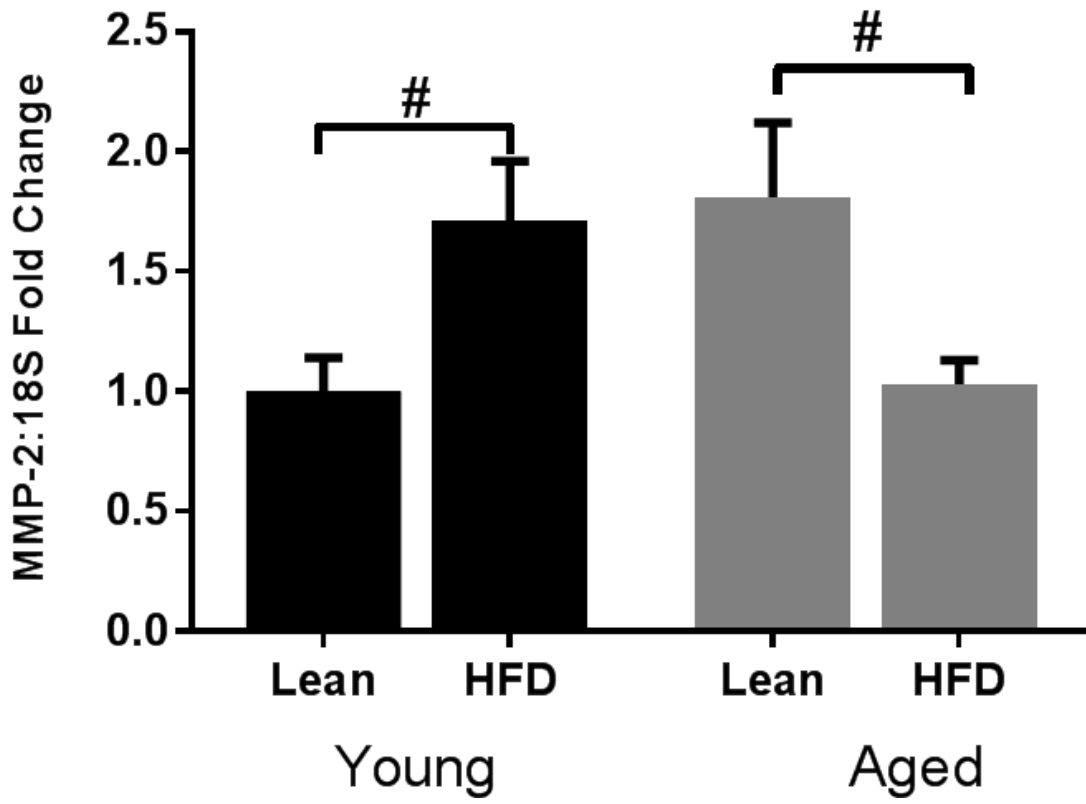
C.
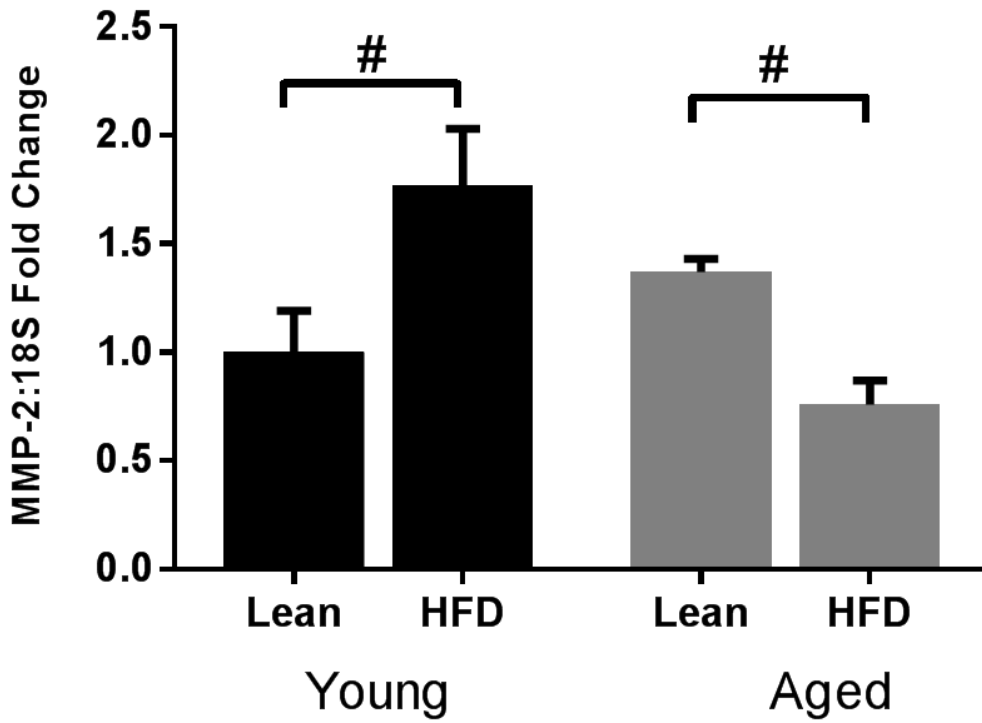
D.
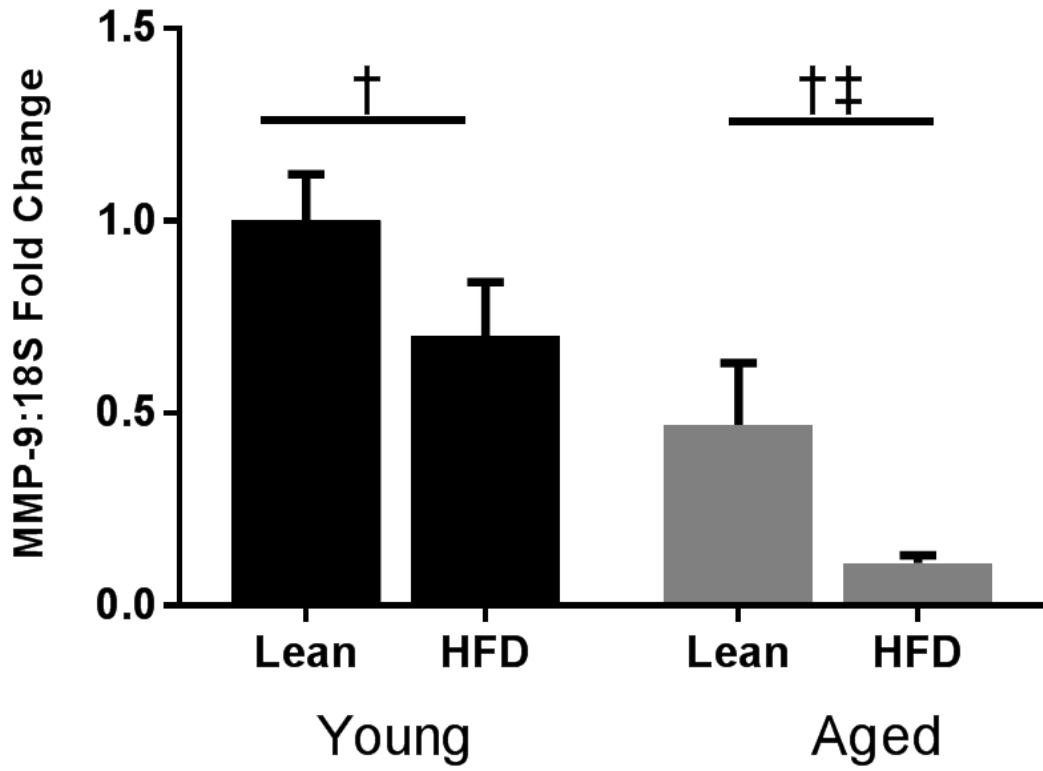
E.
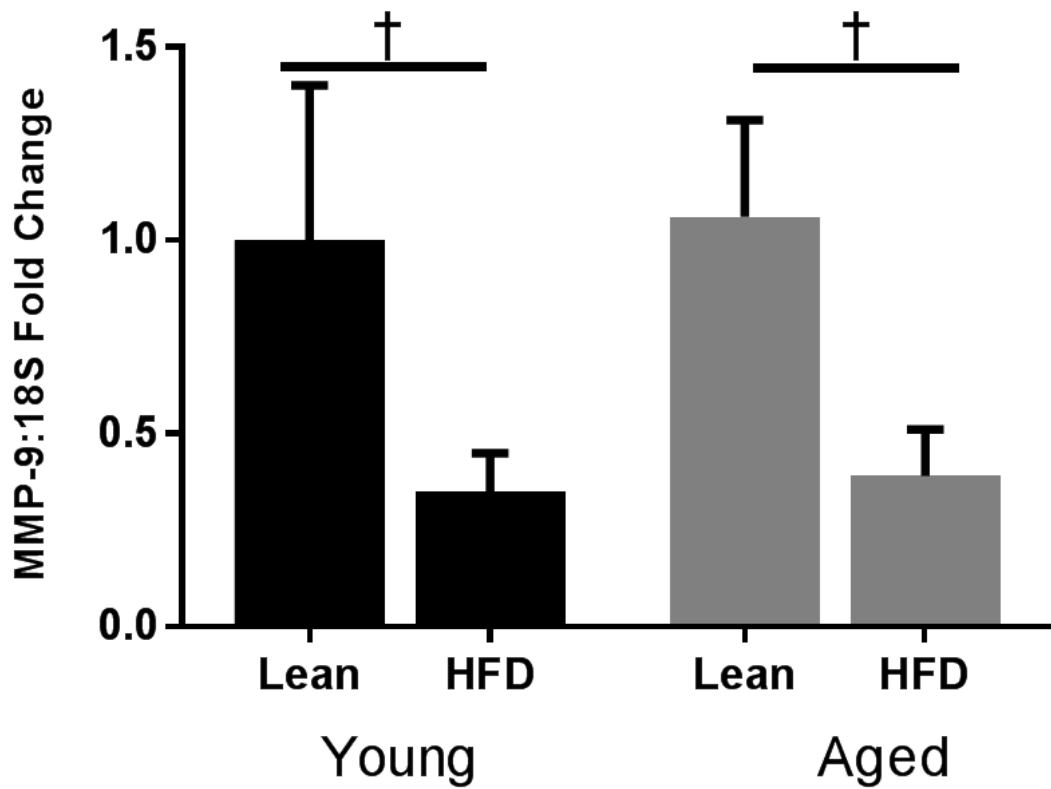
F.
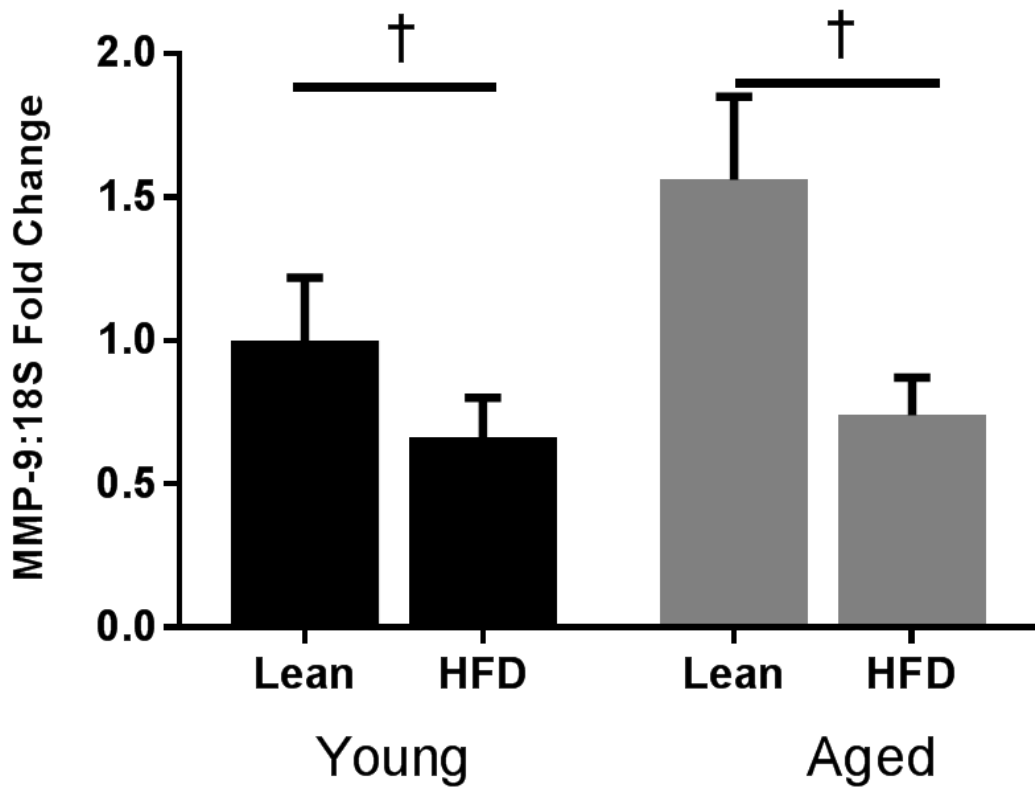
G.
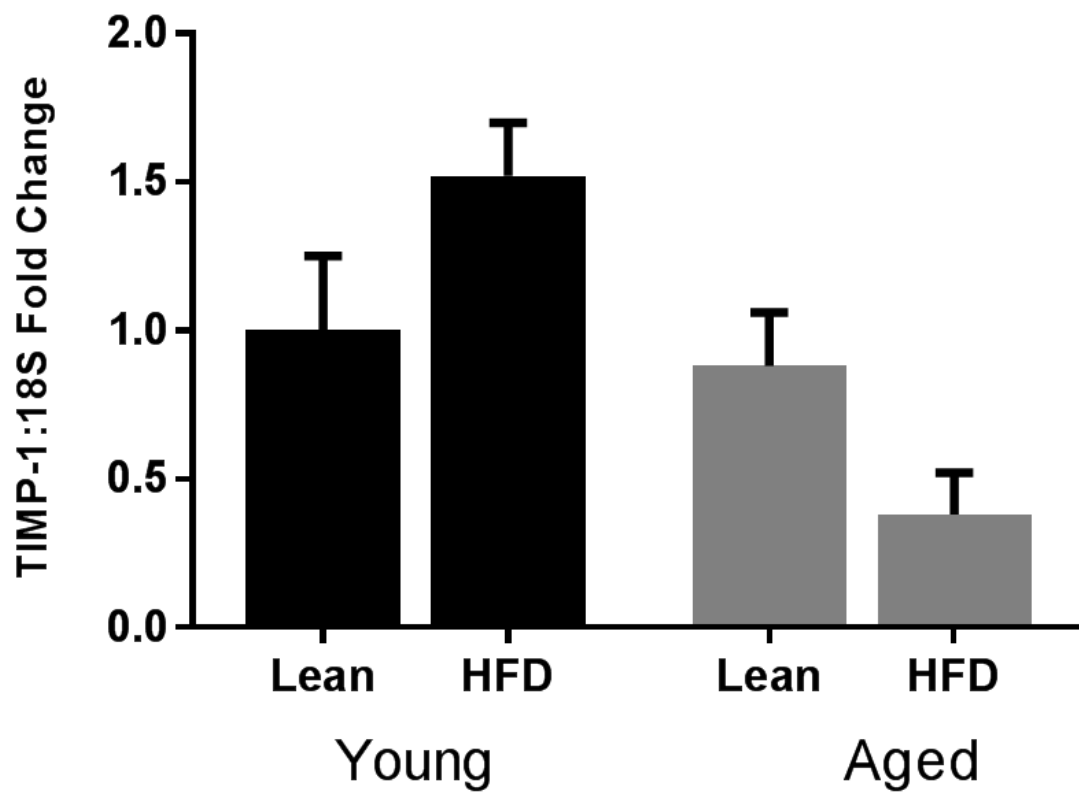
H.
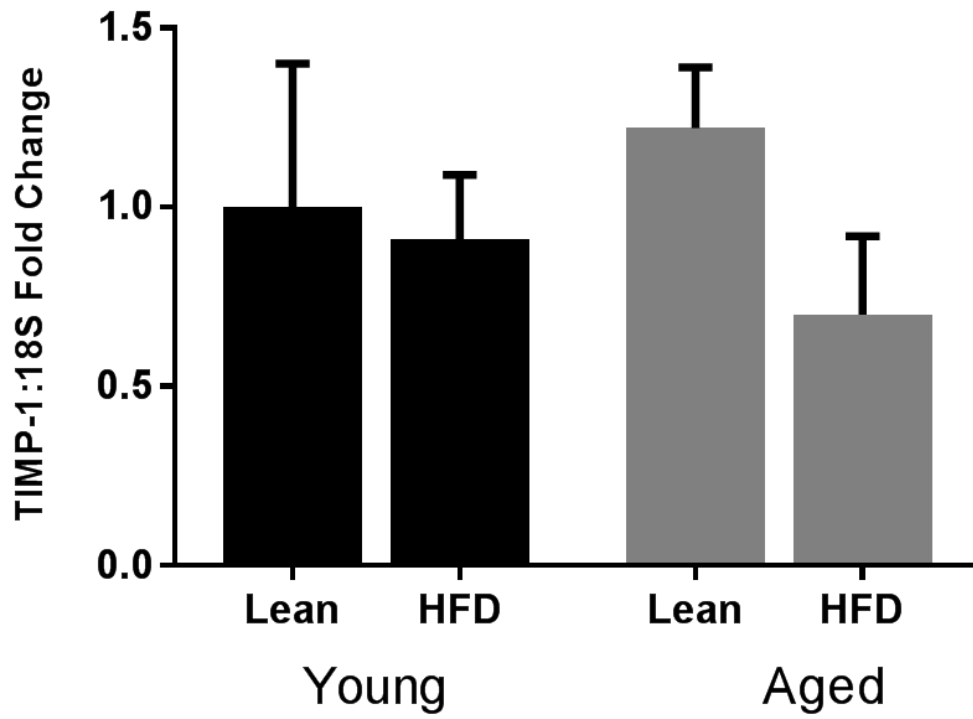
I.
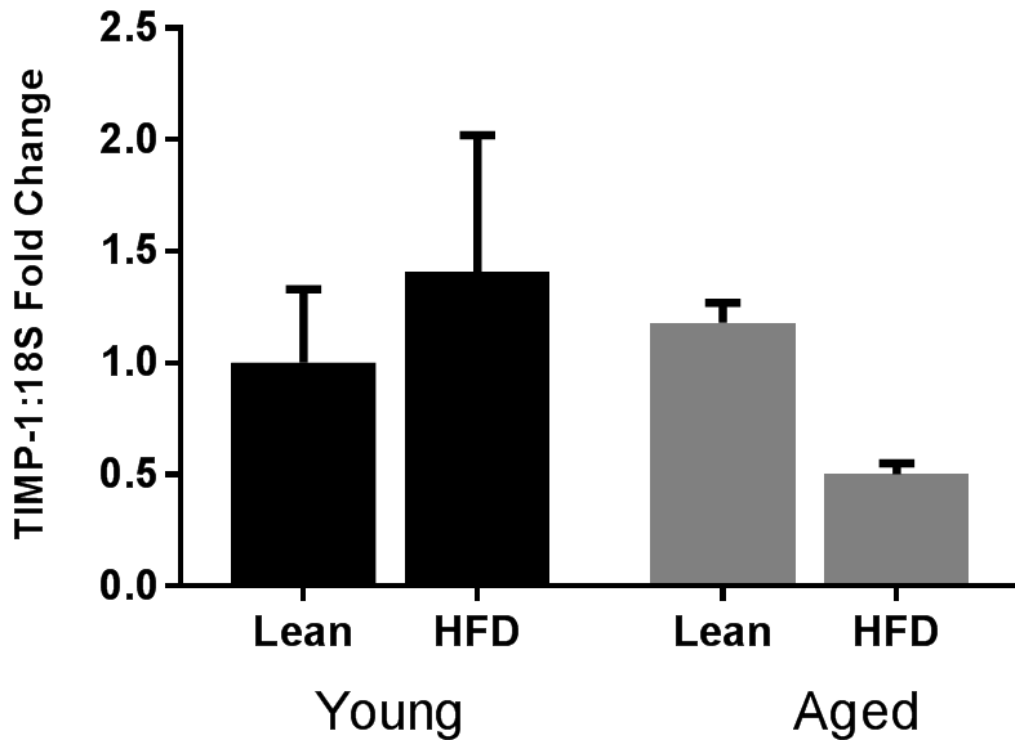
Chapter 4

Diet-induced obesity alters inflammatory signaling in sarcopenic mice at the onset of skeletal muscle regeneration

[1,2]Lemuel A. Brown, [1,2]Richard A. Perry, [1,2]Wesley S. Haynie, [2]David E. Lee, [2]Megan E. Rosa, [2]Jacob L. Brown, [2]Nicholas P. Greene, and [1,2]Tyrone A. Washington

[1]Exercise Muscle Biology Laboratory, [2]Human Performance Laboratory, Department of Health, Human Performance and Recreation, University of Arkansas, Fayetteville AR 72701

Running Title: Aged Diet-induced obesity and muscle regeneration

Corresponding author:
Tyrone A. Washington, Ph.D.
University of Arkansas
Department of Health, Human Performance, and Recreation
155 Stadium Dr. HPER 308H
Fayetteville AR 72701

Office Phone: 479-575-6693
Fax: 479-575-5778
tawashin@uark.edu

Abstract

AIM: Sarcopenic obesity has become a major concern because older adults have become the fastest growing obese population in North America. Sarcopenic obese individuals are associated with major health concerns along with increased risk of disability and will result in reduce quality of life. Aging and obese populations are associated with reduced recovery with injury and systemic low-grade inflammation. The inflammatory response is a major regulator in muscle regeneration which is needed for repair. The regenerative process is also dependent on myogenic regulatory factors (MRFs) for optimal muscle growth. The purpose of this study was to determine how sarcopenic obesity alters MRFs and inflammatory signaling during muscle regeneration in mice. **METHODS:** One hundred two male C57BL6/J mice (4 weeks old) were randomly assigned to either a high fat diet (HFD, 60% fat) or normal chow. Both young mice (12 weeks) and aged mice (22-24 months old) were injected with either PBS (control) or bupivacaine (myotoxin). The TA was excised 3 or 21 days after injection. **RESULTS:** The aged lean injured mice had 9% greater mean cross-sectional area than the control mice 21 days following muscle damage but no changes were observed in aged HFD injured mice. There were no reported changes in MRF gene expression in the aged HFD mice 3 and 21 days post-injection. There was a main effect of diet to increase NF-κB in the aging HFD mice 3 days following muscle damage. NF-κB was 3-fold greater in the aged HFD injured mice compared to the uninjured mice 21 days following muscle damage. **CONCLUSION:** Sarcopenic obese mice had reduced regenerative capacity partially due to impaired inflammatory signaling.

Keywords: aging, high fat diet, cytokines, myogenic regulator factors, adhesion molecules

Introduction

Currently, close to 40% of Americans 65 years of age and older are obese (**CDC**). The majority of these older adults also suffer from an age-related decline in muscle mass known as sarcopenia (Rosenberg, 1989). These individuals would be considered sarcopenic obese which is defined as a metabolic syndrome in which there is excess adipose tissue along with an age-related decline of muscle mass (Choi, 2013; Lim et al., 2010; Lynch, 2011; Rosenberg, 1989). This is alarming because little is known about the symptoms and associated health risks involved with this sub-population. It has been identified that both aging and obesity are associated with chronic systemic low-grade inflammation. Nevertheless, chronic inflammatory signaling negatively impacts numerous physiological processes involved with recovery including skeletal muscle regeneration, which is needed for optimal muscle repair (Hu et al., 2010; Nguyen et al., 2011).

Skeletal muscle regeneration is essential for the repair of damaged muscle fibers. It involves the coordination of inflammatory signaling, satellite cell activation, and extracellular matrix (ECM) remodeling for optimal muscle growth and repair. Similar to damage to other tissues and organs muscle damage evokes an inflammatory response to aid in the recovery process. In fact, the inflammatory response has been regarded as one of the earliest responses after the muscle has been damaged (Abbas et al., 2011; Schiaffino & Partridge, 2008). This is because inflammatory cells are involved in the removal of necrotic muscle tissue as well as regulating myogenic regulatory factors (MRFs) that involved in myoblast proliferation and differentiation that is necessary in the early stages of skeletal muscle regeneration (S. E. Chen et al., 2005; Toth et al., 2011).

After muscle damage occurs, phagocytes circulating in the bloodstream will be

recruited to infiltrate the endothelial wall into the skeletal muscle ECM. Upon arrival, phagocytes will engulf damaged tissue and secrete several cytokines such as TNF-α and IL-6 to assist in myoblast proliferation and differentiation. The expression of pro-inflammatory cytokines will be elevated for several days peaking at around 48-72 hours following muscle damage and reach basal levels a few weeks later (Hirata et al., 2003). In addition, resident macrophages located in the ECM of skeletal muscle tissue will secrete cytokines that will facilitate the influx of phagocytes to the site of muscle injury.

Recruitment of phagocytes contribute to muscle growth and is a part of the muscle regeneration process. The adhesion molecule, ICAM-1, is partially responsible for phagocyte recruitment and infiltration within various tissues (Abbas et al., 2011). Dearth and colleagues examined an overload muscle model and discovered that ICAM-1 expression was increased by more than 10 fold in wild-type mice 3 days following muscle overload-induced damage (Dearth et al., 2013). Furthermore, the percentage of regenerating fibers, as measured by Pax7 protein, were 3.5 fold higher in the wild-type mice compared to the ICAM -/- mice a week following muscle overload (Dearth et al., 2013). The role of pro-inflammatory cytokines and their relationship to the recruitment and infiltration has also been investigated in skeletal muscle. Cultured C2C12 treated cells treated with TNF-α induced ICAM-1 in primary myoblasts (Dearth et al., 2013). Furthermore, Zhang et al. examined macrophage recruitment in IL-6 knockout mice following cardiotoxin-induced muscle damage and observed a decrease in chemokines involved with macrophage infiltration days after muscle damage along with smaller myofibers two weeks following muscle damage (Zhang et al., 2013).

It has been observed in aging and pathophysiological disease that the alteration of inflammatory cytokines can delay or impair the muscle regeneration process (Cesari et al.,

2005). Recently, we examined diet-induced obese mice and discovered reduced IL-6 at basal levels and a blunted response TNF-α mRNA abundance at the onset of muscle regeneration (L. A. Brown et al., 2015). The obese mice also had no change in cross-sectional area and a reduction in skeletal muscle weight relative to tibia length 28 days following muscle damage (L. A. Brown et al., 2015). In the aging literature there have been a few reports finding that either older adults are not able to induce a pro-inflammatory response at the onset muscle regeneration or that there is no difference pro-inflammatory cytokine expression compared to young adults (Hamada et al., 2005; Pedersen et al., 2004). Thus, aging and obesity leads to chronic systemic low-grade inflammation, reduced inflammatory cytokines in skeletal muscle, and the inability to secrete a substantial amount of inflammatory cytokines during muscle regeneration. Whether this is the case for sarcopenic obese mice has yet to be explored.

Therefore the purpose of this study was to investigate how sarcopenic obesity alters inflammatory processes during skeletal muscle regeneration. We hypothesized that impaired muscle regeneration will be a result of altered inflammatory signaling and macrophage recruitment.

Methods

Animals and Housing

One hundred two C57BL/6 mice were purchased from Jackson Laboratories. Animals were housed in the University of Arkansas Central Laboratory Animal Facility. The overall study consisted of 2 separate animal experiments in young adult (3-4 mo) and aged mice (22-24 mo). Experiment 1 examined immunohistochemistry and protein expression, and gene expression 3 days post-bupivacaine injection. Experiment 2 examined immunohistochemistry, muscle morphology, protein expression, and gene expression 21 days post-bupivacaine injection. For experiment 1 and 2 mice were randomly assigned to one of eight groups at 4 weeks of age: 1) young lean uninjured (n = 5); 2) young lean injured (n = 6); 3) young obese uninjured (n = 5-8); 4) young obese injured (n = 6-8); 5) aged lean uninjured (n = 7-8); 6) aged lean injured (n = 7-8); 7) aged obese uninjured (n = 5-6); 8) aged obese injured (n = 6). Mice were fed normal chow (normal; 17% kcals fat Research Diets, New Brunswick, New Jersey) or a high fat diet (HFD; 60% kcals fat, Research Diets, New Brunswick, New Jersey) until they were euthanized. All procedures were approved by the University of Arkansas Institutional Animal Care and Use Committee (IACUC).

Muscle and Tibia Extraction

At either 3-4 mo or 22-24 mo of age, muscle and tibia extractions were performed as previously described (Tyrone A Washington et al., 2013; T. A. Washington et al., 2011). The TA and tibias were extracted while the mice were anesthetized with a subcutaneous injection of a cocktail containing ketamine hydrochloride (90 mg/kg body weight), xylazine (3 mg/kg body weight), and acepromazine (1 mg/kg body weight). The left TA was snap frozen in liquid nitrogen and stored at -80°C for protein and gene expression analysis, the right TA was

cut at the midbelly, mounted in optimum cutting temperature compound (OCT), and then dropped in liquid nitrogen cooled isopentane. Once frozen, samples were stored at -80°C for morphological analysis. After the muscles was dissected out, the tibia was removed and measured with a plastic caliper (VWR, Radnor, PA, USA). Tibia measurements were utilized to normalize muscle weights to an estimate of total body size.

Bupivacaine Injection

At 3 mo or 22-23 mo of age, bupivacaine (Hospira, Lake Forest, IL) injections were performed as previously described (Washington et al., 2013). Mice were anesthetized with a subcutaneous injection of a cocktail containing ketamine hydrochloride (45 mg/kg body weight), xylazine (3 mg/kg body weight), and acepromazine (1 mg/kg body weight). Muscle damage was induced by injecting 0.03ml of 0.75% bupivacaine (Marcaine) in the left and right tibialis anterior muscles (TA). A 25-gauge, 5/8 (0.5 x 16 mm) needle was inserted along the longitudinal axis of the muscle, and the bupivacaine was injected slowly as the needle was withdrawn. The control group was injected with 0.03 ml of phosphate buffered saline (PBS).

Morphological Analysis

Fiber distribution and cross-sectional area (CSA) were performed as previously described (Brown et al., 2016; Washington et al., 2011). Each TA muscle section (n = 6) was stained with hematoxylin and eosin, imaged with a Nikon camera (Sight DS-Vi1) mounted on an Olympus CKX41 inverted microscope at 20X magnification (Olympus), and analyzed with Nikon NIS Elements BR software package (Nikon). Each fiber was traced with a mouse and the number of pixels traced was calibrated to obtain CSA of the muscle. All fibers in the cross section images were quantified unless the sarcolemma was not intact. Approximately 100 fibers were traced per sample.

Western blotting

Muscle tissues were homogenized as previously described (Lee et al., 2016). Approximately 10-40 mg of gastrocnemius, soleus, and TA was homogenized in glass dounce type homogenizers in 0.30 ml of complete protein loading buffer (50 mM Tris·HCl, pH 6.8, 1% sodium dodecyl sulfate (SDS), 10% glycerol, 20 mM dithiothreitol, 127 mM 2-mercaptoethanol, and 0.01% bromophenol blue supplemented with protease inhibitors (Roche) and phosphatase inhibitors (Sigma-Aldrich, St. Louis, MO). After homogenization, samples were transferred to sterile 1.5mL microcentrifuge tubes, heated for 5 minutes at 95°C to denature protein and then centrifuged for 5 minutes at 13,000 rpm. Protein concentrations were determined using a commercially available RC/DC assay kit. Muscle homogenate (40 µg) was fractionated in 10% SDS-polyacrylamide gels. Gels were transferred to polyvinylidene difluoride (PVDF) membranes. Membranes were stained with *Ponceau S* before blotting to verify equal loading of the gels. Membranes were blocked in 5% milk, in Tris-buffered saline with 0.1% Tween-20 (TBST), for 2 hours. Primary antibodies for P-Stat3 (Tyr[705]), Stat3 (Cell Signaling Technologies, Danvers, MA), and NF-κB p65 (Santa Cruz, Dallas, TX) were diluted 1:1000 to 1:2000 in 5% milk, in TBST, and incubated at 4°C overnight. Anti-rabbit and Anti-mouse monoclonal secondary antibodies (Cell Signaling Technologies, Danvers, MA) were diluted 1:2,000 in 5% milk, in TBST, and then incubated at room temperature for one hour. Enhanced Chemiluminescence (ECL) was performed using Fluorochem M imager (Protein Simple, Santa Clara, California) to visualize antibody-antigen interaction. Blotting images were quantified by densitometry using AlphaView software (Protein Simple). The Ponceau-stained membranes were digitally scanned, and the 45-kDa

actin bands were quantified by densitometry and used as a protein loading correction factor for each lane.

RNA Isolation, cDNA synthesis, and quantitative RT-PCR

The following procedures were completed as previously described (N. P. Greene et al., 2015; Nicholas P Greene et al., 2014; Tyrone A Washington et al., 2013). RNA was extracted with Trizol reagent (Life Technologies, Grand Island, NY, USA). TA muscles were homogenized in Trizol. Total RNA was isolated, DNase treated and purity and concentrations were determined using 260/280nm ratios read on a BioTek Take3 microvolume microplate with a BioTek PowerWave XC microplate reader (BioTek Instruments Inc., Winooski, VT). cDNA was reverse transcribed from 1 µg of total RNA using the Superscript Vilo cDNA synthesis kit (Life Technologies, Carlsbad, CA, USA). Real-time PCR was performed, and results were analyzed by using the StepOne Real-Time PCR system (Life Technologies, Applied Biosystems, Grand Island, NY). cDNA was amplified in a 25 µL reaction containing appropriate primer pairs and TaqMan Universal Mastermix (Applied Biosystems). Samples were incubated at 95°C for 4 min, followed by 40 cycles of denaturation, annealing and extension at 95°C, 55°C and 72°C respectively. TaqMan fluorescence was measured at the end of the extension step each cycle. Fluorescence labeled probes for TNFα (FAM dye), IL-6 (FAM dye), ICAM-1 (FAM dye), and 18S (FAM dye) were purchased from Applied Biosystems and quantified with TaqMan Universal mastermix. Cycle threshold (Ct) was determined, and the ΔCt value was calculated as the difference between the Ct value and the 18S Ct value. Final quantification of gene expression was calculated using the ΔΔCT method Ct = [ΔCt(calibrator) – ΔCt(sample)]. Relative quantification was then calculated as $20^{-\Delta\Delta Ct}$.

Melt curve analysis was performed at the end of the PCR run to verify no primer dimers were formed.

Statistical Analysis

All data was analyzed using Statistical Package for the Social Sciences (SPSS version 22.0, Armonk, NY). Results are reported as mean ± SEM. Pre-planned comparisons between lean and obese uninjured mice were conducted using Student's t-tests. For these analyses, lean and obese uninjured were pooled from the 3 and 21 day time-points. A two-way ANOVA was performed to analyze main effects of treatment and diet and if there were any interactions between the dependent variables for 3 and 21 days post-bupivacaine injection. When a significant interaction was detected, differences among individual means were assessed with Fisher's LSD post-hoc analysis. The χ^2 analysis was used to detect differences in the proportion of small fibers ($< 400\ \mu m^2$) and large fibers ($> 900\ \mu m^2$) between treatment groups. Statistical significance was set at $P \leq 0.05$.

Results

Animal weight characteristics and muscle morphology

Body weight in the young HFD mice was 21% greater than young lean mice (Table 1). Body weight in the aged HFD mice was 38% greater than aged lean mice (Table 2). In the young mice there was no difference in muscle weight relative to tibia length 3 days post-bupivacaine injection (Table 1). In the aged mice there was no difference in muscle weight relative to tibia length 3 days post-bupivacaine injection (Table 2). In the young mice there was no difference in muscle weight relative to tibia length 21 days post-bupivacaine injection (Table 1). In the aged mice there was no difference in muscle weight relative to tibia length 21 days post-bupivacaine injection (Table 2).

In the young lean mice, mean cross-sectional area was 20% greater in the injured group compared to the uninjured group 21 days post-bupivacaine injection (Fig. 1B). In the young HFD mice, mean cross-sectional area was not different in the injured group compared to the uninjured group 21 days post-bupivacaine injection (Fig. 1B). In the young lean mice there were 89% less small ($< 400 \, \mu m^2$) fibers in the injured group compared to the uninjured group (Fig. 1C). Also, in the young lean mice there were 7% more large fibers ($> 900 \, \mu m^2$) in the injured group compared to the uninjured group (Fig. 1C). No differences were seen between the uninjured and injured young HFD mice for distribution of myofibers 21 days post-bupivacaine injection (Fig. 1D). In the aged lean mice, mean cross-sectional area was 9% greater in the injured group compared to the uninjured group 21 days post-bupivacaine injection (Fig. 1F). In the aged HFD mice, mean cross-sectional area was not different in the injured group compared to the uninjured group 21 days post-bupivacaine injection (Fig. 1F). In the aged lean mice there were 32% less small ($< 400 \, \mu m^2$) fibers in the injured group

128

compared to the uninjured group (Fig. 1G). Also, in the aged lean mice there were no differences seen between large fibers in the injured group compared to the uninjured group 21 days post-bupivacaine injection. No differences were seen between the uninjured and injured aged HFD mice for distribution of myofibers 21 days post-bupivacaine injection (Fig. 1H).

MRF gene expression

In the young lean mice, MyoD mRNA abundance was not different in the injured group compared to the uninjured group 3 days post-bupivacaine injection (Fig. 2A). In the young HFD mice MyoD mRNA abundance was not different in the injured group compared to the uninjured group 3 days post-bupivacaine injection (Fig. 2A). There was a main effect of diet with a decrease of MyoD mRNA abundance in the young HFD group compared to the lean group 21 days post-bupivacaine injection (Fig. 2B). In the aged lean mice MyoD mRNA abundance was not different in the injured group compared to the uninjured group 3 days post-bupivacaine injection (Fig. 2C). In the aged HFD mice MyoD mRNA abundance was not different in the injured group compared to the uninjured group 3 days post-bupivacaine injection (Fig. 2C). In the aged lean mice, MyoD mRNA abundance was reduced by 76% (Fig. 2D) in the injured group compared to the uninjured group 21 days post-bupivacaine injection. In the aged HFD mice MyoD mRNA abundance was not different in the injured group compared to the uninjured group 21 days post-bupivacaine injection (Fig. 2D). In the young lean mice, myogenin mRNA abundance was 6-fold greater (Fig. 2E) in the injured group compared to the uninjured group 3 days post-bupivacaine injection. In the young HFD mice myogenin mRNA abundance was not different in the injured group compared to the uninjured group 3 days post-bupivacaine injection (Fig. 2E). There was a main effect of diet with a decrease of myogenin mRNA abundance in the young HFD group compared to the

young lean group 21 days post-bupivacaine injection (Fig. 2F). In the aged lean mice, myogenin mRNA abundance was not different in the injured group compared to the uninjured group 3 days post-bupivacaine injection (Fig. 2G). In the aged HFD mice, myogenin mRNA abundance was not different in the injured group compared to the uninjured group 3 days post-bupivacaine injection (Fig. 2G). In the aged lean mice, myogenin mRNA abundance was reduced by 70% (Fig. 2H) in the injured group compared to the uninjured group 21 days post-bupivacaine injection. In the aged HFD mice myogenin mRNA abundance was not different in the injured group compared to the uninjured group 21 days post-bupivacaine injection (Fig. 2H).

ICAM 1 gene expression

In the young lean mice, ICAM-1 mRNA abundance was not different in the injured group compared to the uninjured group 3 days post-bupivacaine injection (Fig. 3A). In the young HFD mice, ICAM-1 mRNA abundance was not different in the injured group compared to the uninjured group 3 days post-bupivacaine injection (Fig. 3A). There was a main effect of diet with a decrease of ICAM-1 mRNA abundance in the young HFD group compared to the young lean group 21 days post-bupivacaine injection (Fig. 3B). In the aged lean mice, ICAM-1 mRNA abundance was not different in the injured group compared to the uninjured group 3 days post-bupivacaine injection (Fig. 3C). In the aged HFD mice ICAM-1 mRNA abundance was not different in the injured group compared to the uninjured group 3 days post-bupivacaine injection (Fig. 3C). There was a main effect of diet with a decrease of ICAM-1 mRNA abundance in the aged HFD group compared to the aged lean group 21 days post-bupivacaine injection (Fig. 3D).

IL-6/STAT3 signaling

In the young lean mice, IL-6 mRNA abundance was 5-fold greater in the injured group compared to the uninjured group 3 days post-bupivacaine injection (Fig. 4A). In the young HFD mice, IL-6 mRNA abundance was not different in the injured group compared to the uninjured group 3 days post-bupivacaine injection (Fig. 4A). In the young lean mice, IL-6 mRNA abundance was 3-fold greater in the injured group compared to the uninjured group 21 days post-bupivacaine injection (Fig. 4B). In the young HFD mice, IL-6 mRNA abundance was not different in the injured group compared to the uninjured group 21 days post-bupivacaine injection (Fig. 4B). There was a main effect of diet with an increase of phosphorylated STAT3 relative to STAT3 in the young HFD group compared to the young lean group 3 days post-bupivacaine injection (Fig. 4C). There was a main effect of diet with an increase of phosphorylated STAT3 relative to STAT3 in the young HFD group compared to the young lean group 21 days post-bupivacaine injection (Fig. 4D).

In the aged lean mice, IL-6 mRNA abundance was not different in the injured group compared to the uninjured group 3 days post-bupivacaine injection (Fig. 5A). In the aged HFD mice, IL-6 mRNA abundance was 3-fold greater 3 days post bupivacaine injection (Fig. 5A). In the aged lean mice, IL-6 mRNA abundance was not different in the injured group compared to the uninjured group 21 days post-bupivacaine injection (Fig. 5B). In the aged HFD mice, IL-6 mRNA abundance was not different in the injured group compared to the uninjured group 21 days post-bupivacaine injection (Fig. 5B). There was a main effect of diet with a decrease of phosphorylated STAT3 relative to STAT3 in the aged HFD group compared to the aged lean group 3 days post-bupivacaine injection (Fig. 5C). In the aged lean mice, phosphorylated STAT3 relative to STAT3was not different in the injured group compared to the uninjured group 21 days post-bupivacaine injection (Fig. 5D). In the aged

HFD mice, phosphorylated STAT3 relative to STAT3 was not different in the injured group compared to the uninjured group 21 days post-bupivacaine injection (Fig. 5D).

TNF-α/NF-κB signaling

There was a main effect of injury with an increase of TNF-α mRNA abundance in the young injured group compared to the young uninjured group 3 days post-bupivacaine injection (Fig. 6A). There was a main effect of diet with a decrease of TNF-α mRNA abundance in the young HFD group compared to the young lean group 21 days post-bupivacaine injection (Fig. 6B). There was no difference of NF-κB in all groups 3 days post-bupivacaine injection (Fig. 6C). There was a main effect of diet with an increase of NF-κB in the young HFD group compared to the young lean group 21 days post-bupivacaine injection (Fig. 6D).

In the aged lean mice, TNF-α mRNA abundance was not different in the injured group compared to the uninjured group 3 days post-bupivacaine injection (Fig. 7A). In the aged HFD mice, TNF-α mRNA abundance was not different in the injured group compared to the uninjured group 3 days post-bupivacaine injection (Fig. 7A). There was a main effect of diet with a decrease of TNF-α mRNA abundance in the aged HFD group compared to the aged lean group 21 days post-bupivacaine injection (Fig. 7B). There was a main effect of diet with an increase of NF-κB in the aged HFD group compared to the aged lean group 3 days post-bupivacaine injection (Fig. 7C). In the aged lean mice, NF-κB was not different in the injured group compared to the uninjured group 21 days post-bupivacaine injection (Fig. 7D). In the aged HFD mice, NF-κB was 3-fold greater (Fig. 7D) in the injured group compared to the uninjured group 21 days post-bupivacaine injection.

Discussion

The primary goal of this study was to examine how sarcopenic obesity alters myogenic and inflammatory signaling in skeletal muscle following injured. We hypothesized that sarcopenic obese mice would have impaired muscle regeneration due to the inability to upregulate inflammatory cytokines at the onset of muscle damage. In addition, we expected to observe a blunted response in ICAM-1 expression following muscle injury. To our knowledge we are the first to demonstrate no changes in frequency of cross-sectional area fiber size 21 days following muscle damage in HFD mice. We also witnessed reduced STAT3 at the onset muscle regeneration and upregulated NF-κB in the early and late stages of muscle regeneration in HFD mice. These alterations within inflammatory signaling would suggest sub-optimal muscle regeneration in aged HFD mice.

There were no differences when examining the TA muscle weight relative to tibia length in the aged lean and aged HFD mice. However, 21 days following myotoxin-induced damage, mean CSA slightly shifted towards the right in the aged lean mice but not in the aged HFD mice. A previous study from our laboratory demonstrated a right shift towards large fibers in young lean mice but not in young HFD mice indicating delayed muscle regeneration (L. A. Brown et al., 2015). We observed a similar pattern in the aged lean and aged HFD mice. Also, 21 days following muscle damage we observed a 20% and 9% increase in young lean and aged lean mice, respectively but no changes in the HFD mice. These data would suggest that there is a delayed or sub-optimal regenerative response in the aged HFD mice.

Next we examined expression of MRFs in all animal groups. To our surprise there was no differences with the upregulation of MyoD in both the young and aged mice at the onset of muscle regeneration. A previous study reported that MyoD was upregulated 5 days after

muscle injury for myoblast proliferation (Marsh et al., 1997). The difference in MyoD

expression in this study compared to our study may be due to high variance reported in gene

expression. As expected young mice upregulated myogenin at the onset of regeneration but

young HFD and aging mice had the inability to upregulate myogenin. Myogenin is an

essential transcription factor for myoblast differentiation. Unlike our findings Marsh and

colleagues found a 2.5-fold upregulation of myogenin in aged rats (Marsh et al., 1997). In

their study they normalized myogenin expression to muscle weight which may could

potentially explain the slight increase they found an expression due to a smaller muscle

weight in old rats (Marsh et al., 1997). It has been reported in numerous studies that aging

skeletal muscle has a reduced satellite pool and senescent cells that may contribute to reduced

activity in muscle cells involved with muscle repair an aging lean and HFD mice

(Chakkalakal, Jones, Basson, & Brack, 2012; Ciciliot & Schiaffino, 2010; Conboy et al.,

2005).

In young mice and old mice we did not observe any changes in ICAM-1 expression

following injury at the early stages of injury. Dearth and colleagues found a 2-fold

upregulation of ICAM-1 in 3 days after overload in mice (Dearth et al., 2013). Monocyte

recruitment is one of the first processes that will occur following tissue injury which can

facilitate macrophage recruitment within minutes following tissue damage (Kharraz et al.,

2013). It is possible that we did not see an upregulation of ICAM-1 in any group because the

3 day time point is too late to detect differences in a myotoxin-induced muscle damage model.

In the late stages of muscle regeneration there was a reduced expression of ICAM-1 in the

HFD mice. Activated inflammatory proteins involved with repair will typically get inhibited

before returning to basal levels. The reduction of ICAM-1 may indicate a delayed

regenerative response in HFD mice.

In this study we noticed that the young lean and aged HFD mice were able to activate IL-6 at the onset of muscle regeneration whereas the young HFD and aged lean mice could not induce IL-6. The young HFD and aged lean mice both exhibit altered inflammatory cytokines and sub-optimal regeneration (L. A. Brown et al., 2015; Chakkalakal et al., 2012). The young HFD mice also had a greater P-STAT3/STAT3 expression 3 and 21 days following muscle injury that may be partially responsible for sub-optimal regeneration in this population. However, the aged HFD mice induced IL-6, but had a severe reduction in STAT3 expression. IL-6 can classically activate STAT3 for anti-inflammatory effects or alternatively signal pathways responsible for apoptosis seen in inflammatory diseases (Kishimoto, 2006). The lack of STAT3 activation in aged HFD may suggest that IL-6 is signaling pathways that may negatively impact muscle regeneration.

TNF-α was also examined because of it has a regulatory role in myoblast differentiation. We observed a similar response for young lean and HFD to upregulate TNF-α 3 days following injury. This was different from our previous study that found a blunted response in TNF-α (L. A. Brown et al., 2015). The differences in diet of the control animal groups between studies (lean diet 10% fat v. normal chow) could be responsible for highlighting the changes in HFD mice in the previous study. There was also a main effect of diet to increase NF-κB 3 days following muscle damage and it remained elevated in the HFD group 21 days following muscle recovery. TNF-α/NF-κB signaling is necessary to carry out apoptosis of damaged muscle fibers (S. E. Chen et al., 2005). However, chronic expression can lead to muscle atrophy that may be responsible in the reduction of CSA seen in our study. Interestingly, the aging mice were unable to upregulate TNF-α. However, we did observe a

135

main effect of diet to increase in NF-κB expression at the onset of muscle regeneration and a 3-fold greater response in the aged HFD mice. It has been demonstrated that NF-κB can be chronically activated independent of TNF-α and will cause atrophy in cancer cachexia (He et al., 2013). It appears that NF-kB could be the major contributor to muscle loss in sarcopenic obesity.

Overall, sarcopenic obesity has a sub-optimal regenerative response to muscle injury. This appears to be partially due to the inability to activate STAT3 and inactivate NF-κB during muscle regeneration. The aged mice also demonstrated a blunted response in myogenin which may be associated with changes in inflammatory signaling. The reductions of inflammatory signaling may be due to reduced macrophage infiltration and should be further explored.

Tables

Table 1

Animal post-bodyweight, tibia anterior muscle wet weight, tibia length, muscle relative to tibia length, and muscle relative to bodyweight, in young male C57BL/6 mice with and without muscle damage

Treatment	Bodyweight (g)	Muscle wet wt (mg)	Tibia (mm)	Muscle/BW (mg g $^{-1}$)	*Muscle/TL (mg mm $^{-1}$)*
3D Lean					
Uninjured	27.84 ± 0.44	51.27 ± 1.08	17.56 ± 0.08	1.84 ± 0.03	2.92 ± 0.07
Injured	28.12 ± 0.74	53.23 ± 1.93	$17.01 \pm 0.23^{\dagger}$	1.90 ± 0.07	3.13 ± 0.08
3D HFD					
Uninjured	$38.68 \pm 1.48^{\ddagger}$	57.08 ± 2.12	17.58 ± 0.20	$1.49 \pm 0.10^{\ddagger}$	3.25 ± 0.13
Injured	$34.63 \pm 1.98^{\ddagger}$	53.96 ± 2.30	$17.10 \pm 0.26^{\dagger}$	$1.57 \pm 0.08^{\ddagger}$	3.15 ± 0.10
21D Lean					
Uninjured	29.98 ± 0.37	58.87 ± 0.77	17.15 ± 0.12	1.96 ± 0.01	3.43 ± 0.04
Injured	30.30 ± 0.86	59.05 ± 1.86	17.20 ± 0.09	1.95 ± 0.04	3.43 ± 0.11
21D HFD					
Uninjured	$39.83 \pm 1.22^{\ddagger}$	56.10 ± 2.43	17.60 ± 0.25	$1.41 \pm 0.08^{\ddagger}$	$3.19 \pm 0.16^{\ddagger}$
Injured	$34.63 \pm 1.98^{\ddagger}$	53.96 ± 2.30	17.10 ± 0.26	$1.57 \pm 0.08^{\ddagger}$	$3.15 \pm 0.10^{\ddagger}$

Values are means $\pm$ SEM. Main effects of treatment distinguished by $\dagger$ and diet by $\ddagger$, $P \leq 0.05$.

Table 2

Animal post-bodyweight, tibia anterior muscle wet weight, tibia length, muscle relative to tibia length, and muscle relative to bodyweight, in aged male C57BL/6 mice with and without muscle damage

Treatment	Bodyweight (g)	Muscle wet wt (mg)	Tibia (mm)	Muscle/BW (mg g $^{-1}$)	*Muscle/TL (mg mm $^{-1}$)*
3D Lean					
Uninjured	34.10 ± 2.62	48.44 ± 1.01	18.50 ± 0.18	1.46 ± 0.08	2.60 ± 0.05
Injured	32.59 ± 0.70	55.52 ± 1.59	$18.18 \pm 0.14^{\dagger}$	1.71 ± 0.06	3.06 ± 0.10
3D HFD					
Uninjured	$58.87 \pm 2.17^{\ddagger}$	46.48 ± 1.42	18.32 ± 0.14	$0.79 \pm 0.04^{\ddagger}$	2.54 ± 0.09
Injured	$56.47 \pm 4.36^{\ddagger}$	45.40 ± 1.76	$18.68 \pm 0.07^{\dagger}$	$0.84 \pm 0.09^{\ddagger}$	2.43 ± 0.09
21D Lean					
Uninjured	32.34 ± 0.69	55.92 ± 0.87	17.80 ± 0.07	1.73 ± 0.04	3.14 ± 0.05
Injured	32.73 ± 0.93	54.36 ± 1.26	$17.98 \pm 0.10^{\ddagger}$	1.66 ± 0.02	3.02 ± 0.06
21D HFD					
Uninjured	$46.72 \pm 3.55^{\ddagger}$	$48.24 \pm 1.95^{\ddagger}$	17.89 ± 0.17	$1.06 \pm 0.10^{\ddagger}$	$2.70 \pm 0.11^{\ddagger}$
Injured	$50.46 \pm 4.45^{\ddagger}$	$49.37 \pm 2.37^{\ddagger}$	$18.22 \pm 0.06^{\ddagger}$	$1.02 \pm 0.12^{\ddagger}$	$2.71 \pm 0.13^{\ddagger}$

Values are means ± SEM. Main effects of treatment distinguished by † and diet by ‡, $P \leq 0.05$.

Figure Legends

Figure 1. Tibialis anterior mean cross-sectional area and fiber distribution 21 days of recovery after bupivacaine-induced injury. (A) Representative H&E staining of muscle cross section of young lean uninjured (a), lean injured (b), HFD uninjured (c), and HFD injured (d); (B) Mean cross-sectional area of the tibialis anterior in young mice. (C) Myofiber distribution in young lean uninjured and lean injured mice (D) Myofiber distribution in young HFD uninjured and HFD injured mice. .(E) Representative H&E staining of muscle cross section of aged lean uninjured (a), lean injured (b), HFD uninjured (c), and HFD injured (d); (F) Mean cross-sectional area of the tibialis anterior in aged mice. (G) Myofiber distribution in aged lean uninjured and lean injured mice (H) Myofiber distribution in aged HFD uninjured and HFD injured mice. Frequency histograms and the frequency of fibers $< 400\ \mu m^2$ and > 900 μm^2 were compared by a χ^2 analysis as previously described (Washington et al., 2011). Values are reported in the frequency percentage of a given fiber size (μm^2). Main effects of injury distinguished by † and diet by ‡. Significant differences between lean uninjured and lean injured and aged uninjured and aged injured distinguished by [#]. $P \leq 0.05$.

Figure 2. Myogenic regulatory factors of skeletal muscle regeneration at 3 days and 21 days of recovery after bupivacaine-induced injury. (A) MyoD mRNA abundance 3 days post-bupivacaine injection in young lean and HFD mice. (B) MyoD mRNA abundance 21 days post-bupivacaine injection in young lean and HFD mice. (C) MyoD mRNA abundance 3 days post-bupivacaine injection in aged lean and HFD mice. (D) MyoD mRNA abundance 21 days post-bupivacaine injection in aged lean and HFD mice. (E) Myogenin mRNA abundance 3 days post-bupivacaine injection in young lean and HFD mice. (F) Myogein mRNA abundance 21 days post-bupivacaine injection in young lean and HFD mice. (G) Myogenin mRNA

abundance 3 days post-bupivacaine injection in aged lean and HFD mice. (H) Myogenin mRNA abundance 21 days post-bupivacaine injection in aged lean and HFD mice. Main effects of injury distinguished by † and diet by ‡. Significant differences between lean uninjured and lean injured and aged uninjured and aged injured distinguished by [#]. $P \leq 0.05$.

Figure 3. ICAM-1 mRNA abundance of skeletal muscle regeneration at 3 days and 21 days of recovery after bupivacaine-induced injury. (A) ICAM-1 mRNA abundance 3 days post-bupivacaine injection in young lean and HFD mice. (B) ICAM-1 mRNA abundance 21 days post-bupivacaine injection in young lean and HFD mice. (C) ICAM-1 mRNA abundance 3 days post-bupivacaine injection in aged lean and HFD mice. (D) ICAM-1 mRNA abundance 21 days post-bupivacaine injection in aged lean and HFD mice. Main effects of injury distinguished by † and diet by ‡. Significant differences between lean uninjured and lean injured and aged uninjured and aged injured distinguished by [#]. $P \leq 0.05$.

Figure 4. IL-6 signaling of skeletal muscle regeneration at 3 days and 21 days of recovery after bupivacaine-induced injury. (A) IL-6 mRNA abundance 3 days post-bupivacaine injection in young lean and HFD mice. (B) IL-6 mRNA abundance 21 days post-bupivacaine injection in young lean and HFD mice. (C) Fold changes in P-STAT3/STAT3 protein 3 days post-bupivacaine injection in young lean and HFD mice. (D) Fold changes in P-STAT3/STAT3 protein 21 days post-bupivacaine injection in young lean and HFD mice. Main effects of injury distinguished by † and diet by ‡. Significant differences between lean uninjured and lean injured and aged uninjured and aged injured distinguished by [#]. $P \leq 0.05$. Abbreviations: YLu, young lean uninjured; Yli, young lean injured; YHu, young high fat diet uninjured; YHi, young high fat diet injured.

Figure 5. IL-6 signaling of skeletal muscle regeneration at 3 days and 21 days of

recovery after bupivacaine-induced injury. (A) IL-6 mRNA abundance 3 days post-bupivacaine injection in aged lean and HFD mice. (B) IL-6 mRNA abundance 21 days post-bupivacaine injection in aged lean and HFD mice. (C) Fold changes in P-STAT3/STAT3 protein 3 days post-bupivacaine injection in aged lean and HFD mice. (D) Fold changes in P-STAT3/STAT3 protein 21 days post-bupivacaine injection in aged lean and HFD mice. Main effects of injury distinguished by † and diet by ‡. Significant differences between lean uninjured and lean injured and aged uninjured and aged injured distinguished by #. $P \leq 0.05$. Abbreviations: ALu, aged lean uninjured; Ali, aged lean uninjured; AHu, aged high fat diet uninjured; AHi, aged high fat diet injured.

Figure 6. TNF-α signaling of skeletal muscle regeneration at 3 days and 21 days of recovery after bupivacaine-induced injury. (A) TNF-α mRNA abundance 3 days post-bupivacaine injection in young lean and HFD mice. (B) TNF-α mRNA abundance 21 days post-bupivacaine injection in young lean and HFD mice. (C) Fold changes in NF-κB65 protein 3 days post-bupivacaine injection in young lean and HFD mice. (D) Fold changes in NF-κB65 protein 21 days post-bupivacaine injection in young lean and HFD mice. Main effects of injury distinguished by † and diet by ‡. Significant differences between lean uninjured and lean injured and aged uninjured and aged injured distinguished by #. $P \leq 0.05$. Abbreviations: YLu, young lean uninjured; Yli, young lean injured; YHu, young high fat diet uninjured; YHi, young high fat diet injured.

Figure 7. TNF-α signaling of skeletal muscle regeneration at 3 days and 21 days of recovery after bupivacaine-induced injury. (A) TNF-α mRNA abundance 3 days post-bupivacaine injection in aged lean and HFD mice. (B) TNF-α mRNA abundance 21 days post-bupivacaine injection in aged lean and HFD mice. (C) Fold changes in NF-κB65 protein

141

3 days post-bupivacaine injection in aged lean and HFD mice. (D) Fold changes in NF-κB65 protein 21 days post-bupivacaine injection in aged lean and HFD mice. Main effects of injury distinguished by † and diet by ‡. Significant differences between lean uninjured and lean injured and aged uninjured and aged injured distinguished by #. $P \leq 0.05$. Abbreviations: ALu, aged lean uninjured; Ali, aged lean uninjured; AHu, aged high fat diet uninjured; AHi, aged high fat diet injured.

Figures

Figure 1

A.

B.

C.

D.

E.

F.

G.

H.

Figure 2

A.

B.

C.

D.
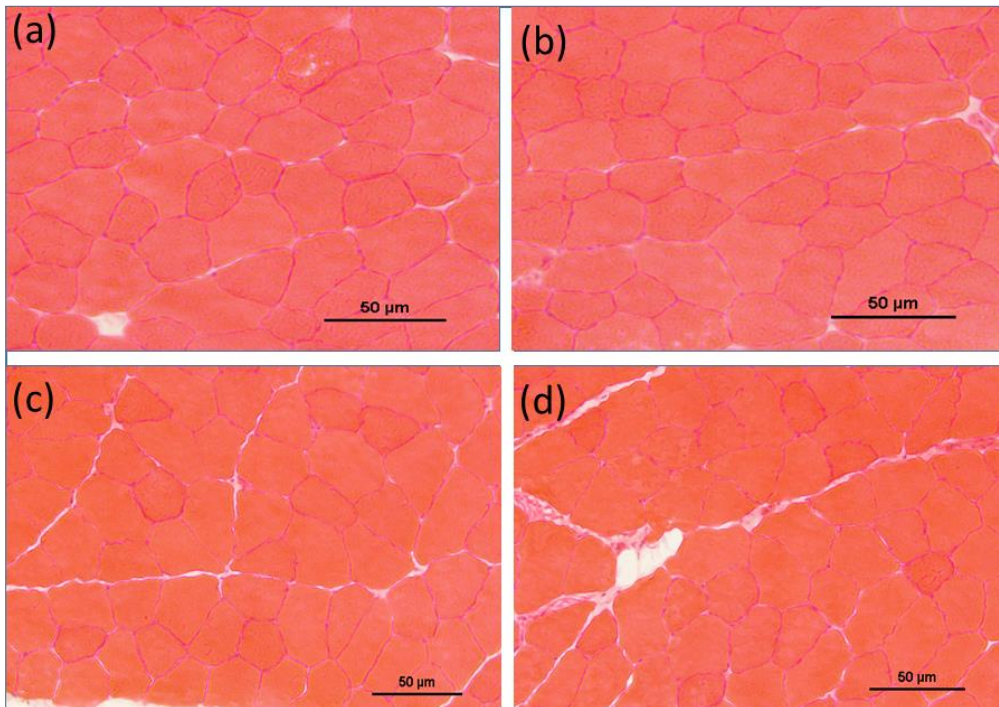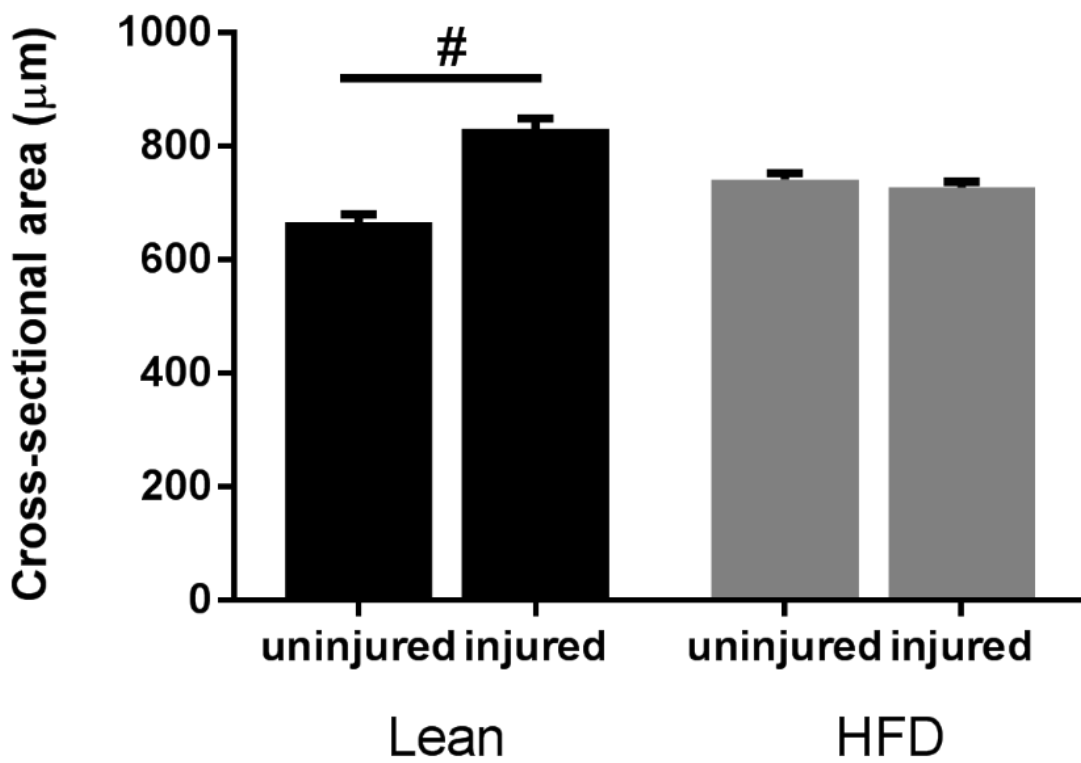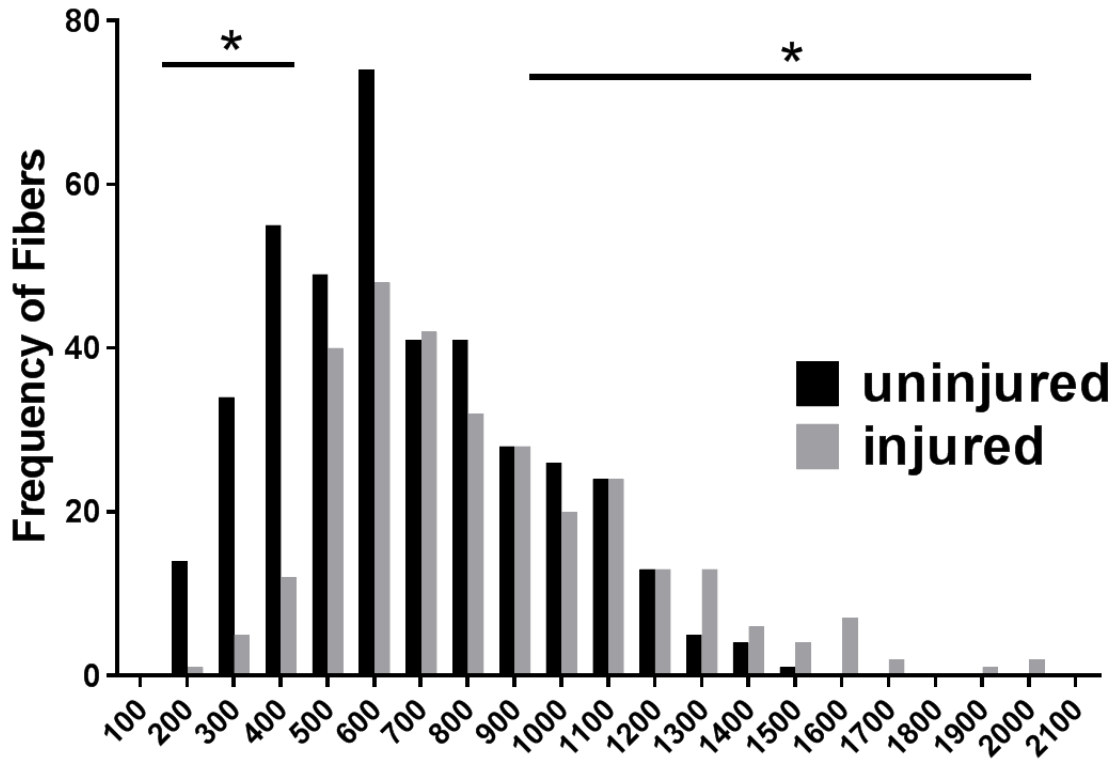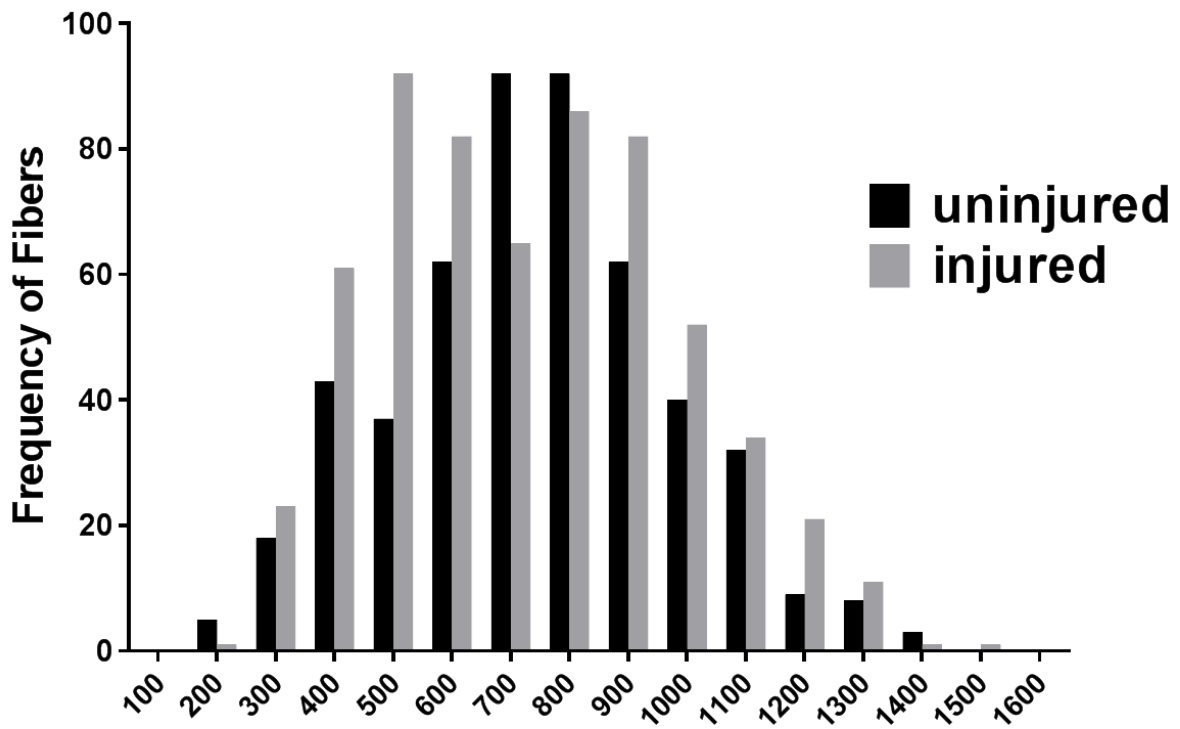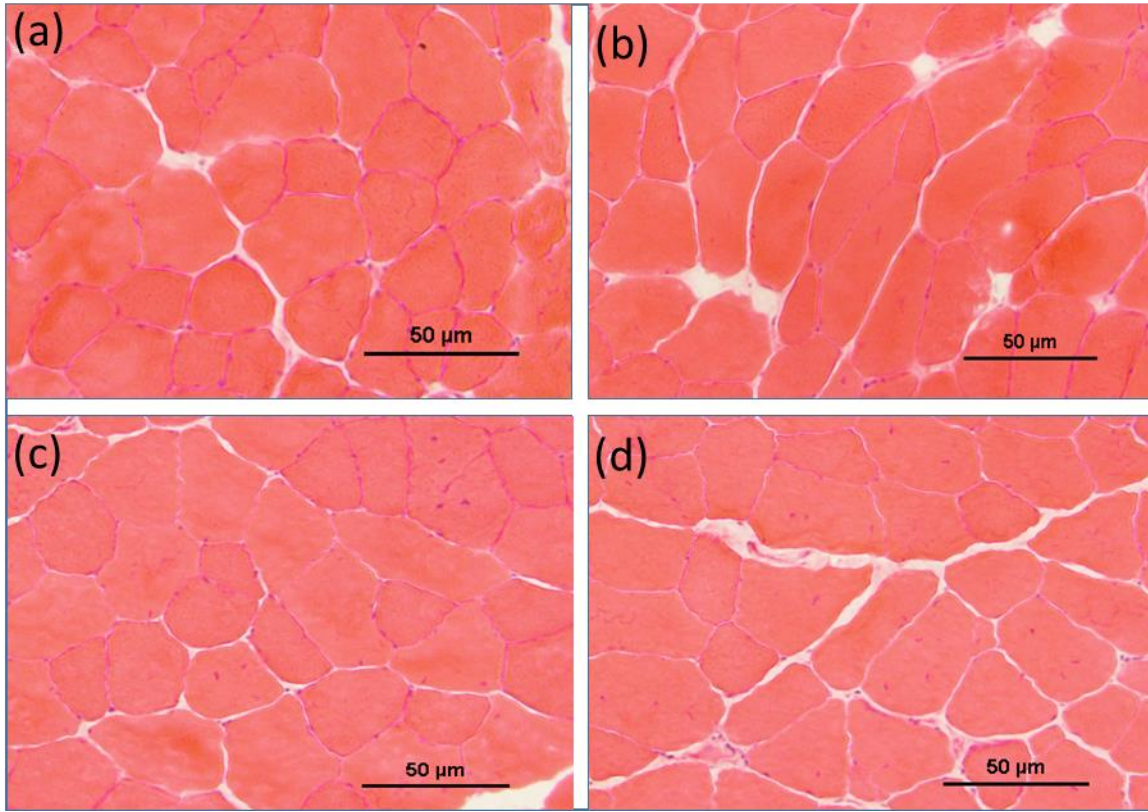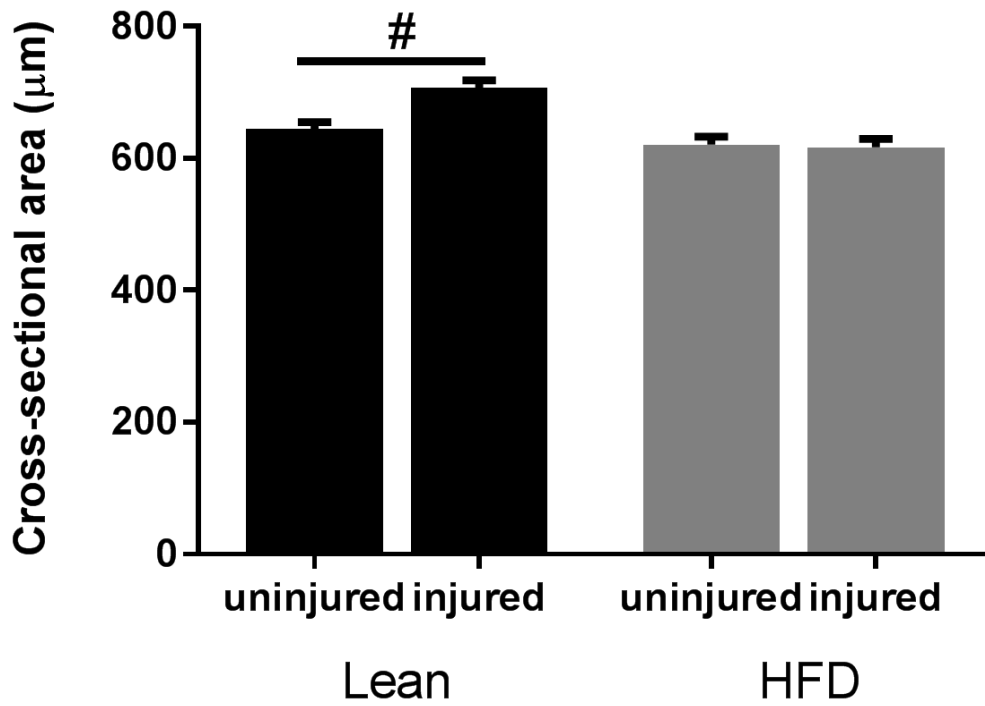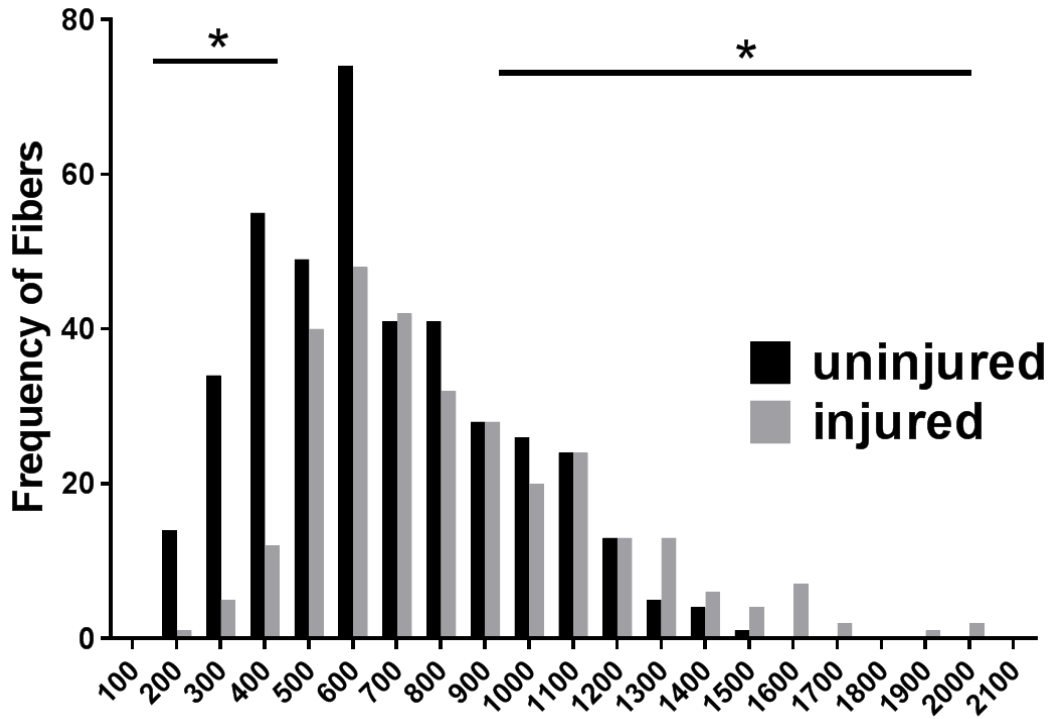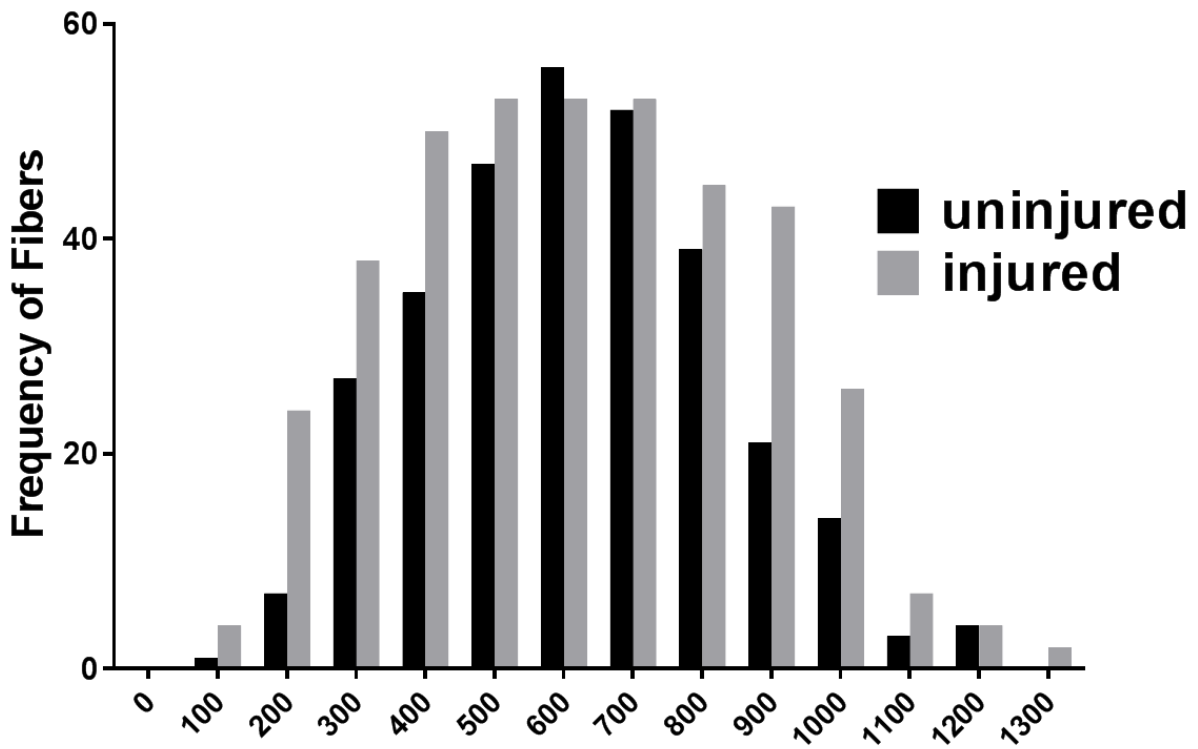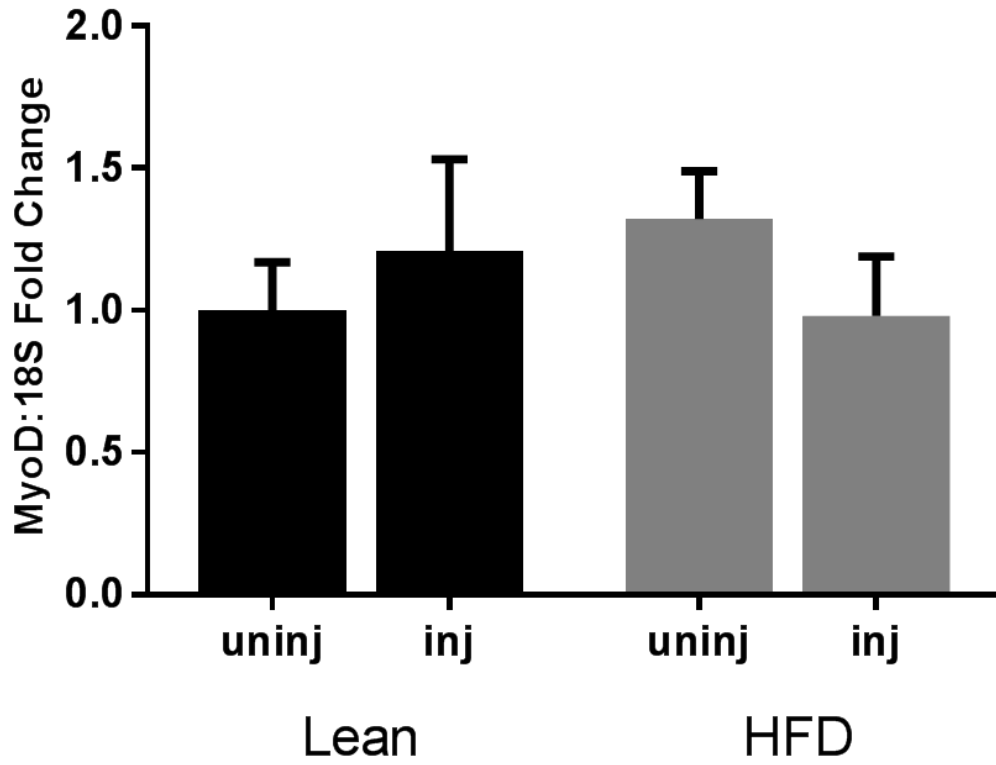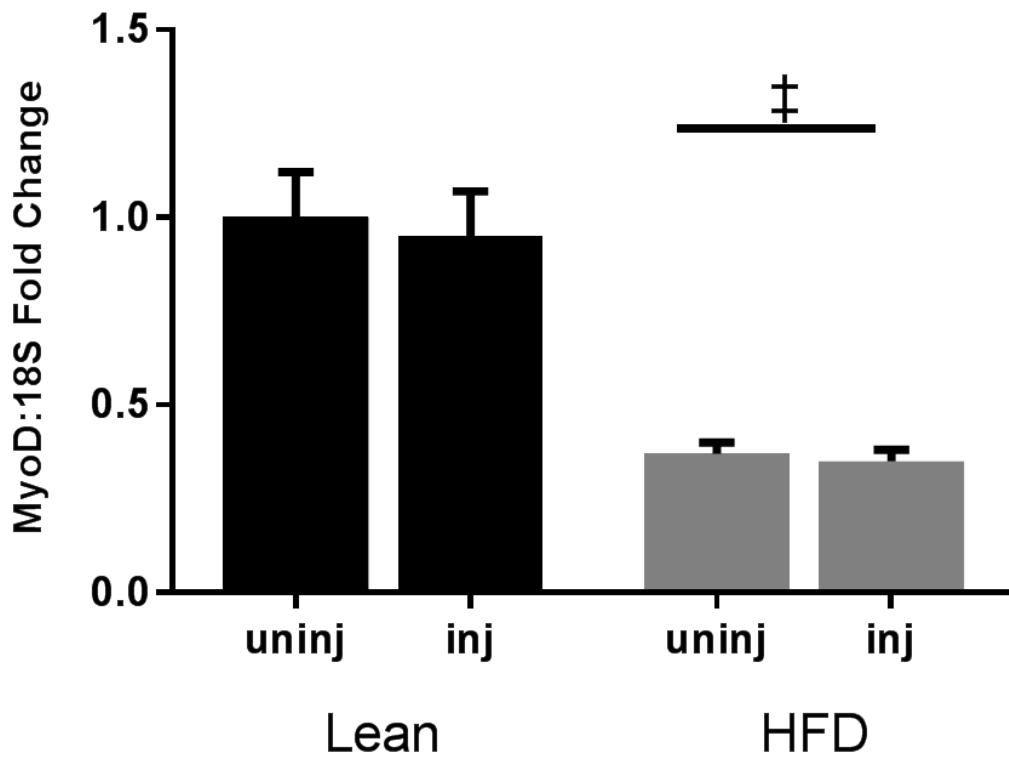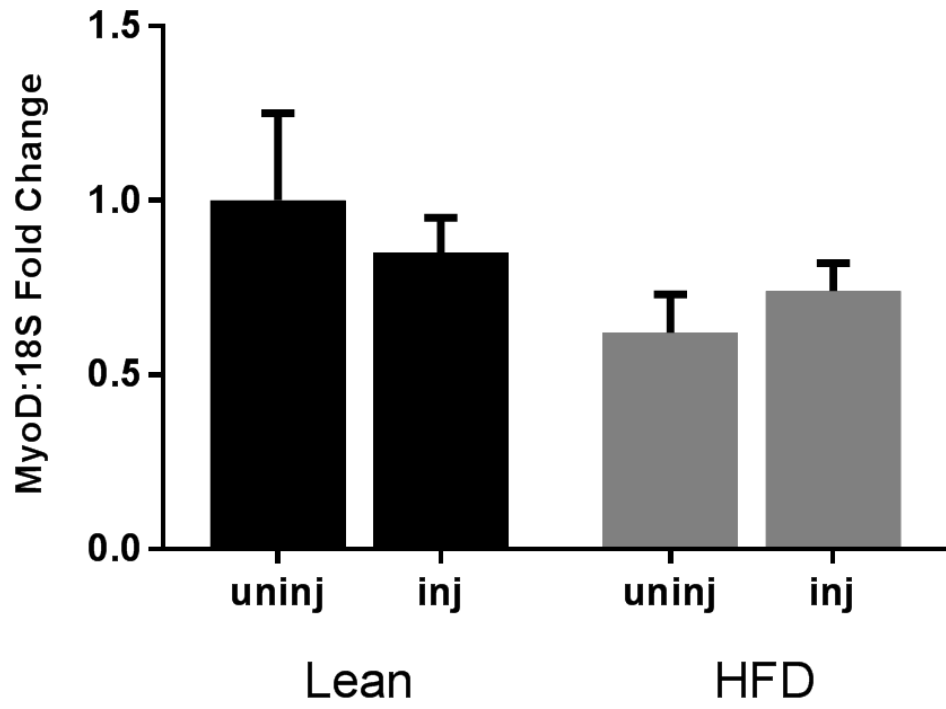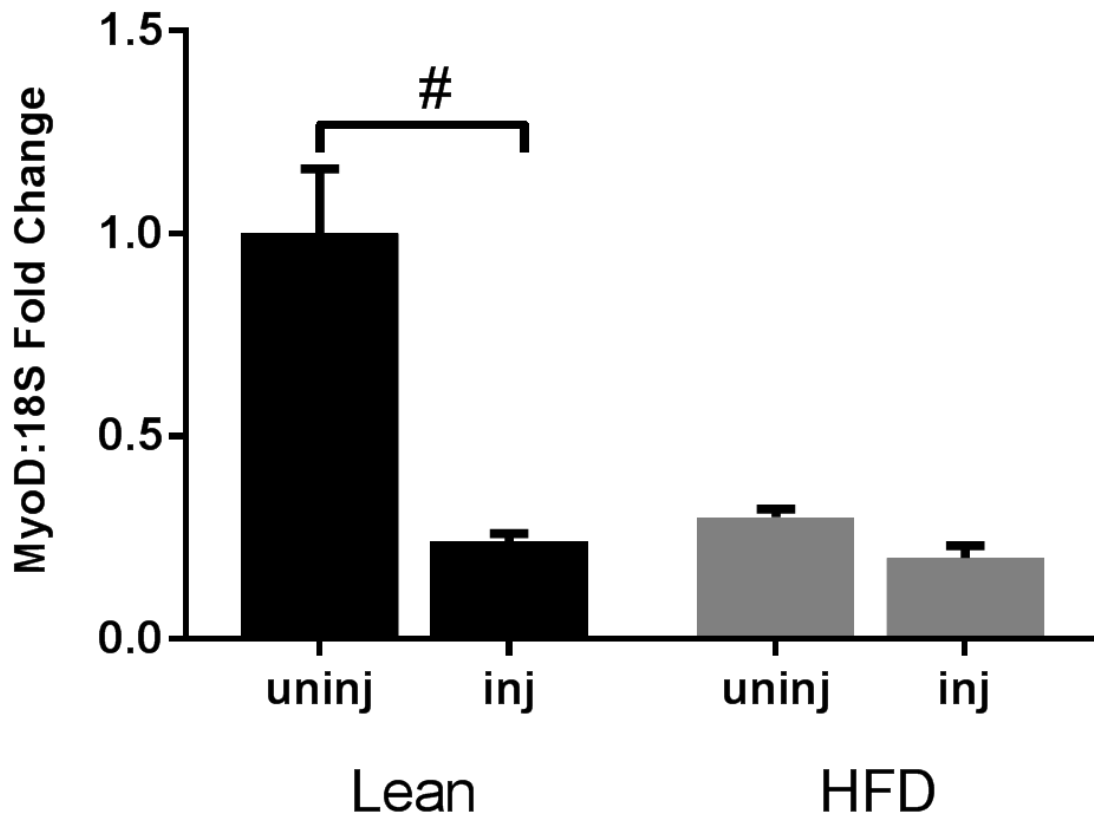
E.
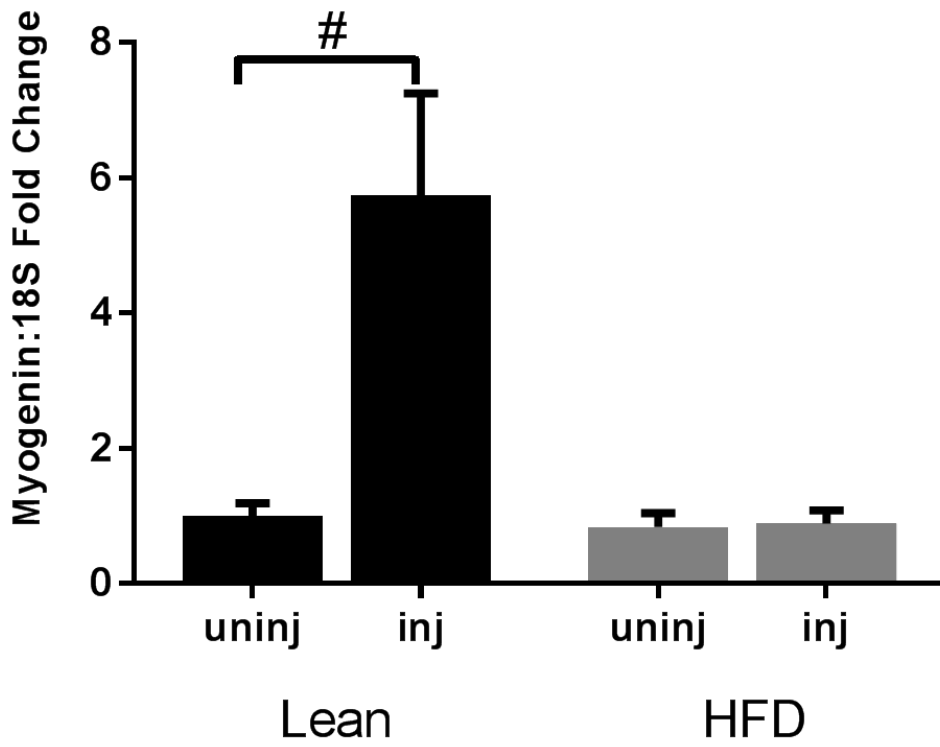
F.
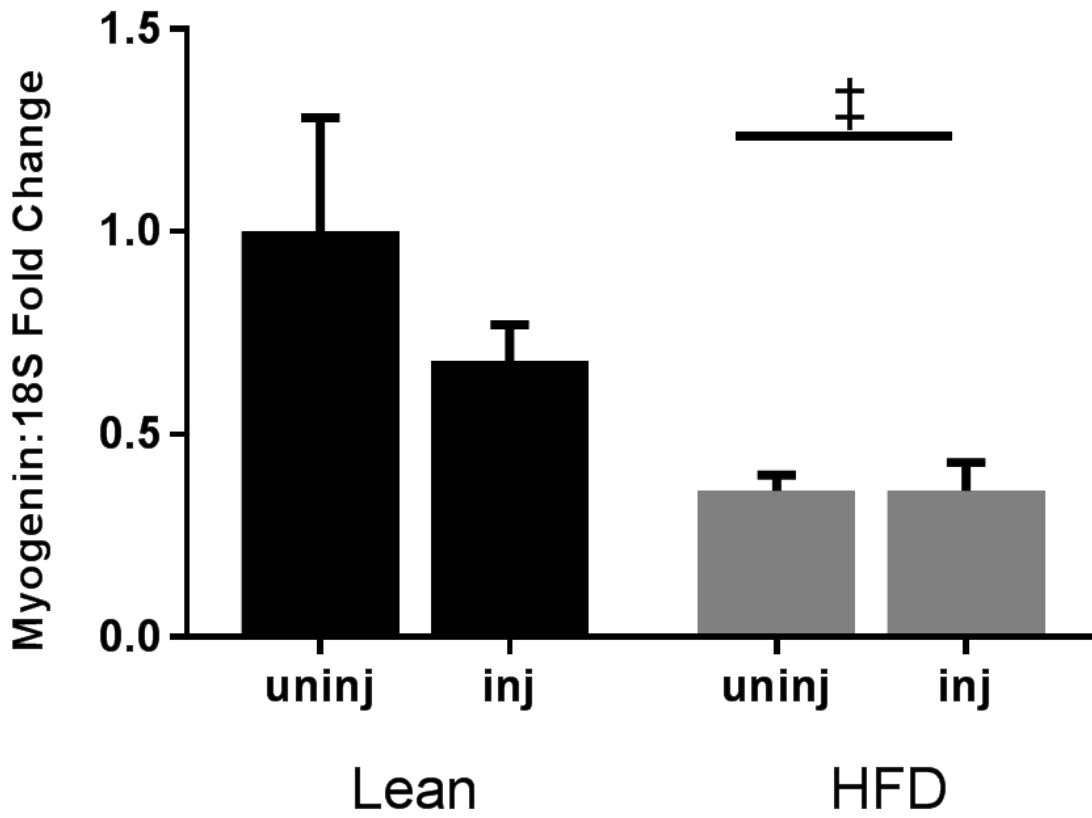
G.
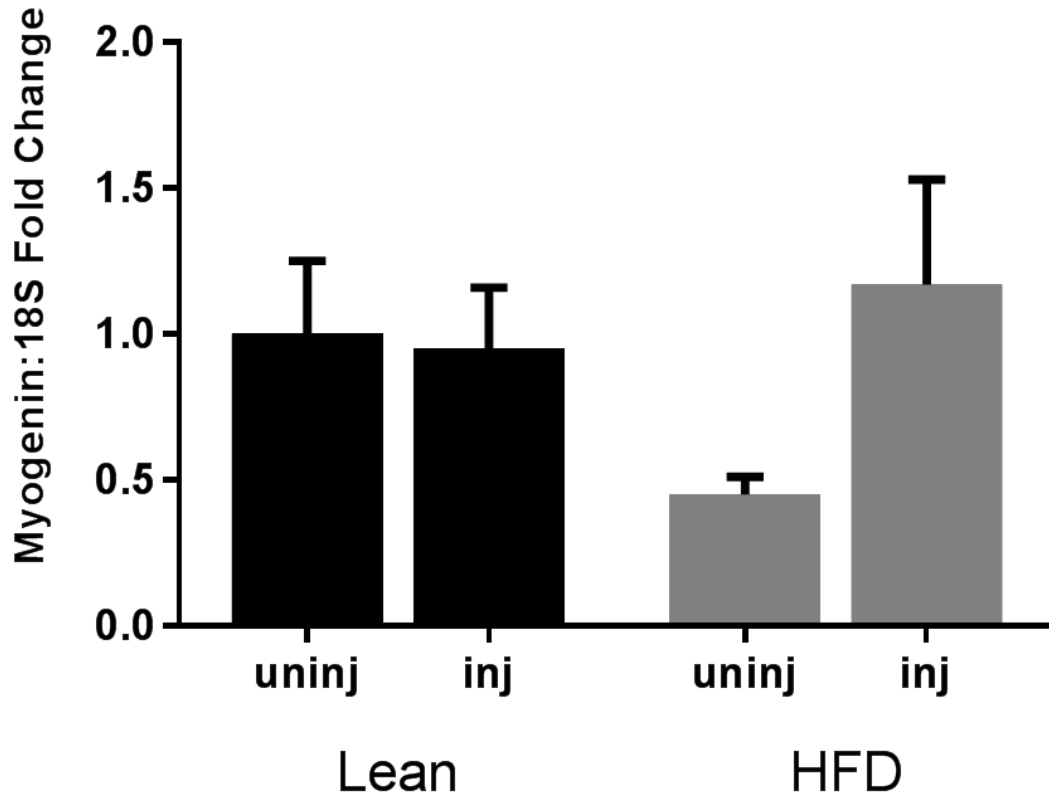
H.
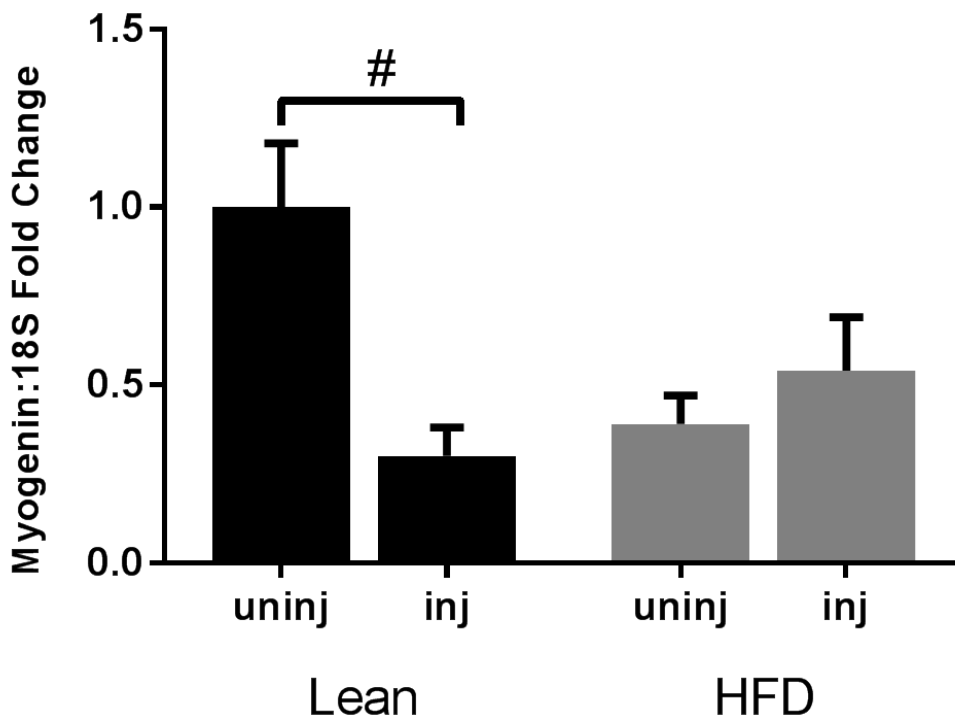
Figure 3

A.

B.

C.

D.

Figure 4

A.

B.

C.

Young 3D
YLu YLi YHu YHi
P-STAT3
STAT3
Ponceau

‡

P-Stat3/Stat3 Protein (Fold Change)

Lean   HFD

uninj   inj   uninj   inj

D.

Young 21D
YLu YLi YHu YHi
P-STAT3
STAT3
Ponceau

‡

P-Stat3/Stat3 Protein (Fold Change)

Lean   HFD

uninj   inj   uninj   inj

154

Figure 5
A.

B.

C.

D.

156
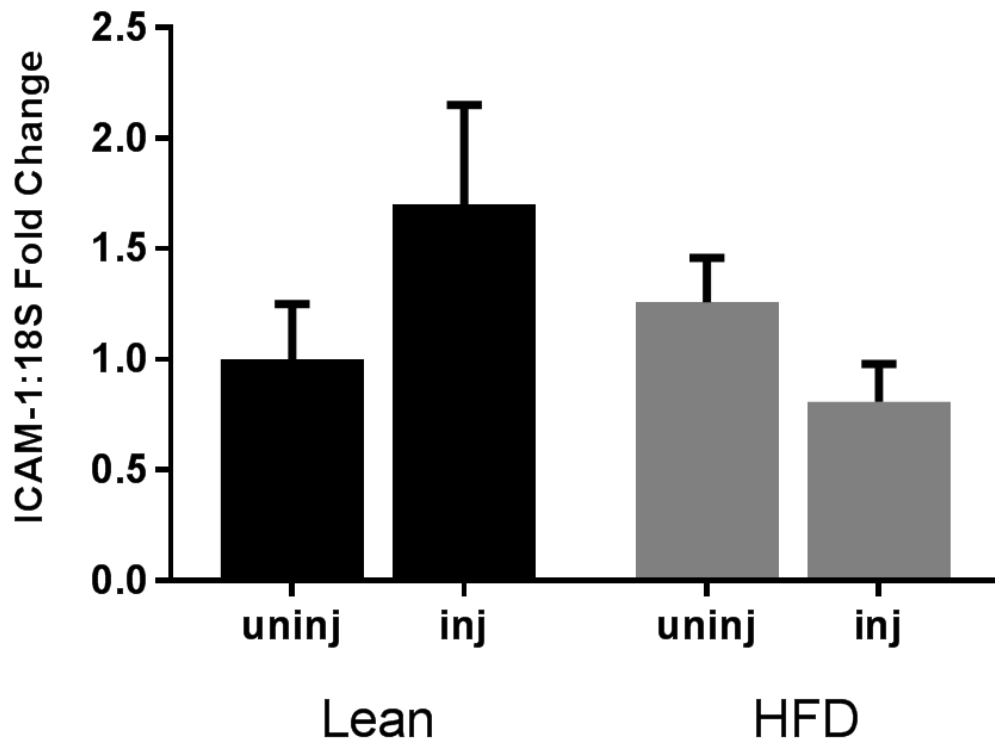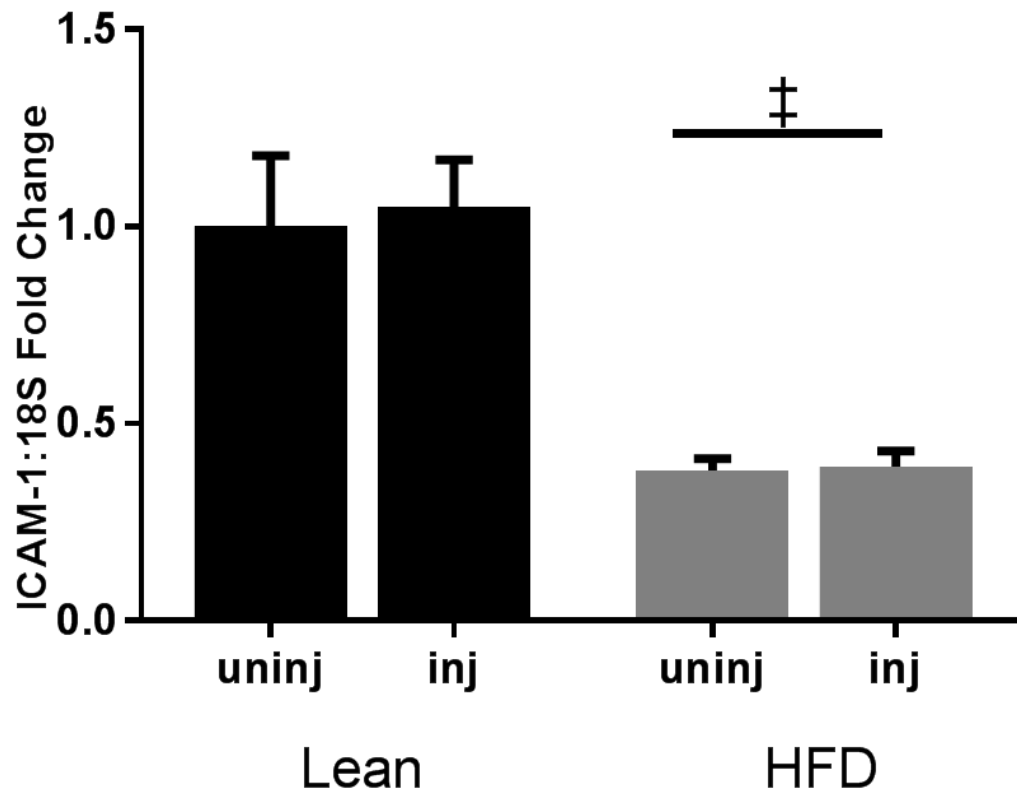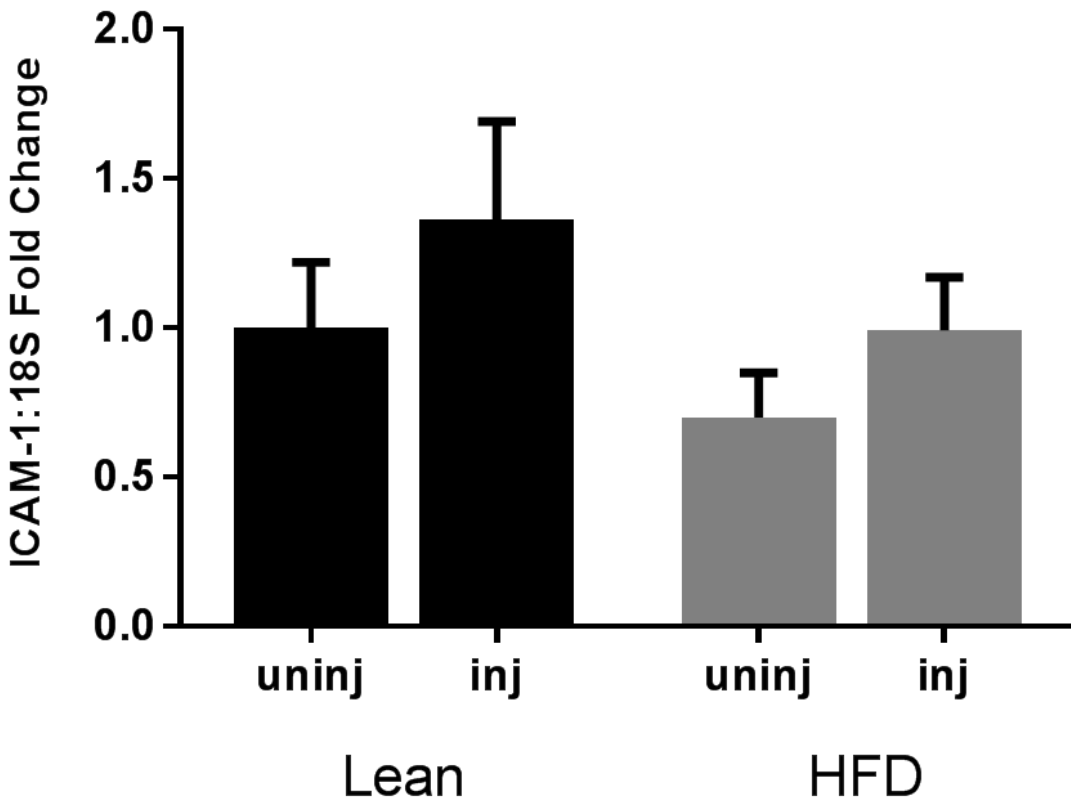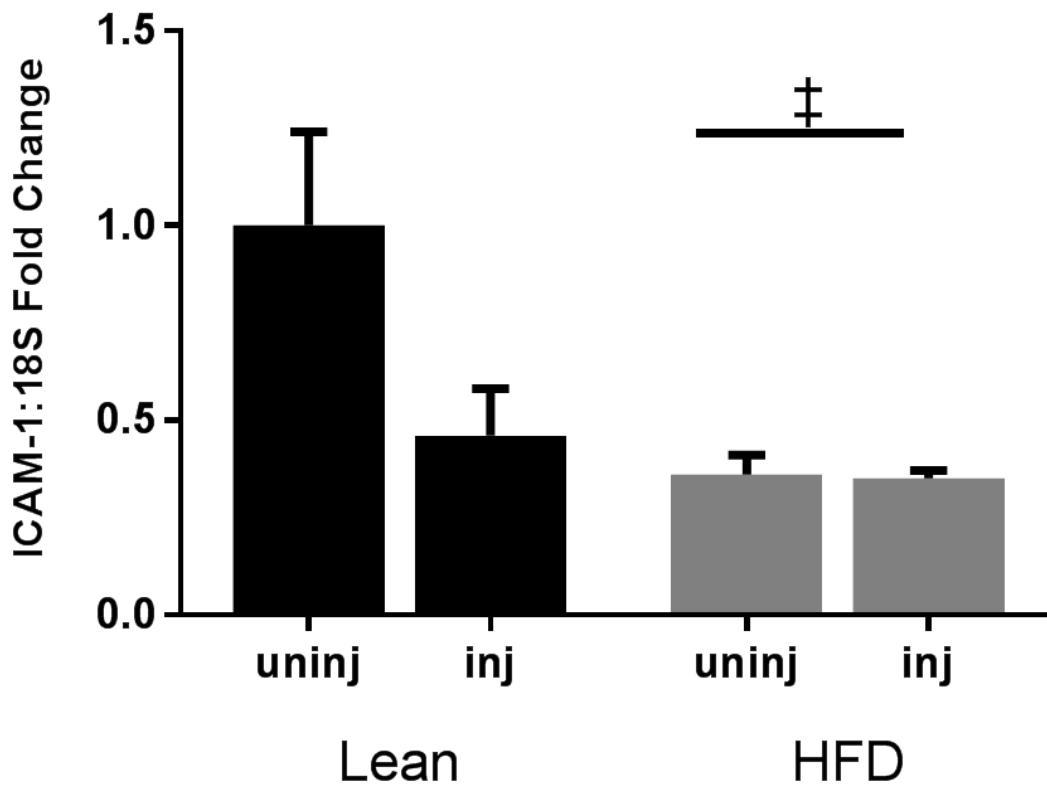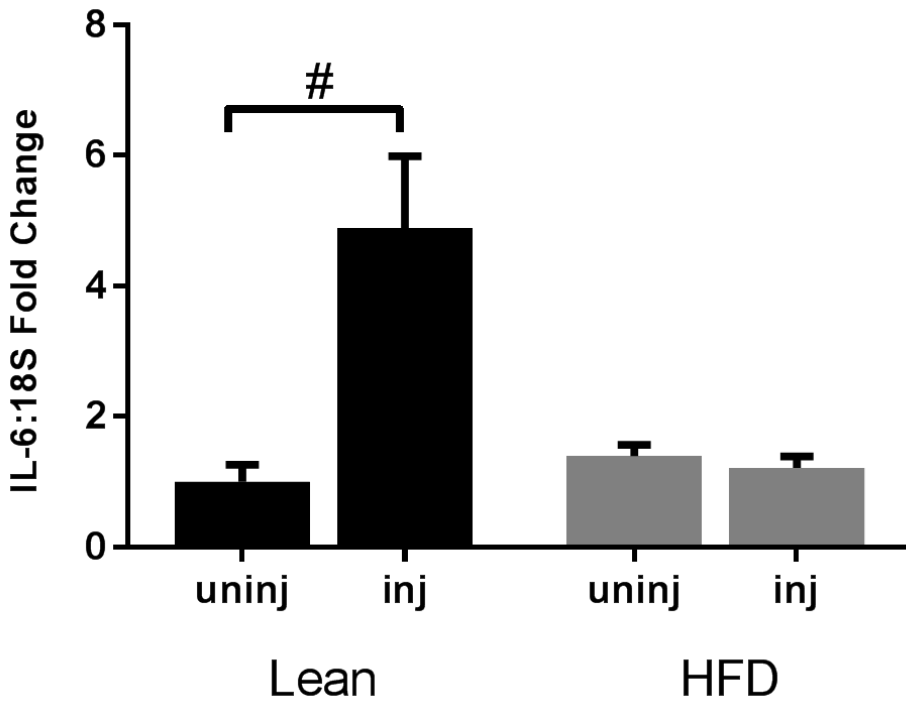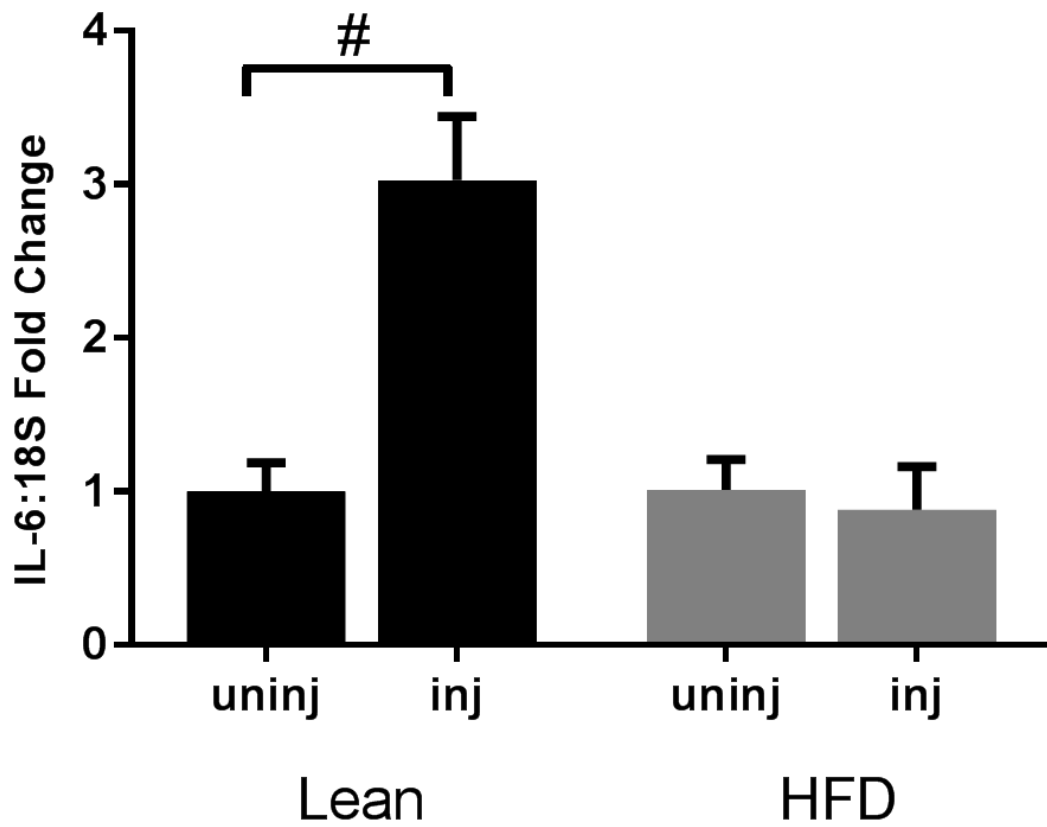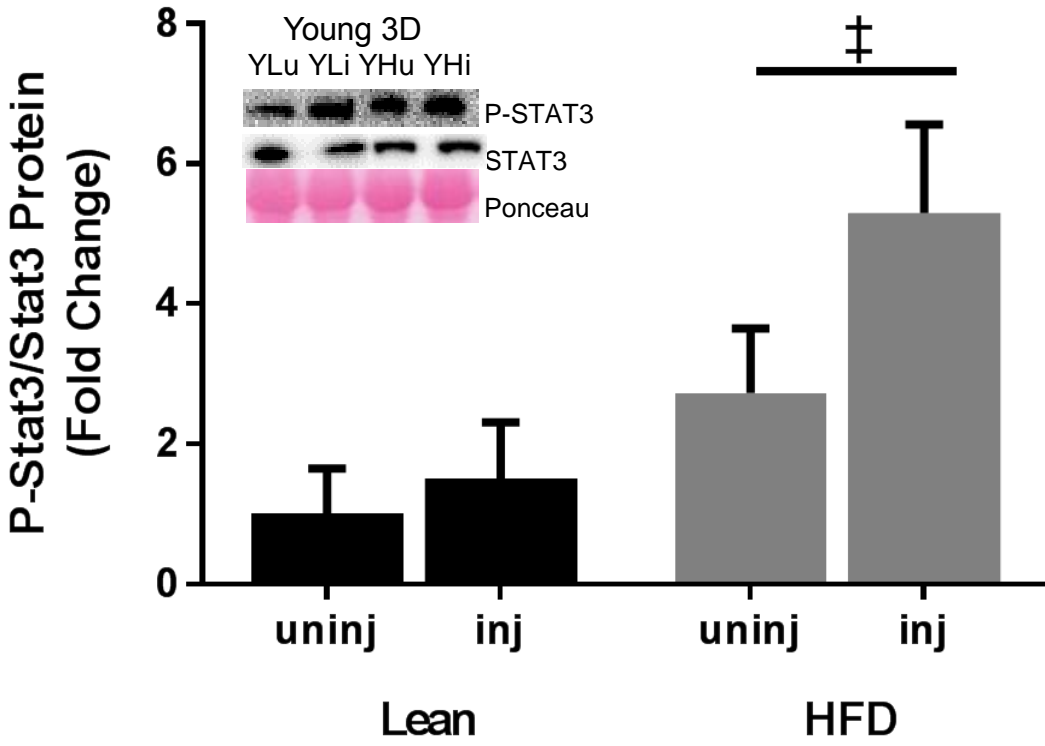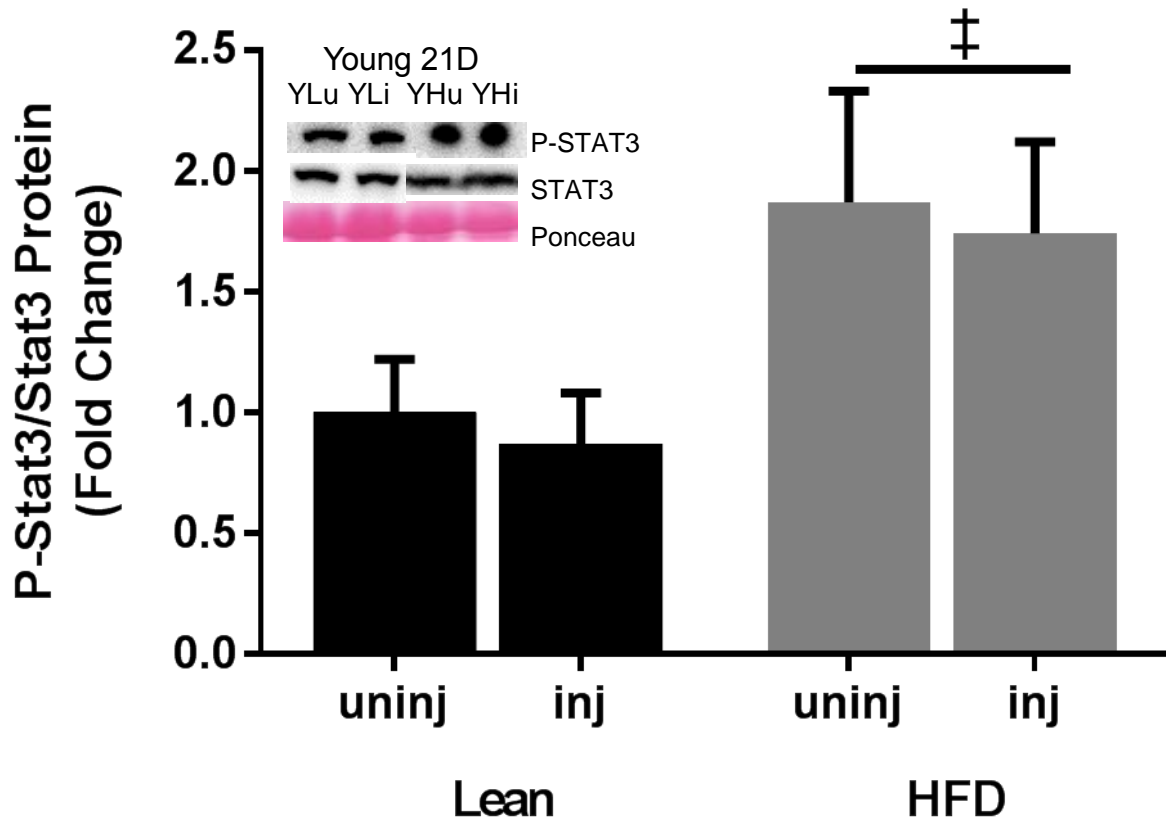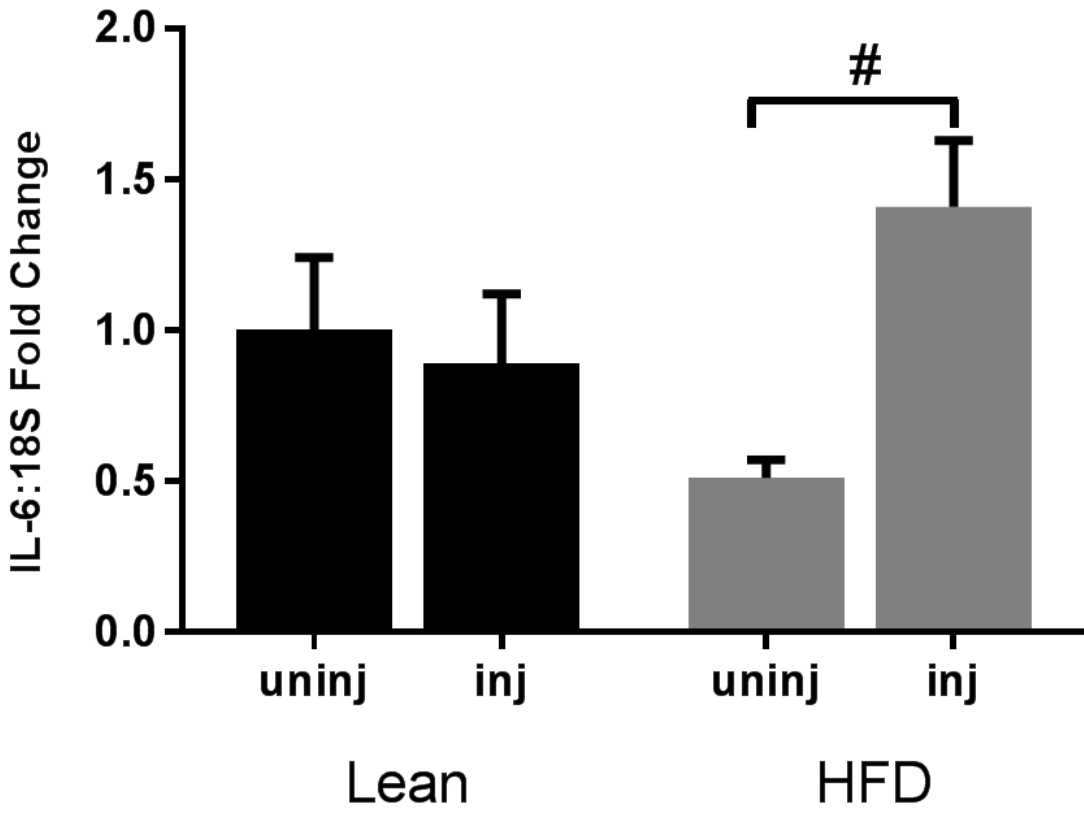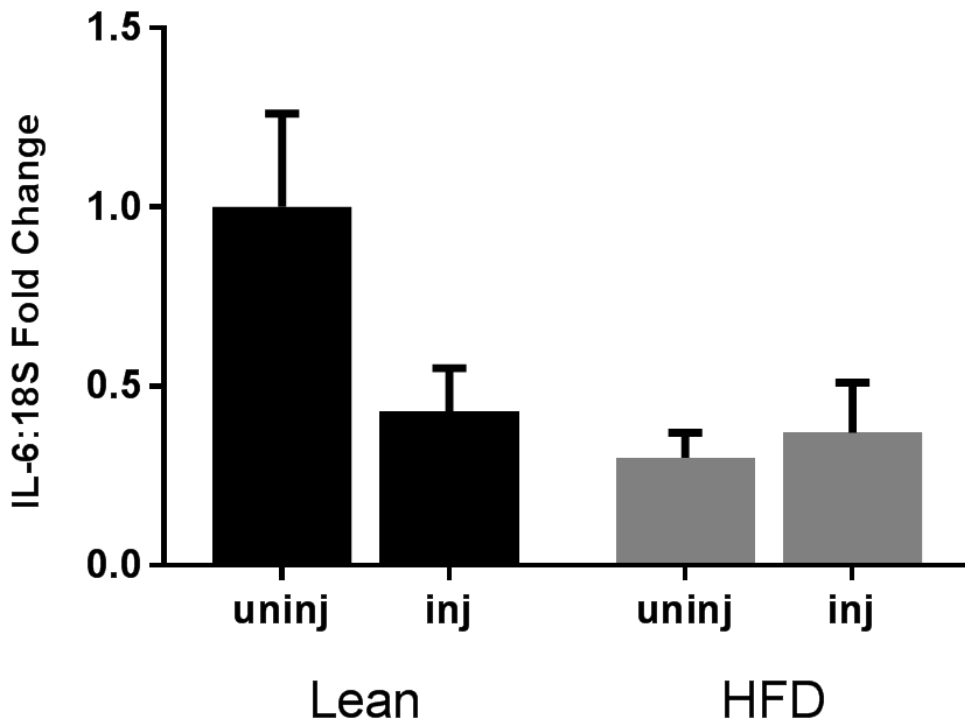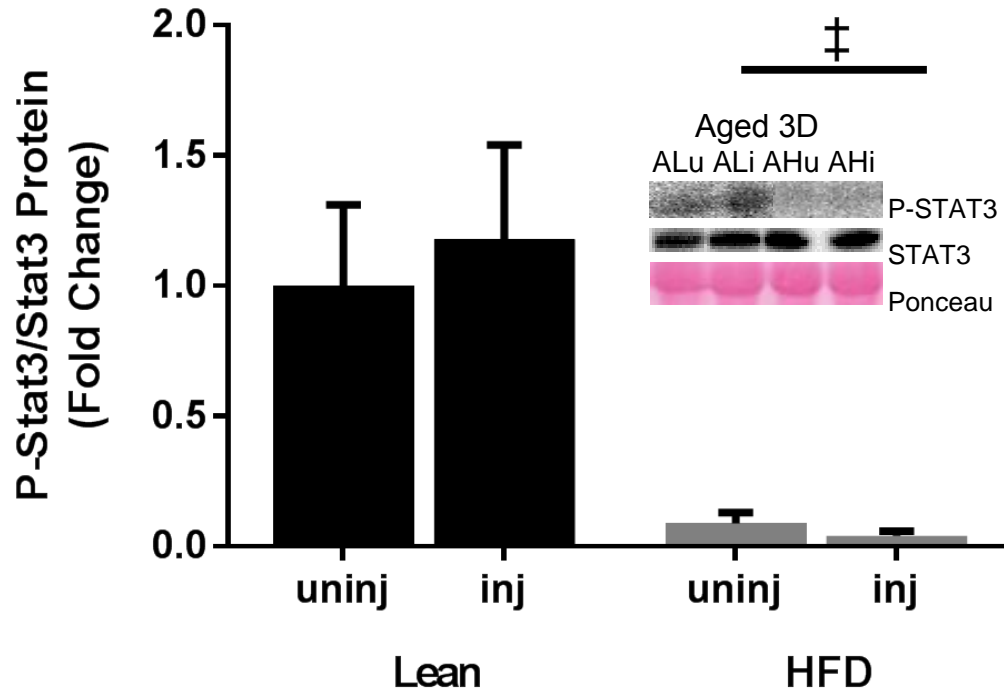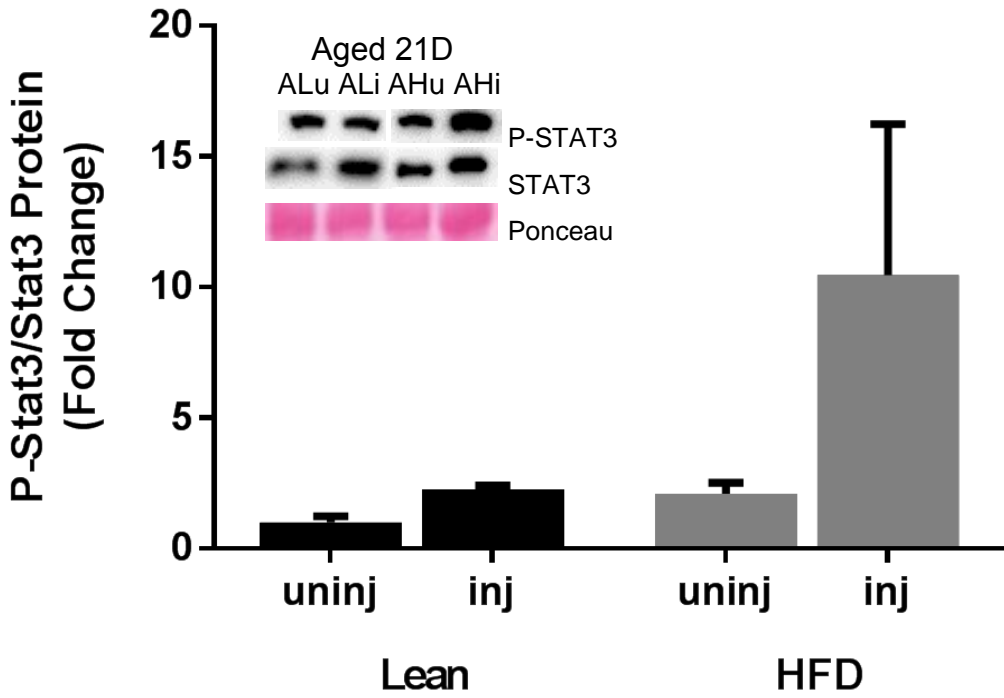
Figure 6

A.
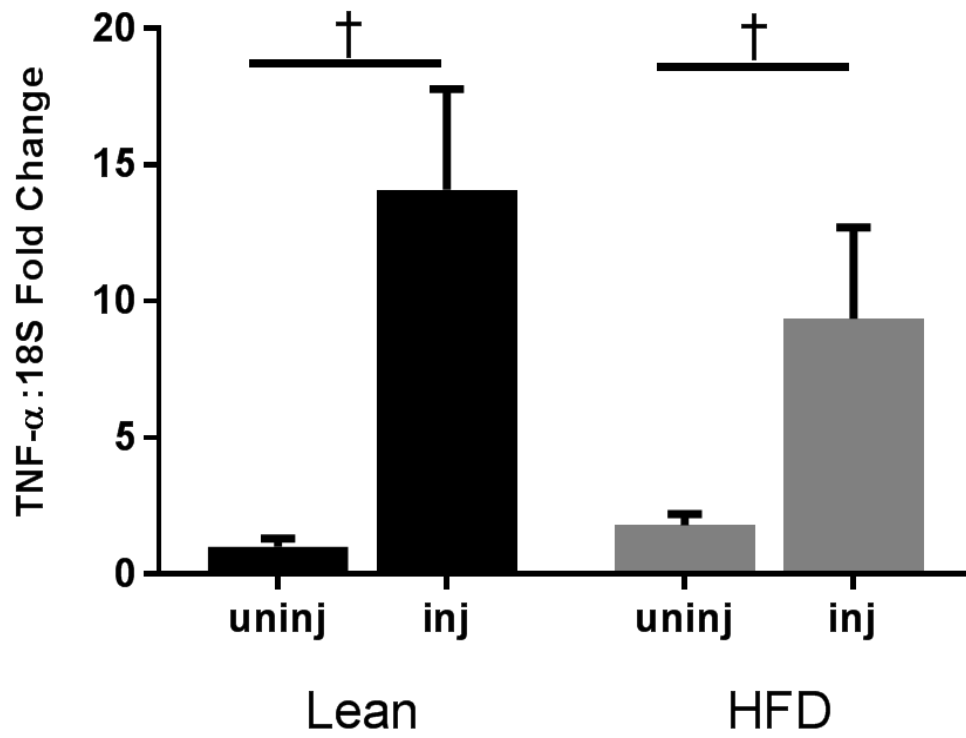
B.
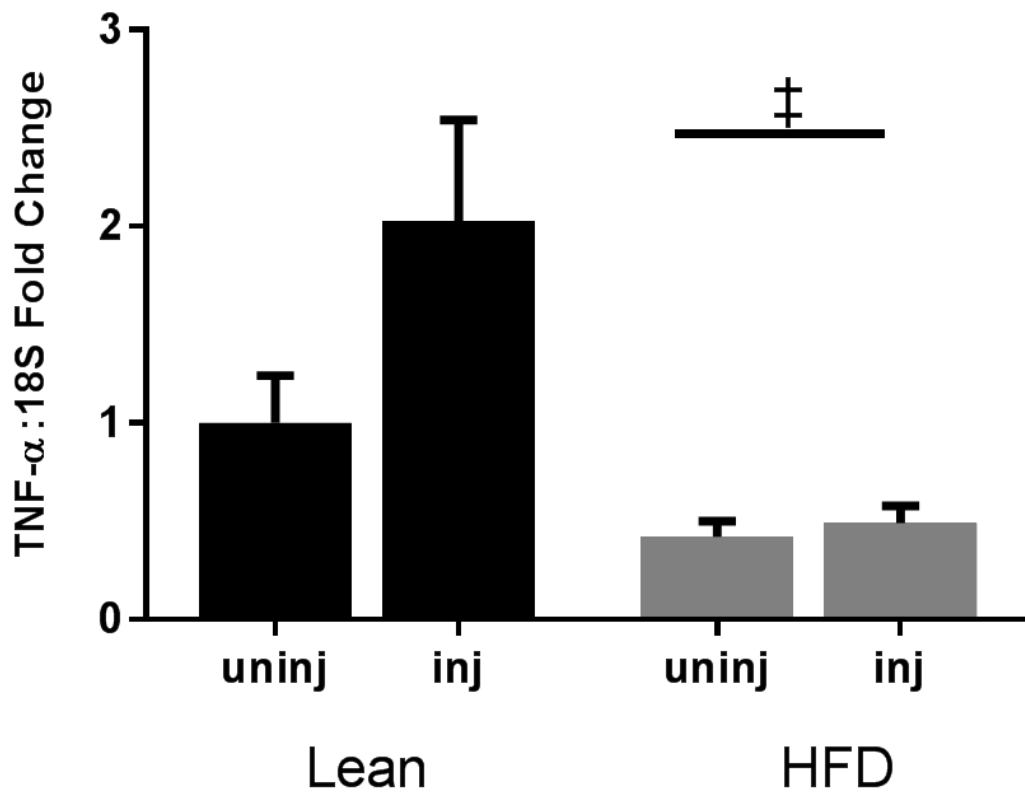
C.
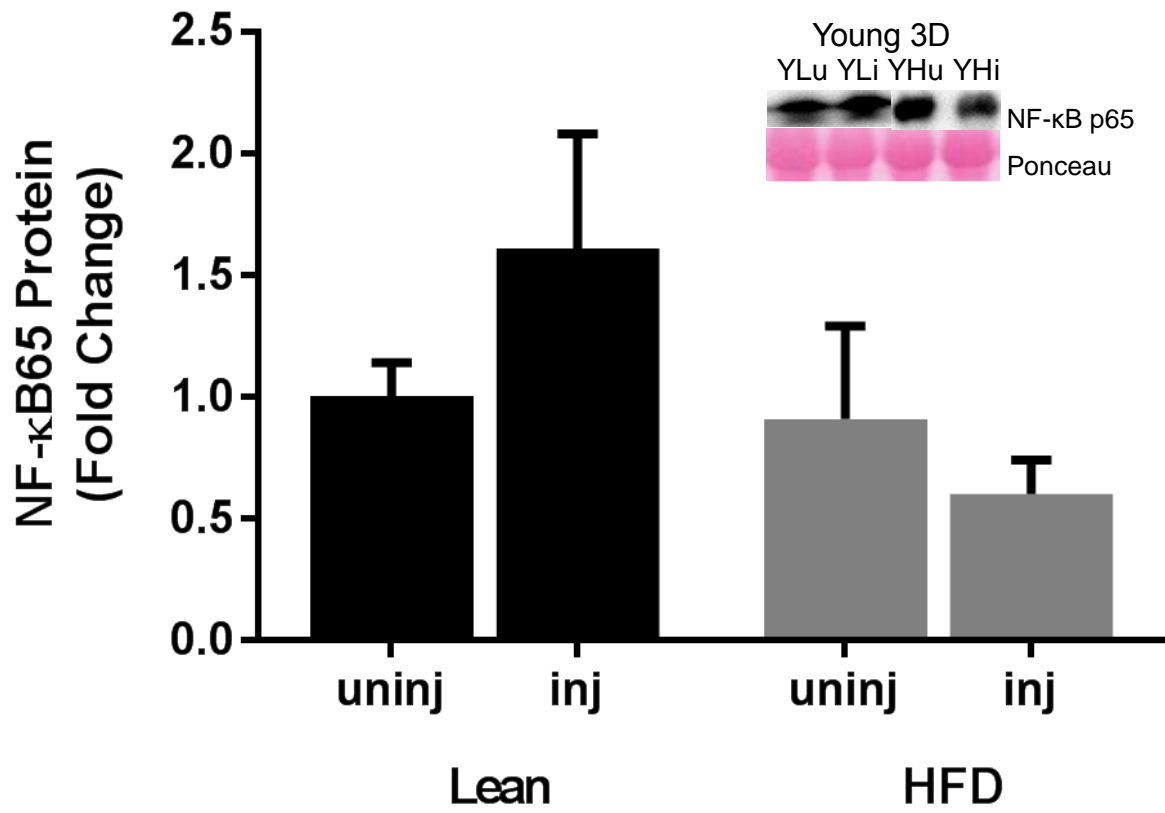
D.
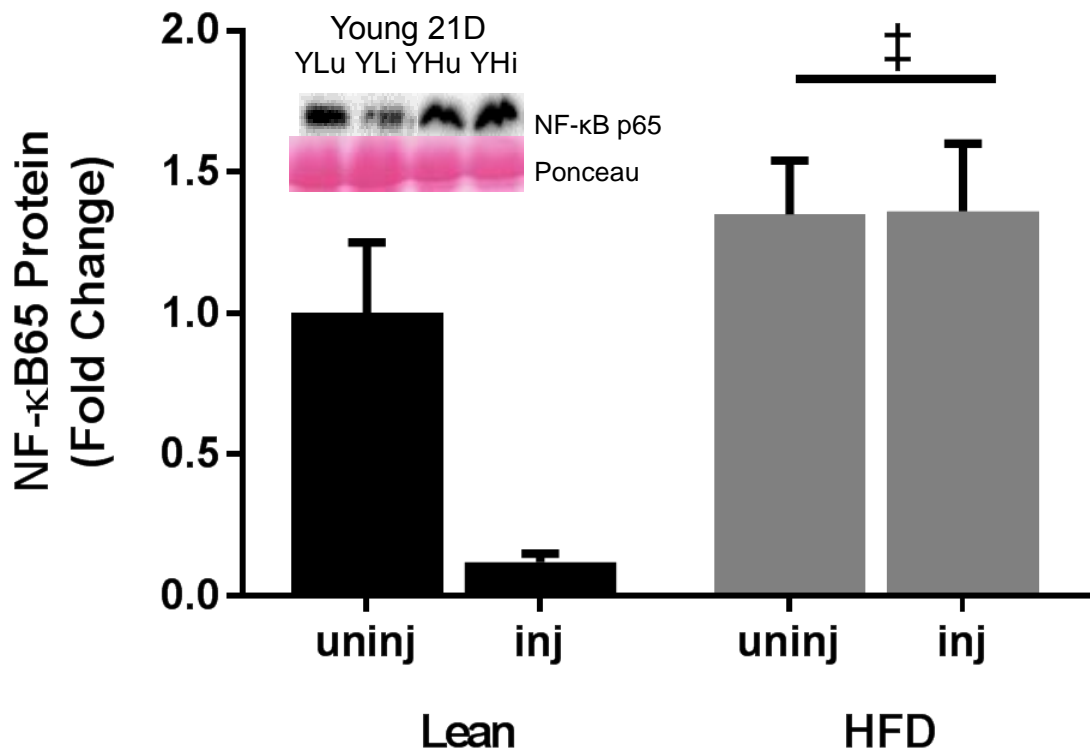
Figure 7

A.
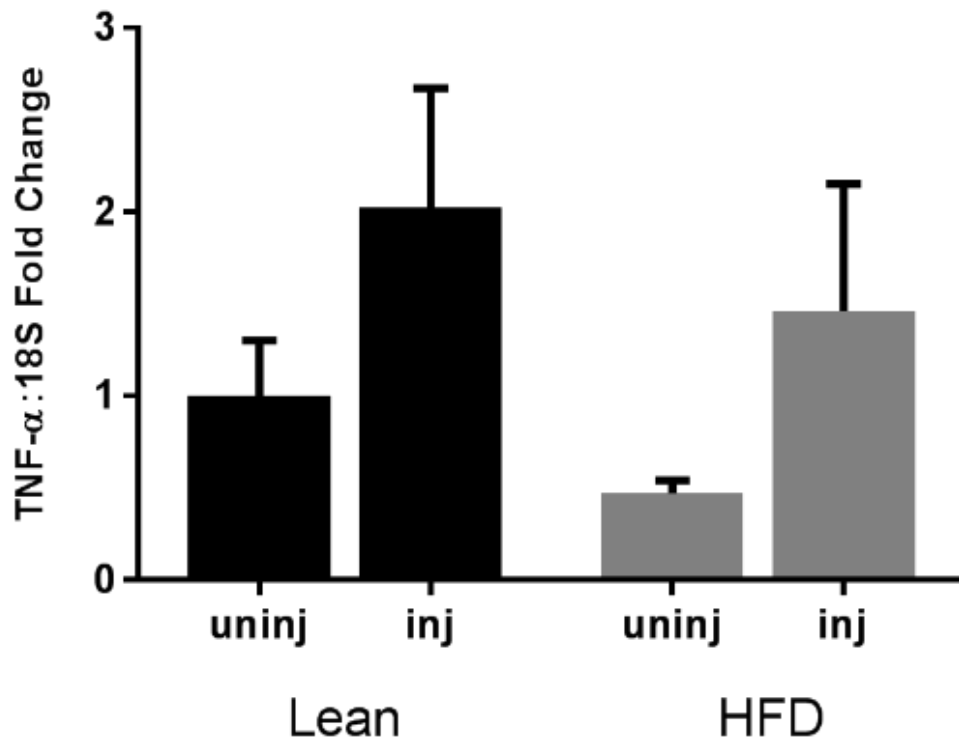
B.
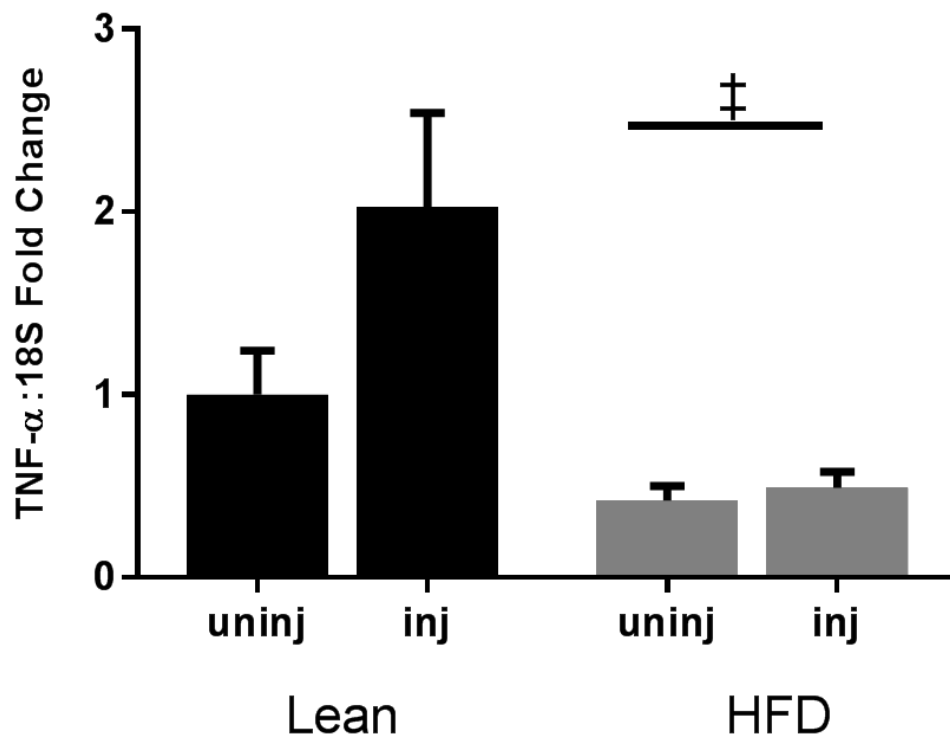
C.
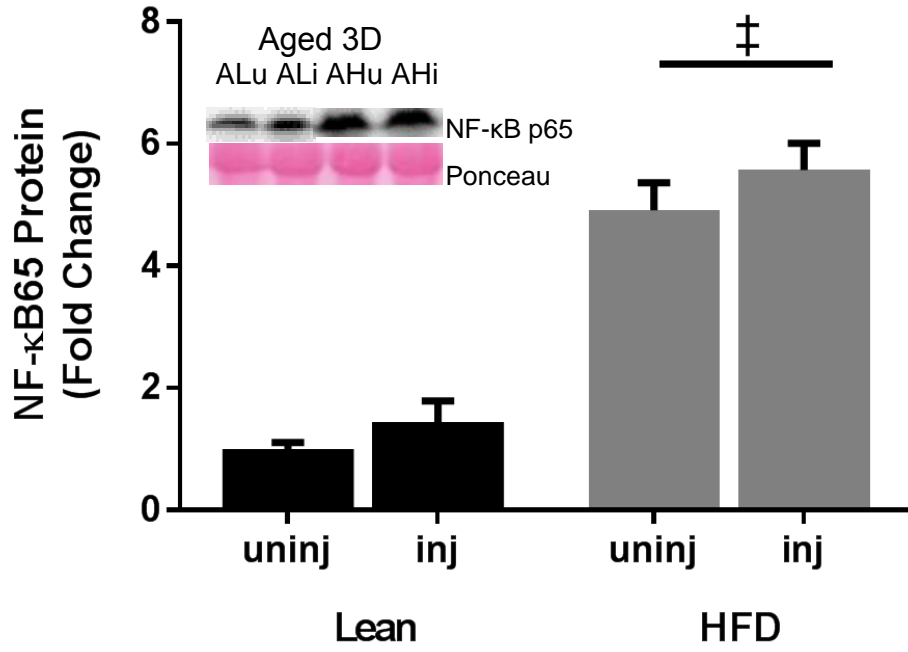
D.
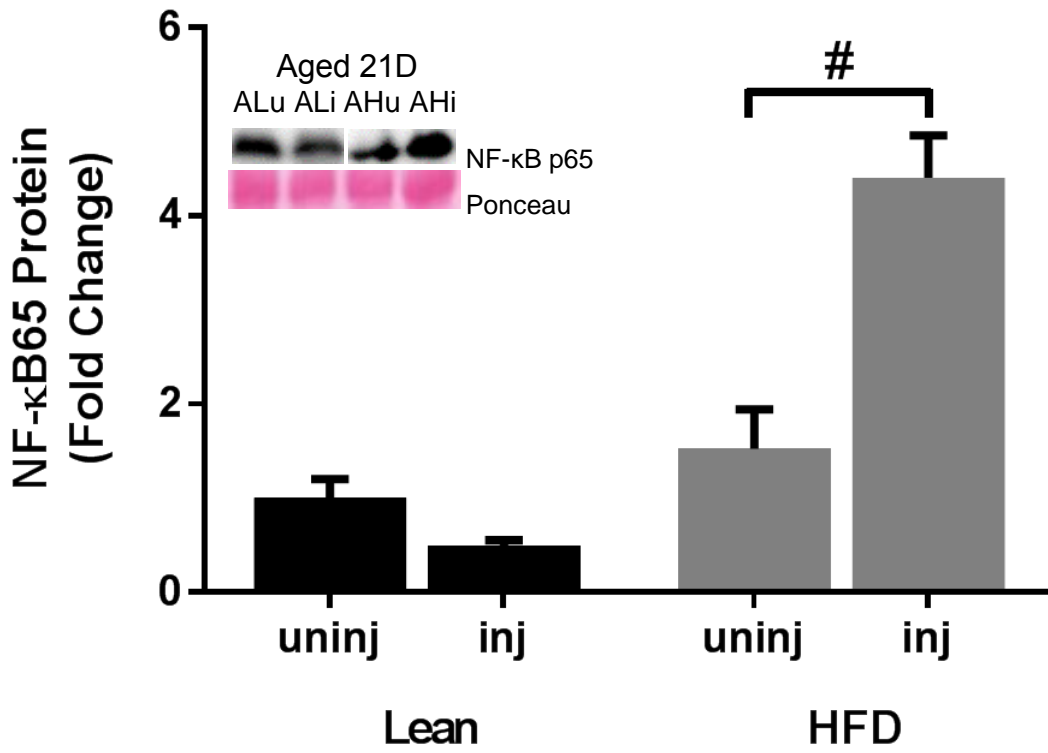
Chapter 5

Diet-induced obesity alters ECM remodeling in sarcopenic mice during skeletal muscle regeneration

[1,2]Lemuel A. Brown, [1,2]Richard A. Perry, [1,2]Wesley S. Haynie, [2]Jacob L. Brown, [3]John T. Kim, [3]Benjamin M. Kasukonis, [2]Thomas A. Blackwell, [2]Megan E. Rosa, [2]David E. Lee, [2]Nicholas P. Greene, [3]Jeffrey C. Wolchok, and [1,2]Tyrone A. Washington

[1]Exercise Muscle Biology Laboratory, [2]Human Performance Laboratory, Department of Health, Human Performance and Recreation, University of Arkansas, Fayetteville AR 72701
[3]Department of Biomedical Engineering, University of Arkansas, Fayetteville AR 72701

Running Title: Aged Diet-induced obesity and muscle regeneration

Corresponding author:
Tyrone A. Washington, Ph.D.
University of Arkansas
Department of Health, Human Performance, and Recreation
155 Stadium Dr. HPER 308H
Fayetteville AR 72701

Office Phone: 479-575-6693
Fax: 479-575-5778
tawashin@uark.edu

Abstract

AIM: Sarcopenic obesity is a vastly growing population worldwide that is tied with several health risks. Both aging and obese individuals are tied with poor regenerative capacity and increased muscle fibrosis. This is alarming because sarcopenic obese individuals exhibit progressive muscle loss which is associated with mortality in aging. The extracellular matrix is essential because it assists in regenerating muscle fibers by releasing growth factors and can protect the musculature from high amounts of stress. The remodeling of the ECM may be impaired in sarcopenic obese individuals. The purpose of this study was to determine how obesity alters extracellular matrix remodeling (ECM) during muscle regeneration in mice. **METHODS:** One hundred two male C57BL6/J mice (4 weeks old) were randomly assigned to either a high fat diet (HFD, 60% fat) or normal chow. Both young mice (12 weeks) and aged mice (22-24 months old) were injected with either PBS or bupivacaine. The TA was excised 3 or 21 days after injection. **RESULTS:** There was a main effect of injury to reduce collagen I and III content in aged injured mice 3 days following myotoxin induced muscle damage. There was a main effect of diet with a decrease of collagen I, collagen III, and MMP-9 gene expression in aged HFD mice 3 days following myotoxin-induced muscle damage. **CONCLUSION:** Sarcopenic obese mice had changes in collagen content and reduced ECM gene expression that suggests impaired ECM remodeling in sarcopenic obese mice.

Keywords: collagen, muscle injury, MMP, fibronectin, regeneration

Introduction

Currently, the worldwide estimation of adults 65 years is 605 million individuals and roughly a third of them are considered obese (Amarya, Singh, & Sabharwal, 2014). This is a major concern because older adults are the fastest growing obese population in the United States. Not to mention, older adults and obesity are associated with increased skeletal muscle fibrosis and reduced insulin sensitivity (Goldspink et al., 1994; Lim et al., 2010; Proctor et al., 1998). As a result, older obese adults have reduced mobility and an increased risk of disability (Fried et al., 2001). Muscle fibrosis in obese and older adults partially stems from improper or sub-optimal skeletal muscle regeneration (L. A. Brown et al., 2015; Smythe et al., 2008).

The skeletal muscle regeneration process is comprised of an inflammatory response, myoblast proliferation and differentiation, and extracellular matrix (ECM) remodeling that will work synergistically for optimal muscle growth and repair. Skeletal muscle ECM can be induced by mechanical stimuli and/or traumatic damage to muscle tissue, which will release the growth factor TGF-β that will induce anti-inflammatory cytokines over time to increase collagen turnover and ECM regulatory proteins necessary for ECM remodeling (Hocevar et al., 1999; Kjaer, 2004). Thus, ECM remodeling takes place in both the early and late stages of skeletal muscle regeneration.

Skeletal muscle ECM is predominately comprised of collagen I and collagen III triple helix polypeptides that are activated transcriptionally during the regenerative process to increase collagen deposition (Kjaer, 2004; Schiaffino & Partridge, 2008). Collagen I has been implicated as the sturdiest collagen fibril whereas collagen III is a naïve collagen fibril that is more pliable and is involved in collagen I production (Kjaer, 2004; Schiaffino & Partridge, 2008). Along with collagen, Matrix metalloproteinases (MMPs), which are zymogen

163

endopeptidases, are activated to degrade collagen for ECM remodeling and myoblast migration (Bourboulia & Stetler-Stevenson, 2010). In regards to muscle regeneration, MMP-2 and MMP-9 have been implicated as essential ECM proteins because of their role in muscle ECM remodeling and satellite cell migration during the regenerative process (Schiaffino & Partridge, 2008). The family of MMPs are controlled by tissue inhibitors of MMPs (TIMPs) that can dock on the active region of MMPs to stop the cleavage of collagen and ECM promoting such as fibronectin (Bourboulia & Stetler-Stevenson, 2010). Physiological changes to this process such as insulin resistance can reduce alter the ECM remodeling and in worst cases cause aberrant signaling of a couple or several proteins that play key roles in the regenerative process.

There have been a few studies examining how chronic injury, aging, and obesity may negatively impact ECM remodeling and the regenerative process. Ireland and colleagues examined ECM gene expression of Collagen I and III in chronic Achilles tendinopathy (Ireland et al., 2001). They observed an upregulation of both collagen I and II with an increase in the collagen III/I ratio (Ireland et al., 2001). These findings are consistent with other studies that witnessed that individuals suffering from traumatic acute or chronic injury exhibited fibrosis and an increase collagen III/I ratio (Ameye et al., 2002). It has been reported that both aging and obesity have higher collagen content in skeletal muscle tissue (Berria et al., 2006; Wood et al., 2014). In aging muscle collagen concentration may be 2-fold higher compared to young and is associated with muscle stiffness (Wood et al., 2014). Moreover, it appears that the increase in fibrosis is due partially to the increase in M2a macrophages present in skeletal muscle that will promote collage deposition (Z. Wang et al., 2000). Thus, changes in ECM proteins and the regulation of these proteins can impair the regenerative process. Whether

these changes exist in Sarcopenic obese individuals has not been demonstrated.

Therefore the purpose of this study was to investigate how Sarcopenic obesity alters the skeletal muscle ECM following a damaging stimulus. We hypothesized that impaired muscle regeneration will be associated with an increase in skeletal muscle fibrosis. We further hypothesized that the induction of collagen III mRNA expression will be drastically increased.

Methods

Animals and Housing

One hundred two C57BL/6 mice were purchased from Jackson Laboratories. Animals were housed in the University of Arkansas Central Laboratory Animal Facility. The overall study consisted of 2 separate animal experiments in young adult (3-4 mo) and aged mice (22-24 mo). Experiment 1 examined immunohistochemistry and protein expression, and gene expression 3 days post-bupivacaine injection. Experiment 2 examined immunohistochemistry, muscle morphology, protein expression, and gene expression 21 days post-bupivacaine injection. For experiment 1 and 2 mice were randomly assigned to one of eight groups at 4 weeks of age: 1) young lean uninjured (n = 5); 2) young lean injured (n = 6); 3) young obese uninjured (n = 5-8); 4) young obese injured (n = 6-8); 5) aged lean uninjured (n = 7-8); 6) aged lean injured (n = 7-8); 7) aged obese uninjured (n = 5-6); 8) aged obese injured (n = 6). Mice were fed normal chow (normal; 17% kcals fat Research Diets, New Brunswick, New Jersey) or a high fat diet (HFD; 60% kcals fat, Research Diets, New Brunswick, New Jersey) until they were euthanized. All procedures were approved by the University of Arkansas Institutional Animal Care and Use Committee (IACUC).

Muscle and Tibia Extraction

At either 3-4 mo or 22-24 mo of age, muscle and tibia extractions were performed as previously described (Tyrone A Washington et al., 2013; T. A. Washington et al., 2011). The TA and tibias were extracted while the mice were anesthetized with a subcutaneous injection of a cocktail containing ketamine hydrochloride (90 mg/kg body weight), xylazine (3 mg/kg body weight), and acepromazine (1 mg/kg body weight). The left TA was snap frozen in liquid nitrogen and stored at -80°C for protein and gene expression analysis, the right TA was

166

cut at the midbelly, mounted in optimum cutting temperature compound (OCT), and then

dropped in liquid nitrogen cooled isopentane. Once frozen, samples were stored at -80°C for

morphological analysis. After the muscles was dissected out, the tibia was removed and

measured with a plastic caliper (VWR, Radnor, PA, USA). Tibia measurements were utilized

to normalize muscle weights to an estimate of total body size.

Bupivacaine Injection

At 3 mo or 22-23 mo of age, bupivacaine (Hospira, Lake Forest, IL) injections were

performed as previously described (Washington et al., 2013). Mice were anesthetized with a

subcutaneous injection of a cocktail containing ketamine hydrochloride (45 mg/kg body

weight), xylazine (3 mg/kg body weight), and acepromazine (1 mg/kg body weight). Muscle

damage was induced by injecting 0.03ml of 0.75% bupivacaine (Marcaine) in the left and

right tibialis anterior muscles (TA). A 25-gauge, 5/8 (0.5 x 16 mm) needle was inserted along

the longitudinal axis of the muscle, and the bupivacaine was injected slowly as the needle was

withdrawn. The control group was injected with 0.03 ml of phosphate buffered saline (PBS).

Tissue histology and image analysis

The following procedures were completed as previously described (Kim et al., 2016).

Each TA muscle cross-section will was cut at 10 µm (n = 3-5) using the cryostat and placed

on a slide. Prior to immunostaining, slides were permeabilized in 0.1% 100X triton then

rinsed in phosphate-buffered solution (PBS, pH 7.4). Slides were then blocked in PBS

containing 4% goat serum and 0.05% sodium azide for 1h at room temperature prior to

incubation in primary antibodies including mouse-anti-collagen I IgG (1:500, Sigma Aldrich),

rabbit polyclonal anti-collagen III (1:1000, Abcam), and mouse-anti-myosin IgG$_{2B}$ (MF-20,

1:10, Developmental Studies Hybridoma Bank, Iowa City, IA) for 4h at 4°C. Following PBS

washes, slides were incubated in the appropriate corresponding Alexa Fluor 488 and 596 (1:500, Life Technologies) labeled secondary antibodies for 30 minutes at room temperature. Images of the slide were acquired with a Nikon camera (Sight DS-Vi1) mounted on an Olympus CKX41 inverted microscope at 20X magnification (Olympus), analyzed with MATLAB. Total ECM area was determined by dividing the number of green pixels by the total number of pixels in the image.

RNA Isolation, cDNA synthesis, and quantitative RT-PCR

The following procedures were completed as previously described (N. P. Greene et al., 2015; Nicholas P Greene et al., 2014; Tyrone A Washington et al., 2013). RNA was extracted with Trizol reagent (Life Technologies, Grand Island, NY, USA). TA muscles were homogenized in Trizol. Total RNA was isolated, DNase treated and purity and concentrations were determined using 260/280nm ratios read on a BioTek Take3 microvolume microplate with a BioTek PowerWave XC microplate reader (BioTek Instruments Inc., Winooski, VT). cDNA was reverse transcribed from 1 µg of total RNA using the Superscript Vilo cDNA synthesis kit (Life Technologies, Carlsbad, CA, USA). Real-time PCR was performed, and results were analyzed by using the StepOne Real-Time PCR system (Life Technologies, Applied Biosystems, Grand Island, NY). cDNA was amplified in a 25 µL reaction containing appropriate primer pairs and TaqMan Universal Mastermix (Applied Biosystems). Samples were incubated at 95°C for 4 min, followed by 40 cycles of denaturation, annealing and extension at 95°C, 55°C and 72°C respectively. TaqMan fluorescence was measured at the end of the extension step each cycle. Fluorescence labeled probes for Collagen I (FAM dye), Collagen III (FAM dye), Firbronectin 1 (FAM dye), MMP-2 (FAM dye), MMP-9 (FAM dye), TIMP-1 (FAM dye), TGF-β (FAM dye), and 18S (FAM dye) were purchased from Applied

Biosystems and quantified with TaqMan Universal mastermix. Cycle threshold (Ct) was determined, and the ΔCt value was calculated as the difference between the Ct value and the 18S Ct value. Final quantification of gene expression was calculated using the ΔΔCT method Ct = [ΔCt(calibrator) – ΔCt(sample)]. Relative quantification was then calculated as $20^{-\Delta\Delta Ct}$. Melt curve analysis was performed at the end of the PCR run to verify no primer dimers were formed.

Statistical Analysis

All data was analyzed using Statistical Package for the Social Sciences (SPSS version 22.0, Armonk, NY). Results are reported as mean ± SEM. Pre-planned comparisons between lean and obese uninjured mice were conducted using Student's t-tests. For these analyses, lean and obese uninjured were pooled from the 3 and 21 day time-points. A two-way ANOVA was performed to analyze main effects of treatment and diet and if there were any interactions between the dependent variables for 3 and 21 days post-bupivacaine injection. When a significant interaction was detected, differences among individual means were assessed with Fisher's LSD post-hoc analysis.

Results

Collagen content

In the young mice, there was no difference in collagen I content in all groups 3 days post-bupivacaine injection (Fig. 1B). In the young mice, there was no difference in collagen III content in all groups 3 days post-bupivacaine injection (Fig. 1D). In the aged mice there was a main effect of diet with a decrease of collagen I content in the HFD group compared to the lean group 3 days post-bupivacaine injection (Fig. 1F). In the aged mice there was main effect of injury with a decrease in collagen I content in the injured group compared to the injured group 3 days post-bupivacaine injection (Fig. 2D). In the aged mice there was a main effect of injury with a decrease of collagen I content in the injured group compared to the uninjured group 3 days post-bupivacaine injection (Fig. 1H). In the young lean mice, collagen I content was 17% greater in the injured group compared to the uninjured group 21 days post-bupivacaine injection (Fig. 2B). In the young HFD lean mice, collagen I content was reduced by 26% in the injured group compared to the uninjured group 21 days post-bupivacaine injection. (Fig. 2B). In the young mice there was main effect of injury with a decrease in collagen III content in the injured group compared to the injured group 21 days post-bupivacaine injection (Fig. 2D). In the aged lean mice, collagen I content was reduced by 22% in the injured group compared to the uninjured group 21 days post-bupivacaine injection (Fig. 2F). In the aged HFD mice there was no difference in collagen I content in the injured group compared to the uninjured group 21 days post-bupivacaine injection (Fig. 2F). In the aged mice there was no difference in collagen III content in all groups 21 days post-bupivacaine injection (Fig. 2H).

Collagen gene expression

There was a main effect of injury with an increase of collagen I mRNA abundance in the young injured group compared to the young uninjured group 3 days post-bupivacaine injection (Fig. 3A). There was a main effect of diet with a decrease of collagen I mRNA abundance in the young HFD group compared to the young lean group 21 days post-bupivacaine injection (Fig. 3B). There was a main effect of diet with a decrease of collagen I mRNA abundance in the aged HFD group compared to the aged lean group 3 days post-bupivacaine injection (Fig. 3C). There was a main effect of diet with a decrease of collagen I mRNA abundance in the aged HFD group compared to the aged lean group 21 days post-bupivacaine injection (Fig. 3D). There was a main effect of injury with an increase of collagen III mRNA abundance in the young injured group compared to the young uninjured group 3 days post-bupivacaine injection (Fig. 3E). In the young lean mice collagen III mRNA abundance was not different in the injured group compared to the uninjured group 21 days post-bupivacaine injection (Fig. 3F). In the young HFD mice collagen III mRNA abundance was not different in the injured group compared to the uninjured group 21 days post-bupivacaine injection (Fig. 3F). There was a main effect of diet with a decrease of collagen III mRNA abundance in the aged HFD group compared to the aged lean group 3 days post-bupivacaine injection (Fig. 3G). In the aged lean mice collagen III mRNA abundance was not different in the injured group compared to the uninjured group 21 days post-bupivacaine injection (Fig. 3H). In the aged HFD mice collagen III mRNA abundance was not different in the injured group compared to the uninjured group 21 days post-bupivacaine injection (Fig. 3H).

Collagen promoter gene expression

There was a main effect of injury with an increase of fibronectin 1 mRNA abundance in the young injured group compared to the young uninjured group 3 days post-bupivacaine injection (Fig. 4A). There was a main effect of diet with a decrease of fibronectin 1 mRNA abundance in the young HFD group compared to the young lean group 21 days post-bupivacaine injection (Fig. 4B). There was a main effect of injury with an increase of fibronectin 1 mRNA abundance in the aged injured group compared to the aged uninjured group 3 days post-bupivacaine injection (Fig. 4C). There was a main effect of diet with a decrease of fibronectin 1 mRNA abundance in the aged injured group compared to the young uninjured group 21 days post-bupivacaine injection (Fig. 4D). There was a main effect of injury with an increase of TGF-β mRNA abundance in the young injured group compared to the young uninjured group 3 days post-bupivacaine injection (Fig. 4E). In the young lean mice, TGF-β mRNA abundance was not different in the injured group compared to the uninjured group 21 days post-bupivacaine injection (Fig. 4F). In the young HFD mice, TGF-β mRNA abundance was not different in the injured group compared to the uninjured group 21 days post-bupivacaine injection (Fig. 4F). In the aged lean mice, TGF-β mRNA abundance was not different in the injured group compared to the uninjured group 3 days post-bupivacaine injection (Fig. 4G). In the aged HFD mice, TGF-β mRNA abundance was not different in the injured group compared to the uninjured group 3 days post-bupivacaine injection (Fig. 4G). In the aged lean mice, TGF-β mRNA abundance was not different in the injured group compared to the uninjured group 21 days post-bupivacaine injection (Fig. 4H). In the aged HFD mice, TGF-β mRNA abundance was not different in the injured group compared to the uninjured group 21 days post-bupivacaine injection (Fig. 4H).

MMPs and TIMP gene expression

In the young lean mice, MMP-2 mRNA abundance was not different in the injured group compared to the uninjured group 3 days post-bupivacaine injection (Fig. 5A). In the young HFD mice, MMP-2 mRNA abundance was not different in the injured group compared to the uninjured group 3 days post-bupivacaine injection (Fig. 5A). There was a main effect of diet with a decrease of MMP-2 mRNA abundance in the young HFD group compared to the young lean group 21 days post-bupivacaine injection (Fig. 5B). In the aged lean mice, MMP-2 mRNA abundance was not different in the injured group compared to the uninjured group 3 days post-bupivacaine injection (Fig. 5C). In the aged HFD mice, MMP-2 mRNA abundance was not different in the injured group compared to the uninjured group 3 days post-bupivacaine injection (Fig. 5C). There was a main effect of diet with a decrease of MMP-2 mRNA abundance in the young HFD group compared to the young lean group 21 days post-bupivacaine injection (Fig. 5D). In the young lean mice, MMP-9 mRNA abundance was not different in the injured group compared to the uninjured group 3 days post-bupivacaine injection (Fig. 5E). In the young HFD mice, MMP-9 mRNA abundance was not different in the injured group compared to the uninjured group 3 days post-bupivacaine injection (Fig. 5E). In the young lean mice MMP-9 mRNA abundance was not different in the injured group compared to the uninjured group 21 days post-bupivacaine injection (Fig. 5F). In the young HFD mice MMP-9 mRNA abundance was not different in the injured group compared to the uninjured group 21 days post-bupivacaine injection (Fig. 5F). There was a main effect of diet with a decrease of MMP-9 mRNA abundance in the aged HFD group compared to the aged lean group 21 days post-bupivacaine injection (Fig. 5G). There was a main effect of diet with a decrease of MMP-9 mRNA abundance in the aged HFD group compared to the aged lean group 21 days post-bupivacaine injection (Fig. 5H). There was a main effect of injury with a

173

decrease of MMP-9 mRNA abundance in the aged injured group compared to the aged uninjured group 21 days post-bupivacaine injection (Fig. 5H). In the young lean mice, TIMP-1 mRNA abundance was 28-fold greater (Fig. 5I) in the injured group compared to the uninjured group 3 days post-bupivacaine injection. In the young HFD mice TIMP-1 mRNA abundance was not different in the injured group compared to the uninjured group 3 days post-bupivacaine injection (Fig. 5I). There was a main effect of diet with a decrease of TIMP-1 mRNA abundance in the young HFD group compared to the young lean group 21 days post-bupivacaine injection (Fig. 5J). There was a main effect of injury with an increase of TIMP-1 mRNA abundance in the aged injured group compared to the aged uninjured group 3 days post-bupivacaine injection (Fig. 5K). In the aged lean mice, TIMP-1 mRNA abundance was reduced by 47% (Fig. 5L) in the injured group compared to the uninjured group 21 days post-bupivacaine injection. In the aged HFD mice TIMP-1 mRNA abundance was not different in the injured group compared to the uninjured group 21 days post-bupivacaine injection (Fig. 5L).

Discussion

The primary goal of this study was to examine how sarcopenic obesity alters extracellular matrix remodeling in skeletal muscle following injured. We hypothesized that there would be no change in collagen I content due to inactivity of senescent muscle cells to upregulate collagen following muscle damage. In addition, we expected to observe excessive MMP activity due to reductions of TIMP-1 activity. To our knowledge we are the first to demonstrate reductions in collagen I content in sarcopenic obese mice and reduced collagen, MMP, and fibronectin gene expression at the early and late stages of muscle injury.

Following muscle damage there appears to be several changes in collagen content due to sarcopenic obesity. We witnessed reductions in collagen I and III content 3 days following myotoxin injection. Aging is associated with muscle fibrosis due to excessive MMP activity and reduced collagen turnover (Kragstrup et al., 2011; Uezumi et al., 2011; Unsold, Bremen, Didie, Hasenfuss, & Schafer, 2014). However, we did not observe any changes in MMP-2 expression and a decrease in MMP-9 expression. Even though MMP expression did not appear to be upregulated in the sarcopenic obese group it is still likely that MMP activity is occurring much earlier than 3 days after muscle damage which would explain the downregulation of MMP-9 and changes in collagen which has a long half-life. Moreover the reduction of collagen III in sarcopenic obese mice could reduce the elastic properties of the muscle fiber and thus increasing susceptibility to traumatic injury following muscle recovery.

This study also demonstrated alterations in collagen RNA expression in sarcopenic obese mice. Collagen I was reduced in aging HFD mice 3 days following damage and was still reduced 21 days following muscle damage. The reduction of collagen I expression is

175

supported by previous literature that reported slow turnover in mature collagen (Avery &

Bailey, 2005, 2006). The reduction of collagen I expression may indicate reduction in

collagen turnover. Furthermore, these animals may be more susceptible towards increased

muscle stiffness because advanced glycation of end products (AGE) occur in a low collagen

turnover environment (Avery & Bailey, 2005, 2006; DeGroot et al., 2001). AGE would also

be more likely to occur in sarcopenic obese individuals because the process favors an insulin

resistant environment as well (DeGroot et al., 2001; Song & Schmidt, 2012). Collagen III had

a similar fate and was reduced in aged HFD mice at the onset of muscle damage. It has been

suggested that collagen III is necessary for the development of collagen I. Without the

development of new collagen I, the sarcopenic obese muscle would be more susceptible to

muscle stiffness via AGE which occurs more so in mature collagen and aging mice (DeGroot

et al., 2001; Wood et al., 2014).

Both TGF-β and fibronectin are involved in promoting collagen synthesis during the

muscle regeneration process. Our results showed a pronounced elevation of fibronectin 3 days

following injury in the aged mice followed by a decrease 21 days after muscle damage. The

aging mice had a similar response in fibronectin demonstrating that fibronectin may not cause

the decrease in collagen observed in aging. This would also indicate that fibrillogenesis

remodeling may not be altered in aging mice. In this study we did not observe any changes in

TGF-β at the onset of muscle regeneration in aging mice. TGF-β is typically upregulated a

few days following muscle damage and will be upregulated for a few weeks to promote

collagen synthesis (Clarke & Feeback, 1996; Kjaer, 2004). Our results would implicate TGF-

β being partially responsible for altered collagen gene expression in aged mice. Hence, no

changes in TGF-β and a reduction in collagen content may elude to an imbalance in collagen turnover.

MMPs and Tissue inhibitors of MMPs (TIMPs) are also regulators of collagen and play a role in collagen turnover. Previously mentioned, MMP-2 and MMP-9 are reduced in aged HFD mice at the onset of muscle regeneration. In support with our findings, TIMP-1 gene expression was upregulated following 3 days following muscle damage in aged HFD mice. However, TIMP-1 returned to basal levels in aged HFD mice at 21 days which would suggest a different regulator to inhibit MMP expression at the later stages of regeneration.

Altogether, these findings illustrate a disruption of ECM remodeling in sarcopenic obesity through the inability of aging muscle to upregulate key ECM proteins. We have identified that HFD mice have reduced collagen and MMP gene expression and an upregulation of fibronectin and TIMP-1 that demonstrates the reductions of collagen content observed may be influenced by increased MMP activity immediately following muscle damage or the influence of other ECM related proteins that promote collagen degradation. Future studies need to focus on elucidating the disruption of ECM gene expression and determine how collagen I and collagen III are being regulated differently in aging and aging obesity.

Figure Legends

Figure 1. Immunofluorescent staining of skeletal muscle regeneration at 3 days of recovery after bupivacaine-induced injury. (A) Representative collagen I staining of muscle cross section of young lean uninjured (a), lean injured (b), HFD uninjured (c), and HFD injured (d). (B) Quantified collagen I content percentage in young lean and HFD mice. (C) Representative collagen III staining of muscle cross section of young lean uninjured (a), lean injured (b), HFD uninjured (c), and HFD injured (d). (D) Quantified collagen III content percentage in young lean and HFD mice. (E) Representative collagen I staining of muscle cross section of aged lean uninjured (a), lean injured (b), HFD uninjured (c), and HFD injured (d). (F) Quantified collagen I content percentage in aged lean and HFD mice. (G) Representative collagen III staining of muscle cross section of aged lean uninjured (a), lean injured (b), HFD uninjured (c), and HFD injured (d). (H) Quantified collagen III content percentage in aged lean and HFD mice. Main effects of injury distinguished by † and diet by ‡. Significant differences between lean uninjured and lean injured and aged uninjured and aged injured distinguished by [#]. $P \leq 0.05$.

Figure 2. Immunofluorescent staining of skeletal muscle regeneration at 21 days of recovery after bupivacaine-induced injury. (A) Representative collagen I staining of muscle cross section of young lean uninjured (a), lean injured (b), HFD uninjured (c), and HFD injured (d). (B) Quantified collagen I content percentage in young lean and HFD mice. (C) Representative collagen III staining of muscle cross section of young lean uninjured (a), lean injured (b), HFD uninjured (c), and HFD injured (d). (D) Quantified collagen III content percentage in young lean and HFD mice. (E) Representative collagen I staining of muscle cross section of aged lean uninjured (a), lean injured (b), HFD uninjured (c), and HFD injured

(d). (F) Quantified collagen I content percentage in aged lean and HFD mice. (G) Representative collagen III staining of muscle cross section of aged lean uninjured (a), lean injured (b), HFD uninjured (c), and HFD injured (d). (H) Quantified collagen III content percentage in aged lean and HFD mice. Main effects of injury distinguished by † and diet by ‡. Significant differences between lean uninjured and lean injured and aged uninjured and aged injured distinguished by [#]. $P \leq 0.05$.

Figure 3. Collagen mRNA abundance of skeletal muscle regeneration at 3 days and 21 days of recovery after bupivacaine-induced injury. (A) Collagen I mRNA abundance 3 days post-bupivacaine injection in young lean and HFD mice. (B) Collagen I mRNA abundance 21 days post-bupivacaine injection in young lean and HFD mice. (C) Collagen I mRNA abundance 3 days post-bupivacaine injection in aged lean and HFD mice. (D) Collagen I mRNA abundance 21 days post-bupivacaine injection in aged lean and HFD mice. (E) Collagen III mRNA abundance 3 days post-bupivacaine injection in young lean and HFD mice. (F) Collagen III mRNA abundance 21 days post-bupivacaine injection in young lean and HFD mice. (G) Collagen III mRNA abundance 3 days post-bupivacaine injection in aged lean and HFD mice. (H) Collagen III mRNA abundance 21 days post-bupivacaine injection in aged lean and HFD mice. Main effects of injury distinguished by † and diet by ‡. Significant differences between lean uninjured and lean injured and aged uninjured and aged injured distinguished by [#]. $P \leq 0.05$.

Figure 4. Fibronectin 1 and TGF-β mRNA abundance of skeletal muscle regeneration at 3 days and 21 days of recovery after bupivacaine-induced injury. (A) Fibronectin 1 mRNA abundance 3 days post-bupivacaine injection in young lean and HFD mice. (B) Fibronectin 1 mRNA abundance 21 days post-bupivacaine injection in young lean and HFD mice. (C)

Fibronectin 1 mRNA abundance 3 days post-bupivacaine injection in aged lean and HFD mice. (D) Fibronectin 1 mRNA abundance 21 days post-bupivacaine injection in aged lean and HFD mice. (E) TGF-β mRNA abundance 3 days post-bupivacaine injection in young lean and HFD mice. (F) TGF-β mRNA abundance 21 days post-bupivacaine injection in young lean and HFD mice. (G) TGF-β mRNA abundance 3 days post-bupivacaine injection in aged lean and HFD mice. (H) TGF-β mRNA abundance 21 days post-bupivacaine injection in aged lean and HFD mice. Main effects of injury distinguished by † and diet by ‡. Significant differences between lean uninjured and lean injured and aged uninjured and aged injured distinguished by [#]. $P \leq 0.05$.

Figure 5. MMP and TIMP mRNA abundance of skeletal muscle regeneration at 3 days and 21 days of recovery after bupivacaine-induced injury. (A) MMP-2 mRNA abundance 3 days post-bupivacaine injection in young lean and HFD mice. (B) MMP-2 mRNA abundance 21 days post-bupivacaine injection in young lean and HFD mice. (C) MMP-2 mRNA abundance 3 days post-bupivacaine injection in aged lean and HFD mice. (D) MMP-2 mRNA abundance 21 days post-bupivacaine injection in aged lean and HFD mice. (E) MMP-9 mRNA abundance 3 days post-bupivacaine injection in young lean and HFD mice. (F) MMP-9 mRNA abundance 21 days post-bupivacaine injection in young lean and HFD mice. (G) MMP-9 mRNA abundance 3 days post-bupivacaine injection in aged lean and HFD mice. (H) MMP-9 mRNA abundance 21 days post-bupivacaine injection in aged lean and HFD mice. (I) TIMP-1 mRNA abundance 3 days post-bupivacaine injection in young lean and HFD mice. (J) TIMP-1 mRNA abundance 21 days post-bupivacaine injection in young lean and HFD mice. (K) TIMP-1 mRNA abundance 3 days post-bupivacaine injection in aged lean and HFD mice. (L) TIMP-1 mRNA abundance 21 days post-bupivacaine injection in aged lean and

HFD mice. Main effects of injury distinguished by † and diet by ‡. Significant differences between lean uninjured and lean injured and aged uninjured and aged injured distinguished by #. $P \leq 0.05$.

Figures

Figure 1
A.

B.

C.

D.

E.

F.

G.

H.

Figure 2

A.

B.

C.

D.
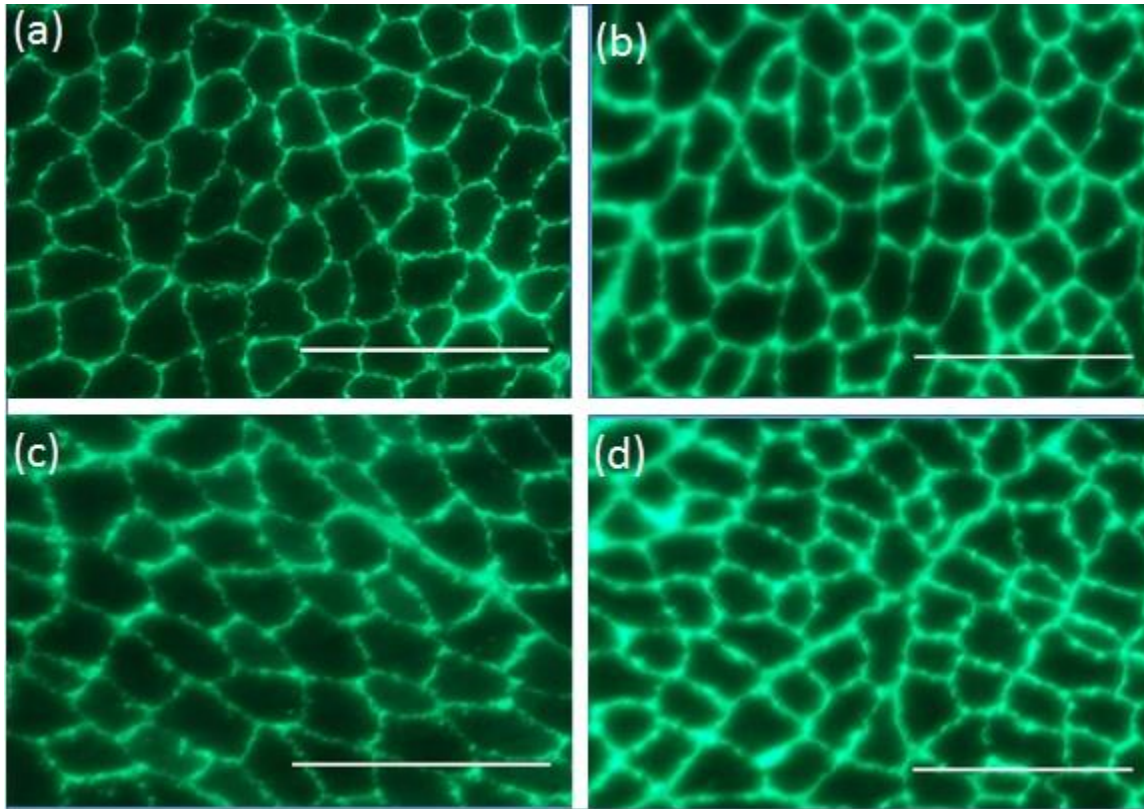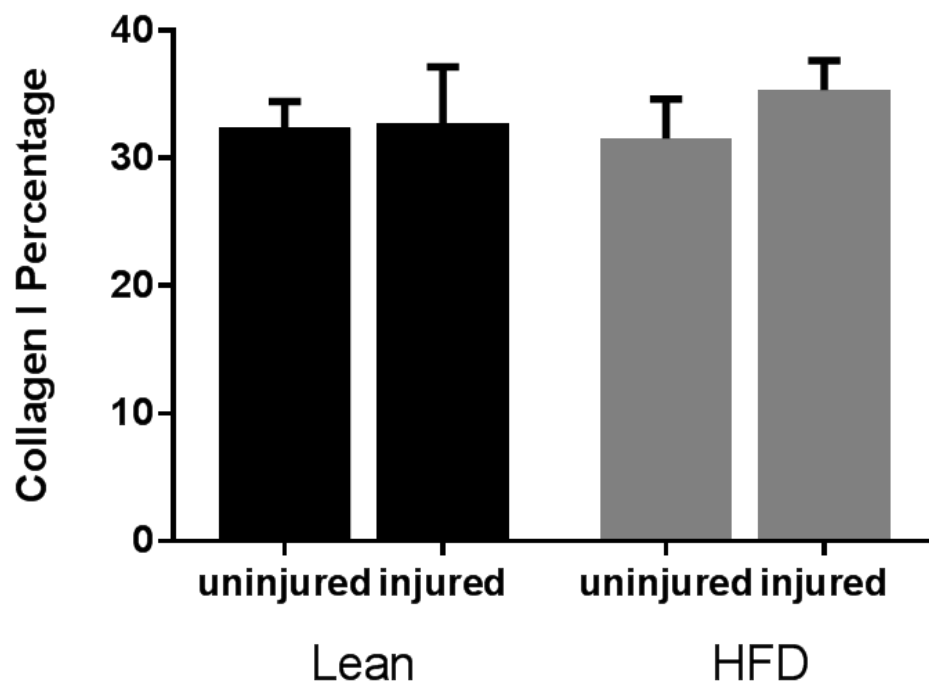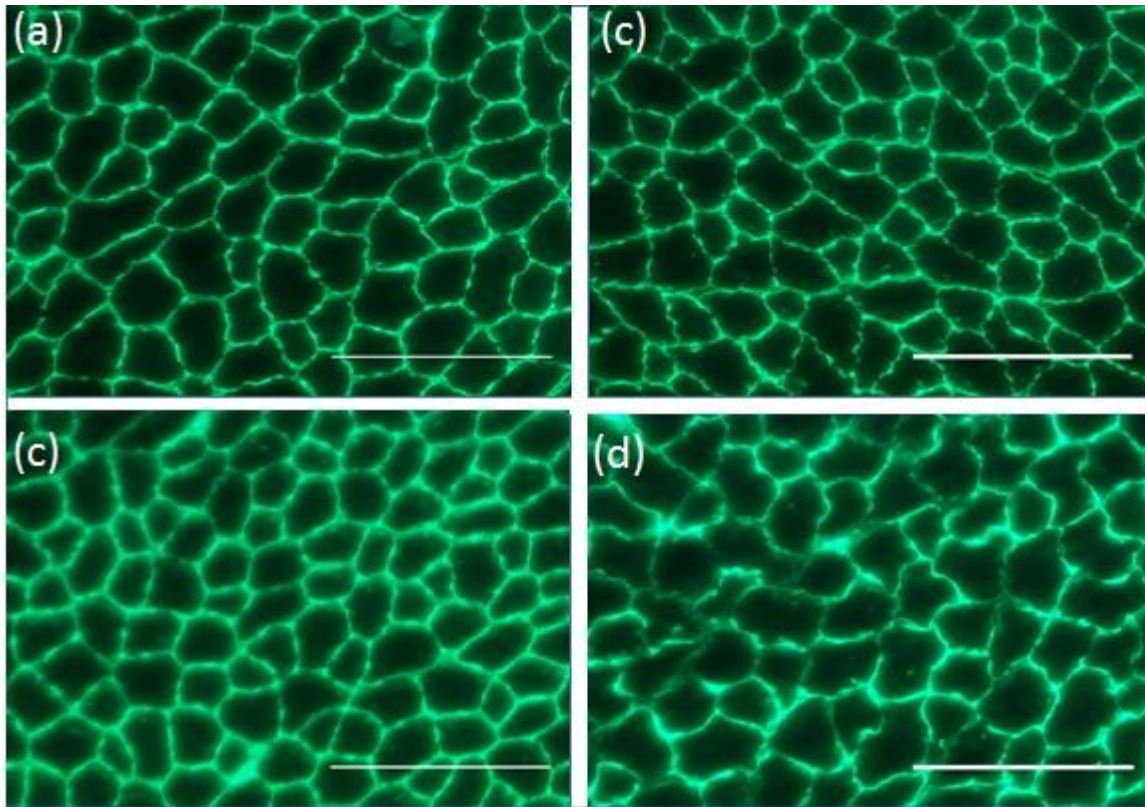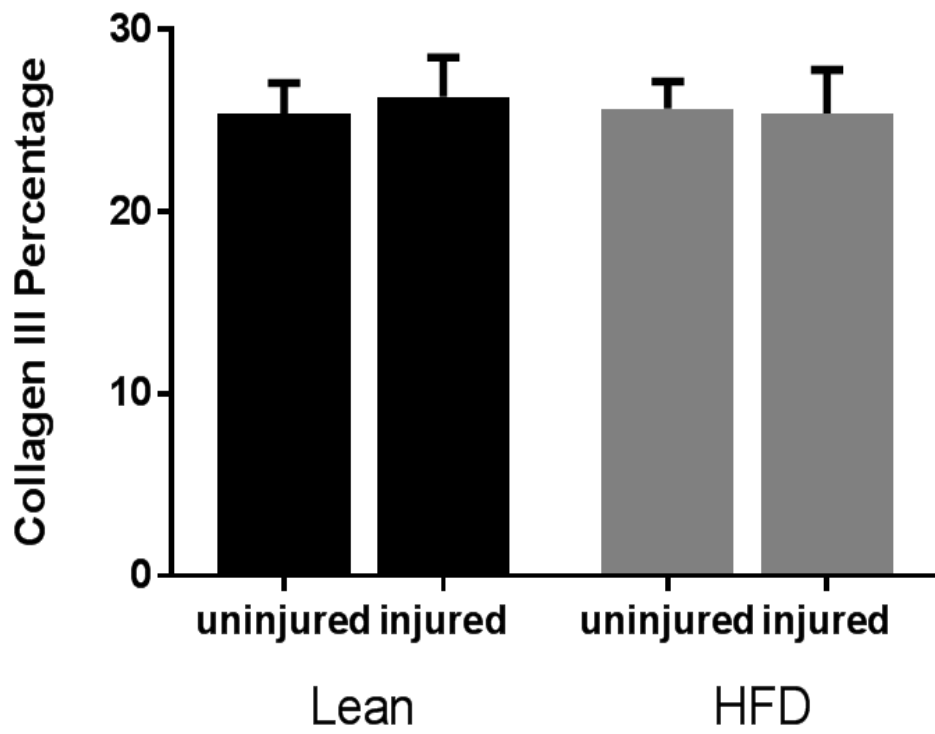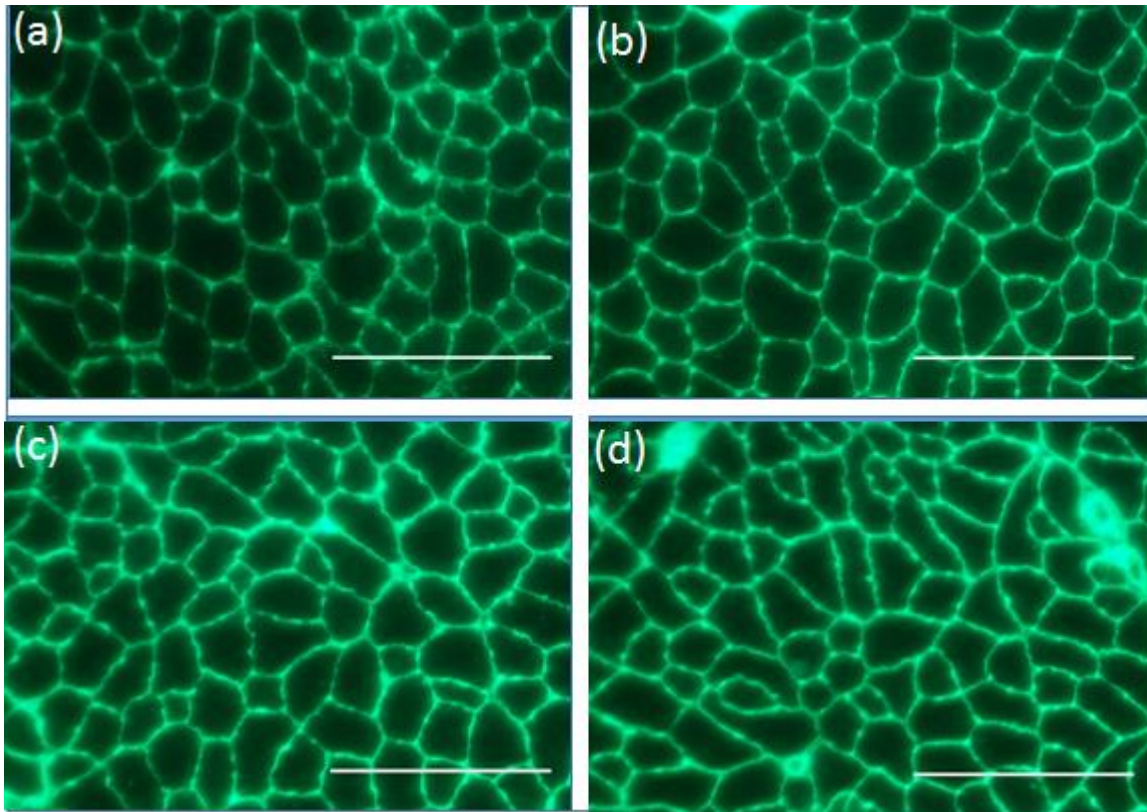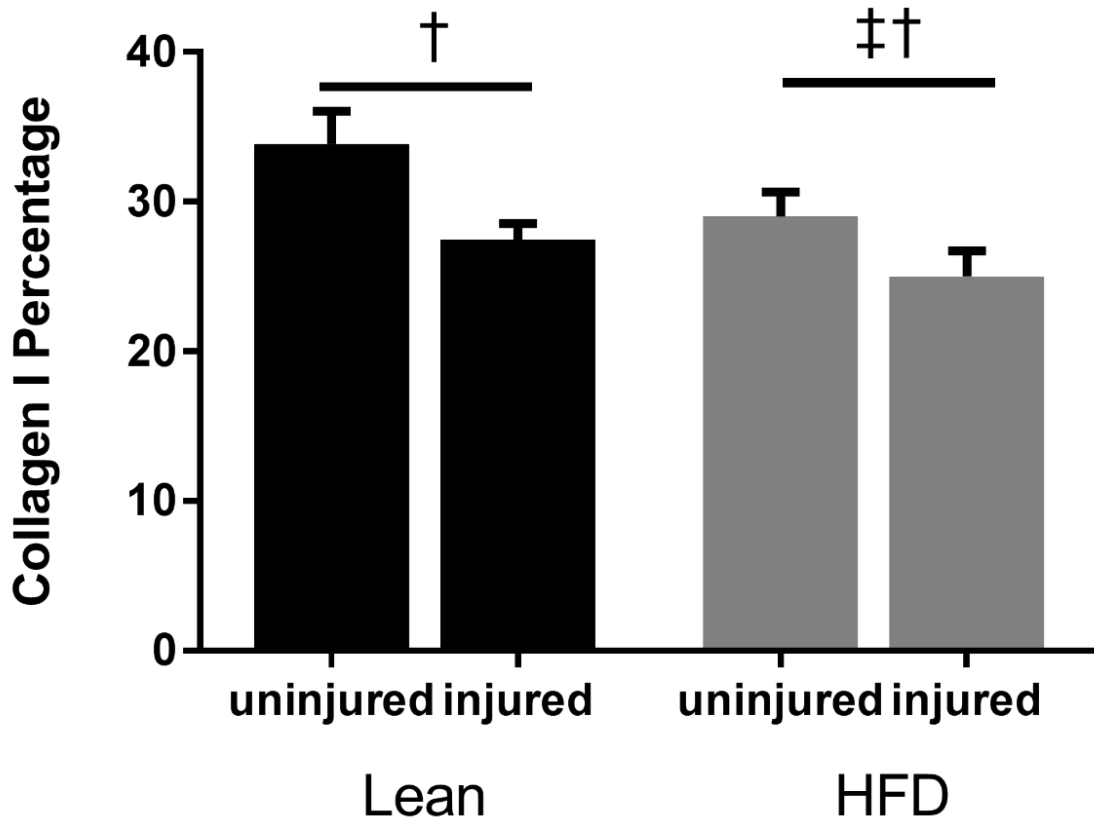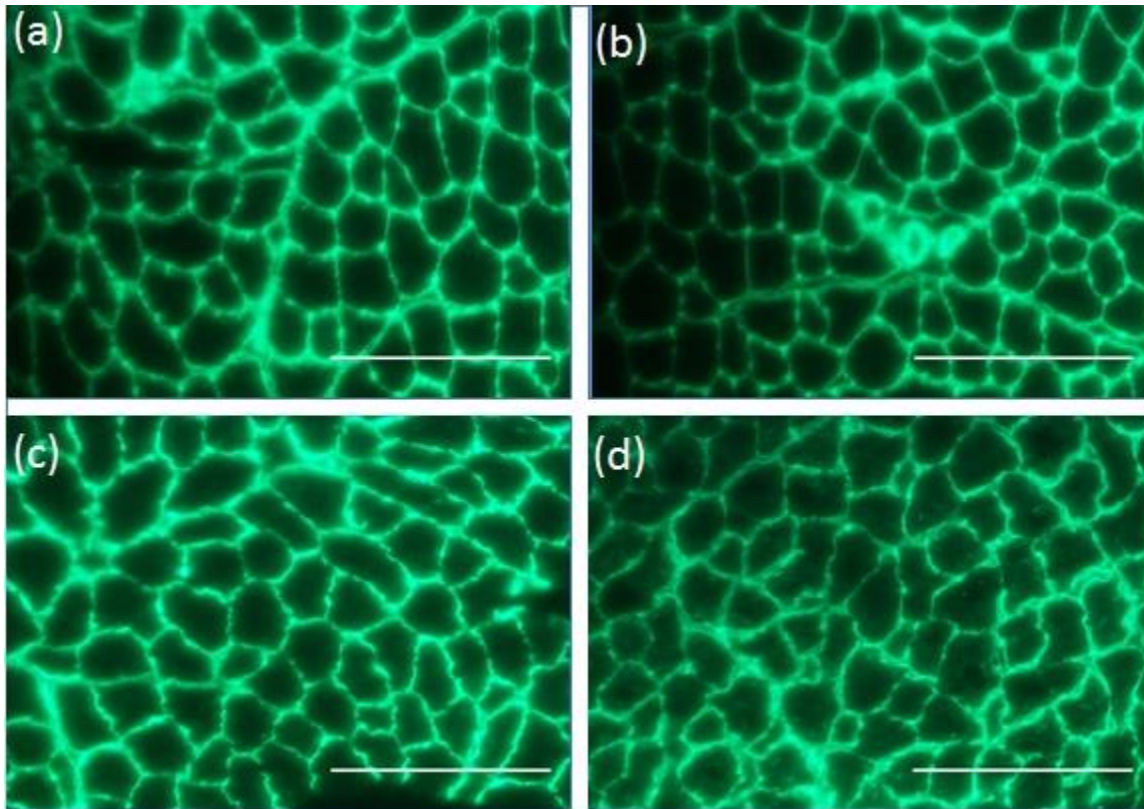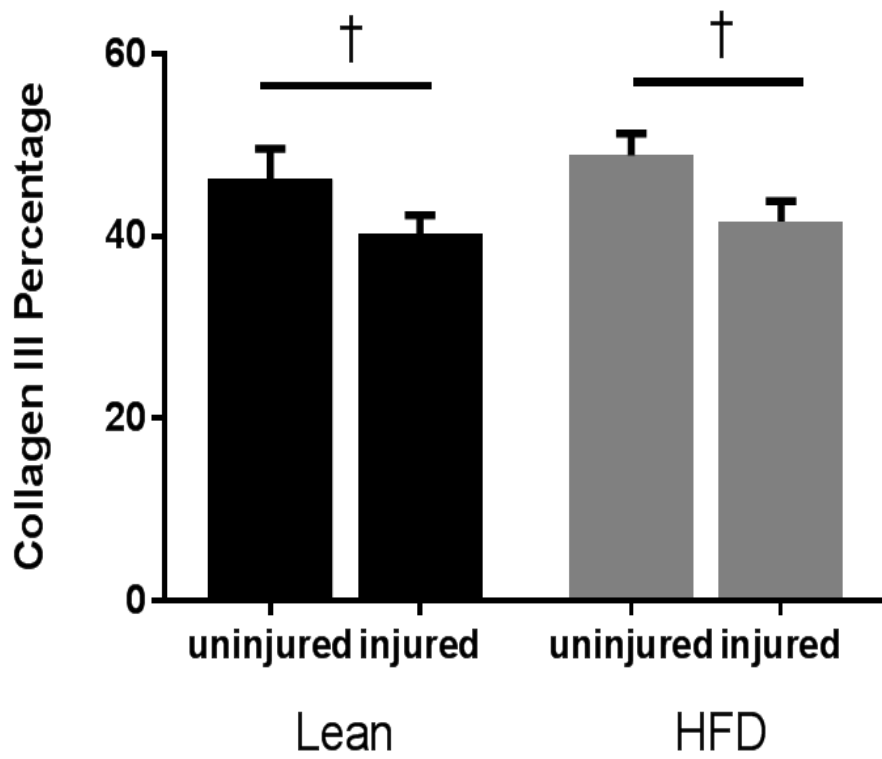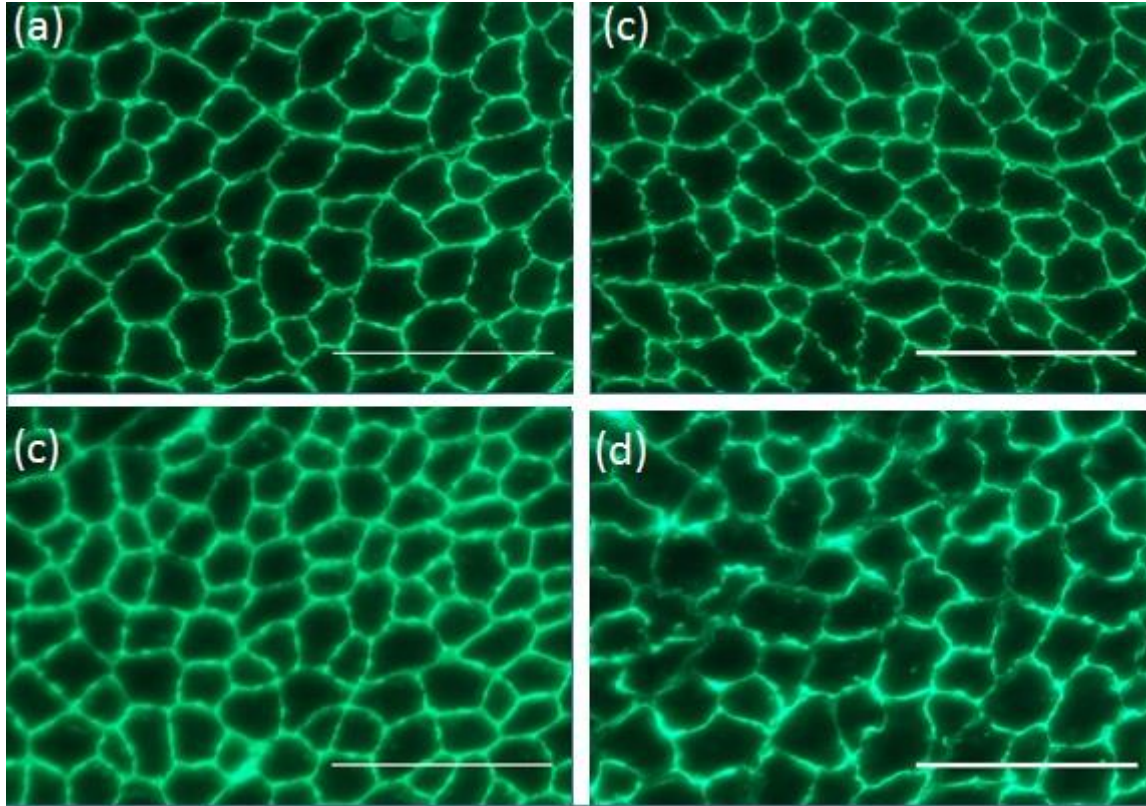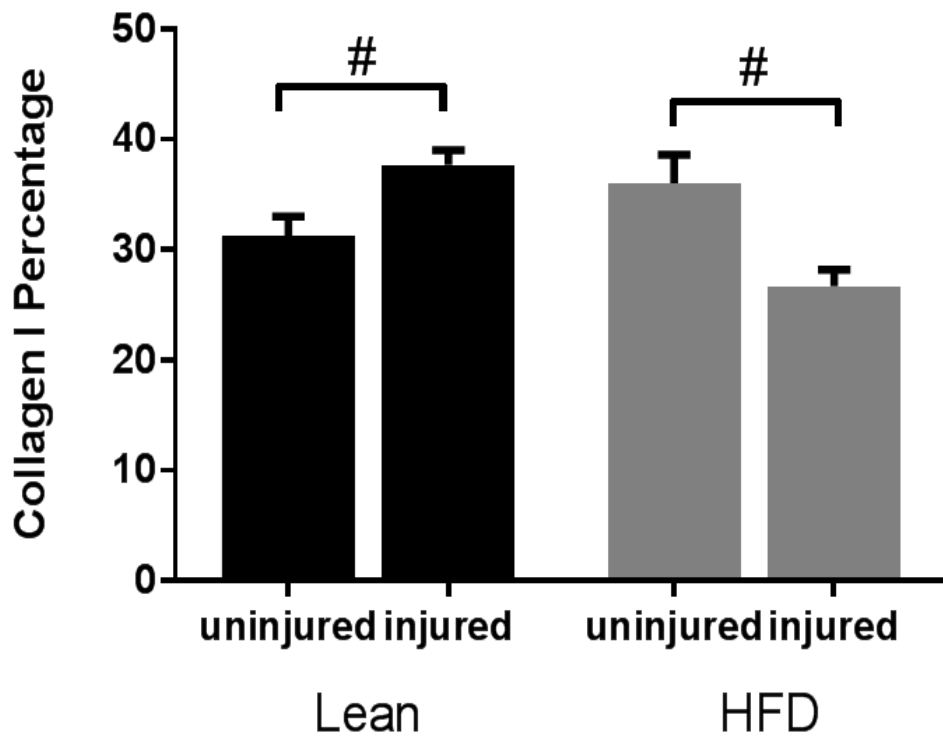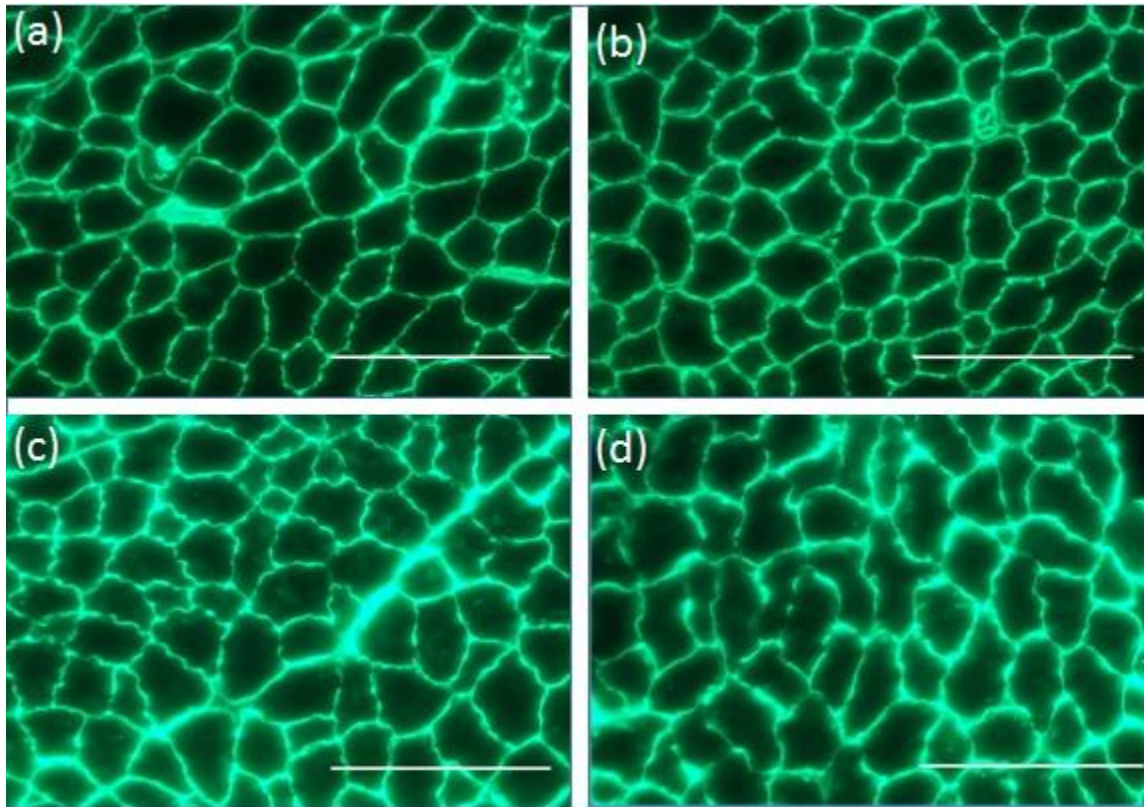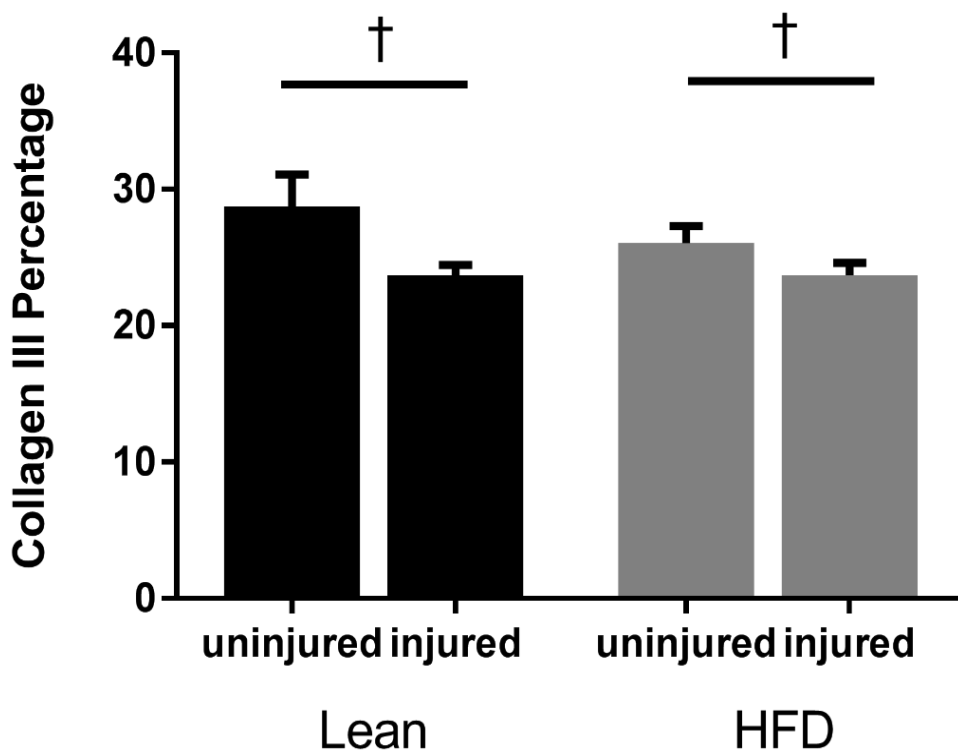
E.
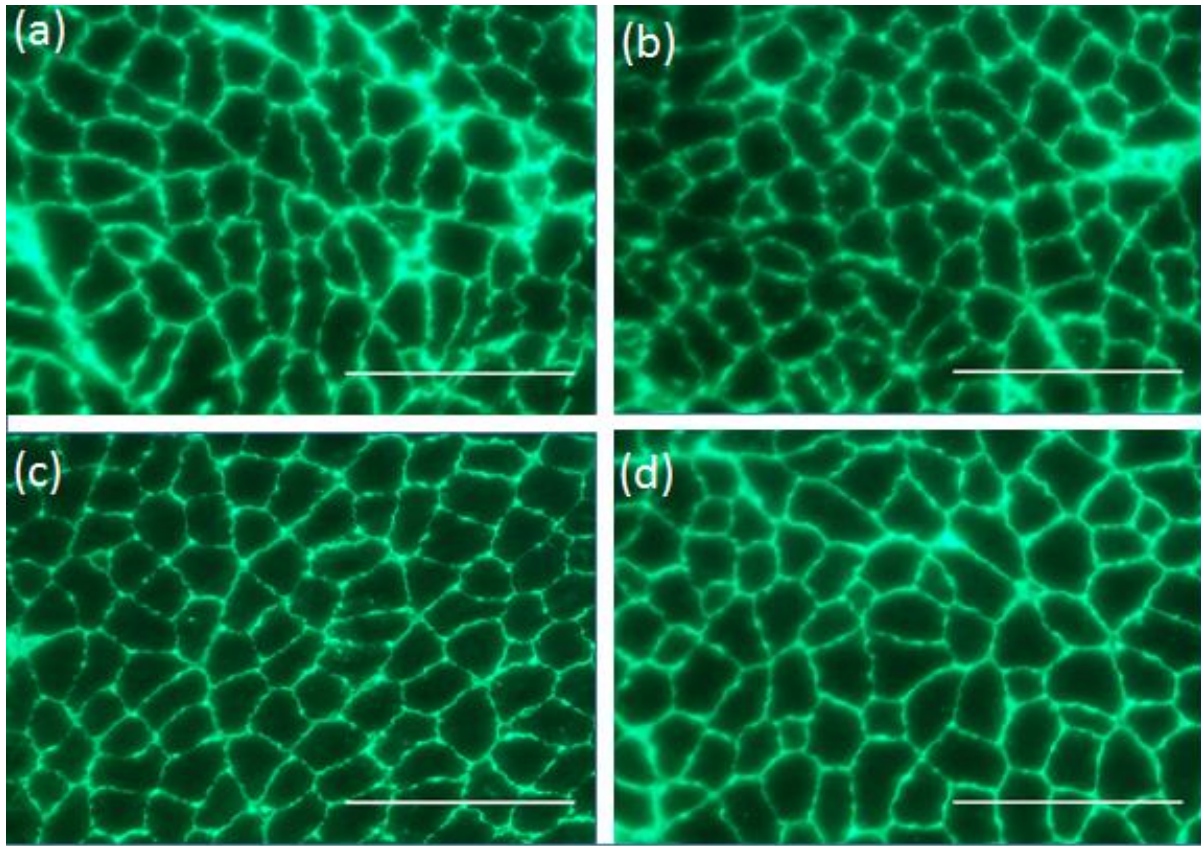
F.
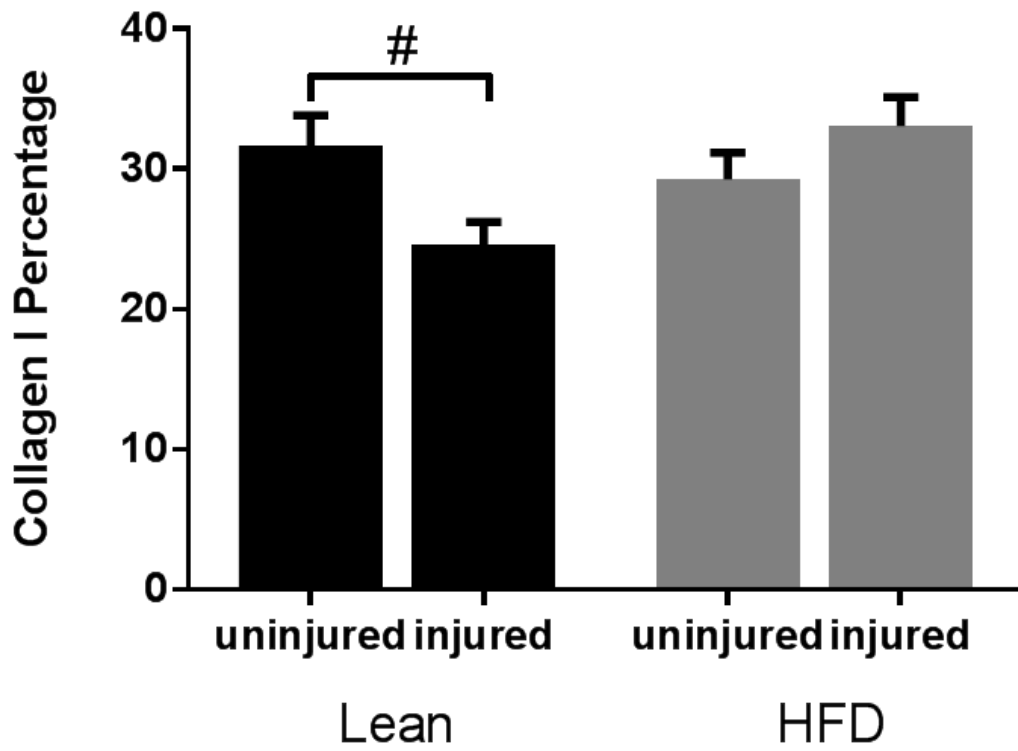
G.
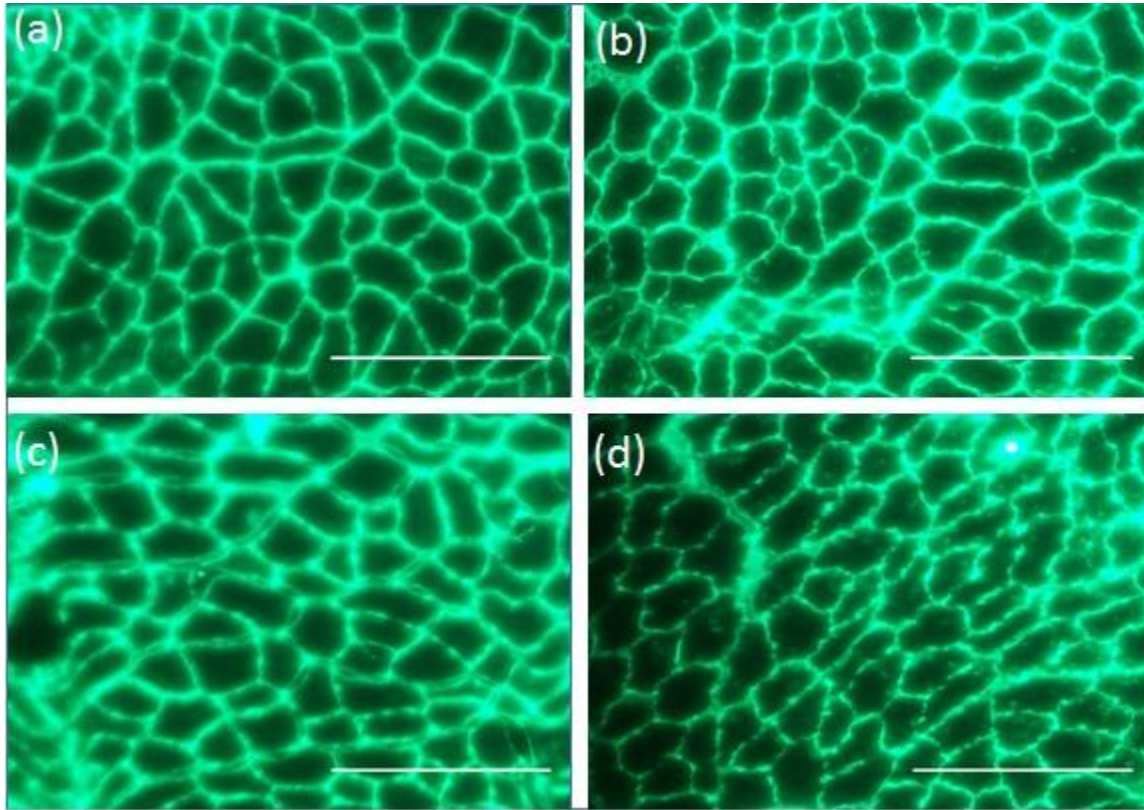
H.
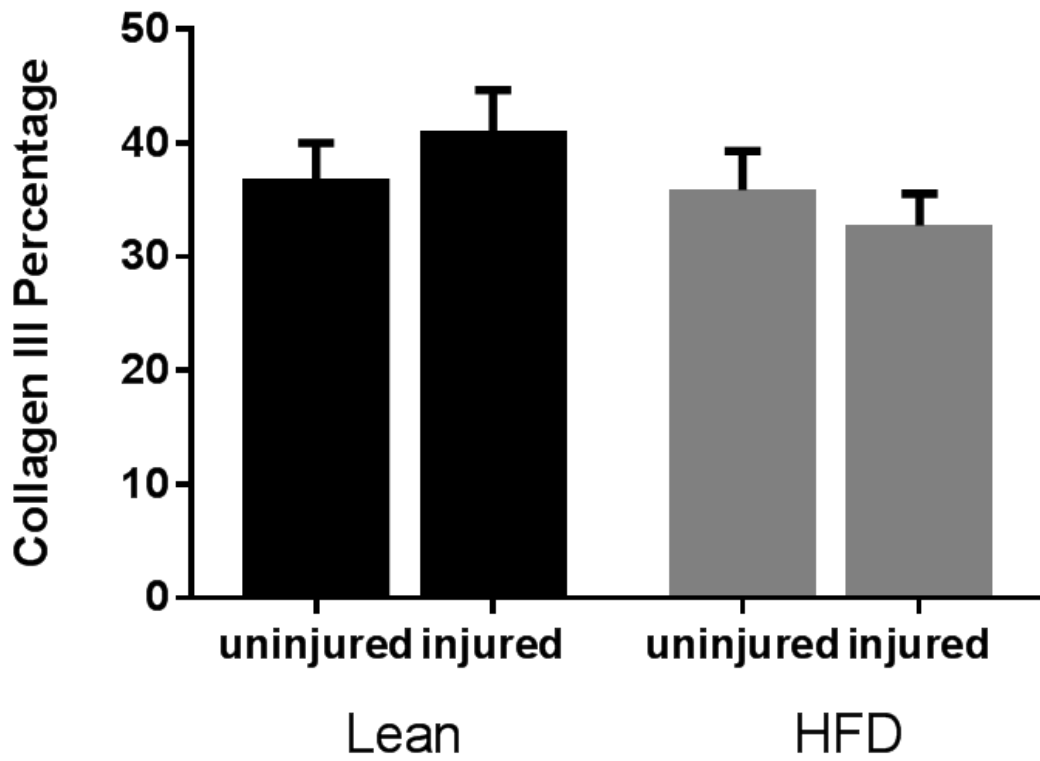
Figure 3

A.
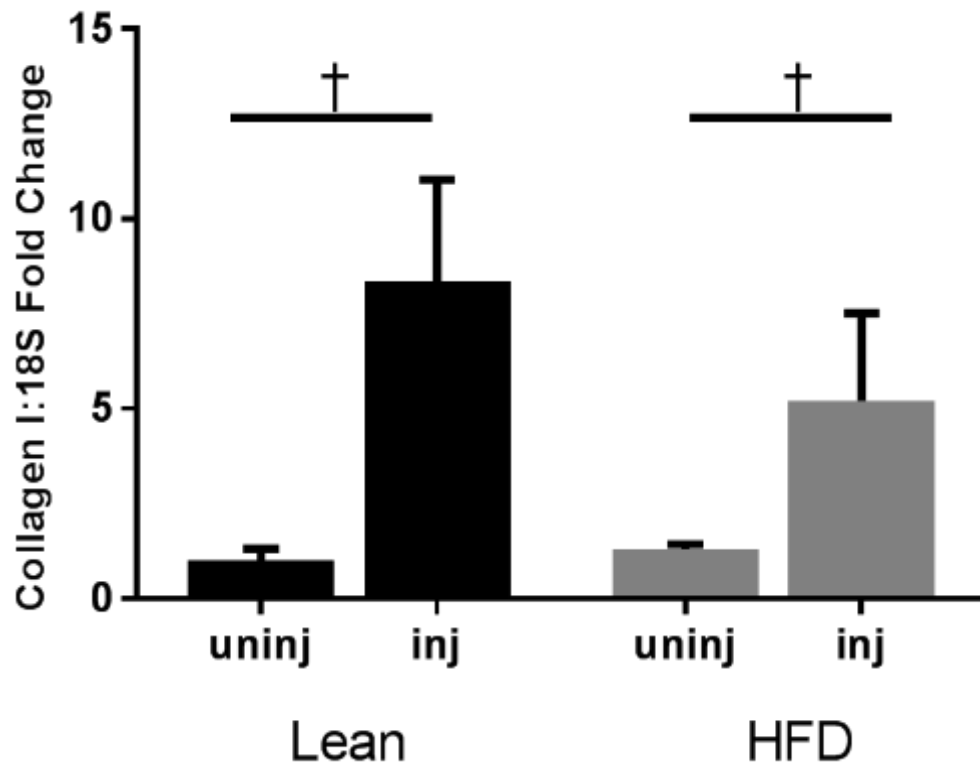
B.
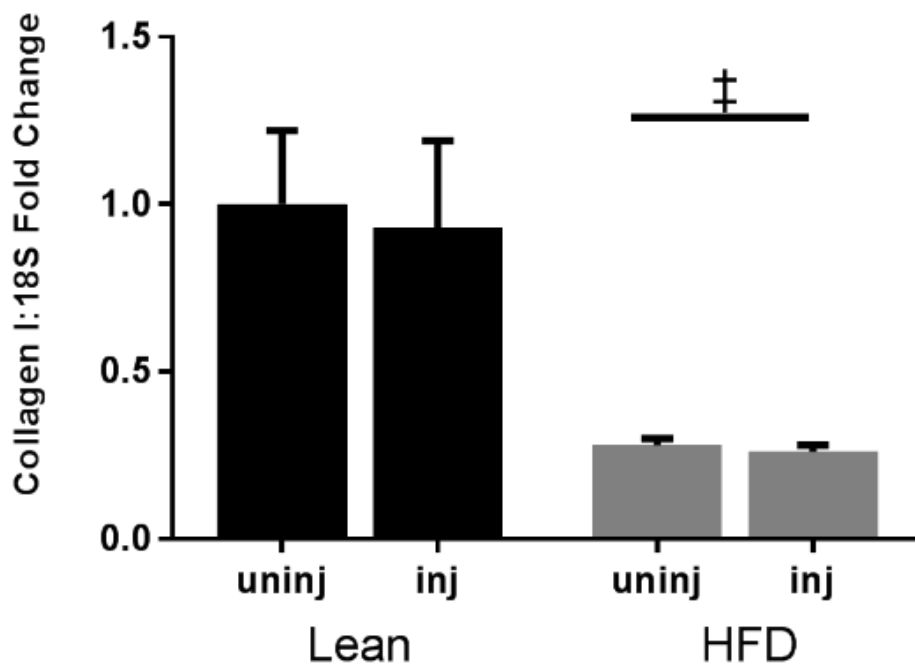
C.
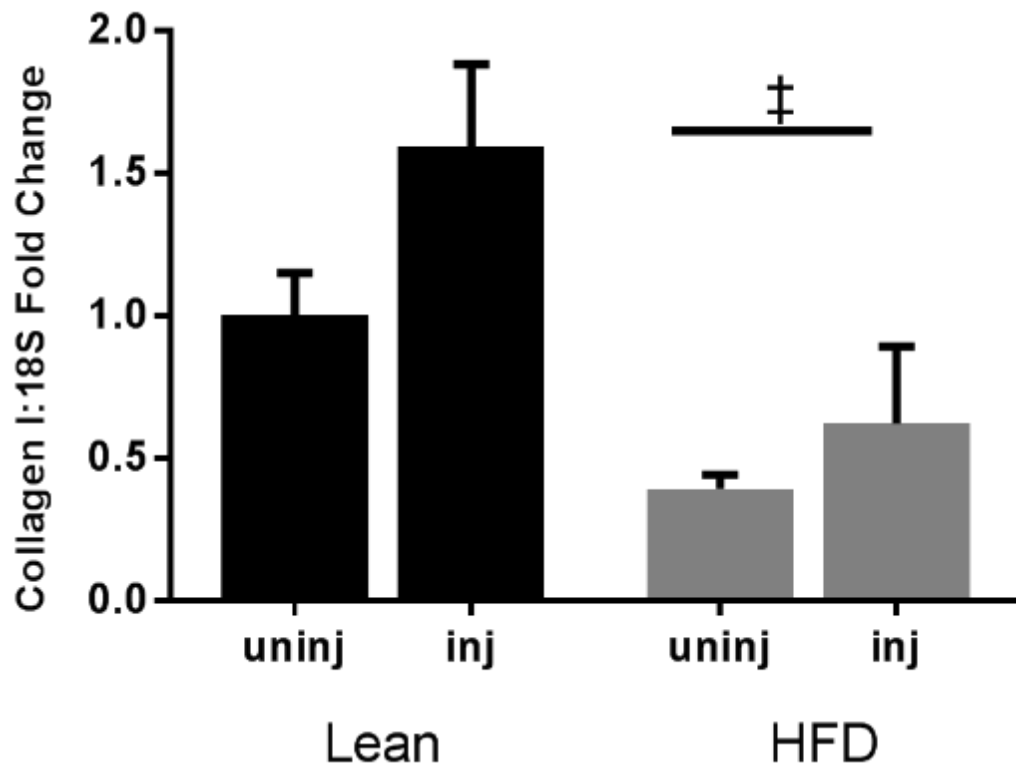
D.
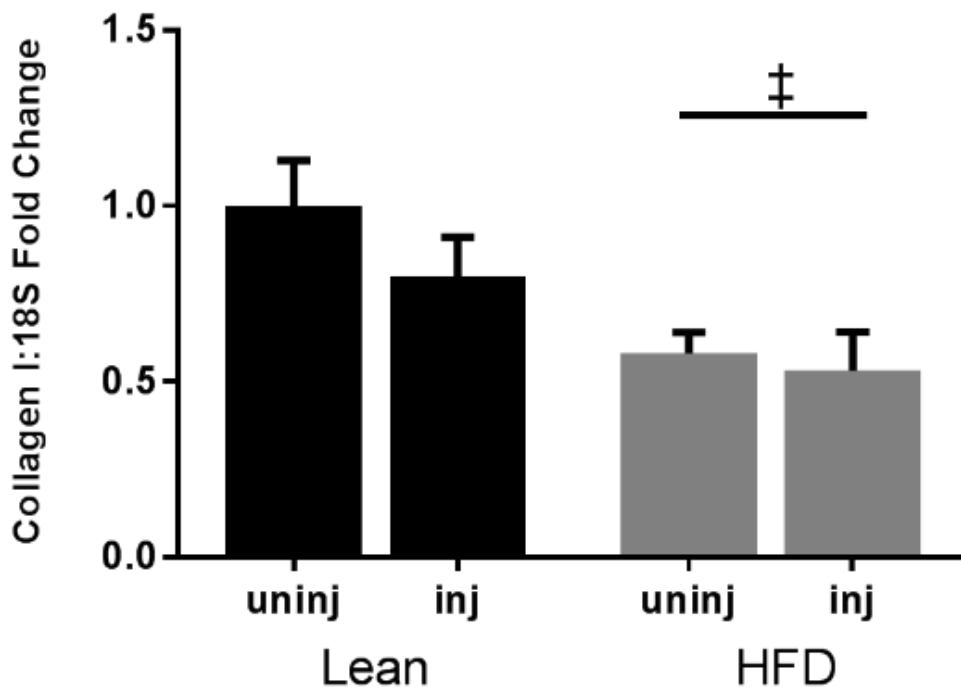
E.
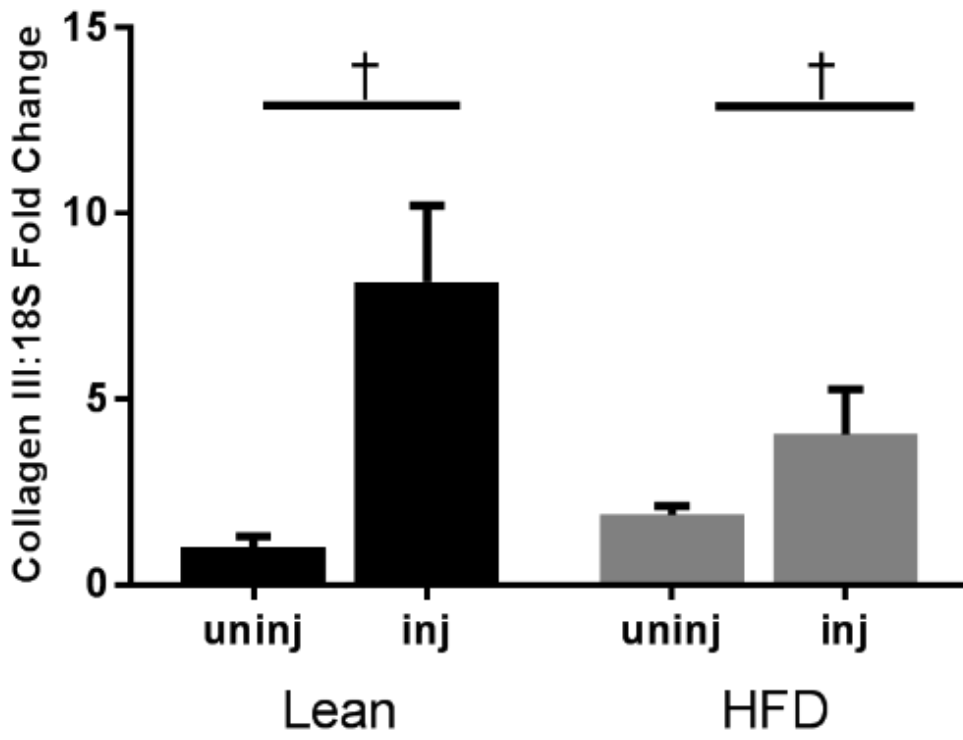
F.
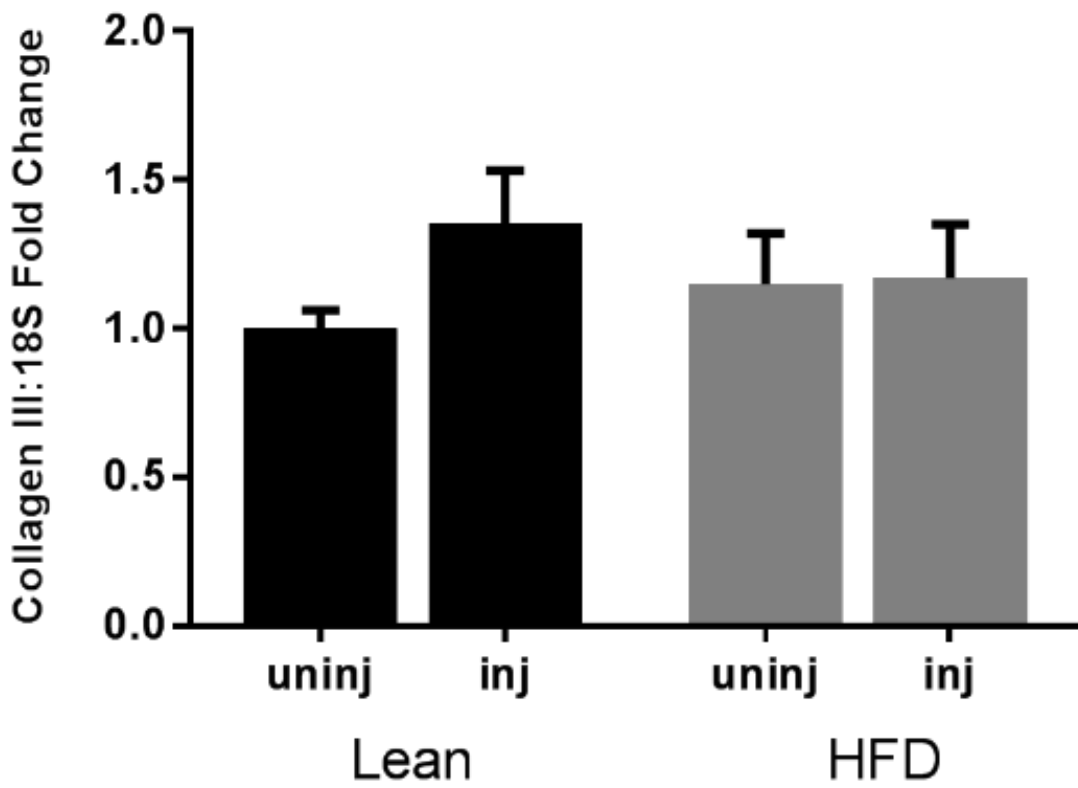
G.
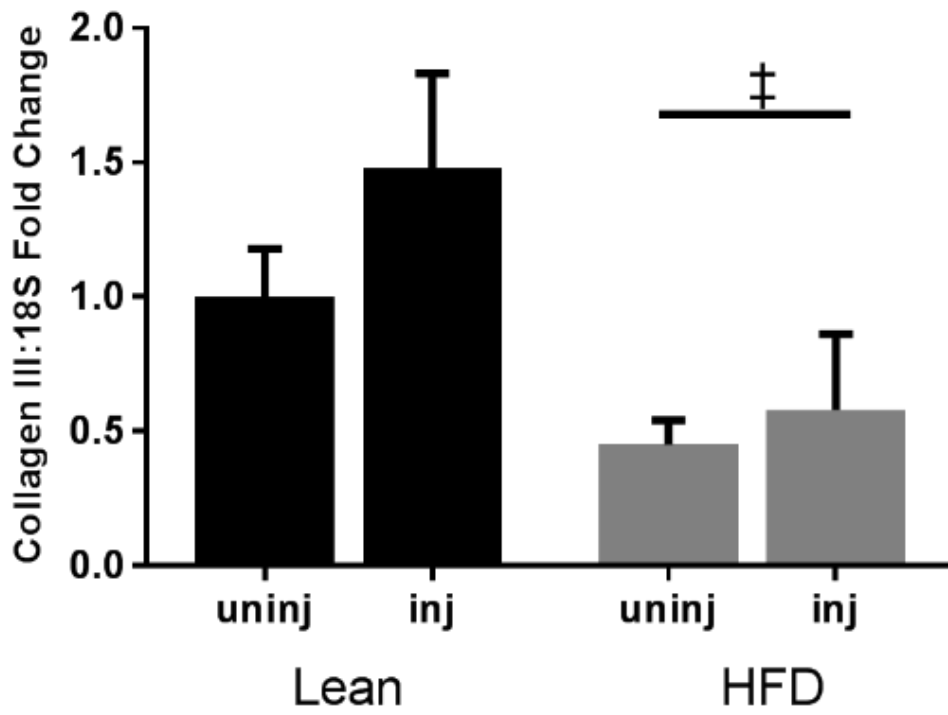
H.
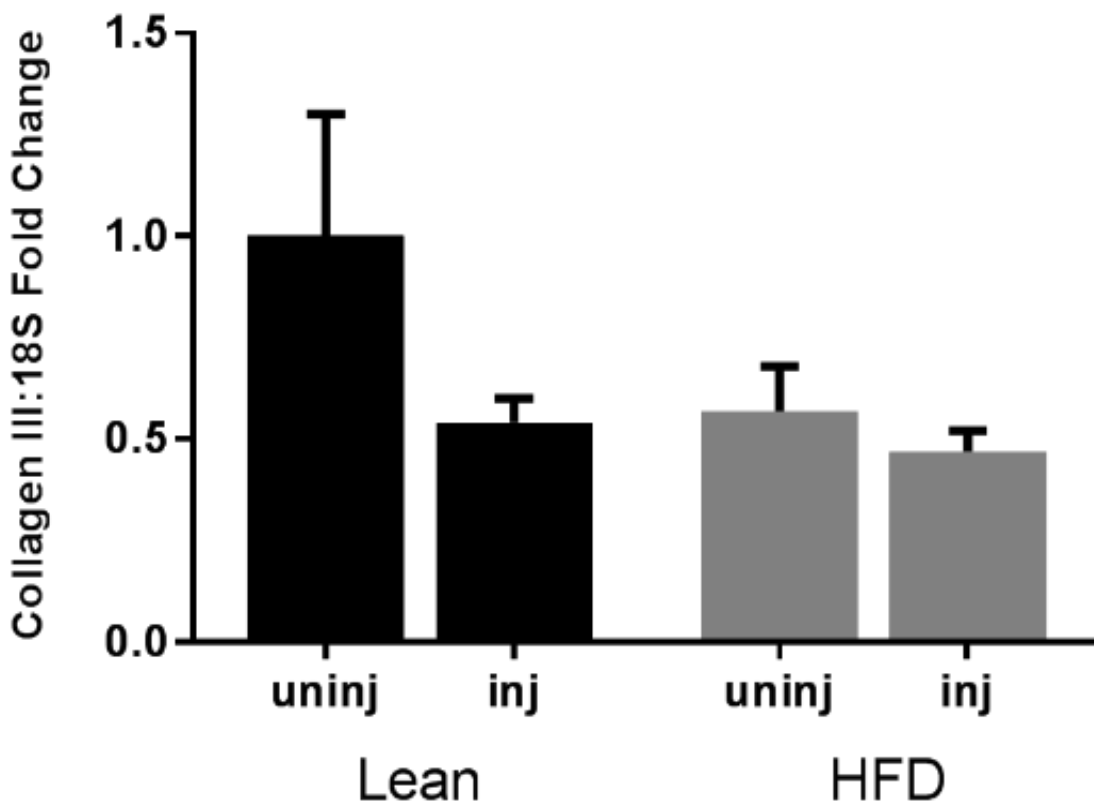
Figure 4
A.
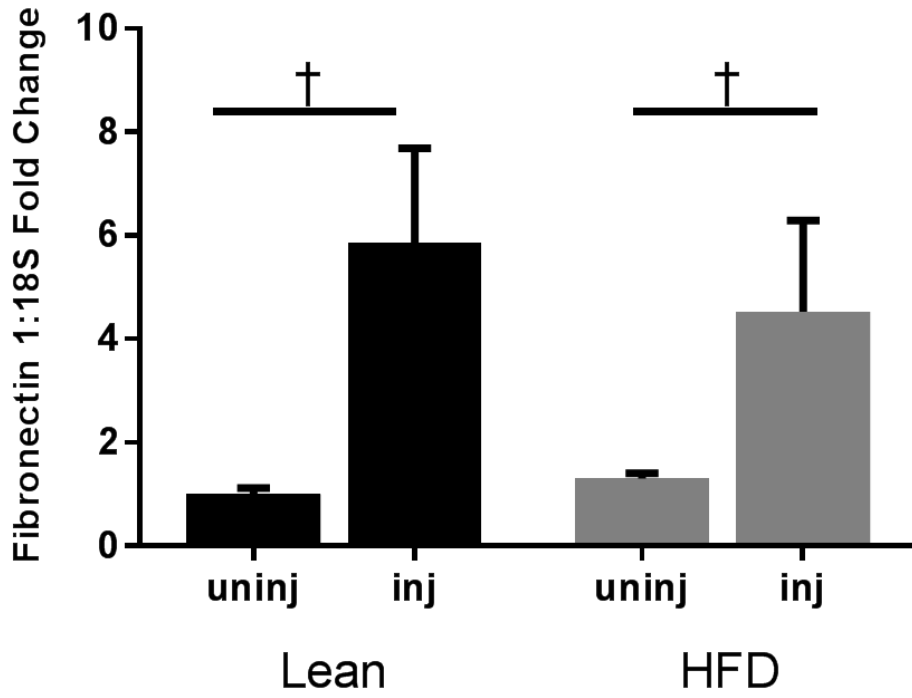
B.
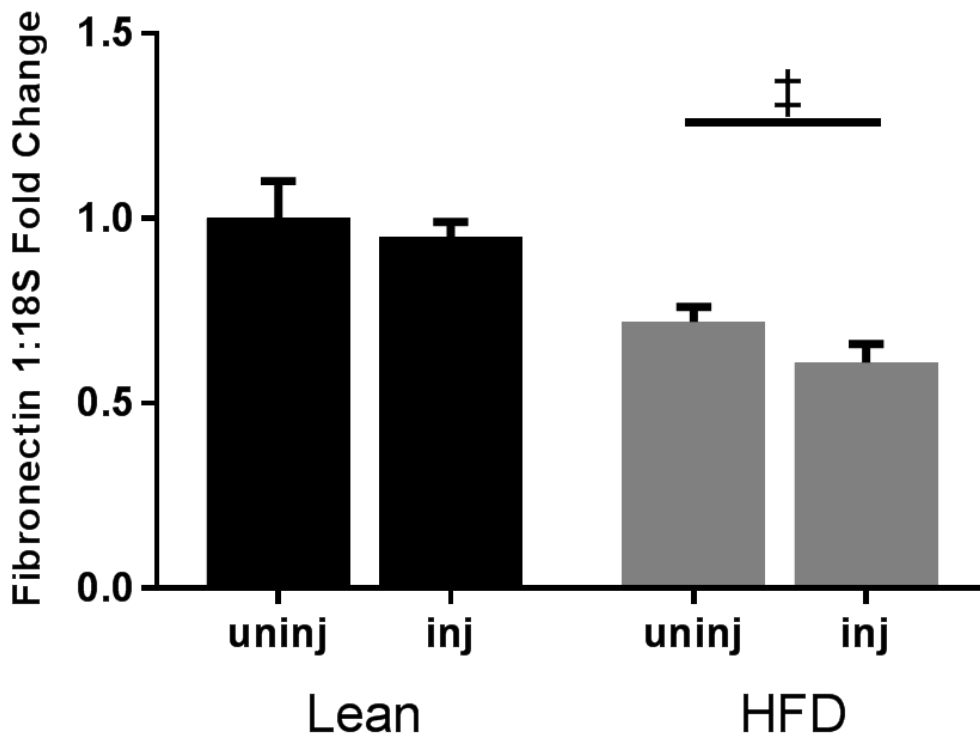
C.
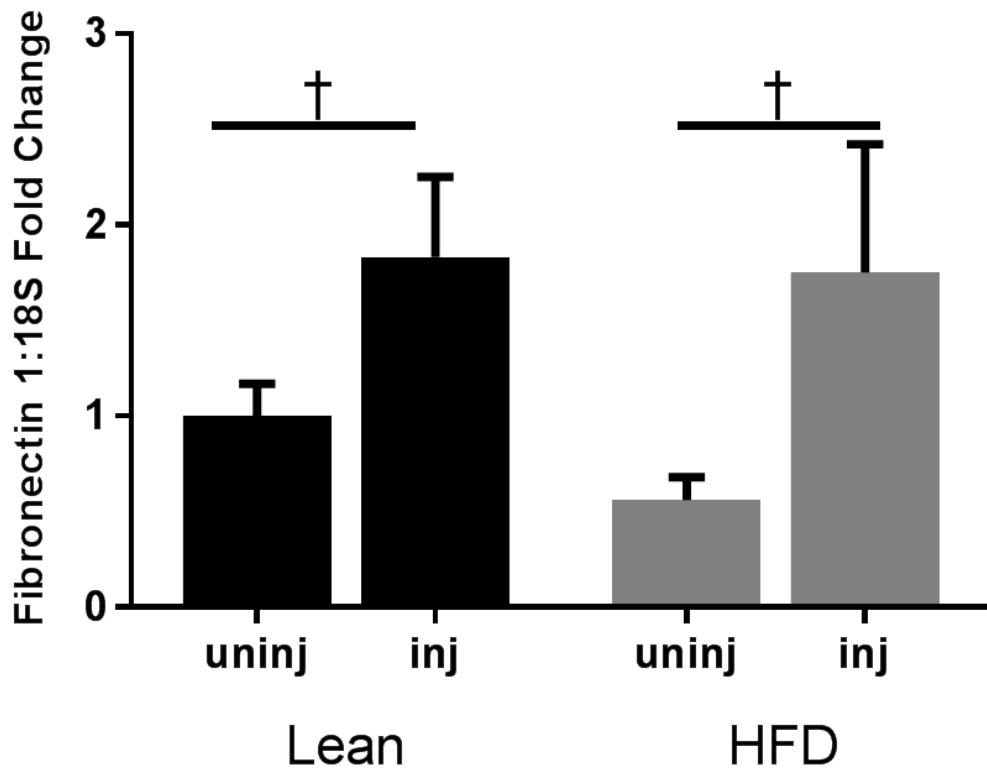
D.
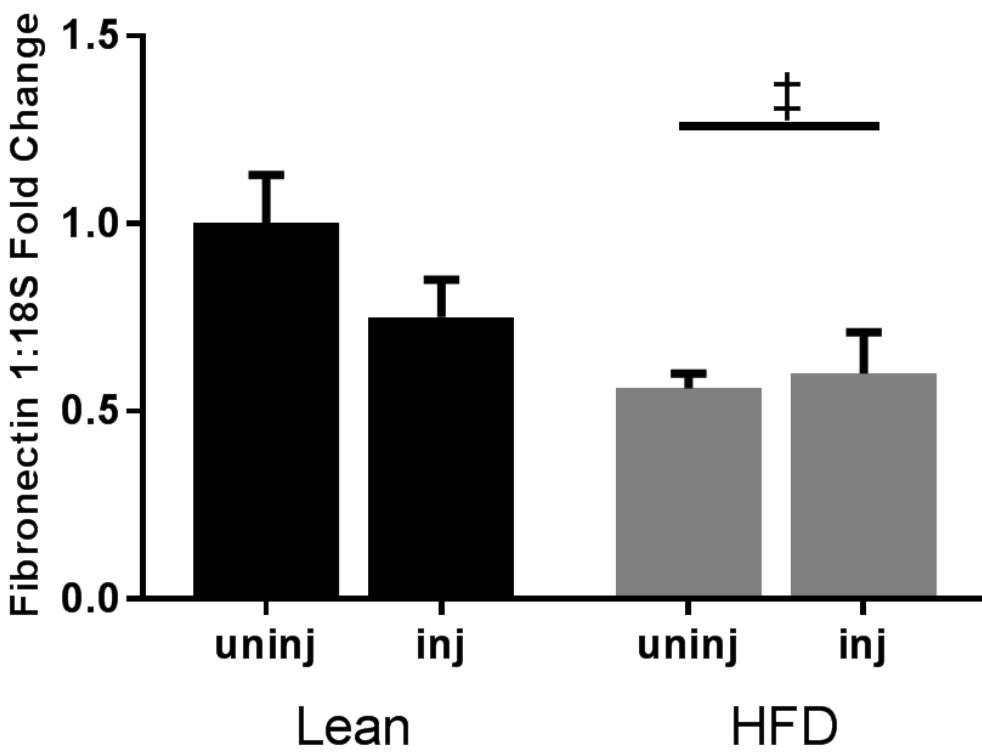
E.
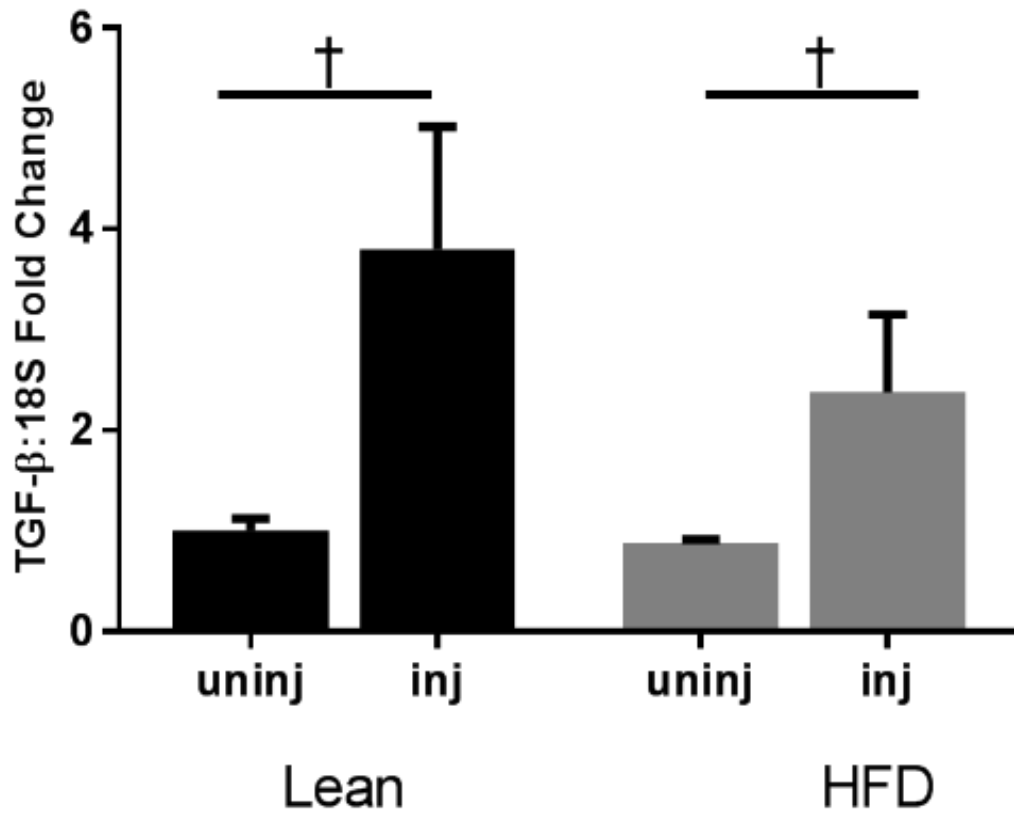
F.
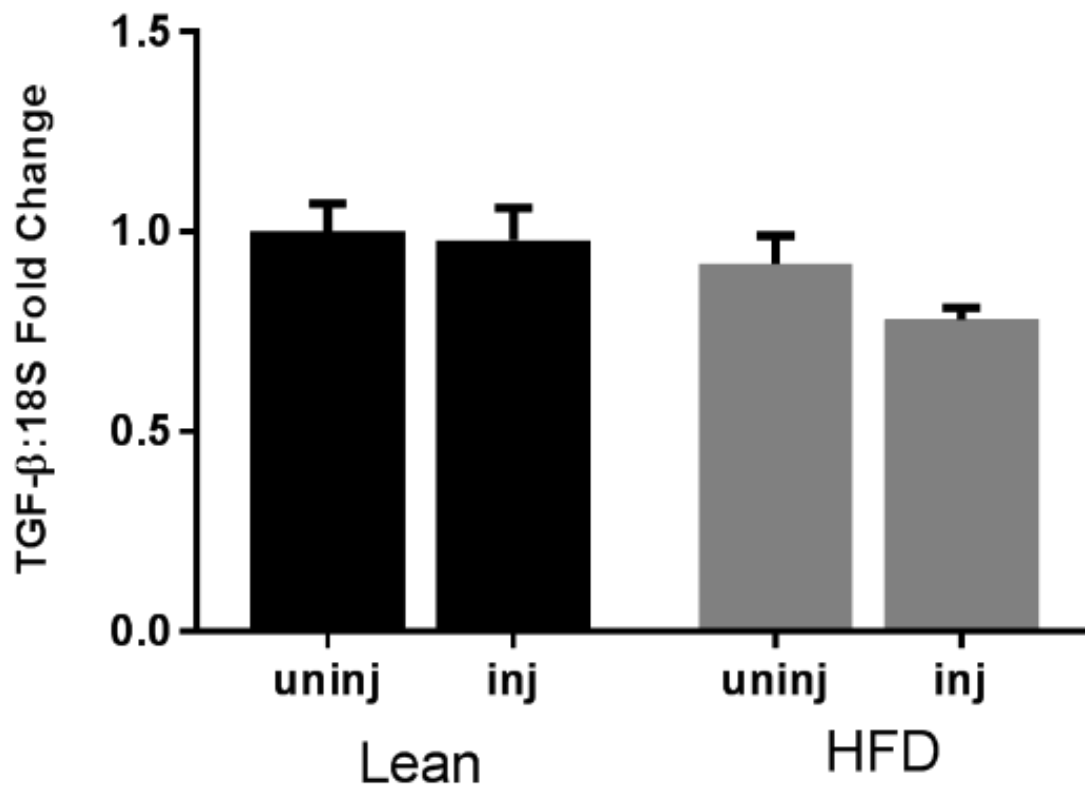
G.
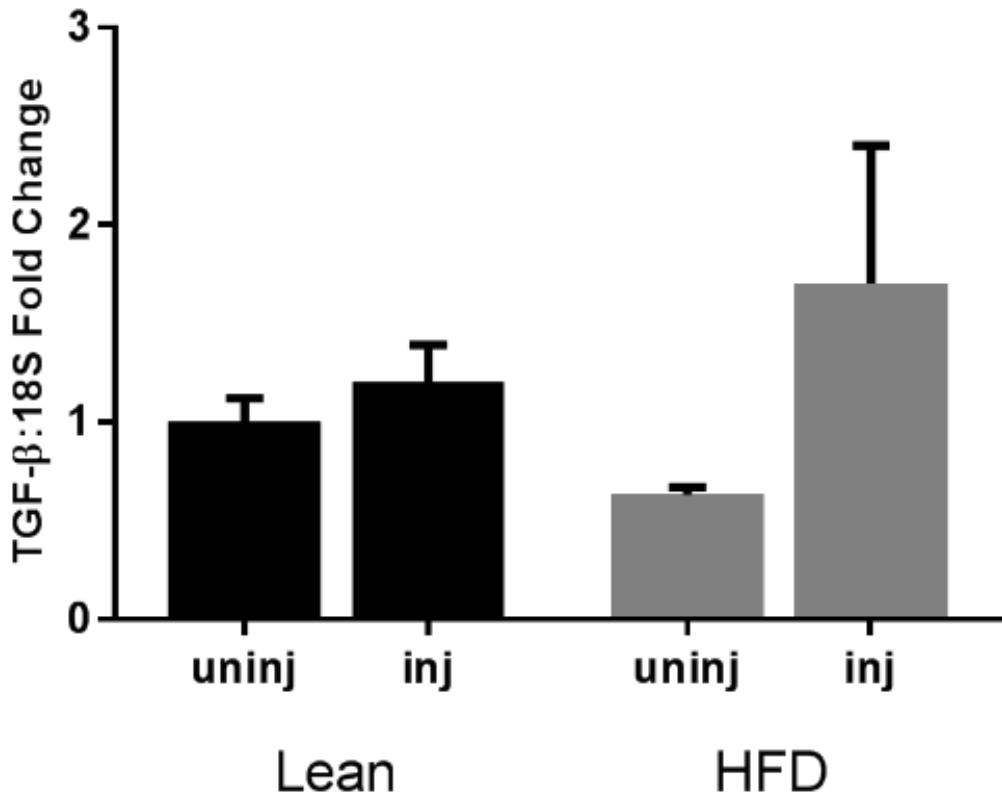
H.
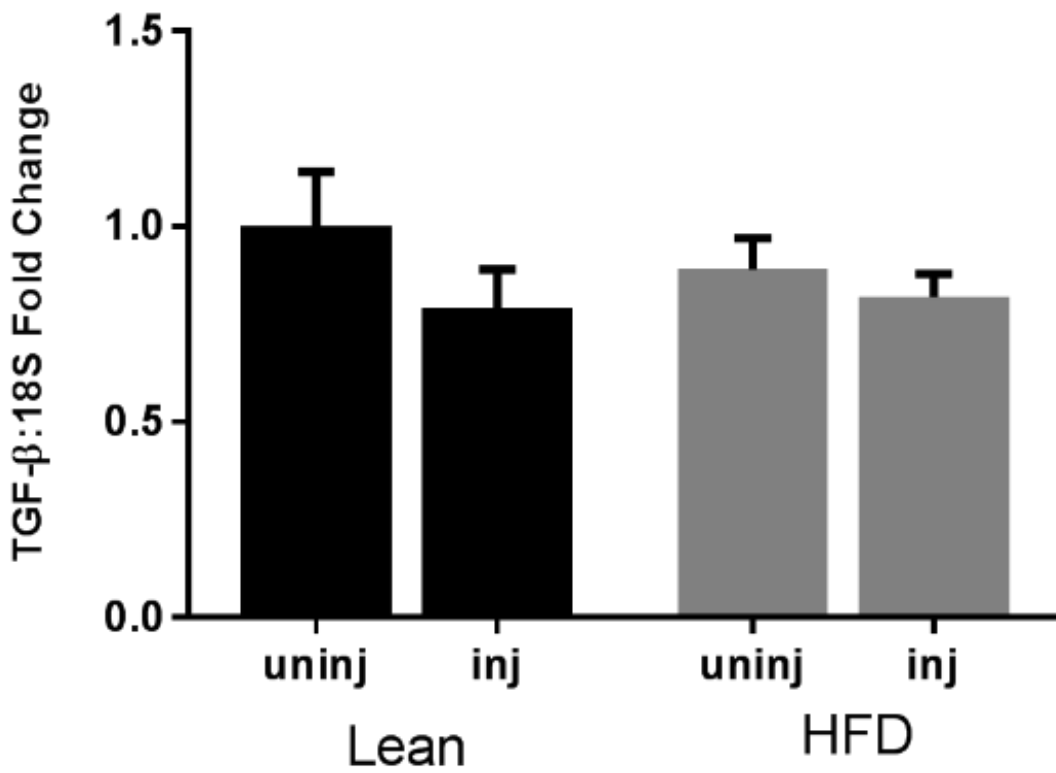
Figure 5

A.
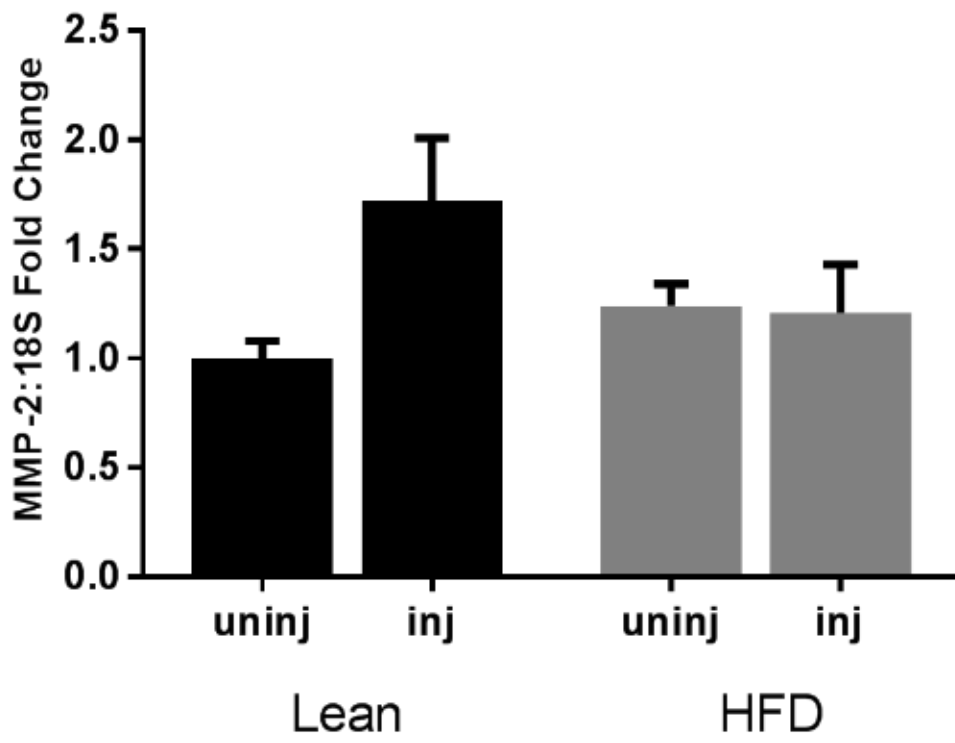
B.
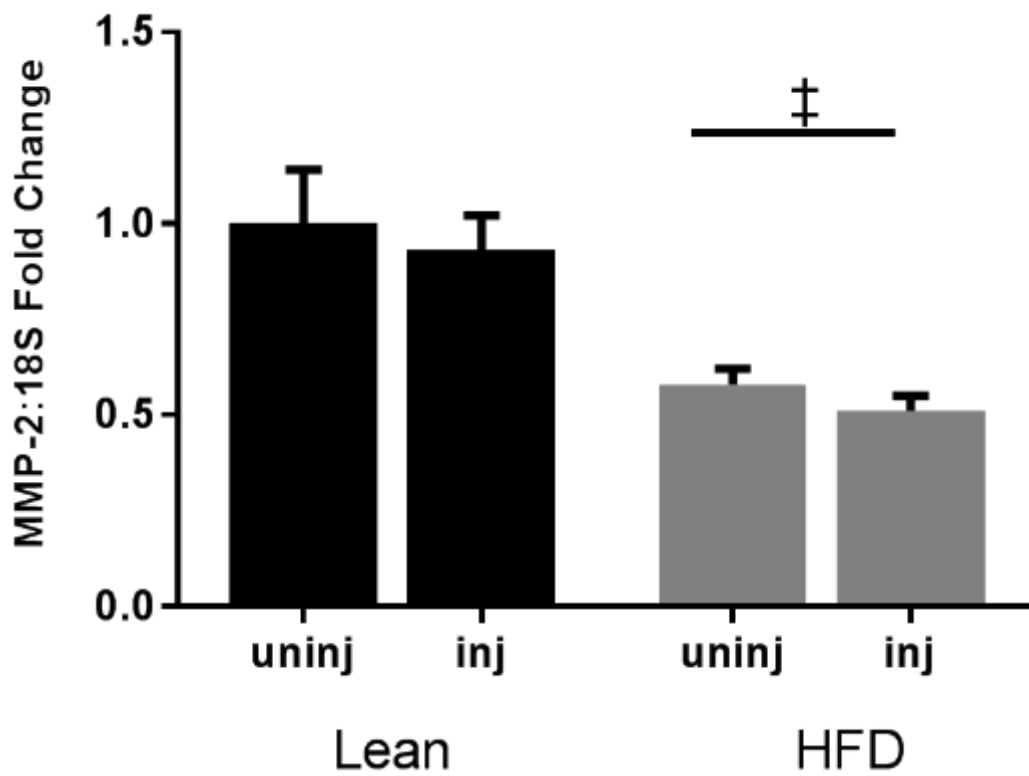
C.
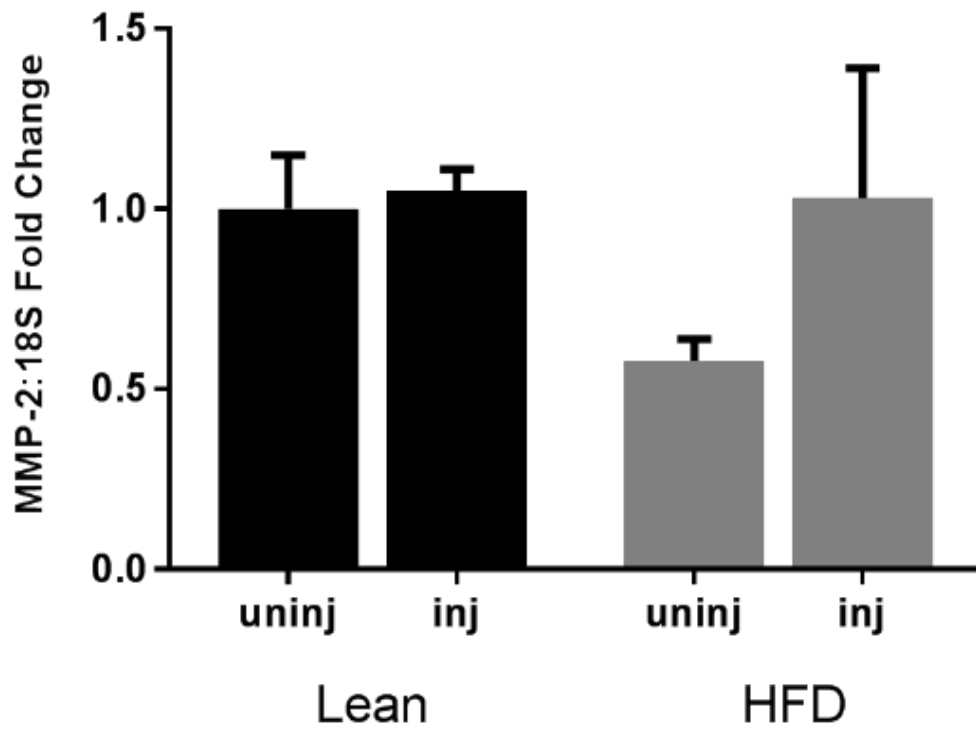
D.
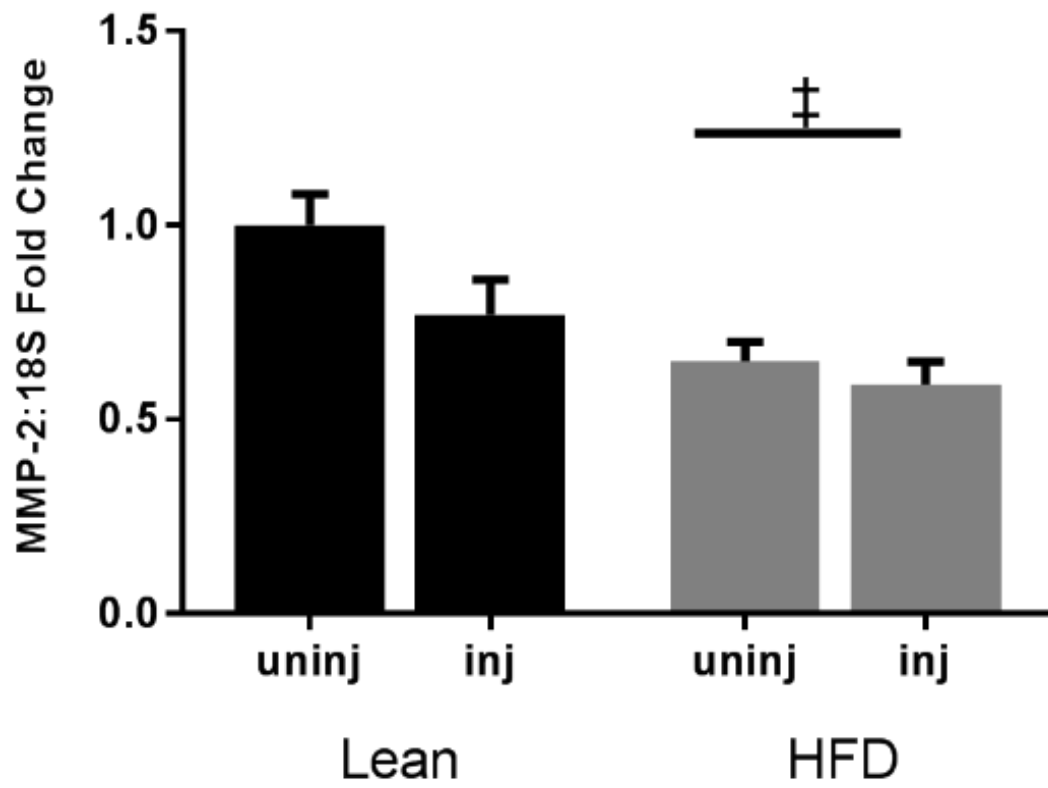
E.
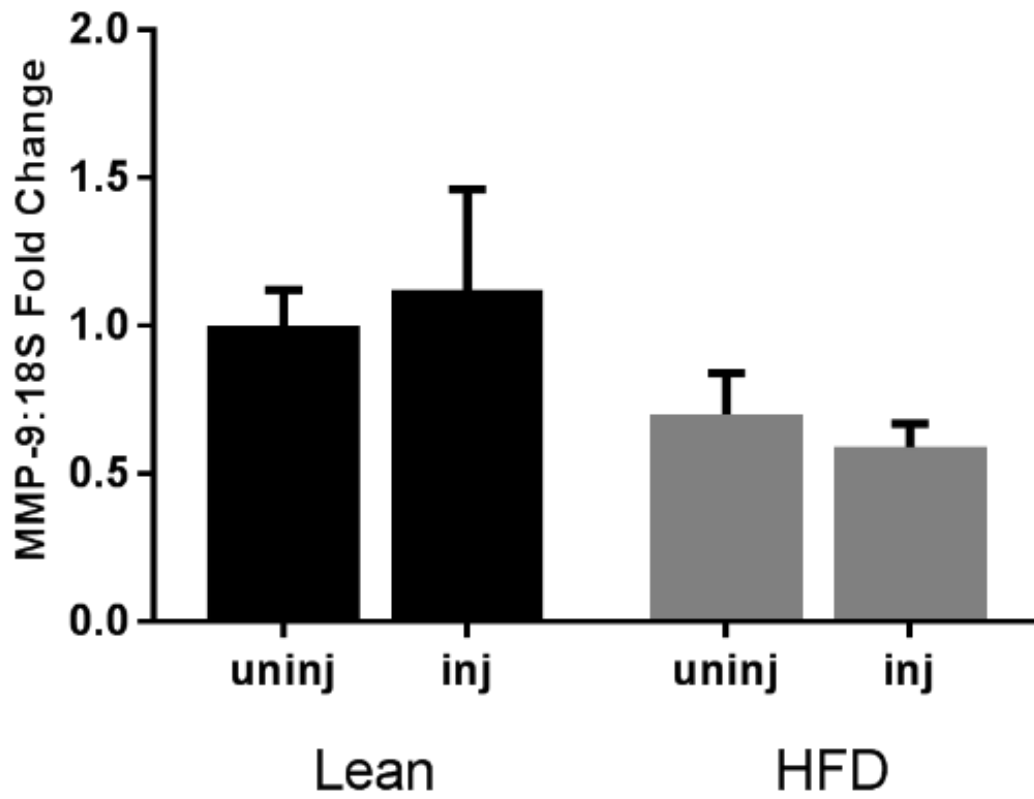
F.
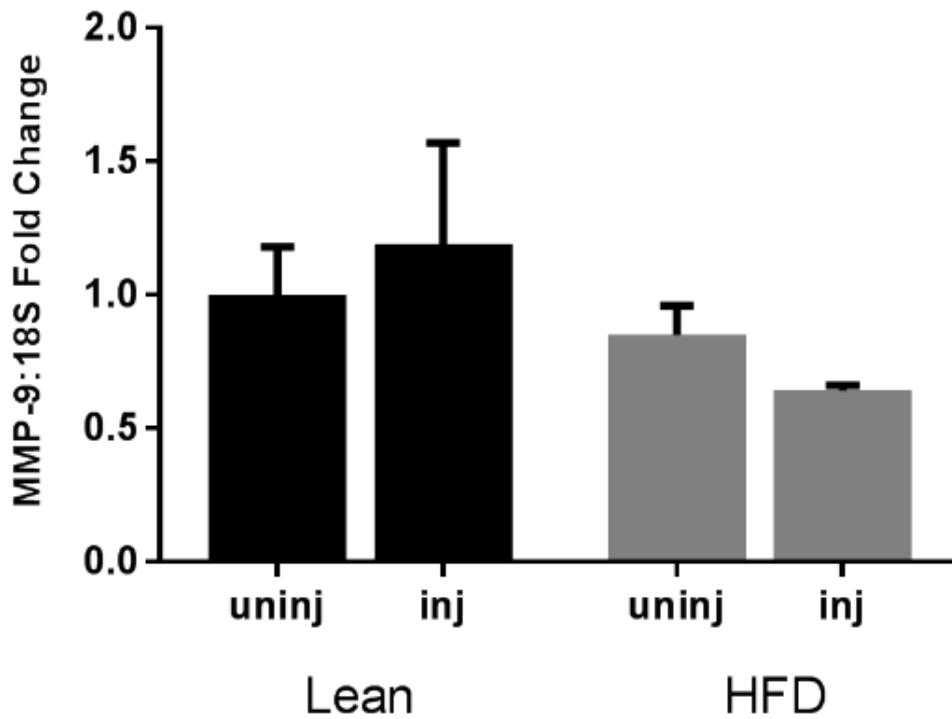
G.
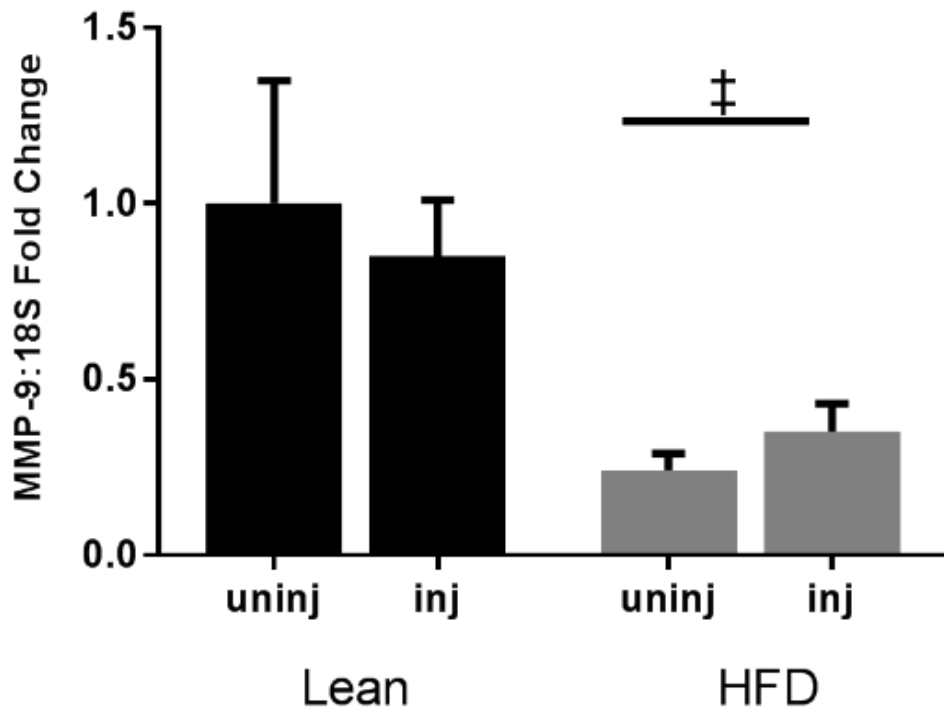
H.
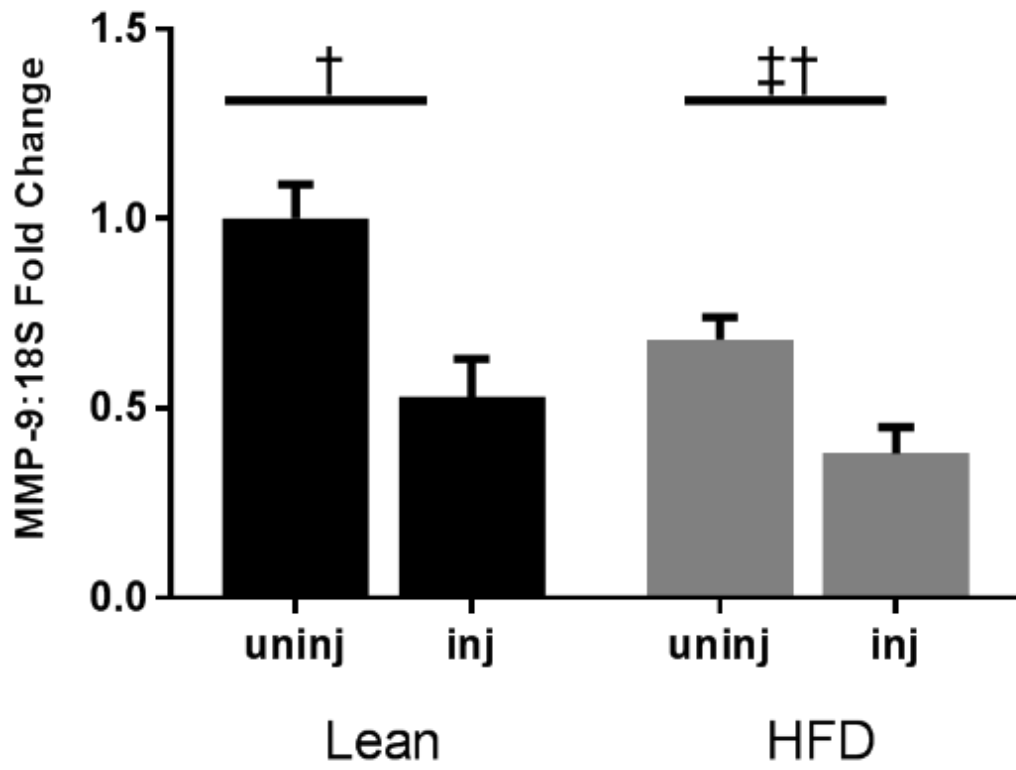
I.
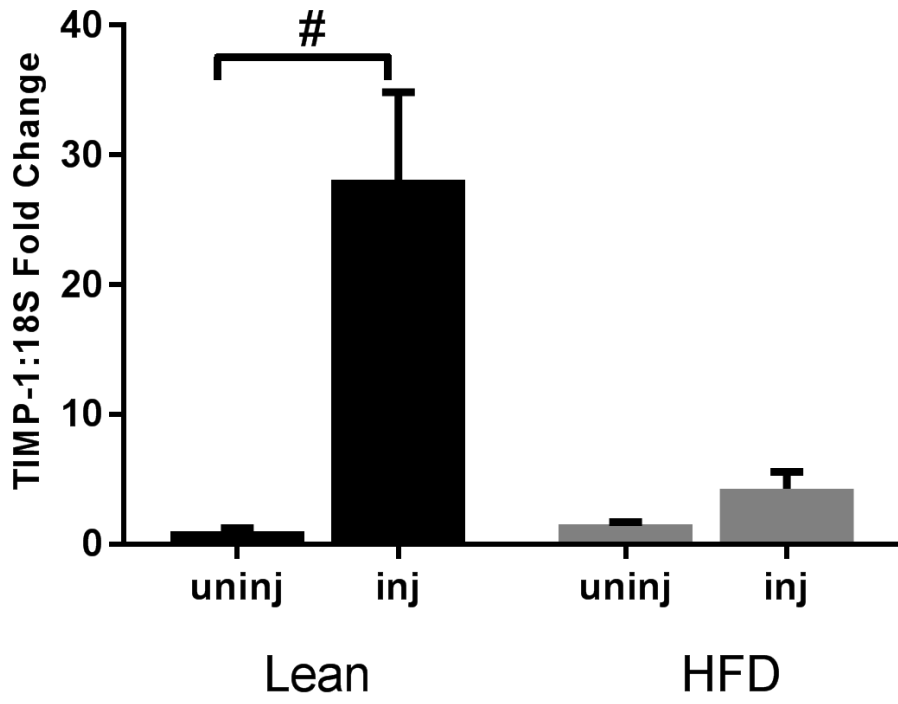
J.
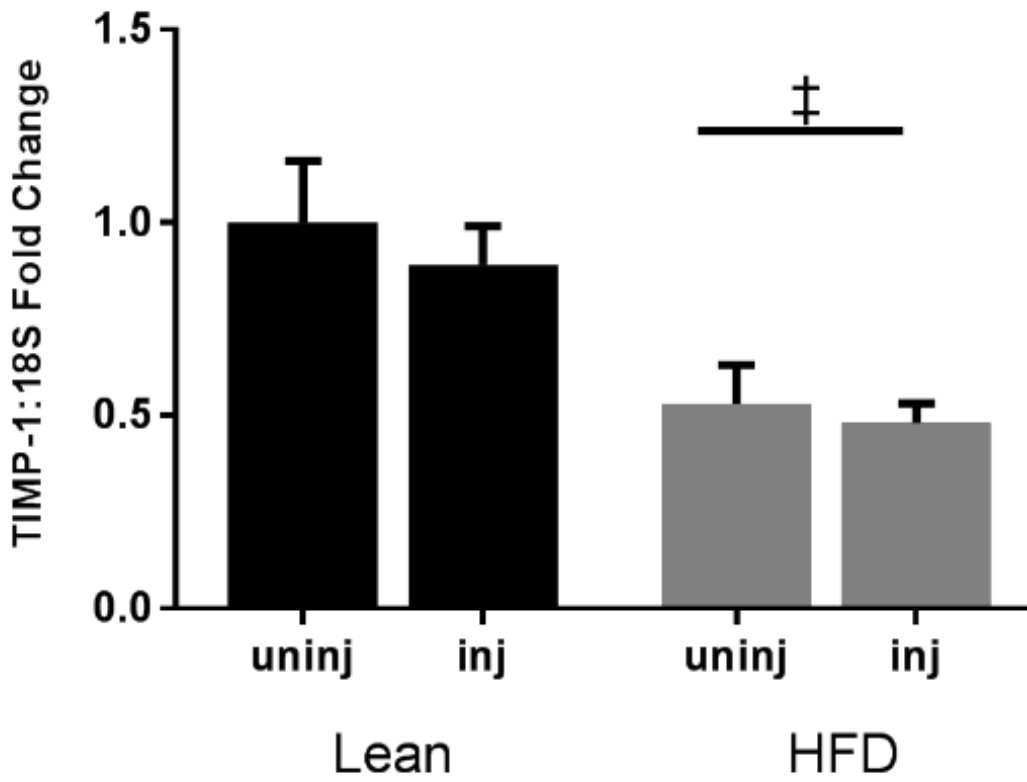
K.
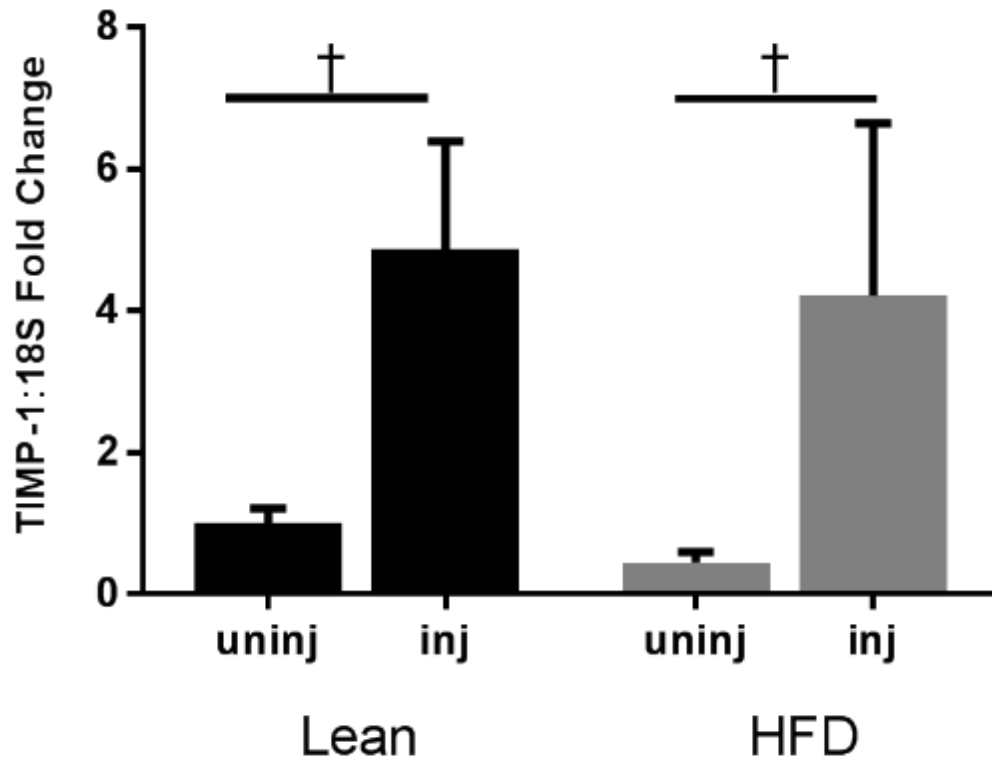
L.
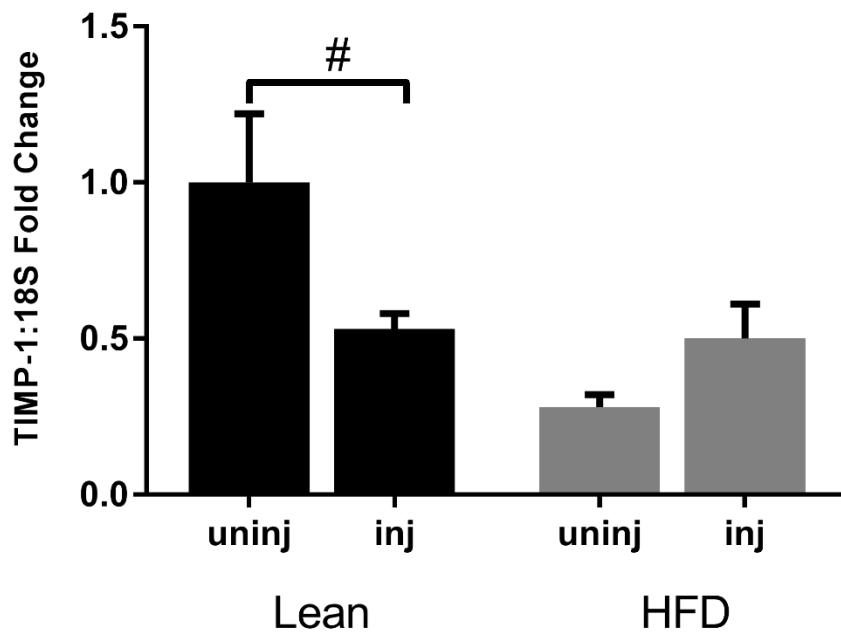
Chapter 6

Overall Discussion

The overall purpose of this project was to determine how sarcopenic obesity alters regenerative capacity and the early and late stages of muscle regeneration in mice. This project has uncovered three major findings in the sarcopenic obese population. First of all, sarcopenic obese muscle has a further reduced capacity to regenerate muscle fibers than sarcopenia or obesity alone. This reduction of regenerative capacity also appears to be linked with a more pronounced loss in skeletal muscle mass. The second major finding was that sarcopenic obese mice had impaired inflammatory signaling. The experiments performed suggest that the role of TNF-α in repair and recovery is lost, whereas IL-6 signaling may lead to alternative pathways that result into sub-optimal regeneration. Finally, this project has demonstrated that ECM remodeling is negatively influenced by the combination of aging and obesity. Altogether, these findings have identified a relatively new population that is susceptible to major losses in muscle and diminished muscle regeneration.

Regenerative capacity is reduced in sarcopenic obese mice

When skeletal muscle is introduced to a mechanical stimuli, the muscle fiber will activate several processes that are tightly regulated and coordinated for optimal growth. Any changes to one of these processes can cause alterations to repair and recovery to the whole muscle but should eventually return back to normal after muscle repair is completed. In degenerative models such as pathophysiological diseases, the muscle fiber will have alterations of these processes at rest that will influence muscle quality over time and reduce the ability for musculature to repair when muscle damage occurs (Argiles et al., 2009; Cai et

al., 2004; Coletti, Moresi, Adamo, Molinaro, & Sassoon, 2005; He et al., 2013). The first aim

of this project identified three major processes that influence regenerative potential or

capacity; myogenesis, the inflammatory response, and ECM remodeling. Each process had

drastic changes in sarcopenic obese mice which ultimately led to muscle mass loss. The major

finding in the first set of experiments is that aging HFD mice have reduced muscle weights

and cross-sectional area. The further progressive loss in muscle mass may have to do with

alterations in all of these processes involved in muscle regeneration. Both resident

macrophages and Satellite cells (SC) are located at the basement membrane of skeletal muscle

at rest (Schiaffino & Partridge, 2008). Changes within the microenvironment can influence

the ability of these proteins to proper function. We observed excessive increases of collagen

III content in aged mice but no changes or reductions in collagen gene expression and

inducers and inhibitors of collagen synthesis and degradation. It is very likely that sarcopenic

obese individuals have lower collagen turnover than either obesity or aging. Low collagen

turnover cultivates muscle stiffness by AGE because crosslinking will occur in an

environments with 1) lower collagen turnover, 2) reduced insulin sensitivity and 3) mature

collagen (Avery & Bailey, 2005, 2006; DeGroot et al., 2001). The constant degrading and

synthesis of collagen observed in healthy adult muscle assists in the movement of SC cells to

migrate to the site of muscle injury and can be regulated by inflammatory cytokines. There

were also basal changes of MyoD and myogenin which could be tied with the increase in

collagen III content in aging mice, because progenitor cells are localized in the ECM and

ECM proteins are involved in SC migration. Collagen turnover is traditionally induced by

anti-inflammatory cytokines and inhibited by pro-inflammatory cytokines. Not many changes

were seen in TGF-β but there were changes in IL-6 and NF-κB. IL-6 when secreted can

activate its downstream target STAT3 which will have anti-inflammatory effects. There was a reduction of STAT3 which may explain why there were no changes in TGF-β and in turn no changes or reductions in collagen gene expression. Perhaps, what was more interesting was the elevation of NF-κB observed in aged HFD mice. NF-κB is usually signaled through TNF-α and can lead to apoptosis in damaged muscle tissue (He et al., 2013). NF-κB appeared to be elevated independent of TNF-α. Chronic elevation of inflammatory cytokines has been implicated in myopathies and may be the major mechanism involved in age-related muscle loss (Cai et al., 2004; He et al., 2013). Thus, regenerative capacity in sarcopenic obesity is reduced and should be more associated with metabolic diseases and myopathies than healthy populations. Any potential treatment to improve regenerative capacity in sarcopenic obesity should be aimed to target the altered genes involved in the regenerative process.

Inflammatory signaling is impaired in sarcopenic obesity

The inflammatory response has a major regulatory role in skeletal muscle regeneration including assisting in myoblast proliferation, differentiation, collagen remodeling, and removal of damaged tissues and recruitment of other inflammatory proteins to overall assist in optimal regeneration. Hence, inflammatory signaling has been examined extensively within the field of muscle regeneration. Because inflammatory signaling has a diverse role in skeletal muscle regeneration, other regenerative processes can be altered and can result in sub-optimal muscle repair. The second set of experiments focused solely on muscle morphology, MRFs and inflammation, but it is very likely that impaired signaling observed in sarcopenic obese mice influenced other areas of muscle regeneration as well.

This project reported a significant reduction not only in young HFD mice but aged

HFD mice which makes this study novel. Furthermore, there were no changes in fiber distribution in aged HFD mice 21 following muscle injury. These results were similar to a previous study investigated in our laboratory demonstrating young HFD had a delayed muscle regeneration response and it was due to impaired signaling. In our first aim we did not see any changes with basal IL-6 in TA which supports the expected increase of IL-6 following muscle damage. However, IL-6 appears to be targeting downstream targets other than STAT3 that can be detrimental to the regenerative process. IL-6 serves many functions in skeletal muscle such as promoting MMP activity, assisting in myoblast proliferation, attracting other inflammatory cytokines to the site of injury. Thus, it is necessary for future studies to determine how alternative signaling is specifically impacting sarcopenic obese mice. The other major finding in aim #2 was impaired TNF-α/NF-κB signaling. TNF-α had a similar response to young lean mice in both the early and late stages of muscle regeneration however, NF-κB was upregulated in all muscles examined for this project. Mentioned earlier, NF-κB may be acting independent of TNF-α to induce apoptosis (He et al., 2013). It is important to note that both aging and obesity are associated with muscle fibrosis. The chronic expression of NF-κB observed in aged HFD mice and upregulation during muscle damage may be compensatory effect to inhibit excess collagen deposition and thus reduce muscle fibrosis. It has been reported that NF-κB can inhibit collagen I. Furthermore, other inhibitors of collagen synthesis do not appear to upregulated following damage. Thus, impaired signaling will contribute sub-optimal regeneration and may influence other aspects of muscle regeneration.

ECM is impaired in sarcopenic obesity

The ECM serves two major functions within skeletal muscle. 1) the ECM will serve as

a reservoir of growth factors and proteins that assist in muscle repair and 2) also supportive structure that will resist tension and compressive force (Kjaer, 2004). One of the major findings reported in the last set of experiments was reduced collagen content in aged mice at the onset of muscle regeneration. The MMP gene expression did not support collagen degradation but it is important to note that MMP gene expression is not always directly related to MMP activity. Furthermore, the rate of collagen synthesis is much lower which could be possibly due to the upregulation of NF-κB. Thus, there could be an imbalance in collage turnover favoring collagen degradation in aging mice. In the first set of experiments we observed a high percentage of collagen in the aged mice compared to the lean mice. During ECM remodeling collagen will release growth factors that will increase collagen turnover. Because there was no increase in collagen turnover it is likely that other factors are involved that may interfere with the remodeling process.

Compared to the other processes in skeletal muscle regeneration, the ECM has a more functional role with force transmission and to resist compressive forces. The reduction of thicker collagen, collagen I, could make the muscle more susceptible to injury while muscle regeneration is still occurring. The aging muscle also had excessive collagen III content which is a more flexible collagen that could contribute to muscle weakness observed in aging. Overall, the alterations in aged HFD mice were similar to lean mice meaning ECM remodeling may not be further impaired in sarcopenic obese individuals. This may also suggest that ECM remodeling could be more tightly regulated than the other regenerative processes discussed in this project.

Appendix

IACUC Approval Letter

UNIVERSITY OF ARKANSAS.

Office of Research Compliance

MEMORANDUM

TO: Dr. Tyrone Washington

FROM: Craig N. Coon, Chairman
          Institutional Animal Care and Use

Committee (IACUC) DATE: September 8, 2014

SUBJECT: IACUC APPROVAL
        Expiration date: September 4, 2017

The Institutional Animal Care and Use Committee (IACUC) has APPROVED
protocol 15004: *'Sarcopenic obesity and skeletal muscle regeneration'*

In granting its approval, the IACUC has approved only the information
provided. Should there be any further changes to the protocol during the
research, please notify the IACUC in writing (via the Modification form)
prior to initiating the changes. If the study period is expected to extend
beyond September 4, 2017 you must submit a new protocol prior to that
date. By policy the IACUC cannot approve a study for more than 3 years at
a time.

The IACUC appreciates your cooperation in complying with University and
Federal guidelines involving animal subjects.

CNC/aem

cc: Animal Welfare Veterinarian

References

Abbas, A. K., Lichtman, A. H. H., & Pillai, S. (2011). *Cellular and Molecular Immunology: with STUDENT CONSULT Online Access*: Elsevier Health Sciences.

Akhmedov, D., & Berdeaux, R. (2013). The effects of obesity on skeletal muscle regeneration. *Front Physiol, 4*, 371. doi: 10.3389/fphys.2013.00371

Amarya, S., Singh, K., & Sabharwal, M. (2014). Health consequences of obesity in the elderly. *Journal of Clinical Gerontology and Geriatrics, 5*(3), 63-67. doi: http://dx.doi.org/10.1016/j.jcgg.2014.01.004

Ameye, L., Aria, D., Jepsen, K., Oldberg, A., Xu, T., & Young, M. F. (2002). Abnormal collagen fibrils in tendons of biglycan/fibromodulin-deficient mice lead to gait impairment, ectopic ossification, and osteoarthritis. *Faseb j, 16*(7), 673-680. doi: 10.1096/fj.01-0848com

Argiles, J. M., Busquets, S., Toledo, M., & Lopez-Soriano, F. J. (2009). The role of cytokines in cancer cachexia. *Curr Opin Support Palliat Care, 3*(4), 263-268. doi: 10.1097/SPC.0b013e3283311d09

Avery, N. C., & Bailey, A. J. (2005). Enzymic and non-enzymic cross-linking mechanisms in relation to turnover of collagen: relevance to aging and exercise. *Scand J Med Sci Sports, 15*(4), 231-240. doi: 10.1111/j.1600-0838.2005.00464.x

Avery, N. C., & Bailey, A. J. (2006). The effects of the Maillard reaction on the physical properties and cell interactions of collagen. *Pathol Biol (Paris), 54*(7), 387-395. doi: 10.1016/j.patbio.2006.07.005

Bailey, A. J. (2001). Molecular mechanisms of ageing in connective tissues. *Mech Ageing Dev, 122*(7), 735-755.

Barrett-Connor, E. (1990). Obesity, hypertension and stroke. *Clin Exp Hypertens A, 12*(5), 769-782.

Batsis, J. A., Barre, L. K., Mackenzie, T. A., Pratt, S. I., Lopez-Jimenez, F., & Bartels, S. J. (2013). Variation in the prevalence of sarcopenia and sarcopenic obesity in older adults associated with different research definitions: dual-energy X-ray absorptiometry data from the National Health and Nutrition Examination Survey 1999-2004. *J Am Geriatr Soc, 61*(6), 974-980. doi: 10.1111/jgs.12260

Benchaouir, R., Meregalli, M., Farini, A., D'Antona, G., Belicchi, M., Goyenvalle, A., . . . Torrente, Y. (2007). Restoration of human dystrophin following transplantation of exon-skipping-engineered DMD patient stem cells into dystrophic mice. *Cell Stem Cell, 1*(6), 646-657. doi: 10.1016/j.stem.2007.09.016

Bernal, F., Hartung, H. P., & Kieseier, B. C. (2005). Tissue mRNA expression in rat of newly described matrix metalloproteinases. *Biol Res, 38*(2-3), 267-271.

Berria, R., Wang, L., Richardson, D. K., Finlayson, J., Belfort, R., Pratipanawatr, T., . . . Mandarino, L. J. (2006). Increased collagen content in insulin-resistant skeletal muscle. *Am J Physiol Endocrinol Metab, 290*(3), E560-565. doi: 10.1152/ajpendo.00202.2005

Biolo, G., Fleming, R., Maggi, S. P., & Wolfe, R. R. (1995). Transmembrane transport and intracellular kinetics of amino acids in human skeletal muscle. *American Journal of Physiology-Endocrinology And Metabolism, 268*(1), E75-E84.

Bishop, J. E., Butt, R., Dawes, K., & Laurent, G. (1998). Mechanical load enhances the stimulatory effect of PDGF on pulmonary artery fibroblast procollagen synthesis. *Chest, 114*(1 Suppl), 25s.

Blaschke, U. K., Eikenberry, E. F., Hulmes, D. J., Galla, H. J., & Bruckner, P. (2000). Collagen XI nucleates self-assembly and limits lateral growth of cartilage fibrils. *J Biol Chem, 275*(14), 10370-10378.

Bode, W., Gomis-Ruth, F. X., & Stockler, W. (1993). Astacins, serralysins, snake venom and matrix metalloproteinases exhibit identical zinc-binding environments (HEXXHXXGXXH and Met-turn) and topologies and should be grouped into a common family, the 'metzincins'. *FEBS Lett, 331*(1-2), 134-140.

Bonfil, R. D., & Cher, M. L. (2011). The role of proteolytic enzymes in metastatic bone disease. *IBMS BoneKEy, 8*(1), 16-36.

Bourboulia, D., & Stetler-Stevenson, W. G. (2010). Matrix metalloproteinases (MMPs) and tissue inhibitors of metalloproteinases (TIMPs): Positive and negative regulators in tumor cell adhesion. *Semin Cancer Biol, 20*(3), 161-168. doi: 10.1016/j.semcancer.2010.05.002

Bowne, D. W., Russell, M. L., Morgan, J. L., Optenberg, S. A., & Clarke, A. E. (1984). Reduced disability and health care costs in an industrial fitness program. *J Occup Med, 26*(11), 809-816.

Brakebusch, C., Bouvard, D., Stanchi, F., Sakai, T., & Fassler, R. (2002). Integrins in invasive growth. *J Clin Invest, 109*(8), 999-1006. doi: 10.1172/jci15468

Brown, J. C., Harhay, M. O., & Harhay, M. N. (2014). Walking cadence and mortality among community-dwelling older adults. *J Gen Intern Med*. doi: 10.1007/s11606-014-2926-6

Brown, L. A., Lee, D. E., Patton, J. F., Perry, R. A., Jr., Brown, J. L., Baum, J. I., . . . Washington, T. A. (2015). Diet-induced obesity alters anabolic signalling in mice at

the onset of skeletal muscle regeneration. *Acta Physiol (Oxf), 215*(1), 46-57. doi: 10.1111/apha.12537

Burks, T. N., & Cohn, R. D. (2011). Role of TGF-beta signaling in inherited and acquired myopathies. *Skelet Muscle, 1*(1), 19. doi: 10.1186/2044-5040-1-19

Burridge, K., & Chrzanowska-Wodnicka, M. (1996). Focal adhesions, contractility, and signaling. *Annu Rev Cell Dev Biol, 12*, 463-518. doi: 10.1146/annurev.cellbio.12.1.463

Butt, R. P., & Bishop, J. E. (1997). Mechanical load enhances the stimulatory effect of serum growth factors on cardiac fibroblast procollagen synthesis. *J Mol Cell Cardiol, 29*(4), 1141-1151. doi: 10.1006/jmcc.1996.0347

Cai, D., Frantz, J. D., Tawa, N. E., Jr., Melendez, P. A., Oh, B. C., Lidov, H. G., . . . Shoelson, S. E. (2004). IKKbeta/NF-kappaB activation causes severe muscle wasting in mice. *Cell, 119*(2), 285-298. doi: 10.1016/j.cell.2004.09.027

Carmeli, E., Moas, M., Reznick, A. Z., & Coleman, R. (2004). Matrix metalloproteinases and skeletal muscle: a brief review. *Muscle Nerve, 29*(2), 191-197. doi: 10.1002/mus.10529

Caron, N. J., Asselin, I., Morel, G., & Tremblay, J. P. (1999). Increased myogenic potential and fusion of matrilysin-expressing myoblasts transplanted in mice. *Cell Transplant, 8*(5), 465-476.

Cassatella, M. A. (1999). Neutrophil-derived proteins: selling cytokines by the pound. *Adv Immunol, 73*, 369-509.

CDC. Center for Disease Control.   Retrieved 7/14/2014

Cesari, M., Kritchevsky, S. B., Baumgartner, R. N., Atkinson, H. H., Penninx, B. W., Lenchik, L., . . . Pahor, M. (2005). Sarcopenia, obesity, and inflammation--results from the Trial of Angiotensin Converting Enzyme Inhibition and Novel Cardiovascular Risk Factors study. *Am J Clin Nutr, 82*(2), 428-434.

Chakkalakal, J. V., Jones, K. M., Basson, M. A., & Brack, A. S. (2012). The aged niche disrupts muscle stem cell quiescence. *Nature, 490*(7420), 355-360. doi: 10.1038/nature11438

Chen, S. E., Gerken, E., Zhang, Y., Zhan, M., Mohan, R. K., Li, A. S., . . . Li, Y. P. (2005). Role of TNF-{alpha} signaling in regeneration of cardiotoxin-injured muscle. *Am J Physiol Cell Physiol, 289*(5), C1179-1187. doi: 10.1152/ajpcell.00062.2005

Chen, S. J., Yuan, W., Mori, Y., Levenson, A., Trojanowska, M., & Varga, J. (1999). Stimulation of type I collagen transcription in human skin fibroblasts by TGF-beta:

involvement of Smad 3. *J Invest Dermatol, 112*(1), 49-57. doi: 10.1046/j.1523-1747.1999.00477.x

Chiquet, M., Matthisson, M., Koch, M., Tannheimer, M., & Chiquet-Ehrismann, R. (1996). Regulation of extracellular matrix synthesis by mechanical stress. *Biochem Cell Biol, 74*(6), 737-744.

Chmelar, J., Chung, K. J., & Chavakis, T. (2013). The role of innate immune cells in obese adipose tissue inflammation and development of insulin resistance. *Thromb Haemost, 109*(3), 399-406. doi: 10.1160/th12-09-0703

Choi, K. M. (2013). Sarcopenia and Sarcopenic Obesity. *Endocrinol Metab (Seoul), 28*(2), 86-89. doi: 10.3803/EnM.2013.28.2.86

Choong, M. F., & Mak, J. W. (1991). Biochemical studies in Presbytis cristata infected with subperiodic Brugia malayi. *Trop Med Parasitol, 42*(1), 71-72.

Ciciliot, S., & Schiaffino, S. (2010). Regeneration of mammalian skeletal muscle. Basic mechanisms and clinical implications. *Curr Pharm Des, 16*(8), 906-914.

Clarke, M. S., & Feeback, D. L. (1996). Mechanical load induces sarcoplasmic wounding and FGF release in differentiated human skeletal muscle cultures. *Faseb j, 10*(4), 502-509.

Coletti, D., Moresi, V., Adamo, S., Molinaro, M., & Sassoon, D. (2005). Tumor necrosis factor-alpha gene transfer induces cachexia and inhibits muscle regeneration. *Genesis, 43*(3), 120-128. doi: 10.1002/gene.20160

Conboy, I. M., Conboy, M. J., Wagers, A. J., Girma, E. R., Weissman, I. L., & Rando, T. A. (2005). Rejuvenation of aged progenitor cells by exposure to a young systemic environment. *Nature, 433*(7027), 760-764. doi: 10.1038/nature03260

Croker, B. A., Krebs, D. L., Zhang, J. G., Wormald, S., Willson, T. A., Stanley, E. G., . . . Alexander, W. S. (2003). SOCS3 negatively regulates IL-6 signaling in vivo. *Nat Immunol, 4*(6), 540-545. doi: 10.1038/ni931

Danielson, K. G., Baribault, H., Holmes, D. F., Graham, H., Kadler, K. E., & Iozzo, R. V. (1997). Targeted disruption of decorin leads to abnormal collagen fibril morphology and skin fragility. *J Cell Biol, 136*(3), 729-743.

De Bleecker, J. L., & Engel, A. G. (1994). Expression of cell adhesion molecules in inflammatory myopathies and Duchenne dystrophy. *J Neuropathol Exp Neurol, 53*(4), 369-376.

Dearth, C. L., Goh, Q., Marino, J. S., Cicinelli, P. A., Torres-Palsa, M. J., Pierre, P., . . . Pizza, F. X. (2013). Skeletal muscle cells express ICAM-1 after muscle overload and ICAM-

1 contributes to the ensuing hypertrophic response. *PLoS One, 8*(3), e58486. doi: 10.1371/journal.pone.0058486

DeGroot, J., Verzijl, N., Budde, M., Bijlsma, J. W., Lafeber, F. P., & TeKoppele, J. M. (2001). Accumulation of advanced glycation end products decreases collagen turnover by bovine chondrocytes. *Exp Cell Res, 266*(2), 303-310. doi: 10.1006/excr.2001.5224

Drake, J. C., Alway, S. E., Hollander, J. M., & Williamson, D. L. (2010). AICAR treatment for 14 days normalizes obesity-induced dysregulation of TORC1 signaling and translational capacity in fasted skeletal muscle. *Am J Physiol Regul Integr Comp Physiol, 299*(6), R1546-1554. doi: 10.1152/ajpregu.00337.2010

Duance, V. C., Restall, D. J., Beard, H., Bourne, F. J., & Bailey, A. J. (1977). The location of three collagen types in skeletal muscle. *FEBS Lett, 79*(2), 248-252.

Engert, J. C., Berglund, E. B., & Rosenthal, N. (1996). Proliferation precedes differentiation in IGF-I-stimulated myogenesis. *J Cell Biol, 135*(2), 431-440.

Fessler, L. I., Timpl, R., & Fessler, J. H. (1981). Assembly and processing of procollagen type III in chick embryo blood vessels. *J Biol Chem, 256*(5), 2531-2537.

Flegal, K. M., Carroll, M. D., Kit, B. K., & Ogden, C. L. (2012). Prevalence of obesity and trends in the distribution of body mass index among US adults, 1999-2010. *Jama, 307*(5), 491-497. doi: 10.1001/jama.2012.39

Fleischmajer, R., MacDonald, E. D., Perlish, J. S., Burgeson, R. E., & Fisher, L. W. (1990). Dermal collagen fibrils are hybrids of type I and type III collagen molecules. *J Struct Biol, 105*(1-3), 162-169.

Freije, J. M., Diez-Itza, I., Balbin, M., Sanchez, L. M., Blasco, R., Tolivia, J., & Lopez-Otin, C. (1994). Molecular cloning and expression of collagenase-3, a novel human matrix metalloproteinase produced by breast carcinomas. *J Biol Chem, 269*(24), 16766-16773.

Fried, L. P., Tangen, C. M., Walston, J., Newman, A. B., Hirsch, C., Gottdiener, J., . . . McBurnie, M. A. (2001). Frailty in older adults: evidence for a phenotype. *J Gerontol A Biol Sci Med Sci, 56*(3), M146-156.

Gaens, K. H., Stehouwer, C. D., & Schalkwijk, C. G. (2013). Advanced glycation endproducts and its receptor for advanced glycation endproducts in obesity. *Curr Opin Lipidol, 24*(1), 4-11. doi: 10.1097/MOL.0b013e32835aea13

Gahmberg, C. G., Tolvanen, M., & Kotovuori, P. (1997). Leukocyte adhesion--structure and function of human leukocyte beta2-integrins and their cellular ligands. *Eur J Biochem, 245*(2), 215-232.

Ge, X., Vajjala, A., McFarlane, C., Wahli, W., Sharma, M., & Kambadur, R. (2012). Lack of Smad3 signaling leads to impaired skeletal muscle regeneration. *Am J Physiol Endocrinol Metab, 303*(1), E90-102. doi: 10.1152/ajpendo.00113.2012

Gillespie, M. A., Le Grand, F., Scime, A., Kuang, S., von Maltzahn, J., Seale, V., . . . Rudnicki, M. A. (2009). p38-{gamma}-dependent gene silencing restricts entry into the myogenic differentiation program. *J Cell Biol, 187*(7), 991-1005. doi: 10.1083/jcb.200907037

Gillies, A. R., & Lieber, R. L. (2011). Structure and function of the skeletal muscle extracellular matrix. *Muscle Nerve, 44*(3), 318-331. doi: 10.1002/mus.22094

Goldspink, G., Fernandes, K., Williams, P. E., & Wells, D. J. (1994). Age-related changes in collagen gene expression in the muscles of mdx dystrophic and normal mice. *Neuromuscul Disord, 4*(3), 183-191.

Greene, N. P., Lee, D. E., Brown, J. L., Rosa, M. E., Brown, L. A., Perry, R. A., . . . Washington, T. A. (2015). Mitochondrial quality control, promoted by PGC-1alpha, is dysregulated by Western diet-induced obesity and partially restored by moderate physical activity in mice. *Physiol Rep, 3*(7). doi: 10.14814/phy2.12470

Greene, N. P., Nilsson, M. I., Washington, T. A., Lee, D. E., Brown, L. A., Papineau, A. M., . . . Fluckey, J. D. (2014). Impaired exercise-induced mitochondrial biogenesis in the obese Zucker rat, despite PGC-1α induction, is due to compromised mitochondrial translation elongation. *American Journal of Physiology-Endocrinology And Metabolism, 306*(5), E503-E511.

Grefte, S. (2011). Improving the regeneration of injured muscle. *Radboud Repository*, 21-48.

Gregor, M. F., & Hotamisligil, G. S. (2011). Inflammatory mechanisms in obesity. *Annu Rev Immunol, 29*, 415-445. doi: 10.1146/annurev-immunol-031210-101322

Gross, J., & Lapiere, C. M. (1962). Collagenolytic activity in amphibian tissues: a tissue culture assay. *Proc Natl Acad Sci U S A, 48*, 1014-1022.

Hamada, K., Vannier, E., Sacheck, J. M., Witsell, A. L., & Roubenoff, R. (2005). Senescence of human skeletal muscle impairs the local inflammatory cytokine response to acute eccentric exercise. *Faseb j, 19*(2), 264-266. doi: 10.1096/fj.03-1286fje

Harwood, R., Grant, M. E., & Jackson, D. S. (1976). The route of secretion of procollagen. The influence of alphaalpha'-bipyridyl, colchicine and antimycin A on the secretory process in embryonic-chick tendon and cartilage cells. *Biochem J, 156*(1), 81-90.

Hashizume, K., Kanda, K., & Burke, R. E. (1988). Medial gastrocnemius motor nucleus in the rat: age-related changes in the number and size of motoneurons. *J Comp Neurol, 269*(3), 425-430. doi: 10.1002/cne.902690309

He, W. A., Berardi, E., Cardillo, V. M., Acharyya, S., Aulino, P., Thomas-Ahner, J., . . . Guttridge, D. C. (2013). NF-kappaB-mediated Pax7 dysregulation in the muscle microenvironment promotes cancer cachexia. *J Clin Invest, 123*(11), 4821-4835. doi: 10.1172/jci68523

Heinrich, P. C., Behrmann, I., Haan, S., Hermanns, H. M., Muller-Newen, G., & Schaper, F. (2003). Principles of interleukin (IL)-6-type cytokine signalling and its regulation. *Biochem J, 374*(Pt 1), 1-20. doi: 10.1042/bj20030407

Hemmavanh, C., Koch, M., Birk, D. E., & Espana, E. M. (2013). Abnormal corneal endothelial maturation in collagen XII and XIV null mice. *Invest Ophthalmol Vis Sci, 54*(5), 3297-3308. doi: 10.1167/iovs.12-11456

Hirata, A., Masuda, S., Tamura, T., Kai, K., Ojima, K., Fukase, A., . . . Takeda, S. (2003). Expression profiling of cytokines and related genes in regenerating skeletal muscle after cardiotoxin injection: a role for osteopontin. *Am J Pathol, 163*(1), 203-215. doi: 10.1016/s0002-9440(10)63644-9

Hiscock, N., Chan, M. H., Bisucci, T., Darby, I. A., & Febbraio, M. A. (2004). Skeletal myocytes are a source of interleukin-6 mRNA expression and protein release during contraction: evidence of fiber type specificity. *Faseb j, 18*(9), 992-994. doi: 10.1096/fj.03-1259fje

Hocevar, B. A., Brown, T. L., & Howe, P. H. (1999). TGF-beta induces fibronectin synthesis through a c-Jun N-terminal kinase-dependent, Smad4-independent pathway. *Embo j, 18*(5), 1345-1356. doi: 10.1093/emboj/18.5.1345

Hotamisligil, G. S., Peraldi, P., Budavari, A., Ellis, R., White, M. F., & Spiegelman, B. M. (1996). IRS-1-mediated inhibition of insulin receptor tyrosine kinase activity in TNF-alpha- and obesity-induced insulin resistance. *Science, 271*(5249), 665-668.

Hu, Z., Wang, H., Lee, I. H., Modi, S., Wang, X., Du, J., & Mitch, W. E. (2010). PTEN inhibition improves muscle regeneration in mice fed a high-fat diet. *Diabetes, 59*(6), 1312-1320. doi: 10.2337/db09-1155

Ingber, D. E., Dike, L., Hansen, L., Karp, S., Liley, H., Maniotis, A., . . . et al. (1994). Cellular tensegrity: exploring how mechanical changes in the cytoskeleton regulate cell growth, migration, and tissue pattern during morphogenesis. *Int Rev Cytol, 150*, 173-224.

Ireland, D., Harrall, R., Curry, V., Holloway, G., Hackney, R., Hazleman, B., & Riley, G. (2001). Multiple changes in gene expression in chronic human Achilles tendinopathy. *Matrix Biology, 20*(3), 159-169.

Iwase, S., Murakami, T., Saito, Y., & Nakagawa, K. (2004). Steep elevation of blood interleukin-6 (IL-6) associated only with late stages of cachexia in cancer patients. *Eur Cytokine Netw, 15*(4), 312-316.

Janssen, I., Heymsfield, S. B., & Ross, R. (2002). Low relative skeletal muscle mass (sarcopenia) in older persons is associated with functional impairment and physical disability. *J Am Geriatr Soc, 50*(5), 889-896.

Jilek, F., & Hörmann, H. (1978). Cold-insoluble globulin (fibronectin), IV Affinity to soluble collagen of various types. *Biol Chem, 359*(1), 247-250.

Joe, A. W., Yi, L., Natarajan, A., Le Grand, F., So, L., Wang, J., . . . Rossi, F. M. (2010). Muscle injury activates resident fibro/adipogenic progenitors that facilitate myogenesis. *Nat Cell Biol, 12*(2), 153-163. doi: 10.1038/ncb2015

Kadler, K. E., Hill, A., & Canty-Laird, E. G. (2008). Collagen fibrillogenesis: fibronectin, integrins, and minor collagens as organizers and nucleators. *Curr Opin Cell Biol, 20*(5), 495-501. doi: 10.1016/j.ceb.2008.06.008

Kamimura, D., Ishihara, K., & Hirano, T. (2003). IL-6 signal transduction and its physiological roles: the signal orchestration model. *Rev Physiol Biochem Pharmacol, 149*, 1-38. doi: 10.1007/s10254-003-0012-2

Kharraz, Y., Guerra, J., Mann, C. J., Serrano, A. L., & Munoz-Canoves, P. (2013). Macrophage plasticity and the role of inflammation in skeletal muscle repair. *Mediators Inflamm, 2013*, 491497. doi: 10.1155/2013/491497

Kherif, S., Lafuma, C., Dehaupas, M., Lachkar, S., Fournier, J. G., Verdiere-Sahuque, M., . . . Alameddine, H. S. (1999). Expression of matrix metalloproteinases 2 and 9 in regenerating skeletal muscle: a study in experimentally injured and mdx muscles. *Dev Biol, 205*(1), 158-170. doi: 10.1006/dbio.1998.9107

Kim, J. T., Kasukonis, B. M., Brown, L. A., Washington, T. A., & Wolchok, J. C. (2016). Recovery from volumetric muscle loss injury: A comparison between young and aged rats. *Exp Gerontol, 83*, 37-46. doi: 10.1016/j.exger.2016.07.008

Kishimoto, T. (2006). Interleukin-6: discovery of a pleiotropic cytokine. *Arthritis Res Ther, 8 Suppl 2*, S2. doi: 10.1186/ar1916

Kiuchi, N., Nakajima, K., Ichiba, M., Fukada, T., Narimatsu, M., Mizuno, K., . . . Hirano, T. (1999). STAT3 is required for the gp130-mediated full activation of the c-myc gene. *J Exp Med, 189*(1), 63-73.

Kjaer, M. (2004). Role of extracellular matrix in adaptation of tendon and skeletal muscle to mechanical loading. *Physiol Rev, 84*(2), 649-698. doi: 10.1152/physrev.00031.2003

Kleinman, H. K., Martin, G. R., & Fishman, P. H. (1979). Ganglioside inhibition of fibronectin-mediated cell adhesion to collagen. *Proc Natl Acad Sci U S A, 76*(7), 3367-3371.

Koskinen, S. O., Wang, W., Ahtikoski, A. M., Kjaer, M., Han, X. Y., Komulainen, J., . . . Takala, T. E. (2001). Acute exercise induced changes in rat skeletal muscle mRNAs and proteins regulating type IV collagen content. *Am J Physiol Regul Integr Comp Physiol, 280*(5), R1292-1300.

Kraemer, W. J., Volek, J. S., Clark, K. L., Gordon, S. E., Puhl, S. M., Koziris, L. P., . . . Sebastianelli, W. J. (1999). Influence of exercise training on physiological and performance changes with weight loss in men. *Med Sci Sports Exerc, 31*(9), 1320-1329.

Kragstrup, T. W., Kjaer, M., & Mackey, A. L. (2011). Structural, biochemical, cellular, and functional changes in skeletal muscle extracellular matrix with aging. *Scand J Med Sci Sports, 21*(6), 749-757. doi: 10.1111/j.1600-0838.2011.01377.x

Kusano, K., Miyaura, C., Inada, M., Tamura, T., Ito, A., Nagase, H., . . . Suda, T. (1998). Regulation of matrix metalloproteinases (MMP-2, -3, -9, and -13) by interleukin-1 and interleukin-6 in mouse calvaria: association of MMP induction with bone resorption. *Endocrinology, 139*(3), 1338-1345. doi: 10.1210/endo.139.3.5818

Langley, B., Thomas, M., Bishop, A., Sharma, M., Gilmour, S., & Kambadur, R. (2002). Myostatin inhibits myoblast differentiation by down-regulating MyoD expression. *J Biol Chem, 277*(51), 49831-49840. doi: 10.1074/jbc.M204291200

Leask, A., Holmes, A., & Abraham, D. J. (2002). Connective tissue growth factor: a new and important player in the pathogenesis of fibrosis. *Curr Rheumatol Rep, 4*(2), 136-142.

Lee, D. E., Brown, J. L., Rosa, M. E., Brown, L. A., Perry, R. A., Washington, T. A., & Greene, N. P. (2016). Translational machinery of mitochondrial mRNA is promoted by physical activity in Western diet-induced obese mice. *Acta Physiologica*, n/a-n/a. doi: 10.1111/apha.12687

Leeman, M. F., Curran, S., & Murray, G. I. (2002). The structure, regulation, and function of human matrix metalloproteinase-13. *Crit Rev Biochem Mol Biol, 37*(3), 149-166. doi: 10.1080/10409230290771483

Lei, H., Leong, D., Smith, L. R., & Barton, E. R. (2013). Matrix metalloproteinase 13 is a new contributor to skeletal muscle regeneration and critical for myoblast migration. *Am J Physiol Cell Physiol, 305*(5), C529-538. doi: 10.1152/ajpcell.00051.2013

Li, X. (2013). SIRT1 and energy metabolism. *Acta Biochim Biophys Sin (Shanghai), 45*(1), 51-60. doi: 10.1093/abbs/gms108

Li, Y. Y., McTiernan, C. F., & Feldman, A. M. (1999). Proinflammatory cytokines regulate tissue inhibitors of metalloproteinases and disintegrin metalloproteinase in cardiac cells. *Cardiovasc Res, 42*(1), 162-172.

Li, Z., Gilbert, J. A., Zhang, Y., Zhang, M., Qiu, Q., Ramanujan, K., . . . Glass, D. J. (2012). An HMGA2-IGF2BP2 axis regulates myoblast proliferation and myogenesis. *Dev Cell, 23*(6), 1176-1188. doi: 10.1016/j.devcel.2012.10.019

Libby, P., & Lee, R. T. (2000). Matrix matters. *Circulation, 102*(16), 1874-1876.

Light, N., & Champion, A. E. (1984). Characterization of muscle epimysium, perimysium and endomysium collagens. *Biochem J, 219*(3), 1017-1026.

Lim, S., Kim, J. H., Yoon, J. W., Kang, S. M., Choi, S. H., Park, Y. J., . . . Jang, H. C. (2010). Sarcopenic obesity: prevalence and association with metabolic syndrome in the Korean Longitudinal Study on Health and Aging (KLoSHA). *Diabetes Care, 33*(7), 1652-1654. doi: 10.2337/dc10-0107

Liu, X., Wu, H., Byrne, M., Krane, S., & Jaenisch, R. (1997). Type III collagen is crucial for collagen I fibrillogenesis and for normal cardiovascular development. *Proc Natl Acad Sci U S A, 94*(5), 1852-1856.

Lo, E. H., Dalkara, T., & Moskowitz, M. A. (2003). Mechanisms, challenges and opportunities in stroke. *Nat Rev Neurosci, 4*(5), 399-415. doi: 10.1038/nrn1106

Lundberg, I., Brengman, J. M., & Engel, A. G. (1995). Analysis of cytokine expression in muscle in inflammatory myopathies, Duchenne dystrophy, and non-weak controls. *J Neuroimmunol, 63*(1), 9-16.

Luz, M. A., Marques, M. J., & Santo Neto, H. (2002). Impaired regeneration of dystrophin-deficient muscle fibers is caused by exhaustion of myogenic cells. *Braz J Med Biol Res, 35*(6), 691-695.

Lynch, G. S. (2011). Overview of Sarcopenia. In G. S. Lynch (Ed.), *Sarcopenia – Age-Related Muscle Wasting and Weakness: Mechanisms and Treatments* (pp. 1-7). Dordrecht: Springer Netherlands.

Mao, Y., & Schwarzbauer, J. E. (2005). Fibronectin fibrillogenesis, a cell-mediated matrix assembly process. *Matrix Biol, 24*(6), 389-399. doi: 10.1016/j.matbio.2005.06.008

Marsh, D. R., Criswell, D. S., Carson, J. A., & Booth, F. W. (1997). Myogenic regulatory factors during regeneration of skeletal muscle in young, adult, and old rats. *J Appl Physiol (1985), 83*(4), 1270-1275.

Martinez, F. O., & Gordon, S. (2014). The M1 and M2 paradigm of macrophage activation: time for reassessment. *F1000Prime Rep, 6*. doi: 10.12703/p6-13

McQuibban, G. A., Gong, J. H., Tam, E. M., McCulloch, C. A., Clark-Lewis, I., & Overall, C. M. (2000). Inflammation dampened by gelatinase A cleavage of monocyte chemoattractant protein-3. *Science, 289*(5482), 1202-1206.

Mecham, R. (2011). *The Extracellular Matrix: an Overview*: Springer Berlin Heidelberg.

Megeney, L. A., Kablar, B., Garrett, K., Anderson, J. E., & Rudnicki, M. A. (1996). MyoD is required for myogenic stem cell function in adult skeletal muscle. *Genes Dev, 10*(10), 1173-1183.

Morikawa, T., Tuderman, L., & Prockop, D. J. (1980). Inhibitors of procollagen N-protease. Synthetic peptides with sequences similar to the cleavage site in the pro alpha 1(I) chain. *Biochemistry, 19*(12), 2646-2650.

Muscaritoli, M., Anker, S. D., Argiles, J., Aversa, Z., Bauer, J. M., Biolo, G., . . . Sieber, C. C. (2010). Consensus definition of sarcopenia, cachexia and pre-cachexia: joint document elaborated by Special Interest Groups (SIG) "cachexia-anorexia in chronic wasting diseases" and "nutrition in geriatrics". *Clin Nutr, 29*(2), 154-159. doi: 10.1016/j.clnu.2009.12.004

Myllyharju, J., & Kivirikko, K. I. (2004). Collagens, modifying enzymes and their mutations in humans, flies and worms. *Trends Genet, 20*(1), 33-43. doi: 10.1016/j.tig.2003.11.004

Nakagawa, Y., Majima, T., & Nagashima, K. (1994). Effect of ageing on ultrastructure of slow and fast skeletal muscle tendon in rabbit Achilles tendons. *Acta Physiol Scand, 152*(3), 307-313. doi: 10.1111/j.1748-1716.1994.tb09810.x

Nguyen, M. H., Cheng, M., & Koh, T. J. (2011). Impaired muscle regeneration in ob/ob and db/db mice. *ScientificWorldJournal, 11*, 1525-1535. doi: 10.1100/tsw.2011.137

Nilsson, M. I., Dobson, J. P., Greene, N. P., Wiggs, M. P., Shimkus, K. L., Wudeck, E. V., . . . Fluckey, J. D. (2013). Abnormal protein turnover and anabolic resistance to exercise in sarcopenic obesity. *Faseb j, 27*(10), 3905-3916. doi: 10.1096/fj.12-224006

Olguin, H. C., Yang, Z., Tapscott, S. J., & Olwin, B. B. (2007). Reciprocal inhibition between Pax7 and muscle regulatory factors modulates myogenic cell fate determination. *J Cell Biol, 177*(5), 769-779. doi: 10.1083/jcb.200608122

Overall, C. M., McQuibban, G. A., & Clark-Lewis, I. (2002). Discovery of chemokine substrates for matrix metalloproteinases by exosite scanning: a new tool for degradomics. *Biol Chem, 383*(7-8), 1059-1066. doi: 10.1515/bc.2002.114

Page-McCaw, A., Ewald, A. J., & Werb, Z. (2007). Matrix metalloproteinases and the regulation of tissue remodelling. *Nat Rev Mol Cell Biol, 8*(3), 221-233. doi: 10.1038/nrm2125

Peake, J., Della Gatta, P., & Cameron-Smith, D. (2010). Aging and its effects on inflammation in skeletal muscle at rest and following exercise-induced muscle injury. *Am J Physiol Regul Integr Comp Physiol, 298*(6), R1485-1495. doi: 10.1152/ajpregu.00467.2009

Pedersen, M., Steensberg, A., Keller, C., Osada, T., Zacho, M., Saltin, B., . . . Pedersen, B. K. (2004). Does the aging skeletal muscle maintain its endocrine function? *Exerc Immunol Rev, 10*, 42-55.

Perry Jr, R. A., Brown, L. A., Lee, D. E., Brown, J. L., Baum, J. I., Greene, N. P., & Washington, T. A. (2016). Differential effects of leucine supplementation in young and aged mice at the onset of skeletal muscle regeneration. *Mech Ageing Dev, 157*, 7-16. doi: http://dx.doi.org/10.1016/j.mad.2016.05.007

Petersen, A. M., & Pedersen, B. K. (2005). The anti-inflammatory effect of exercise. *J Appl Physiol (1985), 98*(4), 1154-1162. doi: 10.1152/japplphysiol.00164.2004

Proctor, D. N., Balagopal, P., & Nair, K. S. (1998). Age-related sarcopenia in humans is associated with reduced synthetic rates of specific muscle proteins. *J Nutr, 128*(2 Suppl), 351s-355s.

Przybyla, B., Gurley, C., Harvey, J. F., Bearden, E., Kortebein, P., Evans, W. J., . . . Dennis, R. A. (2006). Aging alters macrophage properties in human skeletal muscle both at rest and in response to acute resistance exercise. *Exp Gerontol, 41*(3), 320-327. doi: 10.1016/j.exger.2005.12.007

Purslow, P. P., & Duance, V. C. (1990). Strucutre and function of intramuscular connective tissue. *Connective Tissue Matrix, Part 2*, 127-166.

Rantanen, J., Hurme, T., Lukka, R., Heino, J., & Kalimo, H. (1995). Satellite cell proliferation and the expression of myogenin and desmin in regenerating skeletal muscle: evidence for two different populations of satellite cells. *Lab Invest, 72*(3), 341-347.

Rejeski, W. J., Marsh, A. P., Chmelo, E., & Rejeski, J. J. (2010). Obesity, intentional weight loss and physical disability in older adults. *Obes Rev, 11*(9), 671-685. doi: 10.1111/j.1467-789X.2009.00679.x

Relaix, F., Demignon, J., Laclef, C., Pujol, J., Santolini, M., Niro, C., . . . Maire, P. (2013). Six homeoproteins directly activate Myod expression in the gene regulatory networks that control early myogenesis. *PLoS Genet, 9*(4), e1003425. doi: 10.1371/journal.pgen.1003425

Reynolds, S. D., Zhang, D., Puzas, J. E., O'Keefe, R. J., Rosier, R. N., & Reynolds, P. R. (2000). Cloning of the chick BMP1/Tolloid cDNA and expression in skeletal tissues. *Gene, 248*(1-2), 233-243.

Rigamonti, E., & Zordan, P. (2014). Macrophage plasticity in skeletal muscle repair. *2014*, 560629. doi: 10.1155/2014/560629

Rosenberg, I. H. (1989). Summary comments. *Am J Clin Nutr, 50*(5), 1231-1233.

Rubenstein, L. Z., Josephson, K. R., Trueblood, P. R., Loy, S., Harker, J. O., Pietruszka, F. M., & Robbins, A. S. (2000). Effects of a group exercise program on strength, mobility, and falls among fall-prone elderly men. *J Gerontol A Biol Sci Med Sci, 55*(6), M317-321.

Sakaguchi, S., Shono, J. I., Suzuki, T., Sawano, S., Anderson, J. E., Do, M. K., . . . Tatsumi, R. (2014). Implication of anti-inflammatory macrophages in regenerative moto-neuritogenesis: Promotion of myoblast migration and neural chemorepellent semaphorin 3A expression in injured muscle. *Int J Biochem Cell Biol*. doi: 10.1016/j.biocel.2014.05.032

Samstein, B., Hoimes, M. L., Fan, J., Frost, R. A., Gelato, M. C., & Lang, C. H. (1996). IL-6 stimulation of insulin-like growth factor binding protein (IGFBP)-1 production. *Biochem Biophys Res Commun, 228*(2), 611-615. doi: 10.1006/bbrc.1996.1705

Santilli, V., Bernetti, A., Mangone, M., & Paoloni, M. (2014). Clinical definition of sarcopenia. *Clin Cases Miner Bone Metab, 11*(3), 177-180.

Sato, K., Li, Y., Foster, W., Fukushima, K., Badlani, N., Adachi, N., . . . Huard, J. (2003). Improvement of muscle healing through enhancement of muscle regeneration and prevention of fibrosis. *Muscle Nerve, 28*(3), 365-372. doi: 10.1002/mus.10436

Satoh, N., Araki, I., & Satou, Y. (1996). An intrinsic genetic program for autonomous differentiation of muscle cells in the ascidian embryo. *Proc Natl Acad Sci U S A, 93*(18), 9315-9321.

Schaap, L. A., Pluijm, S. M., Deeg, D. J., & Visser, M. (2006). Inflammatory markers and loss of muscle mass (sarcopenia) and strength. *Am J Med, 119*(6), 526.e529-517. doi: 10.1016/j.amjmed.2005.10.049

Schiaffino, S., & Partridge, T. (2008). *Skeletal Muscle Repair and Regeneration*: Springer Netherlands.

Scott, J. E. (1990). Proteoglycan:collagen interactions and subfibrillar structure in collagen fibrils. Implications in the development and ageing of connective tissues. *J Anat, 169*, 23-35.

Serrano, A. L., Baeza-Raja, B., Perdiguero, E., Jardi, M., & Munoz-Canoves, P. (2008). Interleukin-6 is an essential regulator of satellite cell-mediated skeletal muscle hypertrophy. *Cell Metab, 7*(1), 33-44. doi: 10.1016/j.cmet.2007.11.011

Sevilla, C. A., Dalecki, D., & Hocking, D. C. (2010). Extracellular Matrix Fibronectin Stimulates the Self-Assembly of Microtissues on Native Collagen Gels. *Tissue Eng Part A, 16*(12), 3805-3819. doi: 10.1089/ten.tea.2010.0316

Shefer, G., Van de Mark, D. P., Richardson, J. B., & Yablonka-Reuveni, Z. (2006). Satellite-cell pool size does matter: defining the myogenic potency of aging skeletal muscle. *Dev Biol, 294*(1), 50-66. doi: 10.1016/j.ydbio.2006.02.022

Shimizu, N., Yamaguchi, M., Goseki, T., Ozawa, Y., Saito, K., Takiguchi, H., . . . Abiko, Y. (1994). Cyclic-tension force stimulates interleukin-1 beta production by human periodontal ligament cells. *J Periodontal Res, 29*(5), 328-333.

Shumway-Cook, A., Gruber, W., Baldwin, M., & Liao, S. (1997). The effect of multidimensional exercises on balance, mobility, and fall risk in community-dwelling older adults. *Phys Ther, 77*(1), 46-57.

Siwik, D. A., Chang, D. L., & Colucci, W. S. (2000). Interleukin-1beta and tumor necrosis factor-alpha decrease collagen synthesis and increase matrix metalloproteinase activity in cardiac fibroblasts in vitro. *Circ Res, 86*(12), 1259-1265.

Smythe, G. M., Shavlakadze, T., Roberts, P., Davies, M. J., McGeachie, J. K., & Grounds, M. D. (2008). Age influences the early events of skeletal muscle regeneration: studies of whole muscle grafts transplanted between young (8 weeks) and old (13-21 months) mice. *Exp Gerontol, 43*(6), 550-562. doi: 10.1016/j.exger.2008.02.005

Song, F., & Schmidt, A. M. (2012). Glycation & Insulin Resistance: Novel Mechanisms and Unique Targets? *Arterioscler Thromb Vasc Biol, 32*(8), 1760-1765. doi: 10.1161/ATVBAHA.111.241877

Sonnet, C., Lafuste, P., Arnold, L., Brigitte, M., Poron, F., Authier, F. J., . . . Chazaud, B. (2006). Human macrophages rescue myoblasts and myotubes from apoptosis through a set of adhesion molecular systems. *J Cell Sci, 119*(Pt 12), 2497-2507. doi: 10.1242/jcs.02988

Stenholm, S., Harris, T. B., Rantanen, T., Visser, M., Kritchevsky, S. B., & Ferrucci, L. (2008). Sarcopenic obesity - definition, etiology and consequences. *Curr Opin Clin Nutr Metab Care, 11*(6), 693-700. doi: 10.1097/MCO.0b013e328312c37d

Steppan, C. M., Bailey, S. T., Bhat, S., Brown, E. J., Banerjee, R. R., Wright, C. M., . . . Lazar, M. A. (2001). The hormone resistin links obesity to diabetes. *Nature, 409*(6818), 307-312. doi: 10.1038/35053000

Stocker, W., Grams, F., Baumann, U., Reinemer, P., Gomis-Ruth, F. X., McKay, D. B., & Bode, W. (1995). The metzincins--topological and sequential relations between the astacins, adamalysins, serralysins, and matrixins (collagenases) define a superfamily of zinc-peptidases. *Protein Sci, 4*(5), 823-840. doi: 10.1002/pro.5560040502

Stump, C. S., Henriksen, E. J., Wei, Y., & Sowers, J. R. (2006). The metabolic syndrome: role of skeletal muscle metabolism. *Annals of medicine, 38*(6), 389-402.

Thornell, L. E. (2011). Sarcopenic obesity: satellite cells in the aging muscle. *Curr Opin Clin Nutr Metab Care, 14*(1), 22-27. doi: 10.1097/MCO.0b013e3283412260

Tisdale, M. J. (1997). Biology of cachexia. *J Natl Cancer Inst, 89*(23), 1763-1773.

Toth, K. G., McKay, B. R., De Lisio, M., Little, J. P., Tarnopolsky, M. A., & Parise, G. (2011). IL-6 induced STAT3 signalling is associated with the proliferation of human muscle satellite cells following acute muscle damage. *PLoS One, 6*(3), e17392. doi: 10.1371/journal.pone.0017392

Tsuzaki, M., Guyton, G., Garrett, W., Archambault, J. M., Herzog, W., Almekinders, L., . . . Banes, A. J. (2003). IL-1 beta induces COX2, MMP-1, -3 and -13, ADAMTS-4, IL-1 beta and IL-6 in human tendon cells. *J Orthop Res, 21*(2), 256-264. doi: 10.1016/s0736-0266(02)00141-9

Uezumi, A., Ito, T., Morikawa, D., Shimizu, N., Yoneda, T., Segawa, M., . . . Fukada, S. (2011). Fibrosis and adipogenesis originate from a common mesenchymal progenitor in skeletal muscle. *J Cell Sci, 124*(Pt 21), 3654-3664. doi: 10.1242/jcs.086629

Unemori, E. N., Ehsani, N., Wang, M., Lee, S., McGuire, J., & Amento, E. P. (1994). Interleukin-1 and transforming growth factor-alpha: synergistic stimulation of metalloproteinases, PGE2, and proliferation in human fibroblasts. *Exp Cell Res, 210*(2), 166-171. doi: 10.1006/excr.1994.1025

Unsold, B., Bremen, E., Didie, M., Hasenfuss, G., & Schafer, K. (2014). Differential PI3-kinase signal transduction in obesity-associated cardiac hypertrophy and response to ischemia. *Obesity (Silver Spring)*. doi: 10.1002/oby.20888

Urso, M. L., Wang, R., Zambraski, E. J., & Liang, B. T. (2012). Adenosine A3 receptor stimulation reduces muscle injury following physical trauma and is associated with alterations in the MMP/TIMP response. *J Appl Physiol (1985), 112*(4), 658-670. doi: 10.1152/japplphysiol.00809.2011

Van Gaal, L. F., Mertens, I. L., & De Block, C. E. (2006). Mechanisms linking obesity with cardiovascular disease. *Nature, 444*(7121), 875-880. doi: 10.1038/nature05487

Verdijk, L. B., Koopman, R., Schaart, G., Meijer, K., Savelberg, H. H., & van Loon, L. J. (2007). Satellite cell content is specifically reduced in type II skeletal muscle fibers in the elderly. *Am J Physiol Endocrinol Metab, 292*(1), E151-157. doi: 10.1152/ajpendo.00278.2006

Villalta, S. A., Nguyen, H. X., Deng, B., Gotoh, T., & Tidball, J. G. (2009). Shifts in macrophage phenotypes and macrophage competition for arginine metabolism affect

the severity of muscle pathology in muscular dystrophy. *Hum Mol Genet, 18*(3), 482-496. doi: 10.1093/hmg/ddn376

Villareal, D. T., Apovian, C. M., Kushner, R. F., & Klein, S. (2005). Obesity in older adults: technical review and position statement of the American Society for Nutrition and NAASO, The Obesity Society. *Obes Res, 13*(11), 1849-1863. doi: 10.1038/oby.2005.228

Wang, W., Pan, H., Murray, K., Jefferson, B. S., & Li, Y. (2009). Matrix metalloproteinase-1 promotes muscle cell migration and differentiation. *Am J Pathol, 174*(2), 541-549. doi: 10.2353/ajpath.2009.080509

Wang, Z., Juttermann, R., & Soloway, P. D. (2000). TIMP-2 is required for efficient activation of proMMP-2 in vivo. *J Biol Chem, 275*(34), 26411-26415. doi: 10.1074/jbc.M001270200

Washington, T. A., Brown, L., Smith, D. A., Davis, G., Baum, J., & Bottje, W. (2013). Monocarboxylate transporter expression at the onset of skeletal muscle regeneration. *Physiol Rep, 1*(4), e00075.

Washington, T. A., White, J. P., Davis, J. M., Wilson, L. B., Lowe, L. L., Sato, S., & Carson, J. A. (2011). Skeletal muscle mass recovery from atrophy in IL-6 knockout mice. *Acta Physiol (Oxf), 202*(4), 657-669. doi: 10.1111/j.1748-1716.2011.02281.x

Wenstrup, R. J., Florer, J. B., Brunskill, E. W., Bell, S. M., Chervoneva, I., & Birk, D. E. (2004). Type V collagen controls the initiation of collagen fibril assembly. *J Biol Chem, 279*(51), 53331-53337. doi: 10.1074/jbc.M409622200

Wilson, V. J., Rattray, M., Thomas, C. R., Moreland, B. H., & Schulster, D. (1995). Growth hormone increases IGF-I, collagen I and collagen III gene expression in dwarf rat skeletal muscle. *Mol Cell Endocrinol, 115*(2), 187-197.

Wood, L. K., Kayupov, E., Gumucio, J. P., Mendias, C. L., Claflin, D. R., & Brooks, S. V. (2014). Intrinsic stiffness of extracellular matrix increases with age in skeletal muscles of mice. *Journal of Applied Physiology, 117*(4), 363-369. doi: 10.1152/japplphysiol.00256.2014

Xu, T., Bianco, P., Fisher, L. W., Longenecker, G., Smith, E., Goldstein, S., . . . Young, M. F. (1998). Targeted disruption of the biglycan gene leads to an osteoporosis-like phenotype in mice. *Nat Genet, 20*(1), 78-82. doi: 10.1038/1746

Yang, Z., Wang, X., He, Y., Qi, L., Yu, L., Xue, B., & Shi, H. (2012). The full capacity of AICAR to reduce obesity-induced inflammation and insulin resistance requires myeloid SIRT1. *PLoS One, 7*(11), e49935. doi: 10.1371/journal.pone.0049935

Yin, H., Price, F., & Rudnicki, M. A. (2013). Satellite cells and the muscle stem cell niche. *Physiol Rev, 93*(1), 23-67. doi: 10.1152/physrev.00043.2011

Yu, Q., & Stamenkovic, I. (2000). Cell surface-localized matrix metalloproteinase-9 proteolytically activates TGF-beta and promotes tumor invasion and angiogenesis. *Genes Dev, 14*(2), 163-176.

Zammit, P. S., Heslop, L., Hudon, V., Rosenblatt, J. D., Tajbakhsh, S., Buckingham, M. E., . . . Partridge, T. A. (2002). Kinetics of myoblast proliferation show that resident satellite cells are competent to fully regenerate skeletal muscle fibers. *Exp Cell Res, 281*(1), 39-49.

Zhang, C., Li, Y., Wu, Y., Wang, L., Wang, X., & Du, J. (2013). Interleukin-6/signal transducer and activator of transcription 3 (STAT3) pathway is essential for macrophage infiltration and myoblast proliferation during muscle regeneration. *J Biol Chem, 288*(3), 1489-1499. doi: 10.1074/jbc.M112.419788